MOLECULAR ORBITALS

AND

THERMOLYSIS AND HYDROLYSIS MECHANISMS

FOR

Δ^3-1,3,4-OXADIAZOLIN-2-ONES

BY

ANTHONY JAMES PAINE, B.Sc.

A Thesis

Submitted to the School of Graduate Studies

in Partial Fulfillment of the Requirements

for the Degree

Doctor of Philosopy

McMaster University

September 1979

MECHANISTIC ASPECTS OF OXADIAZOLINONE CHEMISTRY

DOCTOR OF PHILOSOPHY (1979) McMASTER UNIVERSITY
(Chemistry) Hamilton, Ontario

TITLE: Molecular Orbitals and Thermolysis and Hydrolysis Mechanisms for Δ^3-1,3,4-Oxadiazolin-2-ones

AUTHOR: Anthony James Paine, B.Sc. (University of Saskatchewan)

SUPERVISOR: Professor J. Warkentin

NUMBER OF PAGES: xviii, 315.

ABSTRACT

The title compounds were first synthesized in 1970, and because of their highly functionalized nature, undergo a medley of quite distinctive reactions.

Interaction between the two main functional groups (azo N=N and carboxylate) was investigated theoretically. CNDO/2 frontier molecular orbital densities, ionization potentials (IPs), and electronic transition energies were calculated for 5,5-dimethyloxadiazolinone (1-Me_2) and the 5,5-diprotio (1-H_2), and 5,5-difluoro (1-F_2) analogs. Bond lengths and angles were not optimized but rather taken from a crystal structure of a closely related system, with an assumed carbonyl bond length of R_{CO} = 1.19 Å. This value is supported by a high infrared stretching frequency (1835 cm^{-1}), X-ray crystal data, and the effect of R_{CO} variation on calculated IPs. The photoelectron spectrum of 1-Me_2 was obtained, and the first three bands assigned as n_N- (10.20 eV), π_{NN} (11.52 eV), and n_{CO} (13.26 eV). This unusually large n_{CO} IP is traced to an inductive effect of the neighbouring strongly electron withdrawing azo group. The IPs obtained by CNDO/2 calculation (12.81, 13.37, and 15.15) are 1.5 to 2.5 eV higher than the experimental values, which is well within the predictive capability of the method. Thus, the theoretical treatment gives a good representation of the MOs of these compounds and may be employed with confidence to provide

insight to the mechanistic studies.

The title compounds thermolyse at 50-100°C in a variety of solvents via two unique competing unimolecular pathways: one furnishing synthetically useful diazoalkane with carbon dioxide, the other, a theoretically interesting 3-piece fragmentation, spawns a molecule each of ketone, carbon monoxide, and dinitrogen. Diazoalkane formation is favoured by polar solvents and electron donating substituents, with a Hammett rho of -1.93 for seven p-substituted 5-methyl-5-phenyloxadiazolinones. Moderate solvent polarity effects, significant secondary kinetic isotope effects (2.1 ± 0.3% per D for 1-$(CD_3)_2$), the Hammett rho, and Frontier Molecular Orbital Theory, all support a concerted mechanism for diazoalkane formation through a transition state with non-synchronous bond rupture.

Neither thermal decomposition mode correlates with Taft steric parameters, E_s, and ketone formation does not correlate with inductive paramerers, σ^*. Interestingly, the enthalpy change during the exothermic three piece fragmentation was calculated to be only -30 ± 2 kcal mol^{-1}, precluding chemiluminescence. A vigorous search for intermediates by esr, ms, CIDNP, trapping, and racemization experiments leads to the conclusion that ketone formation is also concerted.

Synthetic procedures to make oxadiazolinones were augmented with a new oxidation procedure developed for synthesizing oxadiazolinones from ketone semicarbazones which would not cyclize under normal lead tetraacetate oxidation conditions. In the presence

of five equivalents of trifluoroacetic acid, a rapid reaction occurred at lower temperature.

Hydrolysis of dimethyloxadiazolinone was investigated at 20° over 30 orders of magnitude of acidity. Over the range H_o = -6 to pH = 14, the products are carbon dioxide, ketone, and diazene, as expected on the basis of strong kinetic parallels to neutral ester hydrolysis. Large C5 substituent electronic effects seem most consistent with rate limiting breakdown of the tetrahedral intermediate, but ^{17}O carbonyl oxygen isotope exchange was not detected. This is rationalized in terms of Deslongchamps' recent theory of stereoelectronic orbital control of the cleavage of tetrahedral intermediates, and supported by a number of related observations. The observed high reactivity of oxadiazolinones toward nucleophiles is in accord with the theoretical calculations, which predict a very electropositive carbonyl carbon.

Preliminary studies on acid catalysed decomposition of dimethyloxadiazolinone suggest that the thermodynamically favourable N4-protonated form may not be the kinetically active one leading to product 2-propanol over the acid range $-16 < H_o < -6$. Oxadiazolinones bearing C5 substituents capable of forming benzyl or t-butyl cations are more sensitive to acid catalysis, and may, in fact, lose R^+ in 40-60% H_2SO_4 on the way to as yet uncharacterized products.

ACKNOWLEDGEMENTS

After four years of study touching on almost every aspect of physical organic chemistry, it is difficult to single out and individually thank everyone to whom I feel indebted. There are many.

First, the financial support from the National Research Council (now NSERC) in the form of a Postgraduate Scholarship from 1975-79; and from McMaster University, in the form of a Dalley Fellowship, intermittent scholarship funds, and teaching assistantships, is gratefully acknowledged.

The entire Chemistry Department at McMaster has had a major influence on this work through the free interchange of ideas and attitudes (scientific or otherwise) catalysed by easy accessibility to everyone, right up to Chairman D.B. MacLean himself. Professors R.F. Childs and A.J. Yarwood were patient members of my supervisory committee, while Professor D.P. Santry gleefully attempted my conversion to a theoretical chemist, and Professor N.H. Werstiuk encouraged my development in photoelectron spectroscopy. Professor G.W. King graciously lent me digitizing equipment which saved many months of repetetive manual kinetic analysis in over 1500 kinetic runs.

Stimulating discussions and genuine friendship amongst colleagues in the laboratory figured strongly in the directions pursued by this research. Dr. G.A. MacAlpine was a gigantic influence, while co-workers Luba Taguchi and Janet Fulton

nurtured me as a rookie, prior to their own graduation. Many other students and special friends all deserve some credit for this final achievement and for lessons learned along the way. Prominent among these people is my wife, Wendy Fraser-Paine, who struggled (with variable success) to blend other things besides chemistry into my life at McMaster.

For their contribution to the pivotal spectroscopic portions of this thesis, I express gratitude to Messrs. Brian Sayer and Ian Thompson.

I am especially indebted to my supervisor, Professor John Warkentin, for achieving the right combination of a constructively guiding hand and free rein to do what I wanted. His generous encouragement to write and review journal articles, attend conferences, and give lectures has been extraordinarily valuable for both my professional and personal development.

Finally, I thank Rose Vonau for her patience, her skill, and her perseverance in undertaking to type this massive project.

TABLE OF CONTENTS

	Page
Abstract	iii
Acknowledgements	vi
List of Figures	xiv
List of Tables	xvi
INTRODUCTION	1
I.1 Why Mechanistic Studies?	1
I.2 Why Oxadiazolinones?	2
Chapter I1 - Thermolysis of Acyclic Azo Compounds	5
I1.1 Monosubstituted Diazenes	6
I1.2 Thermolysis of trans-Diazenes	7
I1.2.1 Isotope Effects	7
I1.2.2 Substituent Effects	11
I1.2.3 Solvent Viscosity and Pressure Effects	15
I1.2.4 The Role of CIDNP	17
I1.3 Thermolysis of Acyclic cis-Diazenes	20
I1.4 Thermolysis of Acyclic Azocarbonyl Compounds	23
I1.5 α-Hydroxydiazenes	28
Chapter I2 - Thermolysis of Cyclic cis-Diazenes	32
I2.1 Diazirines	34
I2.2 Diazetine	35

		Page
I2.3	Δ^1-Pyrazolines	38
	I2.3.1 Alkyl or Aryl Substitution	38
	I2.3.2 Substitution by Electronegative Groups	40
I2.4	3,4,5,6-Tetrahydropyridazines	46
I2.5	Oxadiazolines	48
I2.6	Cyclic α-Carbonyldiazenes	56
I2.7	Molecules From the Warkentin Laboratory	62
I2.8	Concluding Remarks	67
Chapter I3 - Hydrolysis of Diazene Carbonyls		70
I3.1	Acyldiazenes	70
I3.2	Diazenecarboxylates	76
METHODS, RESULTS, AND DISCUSSION		80
Chapter R1 - SCF Molecular Orbitals and the Photoelectron Spectrum of 5,5-Dimethyl-Δ^3-1,3,4-oxadiazolinone		80
R1.1	Estimation of Bond Lengths and Angles	81
R1.2	Calculation	83
R1.3	Results and Discussion	84
R1.4	The Photoelectron Spectrum of Dimethyloxadiazolinone	90
R1.5	Electronic Transition Energies	95
R1.6	Effects of Variation in R_{CO}	97
R1.7	CNDO/2 MOs for Carbon Dioxide and Diazomethane	98
R1.8	Concluding Remarks	99

		Page
Chapter R2 - Thermolysis of Δ^3-1,3,4-Oxadiazolin-2-ones		101
R2.1	Beginnings	103
R2.2	Mechanistic Alternatives	104
R2.3	Product Distributions	106
R2.4	Kinetic Investigations	108
	R2.4.1 Solvent Effects	108
	R2.4.2 Thermochemistry and Activation Parameters	111
	R2.4.3 Secondary Deuterium Kinetic Isotope Effects	115
	R2.4.4 Alkyl Substituent Effects	115
	R2.4.5 Aryl Substituent Effects	115
R2.5	Mechanism of Diazoalkane Formation	116
R2.6	Mechanism of Ketone Formation	119
R2.7	On the Variety of Product Types from Thermolyses of 5-Membered Ring Diazenes	127
	R2.7.1 A Relative Extrusibility Scale from Group Values	128
	R2.7.2 Testing the Method	135
	R2.7.3 2- and 3-Piece Fragmentations in Oxadiazolines	135
R2.8	Concluding Remarks	140
Chapter R3 - Dimethyloxadiazolinone Hydrolysis Mechanisms		142
R3.1	Neutral (and Base Catalysed) Hydrolysis	143
	R3.1.1 Product Distributions	143
	R3.1.2 Kinetic Studies	145
	R3.1.3 Building a Model	155
	R3.1.4 Substituent Effects	158
	R3.1.5 Carbonyl Oxygen Isotope Exchange	162

Page

R3.1.6 Stereoelectronic Control of the Cleavage of the Tetrahedral Intermediate 166

R3.1.7 Completing the Conversion to Products 172

R3.2 Acid Catalysed Decomposition at 20°C 176

R3.2.1 The Basicity of Dimethyloxadiazolinone 176

R3.2.2 Site of Protonation 180

R3.2.3 Other Substituents 184

R3.3 Concluding Remarks 187

EXPERIMENTAL 190

Chapter E1 - Synthesis 191

E1.1 General Procedure for LTA Oxidation of Dialkyl Ketone Semicarbazones (Method A) 191

E1.2 LTA Oxidation of Semicarbazones of p-Substituted Acetophenones (Method B) 192

E1.3 LTA Oxidation of d-Camphor Semicarbazone 197

E1.4 Synthesis of ^{17}O Carbonyl Labelled Oxadiazolinones 199

E1.5 Photoelectron and UV-Visible Spectroscopy 201

Chapter E2 - Thermolysis 202

E2.1 Materials 202

E2.2 Kinetics 202

E2.2.1 UV Method 203

E2.2.2 IR Method 204

E2.3 Product Distributions 205

E2.4 Other Experiments 206

Page

E2.4.1 Thermochemistry 206

E2.4.2 Chemiluminescence 207

E2.4.3 Electron Spin Resonance 208

E2.4.4 Chemically Induced Dynamic Nuclear Polarization 208

E2.4.5 PMR Test of Interconversion of 159a and 159b 209

E2.4.6 Estimation of an E_T value for TFA 210

Chapter E3 - Hydrolysis 212

E3.1 Product Distributions 212

E3.1.1 PMR Product Analyses 212

E3.1.2 Gas Evolution Experiments 214

E3.1.3 Identification of C2 Gas by GC-FT-IR 214

E3.1.4 Other Substituents 215

E3.1.5 Diimide Trapping Experiments 216

E3.1.6 Behaviour of Dimethyloxadiazolinone in FSO_3H 217

E3.1.7 Behaviour of Methyl-t-butyloxadiazolinone in FSO_3H 218

E3.1.8 UV-Visible Attempts to Estimate the Basicity of 1-Me_2 218

E3.2 Kinetics 220

E3.2.1 General UV Method 220

E3.2.2 NMR Kinetics 225

APPENDICES 231

Appendix 1 - Error Analysis and Curve Fitting Procedures 231

		Page
A1.1	Error Propagation	231
A1.2	Curve Fitting	234
	A1.2.1 Polynomial Functions	235
	A1.2.2 Non-Linear Functions	239
Appendix 2 - Kinetic Methods		255
A2.1	Treatment of First Order Reactions	255
	A2.1.1 Parallel First Order Reactions	258
A2.2	First Order Two Stage Reactions	260
A2.3	Activation Parameters	265
Appendix 3 - Miscellaneous Tables and Figures		267
REFERENCES		291

LIST OF FIGURES

		Page
R1	Bond lengths and angles in dimethyloxadiazolinone	81
R2	π MOs of oxadiazolinone 1-H_2	86
R3	Calculated and observed energy levels of oxadiazolinones	87
R4	CNDO/2 net charge densities	88
R5	The photoelectron spectrum of dimethyloxadiazolinone	91
R6	Correlation diagram using measured valence IPs	92
R7	Absorption spectrum of dimethyloxadiazolinone	97
R8	Valence orbital energy depends on choice of R_{CO} for 1-H_2	98
R9	Product distribution as a function of solvent polarity for thermolysis of 1-Me_2	107
R10	Product distribution as a function of substituent for thermolysis of 1-Me,Ar	109
R11	Effect of solvent polarity on rates of 2-diazopropane (k_2) and acetone (k_3) formation from 1-Me_2	109
R12	Hammett plot for ketone formation from 1-Me,Ar	117
R13	Hammett plot for diazoalkane formation from 1-Me,Ar	117
R14	Charge densities (q) and frontier MOs for cycloaddition	119
R15	A Bronsted plot for neutral hydrolysis of 1-Me_2	147
R16	Acidity dependence of the solvent catalysed rate	149
R17	Order in water in 0.200 M HCl	151
R18	Apparent order in water in aqueous sulfuric acid	151
R19	Concentration and rate profiles in aqueous H_2SO_4	154
R20	Limiting types of ester hydrolysis	156
R21	Alkyl substituent electronic effects in 0.200 M HCl	159

		Page
R22	Hypothetical intensity vs time curves for two oxygen isotope exchange experiments	163
R23	Application of the X-method to the acid catalysed decomposition of l-Me_2	179
R24	Rate profiles for l-Me_2, l-Me,t-Bu, and l-Me,$PhCH_2$ in aqueous sulfuric acid	186
E1	The position of λ_{max} as a function of acidity	219
E2	Absorbance-time behaviour of solutions containing thiophenol	222
E3	Sample ^{17}O nmr kinetic run	228
A3.1	Hydroxide ion buffer catalytic constant	287
A3.2	Tris(hydroxymethyl)aminomethane buffer catalytic constant	287
A3.3	Diethylmalonate dianion buffer catalytic constant	288
A3.4	Hydrogen phosphate dianion buffer catalytic constant	288
A3.5	Maleate dianion buffer catalytic constant	289
A3.6	Acetate ion buffer catalytic constant	289
A3.7	Formate anion buffer catalytic constant	290
A3.8	Apparent order in water for hydrolysis of l-$(PhCH_2)_2$ in aqueous DMF	290

LIST OF TABLES

		PAGE
I1	Kinetic isotope effects in a series of trans-diazenes	11
I2	Effects of substitution on the relative thermolysis rates of symmetrical arylazoalkanes, pyrazolines, and azoalkanes	14
R1	Change in bond length and stretching frequency of the carbonyl group as a function of substituent	82
R2	Valence orbital parameters for dimethyloxadiazolin-2-one	88
R3	Calculated and observed excitation energies for dimethyloxadiazolin-2-one	96
R4	Gas phase thermochemistry	112
R5	Activation parameters for thermolysis of 5,5-dimethyl-oxadiazolinone over the temperature range 50-95°	113
R6	Phenyl Stabilizations of $\Delta G^{\ddagger}$ for several diazene systems	124
R7	Relative heats of extrusion of various molecular fragments	132
R8	Conjugative interactions in R—X—Y—R	134
R9	Models of the heat of formation of dimethyloxadiazolinone	136
R10	Thermodynamic estimates and kinetic data for potential 2-and 3-piece fragmentations of selected pyrazoline derivatives	139
R11	Nmr shifts of 1-Me_2 in acetone-d_6 and FSO_3H at -60°	181
E1	Pmr data for dialkyl substituted oxadiazolinones	193
E2	Synthesis of p-substituted acetophenone oxadiazolinones	194
E3	Nmr assignment of stereochemistry in camphor oxadiazolinones	198

		Page
E4	Gas yields from hydrolyses of 1-Me_2	214
E5	Summary of ^{17}O nmr kinetic results in 0.200 M HCl	229
A1.1	Input data cards for sample listing of LSQ	244
A1.2	Results of the LSQ fit of Equation A1.30	244
A3.1	Valence orbital parameters for oxadiazolinone (1-H_2)	267
A3.2	Valence orbital parameters for difluorooxadiazolinone (1-F_2)	268
A3.3a	Effect of carbonyl bond length variations on the CNDO/2 energy levels of Δ^3-1,3,4-oxadiazolin-2-one	269
A3.3b	Effect of carbonyl bond length variations on the CNDO/2 net charge densities of Δ^3-1,3,4-oxadiazolin-2-one	270
A3.4	Solvent effects on thermolysis of dimethyloxadiazolinone at 85.0°C	271
A3.5	Temperature dependence of dimethyloxadiazolinone thermolysis	272
A3.6	β-Deuterium secondary kinetic isotope effects in thermolysis of 1-Me_2 at 85.0°C	273
A3.7	Alkyl substituent effects on thermolysis of oxadiazolinones in 1,2-dichloroethane at 85.0°C	274
A3.8	Thermolysis of p-substituted acetophenone oxadiazolinones in acetonitrile at 50.0°C	275
A3.9	Estimations of ΔH°_2 and ΔH°_3 for systems found in Table R10	276
A3.10	Buffer catalysis summary for hydrolysis of 1-Me_2 in the pH range 1-9	278
A3.11	Dilution effects on hydrolysis of 1-Me_2 at 20.0° in 0.200 M HCl	279
A3.12	Decomposition of 1-Me_2 in aqueous sulfuric acid at 20.0°C	280

		Page
A3.13	Properties of aqueous sulfuric acid at 20.0°C	281
A3.14	Alkyl substituent effects on oxadiazolinone decomposition in 0.200 M HCl	282
A3.15	Model neutral ester hydrolyses	283
A3.16	Decomposition of 1-Me_2 in FSO_3H by pmr	284
A3.17	Application of the X-method to acid catalysed decomposition of 1-Me_2	284
A3.18	Decomposition of 1-Me,t-Bu and 1-Me,$PhCH_2$ in aqueous sulfuric acid at 20.0°C	285
A3.19	Substituent effects in 63% sulfuric acid	286

INTRODUCTION

I.1 Why Mechanistic Studies?

Continuous improvement in the human condition depends upon contributions from science and technology, where technology harnesses the principles, ideas, and understanding of the physical, chemical, and biological sciences. Tremendous technological potential is critically predicated on a constant and vigorous supply of ideas from basic scientific research. Chemistry contributes through the systematic study of the composition and properties of substances and the reactions by which they are produced from, or converted into, other substances. Chemical reactions are vital components in the human environment (immediate and universal), as well as in the processes of life itself. Life is chemistry. To serve our need for energy, food, medicines, and a host of increasingly sophisticated materials, the development of new chemistry obviously demands comprehensive understanding of the principles governing chemical reactions.

Chemical reactions occur in a sequence of simple steps, the sum of which describes the mechanism of the reaction. Through an understanding of the sequence and molecular composition of the individual steps, and their significance in the overall reaction, comes predictive capability in the form of chemical principles of reactivity. Such principles spare scientists the repetitive ennui of examining every single example of literally billions of chemical reactions,

because similar reactions may be classified and results from one member of a group extrapolated (with due care) to encompass others. This is particularly true of organic functional group reactions. Chemical principles of reactivity deduced from one experiment are subject to refinement, clarification, extension, limitation, or even rejection, through never-ending scientific scrutiny.

I.2 Why Oxadiazolinones?

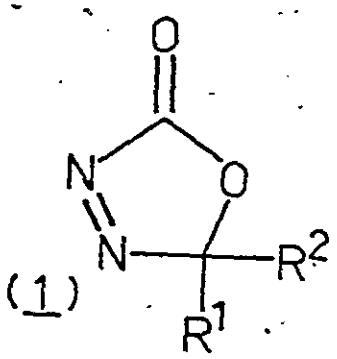

(1)

This thesis probes the chemical reactivity of Δ^3-1,3,4-oxadiazolin-2-ones* (1), particularly in thermolysis and hydrolysis reactions. Because of its highly functionalized structure (ester or lactone carbonyl group flanked by a conjugating nitrogen-nitrogen double bond), a priori application of already known principles of chemical reactivity for each of the constituent parts leads to uncertainty in predictions of chemical reactivity for the whole molecule. For example, azo compounds are characterized by radical-generating thermolyses, cycloaddition reactions of the Diels-Alder type, and stable, nitrogen-protonated species in mildly acidic solution. Carbonyl compounds are characterized by easy surrender to nucleophilic attack in a wide variety of addition reactions. Esters undergo typical replacement reactions of carboxylic acid derivatives, and α,β-unsaturated carbonyls may entertain 1,4 or 1,2

---

*Henceforth, unless otherwise noted, the somewhat more digestible term "oxadiazolinone" will refer to this particular isomer.

nucleophilic attack. As we shall see, not all of these characteristics are present in oxadiazolinones — the whole is not the sum of the parts.

In the interest of brevity, the balance of this thesis necessarily assumes that readers are reasonably familiar with: the syntheses, properties, and reactions of diazoalkanes[1-9]; chemically induced dynamic nuclear polarization (CIDNP)[10-20] (especially with regard to biradicals[21-23]); photoelectron spectroscopy (PES)[24-33] of azo compounds[34-38]; molecular orbital calculations[39-41]; frontier MO theory[42-54] (especially the simple yet elegant charge-controlled vs orbital-controlled theory of Klopman[47,55] which rationalizes Pearson hard-soft acid-base principles[56,57]); 1,3-dipolar cycloadditions[49,58-70] (including the controversy between Huisgen[65-67] and Firestone[68-70] on the mechanism: concerted vs biradical); and the Bader-Salem-Pearson theory of unimolecular reactions[71-76].

E_T is the solvent polarity parameter of choice throughout this thesis. The slope of a linear log k vs E_T plot will henceforth be known as a: for example, $\log k = a \cdot E_T + b$. For excellent reviews of solvent polarity parametersin general, and E_T values for specific solvents in particular, see Reichardt (1965,1979)[77]. Taft (1977)[78] also has a promising solvent polarity scale.

Generation of diazoalkanes, which are useful synthetic intermediates, from oxadiazolinones under a variety of conditions has motivated this study. In many respects, the mechanistic studies reported herein are unique because they tackle thermolysis and hydrolysis decomposition mechanisms for azo carbonyl compounds from a largely kinetic viewpoint. The chemical literature will be shown to be rife

with arguable, largely unsupported, mechanistic inferences drawn from product studies alone. This being the case, conclusions drawn in this study have a wide applicability to azocarbonyl compounds in general, and contribute to a pooled understanding of functional group interdependency in chemical reactivity.

The following Introduction to this thesis has been organized into three chapters. First, Chapter I1 reviews the literature on the thermolysis of acyclic azo compounds, including cis and trans isomers, α-carbonyldiazenes, and α-hydroxydiazenes. In Chapter I2, thermolyses of 3- to 6-membered ring cyclic diazenes are discussed, with particular emphasis on Δ^1-pyrazolines, α-carbonyl systems, and Δ^3-1,3,4-oxadiazolines. This bias reflects a greater relevance to oxadiazolinones. Sadly, not much information is available on hydrolysis of diazene carbonyls (Chapter I3).

After the introduction, there are three chapters of Methods, Results, and Discussion: (R1)SCF MOs and the photoelectron spectrum of dimethyloxadiazolinone; (R2) thermolysis of oxadiazolinones; and (R3) hydrolysis of oxadiazolinones. These are followed by three Experimental chapters: (E1) synthesis; (E2) thermolysis; and (E3) hydrolysis, then by three appendices: (A1) error propagation and curve fitting; (A2) kinetic methods; and (A3) miscellaneous tables and figures. In each of these four main units, section titles, figures, tables, equations, and schemes are identified by a prefix letter I, R, E, or A, respectively, to facilitate cross referencing.

II Thermolysis of Acyclic Azo Compounds

Acyclic azo compounds (diazenes) can exist in either the trans (E) or cis (Z) configurations, and each has its own reactivity patterns. The trans-isomer is generally about 6 kcal mol^{-1} more stable than the cis, an amount approximately equal to their activation energy difference.[79] More stable than the trans-diazene (by about 9 kcal mol^{-1}), is a tautomeric hydrazone (3), which can be formed by acid or base catalysed isomerization of azo compounds bearing an α-hydrogen (Equation II).[80] The presence of ubiquitous hydrazone impurities has harassed measurement of reliable thermodynamic data for azoalkanes,[81,82] and has tended to restrict study to those compounds which do not tautomerize.

[II] $$R_2CH-N=N-R \rightleftharpoons R_2C=NNHR$$
(2) (3)

Properties of azo compounds depend strongly on the nature of the attached groups. Homolysis to free radicals is first order and solvent insensitive, but occurs over an enormous temperature range. At one extreme are the highly stable azo dyes and azobenzene (4) which is stable at 600°C in the gas phase[83], while at the other extreme, azotriphenylmethane (5) is unstable at -40° in solution[36] and 6 is not isolable, even at -80° (ref. 84).

$Ph-N=N-Ph$ (4) $\qquad$ $PH_3C-N=N-CPh_3$ (5) $\qquad$ 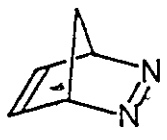 (6)

The question of whether an azo compound fragments to radicals

via a 1-step or 2-step mechanism (Equations I2 and I3), respectively) was first addressed in 1929 by Ramsperger who favoured a concerted mechanism for both symmetrical and unsymmetrical diazenes.[85] Activation parameters, isotope effects, cage studies, and CIDNP experiments have made the past 10 years the most definitive and fruitful. Recent gas phase studies summarized by Crawford in 1972 were interpreted in terms of the two-step mechanism involving a diazenyl radical intermediate (7)[86]. However, solution results fit a continuously graduating mechanism between the two extremes implied by Equations I2 and I3, depending on the relative stabilities of the two alkyl radicals.

[I2] $R{-}N{=}N{-}R \longrightarrow R\cdot + N_2 + \cdot R$ 1-step, concerted

[I3] $R{-}N{=}N{-}R \underset{?}{\rightleftharpoons} \underset{7}{R{-}N{=}N\cdot} + \cdot R \longrightarrow R\cdot + N_2 + \cdot R$ 2-step

II.1 Monosubstitued Diazenes

Diazene itself, as well as any monosubstituted derivative (8), is exceedingly unstable and decomposes in the gas phase by complicated radical chain processes[87] or in solution by complex bimolecular (non-chain) mechanisms[88-90] (Equation I4). For the solution reaction of phenyldiazene (8; R = Ph) Kosower (1971) notes that

[I4] $\underset{(8)}{R{-}N{=}N{-}H} \longrightarrow \underset{50\text{-}80\%}{RH} + \underset{\text{major}}{RNHNHR} + N_2$; R=alkyl, aryl, or H

solvent effects are small, the Hammett rho is small, k_H/k_D values around 4-5 are obtained when NH is replaced by ND, and added radicals do not affect the rate but do divert the reaction course to other

products.[88] Ruling out dissociation to phenyldiazenyl radicals and hydrogen atoms, electron transfer mechanisms, and hydride transfer, Kosower favoured bimolecular thermal conversion to a triplet pair as the rate determining step to decomposition. Shevlin (1978) reported CIDNP studies which were interpreted in terms of an H atom transfer mechanism[91] (Equation I5).

[I5] $2Ar-N{=}N-H \longrightarrow \overline{Ar-N{=}N\cdot \quad \cdot N(NH_2)-Ar} \longrightarrow$ products

Heesing (1976) reported on solution chemistry of monosubstituted diazenes,[92] and Willis and Back (1977) on gas phase reaction of diazene with olefins.[93]

In contrast to monosubstituted diazenes, disubstituted compounds are usually well behaved, and follow first order kinetics in solution, and in the gas phase when induced decomposition is suppressed with a radical scavenger such as NO or propylene[86]. There are, apparently, special features of the N=N—H bonds of 8 which have not yet been fully explained.

I1.2 Thermolysis of trans-Diazenes

I1.2.1 Isotope Effects

Secondary deuterium kinetic isotope effects can be a sensitive criterion of reaction mechanism[94-98]. Secondary effects observed for the allylic diazenes 9 to 12 led Crawford (1972) to conclude that only one CN bond was ruptured in the rate determining step (RDS) of the gas phase decomposition.[86] By themselves, the total k_H/k_D values for 9 and 10 could support either mechanism. However, a concerted

(9) 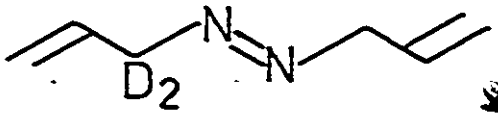 $k_H/k_D = 1.14 \pm 0.02$

(10) 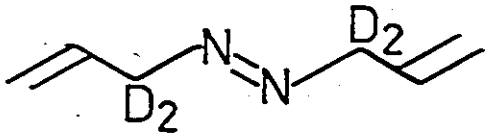 $k_H/k_D = 1.26 \pm 0.02$
rel. rate = 1.00

(11) 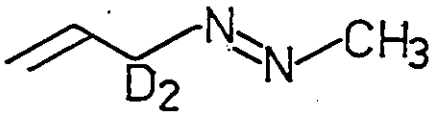 $k_H/k_D = 1.28 \pm 0.05$
rel. rate = 0.14

(12) 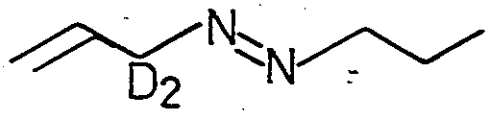 rel. rate = 0.34

process should show equal α-effects for 9 and 11 while a 2-step process, first producing the stabler allyl radical together with methyldiazenyl radical (7; R = CH_3) should show equality between 10 and 11, as observed.

To enhance his conclusion, Crawford noted that, after correcting for the statistical factor of 2 in the thermolysis of 10, the rate is only 1.5 times as great as that of 12. This is the order of magnitude expected from a steric effect, since rate ratios of 1:1 to 1.5 had been noted previously for meso- and dl-azoalkanes RR'R"CN=NCRR'R" in solution. Using group additivity rules[99-102], Crawford computed that the endothermicity (ΔH_r^o) of Equation I6 closely matched the activation enthalpy ($\Delta H^{\ddagger}$) for decomposition of 13, suggesting virtually complete rupture of the CN bond at the

transition state.[86] Benson (1970) concluded from similar thermokinetic considerations that a stepwise mechanism obtains for all azo compounds.[101]

[I6] 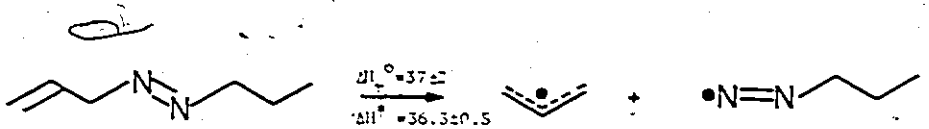

[I7] $$E_a = \alpha D_{RH} + \alpha' D_{R'H} - \text{Constant}$$

One can go even further, expressing the activation energy for a general azoalkane R—N=N—R' as a linear free energy relationship, as in Equation I7. There, E_a is seen to depend on the stabilities of both radicals formed (as reflected in their bond dissociation energies, D_{RH} or $D_{R'H}$, which is lower for stabler radicals), with a scaling factor, α or α', for each. In Crawford's case, say R· is the stabler radical. For Equation I7 to describe the available literature data for both symmetrical and unsymmetrical azo compounds, Crawford found $\alpha \sim 1.0$ and $\alpha' \sim 0$, formalizing the suggestion that only the RH bond is broken in the RDS.[86] This is currently accepted as the proof that dialkyldiazene decomposition in the gas phase must occur in two steps, via the diazenyl radical of Equation I3.

On the other hand, Seltzer (1967) has reported a correlation between primary nitrogen isotope effects and secondary α-D isotope effects for solution thermolysis of 1-phenylethyldiazenes 14 to 16 (Table II), interpreting his data in terms of a gradation of mechanism from concerted in the symmetrical case to stepwise in the asymmetrical

case.[103]

Rough equivalence of k_{16a}/k_{16b} and k_{15a}/k_{15b} at a lower value than k_{14a}/k_{14b} suggests that 15 and 16 each release one α-phenylethyl radical in their rate determining steps while 14 releases two. The small inverse α-effect on methyl labelling 16c, and the low ^{13}C KIE in the azomethyl group of 16 (0.68 ± 0.06%) both deny rupture of the N—CH_3 bond at the transition state. Diazene 16 must therefore decompose via an intermediate methyldiazenyl radical in a 2-step process, whereas 14 goes by a one step mechanism. In the middle, a transition state of non-synchronous, but concerted, bond rupture for 15 is reflected in the intermediate value of k_{15a}/k_{15c} = 1.040 and the smoothly increasing primary nitrogen effect as the N_2 character of the transition state is deduced to increase from 16 to 15 to 14 (Table II). Other work, in which the methyl groups of 14 have been replaced by $PhCH_2$, CH_3CH_2, or OCH_3 groups has consistently reproduced values of k_H/k_D around 1.20 ± 0.01, as in 14 (refs. 103-109).

Zimmerman (1976), however, effectively reminds us that the concerted/stepwise formulation of mechanism is not a dichotomy, but rather represents extreme paths on an energy surface — a mechanistic continuum.[110] It is also noteworthy that interpretation of observed α-D effects tacitly assumes rehybridization of carbon (from sp^3 to sp^2) upon radical formation (for example, Streitweiser (1958)[94] and others[95-98]).

Table II Kinetic isotope effects in a series of trans-diazenes.

Diazene		^{15}N KIE[a]	α-D KIE[b]
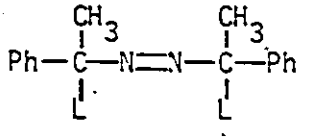	14a: L = H 14b: L = D	2.29 ± 0.14	k_{14a}/k_{14b} = 1.194 ± 0.003
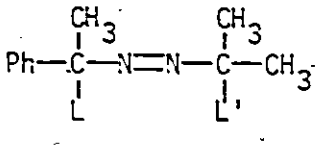	15a: L = L' = H 15b: L = D; L' = H 15c: L = H; L' = D	1.52 ± 0.05	k_{15a}/k_{15b} = 1.164 ± 0.012 k_{15a}/k_{15c} = 1.040 ± .010
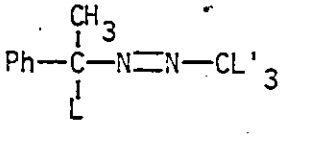	16a: L = L' = H 16b: L = D; L' = H 16c: L = H; L' = D	1.32 ± 0.08	k_{16a}/k_{16b} = 1.151 ± 0.003 k_{16a}/k_{16c} = 0.97 ± 0.01

[a] The ^{15}N KIE is expressed as a percentage: $100(k_{14}/k_{15}-1)$. From Seltzer (1967).[103]

[b] Recently corrected values by Schepple (1975).[104]

II.2.2 Substituent Effects

Classically, information on bond ruptures and transition state geometry for disubstituted diazenes has been obtained from structure-reactivity relationships. For example, rate constants and activation parameters for various structural variations have been examined by Ramsperger (1929)[85], Cohen and Wang (1955)[111], Overberger (1959)[112], Steel and Laidler (1961)[113], Timberlake (1975)[114], and Engel (1975).[115]

It is of interest to use Engel's 1975 compilation of reasonably accurate activation parameters for 20 dialkyldiazene thermolyses in both the gas and solution phase,[115] to compute α' values to fit an

equation like I7. The α' values directly measure the relative contribution of the least stable radical to the activation energy of the RDS. On going from 14 to 15 to 16, α' does decrease (0.50, 0.36, 0.26 respectively) as expected for increasing asymmetry of substitution. The large value for 16, however, emphasizes the importance of the methyl radical stability to the transition state energy! The value 0.26 is intermediate between the zero value for stepwise thermolysis of 12 and the 0.5 value for concerted thermolysis of 14. In fact, almost all other dialkyldiazenes show α' values in the range 0.25 to 0.50, in either gas or solution phase, with higher values corresponding (as expected for a mechanistic continuum) to more symmetrically substituted cases. The LFER criterion in Equation I7 leads to the conclusion that all azo decompositions are concerted, but some are non-synchronous. Only Crawford's systems 9 - 13 are exceptions, and the unrealistic values of $\alpha \sim 1.7$ and $\alpha' \sim -0.7$ which one could compute for 13 are uniquely bizarre among azo compounds. It is noteworthy that a trapping agent (NO) was needed to suppress induced decomposition in Crawford's gas phase work, and the results were appropriately corrected for this.[86] It would be most unusual for the gas phase to be significantly different from solution when there is so little effect of solvent polarity on reaction rate, however, as Engel notes, it would indeed be interesting to thermolyse 9 - 13 in solution.

Optically active 16 is racemized a few percent during decomposition[116] and Seltzer (1972) interpreted this as favouring the 2-step mechanism, with return from the diazenyl-containing radical

pair giving rise to some racemization. However, the observed ratio of optical activity loss rate (k_α) to nitrogen loss rate (k_{N_2}) had to be corrected for five times as much induced racemization,[116] making it somewhat risky to ascribe too much significance to the puny 1-3% residual racemization observed in such studies.

Kopecky (1969), Greene (1970), and again Kopecky (1977) found cage coupling products from optically active azo compounds to be formed with net retention.[117-119] In 1976, however, Kopecky uncovered one case where the cage coupling product had been formed with a few percent net inversion, which was interpreted as consistent with a 2-step mechanism.[120] Once again, the inversion of stereochemistry was considerably suppressed by radical scavengers.

Table I2 shows that para-substitution of phenyl rings, whether by electron donors or acceptors, mildly accelerates decomposition. The range of rate from aromatic substitution is less than a factor of 3 in any given columnar series, and the relative effect of a substituent decreases as the temperature and azo compound stability increase across the row. Thus, it seems unlikely that the isokinetic temperature lies in the range 40-150°, and the lack of correlation with Hammett substituent constants (even the "improved" $\sigma^\cdot$ scale of Jackson (1979)[121]), indicates no charge buildup in the decomposition transition state. Perhaps ponderal, subtle steric, or mass effects are involved — the rate differences are too small to say much more.

In complete contrast, the final column in Table I2 shows that

Table I2 Effects of substitution on the relative thermolysis rates of symmetrical arylazoalkanes, pyrazolines, and azoalkanes.[114,a]

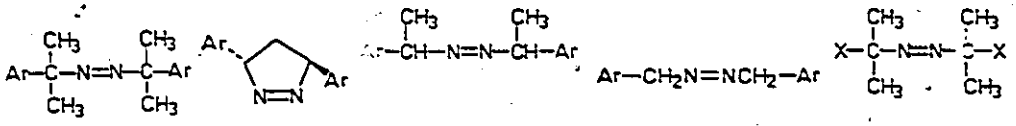

	(17)	(18)	(19)	(20)	(21)
Rel. rate at:	40°	80°	105° [b]	150°	100°
H	1.0	1.0	1.0	1.0	1.0
CH_3	1.46	1.38	1.15	1.07	560
CH_3O	2.06	1.48	1.33	1.30	5800
Cl	2.67	1.92	2.01	1.50	720000
Ph				2.04	$2.3X10^9$

[a] Ar refers to p-X-C_6H_4.

[b] Some of these do not exactly match ref. 114, as the original papers were consulted.

substitution on α-carbon is quite critical. A rate range of > 10^9 ($\Delta\Delta G^{\ddagger}$ = 16 kcal mol^{-1} at 100°) is observed for 21 symmetric trans-21 compiled in 1975 by Timberlake.[114] Reactivity differences are almost entirely accounted for by variations in $\Delta H^{\ddagger}$, since $\Delta S^{\ddagger}$ is around 10 ± 6 eu for almost every case. Interesting exceptions are $\Delta S^{\ddagger}$ = 4, -3, and -13 eu for 21: X = $PhCH_2$, PhO, and PhS, respectively. The relative rates are 1:3:420, the order expected on the basis of increasing radical stabilization ability, in spite of the increasingly unfavourable entropy term in the faster reaction (G = H - TS). Certainly these interesting discrepancies in $\Delta S^{\ddagger}$ deserve more attention

than they have received.[114,122-124] Perhaps there is a peculiar geometric or steric constraint on the transition state for X = PhS which arises from a requirement to line up S atom orbitals with the developing radical centre for maximum transition state stabilization. Replacing the methyl groups of 21 with H atoms would be a useful experiment, but one plagued by the azo-hydrazone tautomerism mentioned earlier.

Solvent polarity effects on thermolysis rates of trans-azo compounds are quite small — seldom more than ± 10% over wide ranges of solvent polarity.[125] Even these may not be polarity effects as solvent viscosity effects may be quite significant.[126]

II.2.3 Solvent Viscosity and Pressure Effects

In 1970, Pryor developed a qualitative and semiquantitative test for cage return of possible diazenyl radical intermediates.[126] For a generalized diazene, decomposition may be described by Equation I8.

[I8] $$R{-}N{=}N{-}R' \underset{k_{-1}}{\overset{k_1}{\rightleftharpoons}} \left\{ \begin{array}{c} \overline{R{-}N{=}N\bullet \quad \bullet R'} \\ \text{or} \\ \overline{R\bullet \quad N_2 \quad \bullet R'} \end{array} \right\} \begin{array}{l} \xrightarrow{k_D} R{-}N{=}N\bullet + R'\bullet \\ \xrightarrow{k_\beta} \overline{R\bullet \quad \bullet R'} + N_2 \end{array}$$

[I9] (a) $$k_{obs} = \frac{k_1(k_D + k_\beta)}{(k_D + k_\beta + k_{-1})}$$ (b) $$\frac{1}{k_{obs}} = \frac{1}{k_1} + \frac{C \cdot k_{-1} \cdot \eta^x}{k_1}$$

He argued that if only k_D depends on solvent viscosity (η), if k_D is inversely proportional to η^x (where $x \sim 0.5$), and if $k_D >> k_\beta$, then Equation I9 b describes the solvent viscosity dependence of the observed rate constant.

Now, if one accepts that a molecule which decomposes by simultaneous rupture of two bonds breaks into too many pieces to recombine, then k_{-1} must be zero for concerted homolysis, and no solvent viscosity dependence is anticipated. On the other hand, compounds which decompose by a one-bond scission, giving a diazenyl radical in the initial cage, may give cage return in solution by simple radical recombination, and k_{-1} may be non-zero, giving rise to solvent viscosity dependence in k_{obs}. Therefore, experimental observation of solvent viscosity dependence obeying Equation I9 b strongly supports the two-step homolysis mechanism, but the absence of any effect is inconclusive. Solvents for such studies must be carefully chosen to avoid possible solvation effects on the rate.[126]

Pryor found that for decomposition of 22 at 60°, k_{obs} decreases smoothly from n-pentane, through nonane, to octadecane: relative rate 1.0, 0.80, 0.61; relative η 1.0, 2.04, 7.10, respectively. In fact, for 10 n-alkane solvents linear plots of k_{obs}^{-1} vs $\eta^{-1/2}$ were obtained. Similar results prevailed for 23, but 24 showed no sensitivity to solvent, ruling out cage return and implicating a possible concerted mechanism for the latter case. The fraction of cage return, $f_r = k_{-1}/(k_D + k_\beta + k_{-1})$, calculated for 22 decreases with increasing temperature, from 0.25 at 50° to 0.13 at 80°, as expected.[126] Considering that so little racemization is observed,

this is an enormous amount of return.

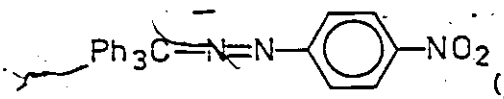

(22)

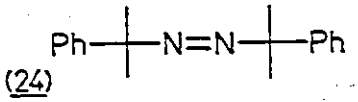

(24)

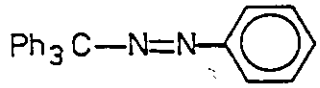

(23)

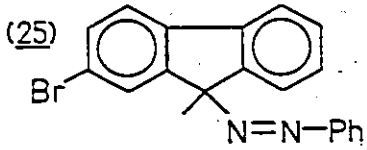

(25)

In 1973, Seltzer compared k_α to k_{N_2} for decomposition of optically active 25 in a series of n-alkane solvents.[127] His results reveal that, phenyldiazenyl/fluorenyl radical pairs are formed and that at 80° in n-heptane, 19% of these pairs return with retention, while 3% return with inversion. In more viscous octadecane more return is calculated (42% with retention, 5% with inversion). Return is enhanced by both lower temperature (Pryor) and increased viscosity (Seltzer) because both discourage diffusion from the radical cage (k_D).

Increased pressure is anticipated to suppress k_D (and k_β if it is significant), thereby lowering k_{obs} and inflating $\Delta V^{\ddagger}$ over the value of +4 $cm^3\ mol^{-1}$ observed for symmetrical azoalkanes.[128] Neuman (1970) found $\Delta V^{\ddagger}$ = +20 $cm^3\ mol^{-1}$ for 22, proving that $\Delta V^{\ddagger}$ does not necessarily reflect the volume change on homolytic scission (k_1), unless it is irreversible ($k_{obs} = k_1$ in such a case).[128,129]

II.2.4 The Role of CIDNP in Thermolyses of trans-Diazenes

Chemically induced dynamic nuclear polarization (CIDNP) refers to the 15 year old phenomenon of transient emission (E)

and enhanced absorption (A) signals observed in nmr spectra of solutions in which radical reactions occur.[10-20] These effects are a consequence of non-Boltzmann nuclear spin distributions which arise because of coupling between nuclear and electron spin states in a radical pair or diradical. CIDNP is capable of discriminating between one and two step decomposition mechanisms, even if the intermediate diazenyl radical has a lifetime on the order of 10^{-10} seconds. According to the CIDNP rules, diamagnetic products from a radical pair containing diazenyl will show net (E or A) polarizations because the g factors will be different for carbon and nitrogen centred radicals. On the other hand, products from a pair of carbon centred radicals will show multiplet (AE or EA) effects, because the g factors will be almost identical. Furthermore, as was noted in the preceding section, recombination of the two radicals-and-nitrogen sandwich (formed by the 1-step mechanism) is most unlikely, so CIDNP in the starting material is only possible from a two step process. Of these two criteria, the former has been widely used by workers in the field, however, this author believes that the latter criterion must also be met to enhance confidence in the intermediacy of diazenyl radicals.

Closs (1970)[130] reported that thermolysis of $PhCH_2—N{=}N—CHPh_2$ gave a pmr CIDNP spectrum displaying only multiplet effects — indicative of two carbon centred radicals in the pair, and a concerted mechanism. No polarization of starting material was reported. If the diazenyl radical intervened in this process, its lifetime was less than 10^{-10} seconds, the time needed to evolve some triplet character by the Δg

effect.

Less symmetrical azo compounds show much different results. Thermolysis of trans-23 at 80° showed net effects in pmr spectra of diamagnetic products benzene (cyclohexanone solvent) or chlorobenzene (CCl_4 solvent). No spectra accompanied this 1974 report (Seifert and Gerhardt[131]), so it is not clear if 23 was polarized. In 1978, Porter reported ^{15}N CIDNP spectra from 97% enriched trans-23 at 60° which clearly show enhanced absorption in the starting material, and emission in the N_2 escape product,[132] consistent with Equation I10.

[I10]

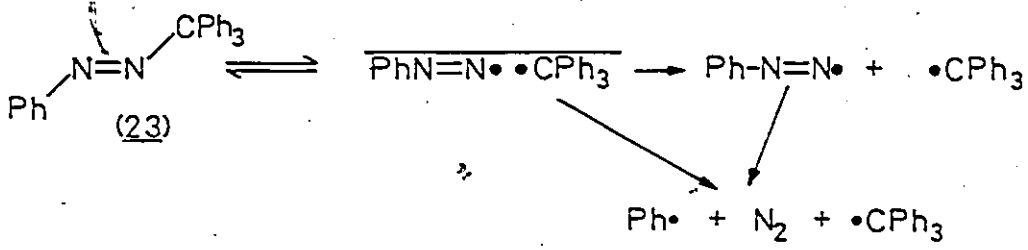

Proton and ^{13}C CIDNP observed by Shevlin (1978) from monoaryldiazene decomposition[91] (Equation I5, page 7) is similar to that observed by Seifert and Gerhardt (above), because no polarization of the initial aryldiazene was observed. Actually, in Shevlin's case, the aryldiazene was continuously produced at 80° (by three methods) at a temperature just sufficiently high to make decomposition rapid enough to display CIDNP, but so high that the aryldiazene had but a fleeting existence and no nmr signals corresponding to it were observed. While three independent methods of generation make it likely that polarized products do come from the aryldiazene, only

the product net vs multiplet effect criterion suggests that diazenyl radicals are involved. As was noted previously, in Section II.1.], phenyldiazene decomposition is bimolecular, and hence much different from thermolysis of disubstituted diazenes (Equation I5).

Kopecky (1976) reported a small amount of polarization during 180° pyrolysis of trans-$Ph_2CH—N{=}N—Ph$, consistent with phenyldiazenyl intermediacy.[120]

Except for these few examples, no other well-characterized CIDNP studies have been reported for trans-diazenes. This is probably because the spectra (especially pmr) are quite complicated, and thermolysis temperatures in excess of 200°, necessary for sufficiently rapid decomposition, are experimentally inaccessible in nmr spectrometers. The most successful CIDNP studies are at lower temperature, as one might expect from Pryor's work in the previous section, which showed that the fraction of return was very temperature dependent. In contrast, the much more labile cis-isomers have been somewhat better characterized in CIDNP experiments conducted at much lower temperatures (Section II.3)

II.3 Thermolysis of Acyclic cis-Diazenes

Very few acyclic cis-diazenes have been thermolysed, and only meagre mechanistic information is available. The cis-isomers are formed from those trans-isomers which do not photodissociate directly to radicals in solution (as is normal in azo photolyses[133,134]), but rather undergo trans to cis photoisomerization at low temperature.[115] Sometimes, low temperature chromatography may permit isolation of

the labile cis-diazene[132,135], and trifluoroacetic acid converts it back to the trans. Thermolysis occurs around room temperature.

Work by Porter's group[132,135-141] in the 1970's has firmly established the presence of the phenyldiazenyl (27) or 1-norbornyldiazenyl (38) radicals in thermolysis of cis-26, 28, 29 and 31, or cis-32 respectively. Proton, ^{13}C, and in 1978, ^{15}N CIDNP studies of cis-26 show net polarizations in the starting material, hydrocarbon products, and trans-diazene during decomposition at 30°, consistent with Equation III. In support of this mechanism, thermolysis of optically active cis-28 yields substantially racemized trans-28, the degree of racemization increasing as solvent viscosity decreases, suggesting that R· of short lived radical pair $\overline{PhN_2 \cdot \cdot R}$ has time to invert its configuration.* Furthermore, thermolysis of cis-29 yields some trans-30 on return from the diazenyl radical pair[139], and thermolysis of cis-26 in the presence of trityl radical gave a few percent of trans-23. Trityl had trapped the intermediate diazenyl radical (Equation III)!

In contrast to systems 26 to 34, cis-35 is thermally stable toward decomposition, reverting to trans-35 by some nondissociative mechanism (1976 theoretical study by Howell[142], 1975 thermodynamic and kinetic study by Haberfield[143]), much like azobenzene, azomethane, azoisopropane (37), azo-1-pentane (38), and azo-1-octane.[133,134,136] It may be tempting to ascribe this difference in reactivity between

*Kopecky (1977)[119] could detect no racemization of trans-34 during thermolysis at 175°, nor photolysis at 15°. Photodecomposition of trans-28 occurred via thermolysis of the cis-isomer.[137,138]

[III]

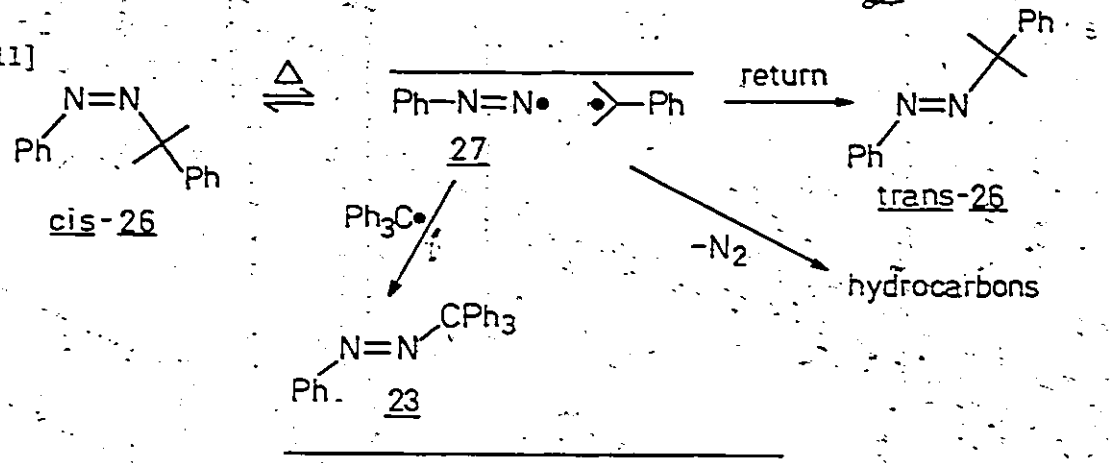

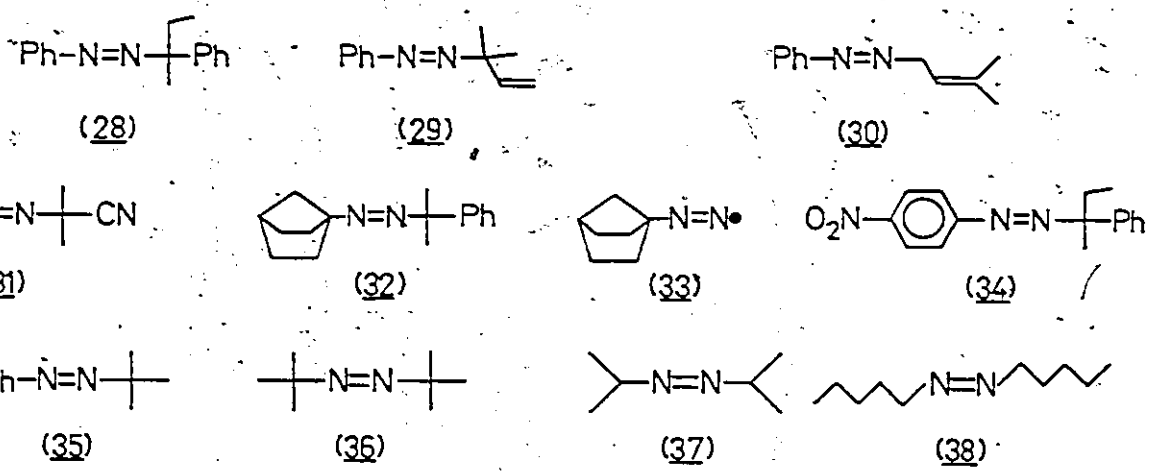

cis-26 and cis-35 to the difference in stability between the t-butyl radical and the benzyl radical in Equation III, but Mill and Stringham (1969) found that cis-36, and others, do undergo room temperature homolysis, presumably by a 1-step mechanism.[144]

Engel (1975) compared activation parameters for five pairs of cis and trans isomers, concluding that cis-dialkyldiazenes inherently decompose with a 7-8 kcal mol^{-1} lower $\Delta G^{\ddagger}$ than the trans, reflecting their ground state energy difference.[115] This $\Delta\Delta G^{\ddagger}$ may be greatly increased by accelerating steric strain: cis-di-t-butyldiazene (36) is 18.7 kcal mol^{-1} kinetically less stable than trans-

36. From his study of activation parameters, Engel concluded that both cis and trans azoalkanes decompose by a one step mechanism, even when unsymmetrically substituted, because the stability of both incipient radicals contributes to the transition state energy.

Rüchardt (1976) showed that the thermolysis rate of cis-36 is solvent sensitive, decreasing by a factor of 60 from pentane to methanol.[145] An excellent linear correlation of log k vs E_T had a moderately large negative slope of - 0.071 ± 0.002 (r = 0.9993 for 5 solvents). Such a slope factor means that the cis-azo starting material is much better solvated in polar solvents that the non polar transition state leading to radical intermediates. The cis-isomers must therefore have a reasonably large dipole moment, in contrast to the trans (with $\mu = 0$), which is lost in the RDS. In fact, Ackermann isolated pure cis-dimethyldiazene in 1977, and found $\mu = 3.2$ D[146] (compare to only 2.88 D for acetone[147]). Solvent sensitivity is mostly due to variations in $\Delta H^{\ddagger}$ (18.6 to 22.5 kcal mol^{-1} from pentane to methanol), as $\Delta S^{\ddagger}$ (ca. 10 eu) remained the same within experimental error.[145]

II.4 Thermolysis of Acyclic Azocarbonyl Compounds

Pyrolysis of trans-azodicarboxylates (diazenedicarboxylates, azodiformate esters, 39), trans-azodiacyls (dicarbonyldiazenes, 40), and trans-azobisformamides (diazenedicarboxamides, 41) has received less attention than even cis-diazenes because the reaction is much more complex. Whereas diazenes decompose with a clean first order rate to alkyl radicals which normally undergo recombination or disproportion-

ation, alkoxycarbonyl or acyl radicals apparently generated on thermolysis of azocarbonyl compounds generally induce secondary decomposition, as evidenced by nonlinear, concentration-dependent kinetics and low recombination yields. In fact, product yields are highly variable and no study has completed a mass balance. Thermochemical and kinetic data are exceedingly rare, making mechanistic ruminations somewhat speculative and biased. It is instructive to consider the examples which have been studied.

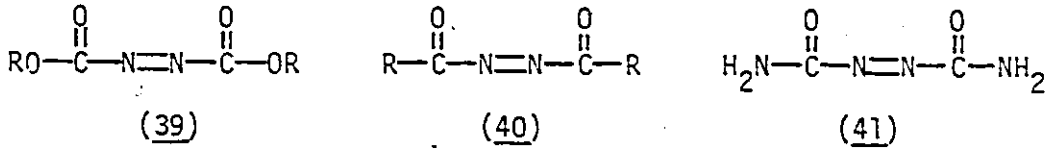

(39) (40) (41)

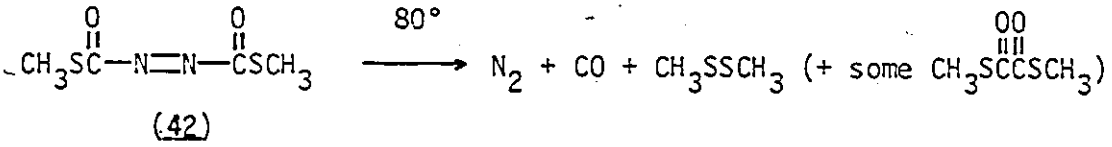

[I12]

(42)

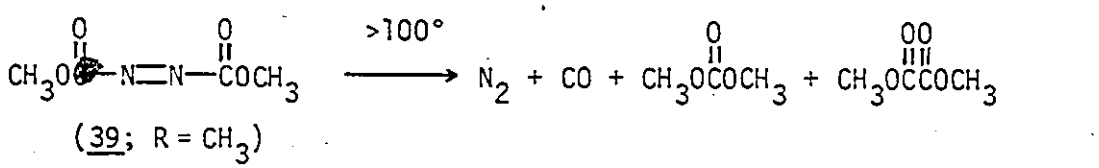

[I13]

(39; R = CH_3)

Arndt, Milde, and Eckert (1923) demonstrated facile loss of both N_2 and CO from 42 (Equation I12).[148] Stolle and Reichert (1929) and later Fedetova and coworkers (1956) studied dimethylazodicarboxylate (39; R = CH_3).[149,150] Thermal decomposition occurs above 100°, sometimes explosively, with quantitative nitrogen evolution[150] (Equation I13). Ingold (1973) repudiated a claim of diazenyl esr signals from matrix photolysis of 39.[151]

Thermodynamic arguments[152] and experimental observation[153]

lead to the conclusion that alkoxycarbonyl radicals $RO_2C\cdot$ lose CO_2 preferentially over CO: the former reaction 11 kcal mol^{-1} exothermic, while the latter 25 kcal endothermic for $R = CH_3$. This would seem to make formation of dimethylcarbonate in Equation I13 an interesting reaction. It is conceivable that CO and N_2 loss are concerted, but this hypothesis is untested.

In contrast, acyl radicals RCO may easily lose carbon monoxide (see Perkins (1974)[153]). If R is primary this process is 15 kcal endothermic and only occurs above 100°, but it can be reversed by a few hundred or a thousand atmospheres of CO pressure.[154]

Curtin (1960) observed a maximum of 70% recombination/disproportionation products in system 43, Equation I14.[154]

[I14] $Ph_3CCH_2\overset{O}{\overset{\|}{C}}-N=N-\overset{O}{\overset{\|}{C}}CH_2CPh_3$ (43) $\xrightarrow[\text{decalin}]{180°}$ $Ph_3CCH_2\overset{O}{\overset{\|}{C}}-\overset{O}{\overset{\|}{C}}CH_2CPh_3$ 45% + Ph_2CHCH_2Ph 11% + $Ph_2C{=}CHPh$ 14%

110°, benzene: 58% 25% 8% 6% 10%

[I15] $Ph-\overset{O}{\overset{\|}{C}}-N=N-\overset{O}{\overset{\|}{C}}-Ph$ (39; R = Ph) $\longrightarrow$ N_2 + 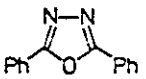 + $PhCH$ + $PhCOH$ + $PhCNHNHCPh$ + others

20°, EtOH: 83% — 61% 64% 10%

In 1956, Leffler found decomposition products from dibenzoyldiazene (39; R = Ph) to be complex and numerous, as well as solvent and O_2 dependent (Equation I15).[155] Unfortunately, no inhibitor could be found which suppressed the complicating reactions and simplified the very nonlinear kinetics. Large accelerating effects of electron

withdrawing groups, acids, and nucleophilic solvents were noticed, and the effect of ethanol solvent was attributed to nucleophilicity. Mackay, Marx, and Waters reported in 1964 that this reaction releases 15-35% CO_2 in aromatic solvents (a fact overlooked by Leffler eight years earlier) and decided that evidence for free benzoyl radicals was inconclusive because only a trace of the well known coupling product, benzil was produced.[156] For 39 ; (R = ethyl), Curtin (1960) found a rate increase of about a factor of 200 on passing from toluene to methanol.[154]

Triphenylmethylazocarboxylates (44; R = Me, Ph) were investigated by Zabel in 1972 (Equation I16).[157] Nitrogen was eliminated with 95% efficiency and no CO_2 or CO was detected. The products were rationalized as arising from recombination of trityl and alkoxycarbonyl radicals presumably before anticipated solvent attack or H abstraction by $RO_2C\cdot$ could occur. The absence of CO in Equation I16, when compared to Equation I13, is consistent with the lower temperature of the I16 thermolysis.

Herweh and Fantazier(1974) examined thermal decomposition of azodicarboxamide (41) at 100° in DMSO.[158] This is perhaps the most complete study on any of these systems to date. The reaction rate is slighly concentration dependent, but they rationalized it in terms of Equation I17, with $\Delta H^{\ddagger}$ = 27.4 kcal mol^{-1} and $\Delta S^{\ddagger}$ = -8 eu. After rate determining trans to cis isomerization, the key cyclization step was postulated to produce triazolinedione 45a which fragmented to lose CO and N_2. Although they wrote the 45a $\rightleftharpoons$ 45b equilibrium, numerous other cyclized intermediates (for example 46 to 48) could

[I16] 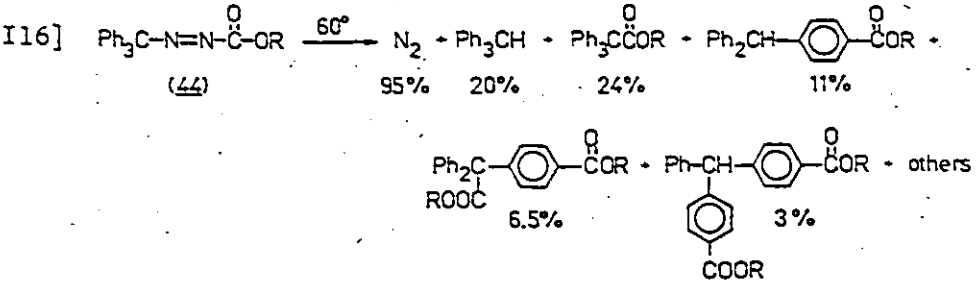

[I17] 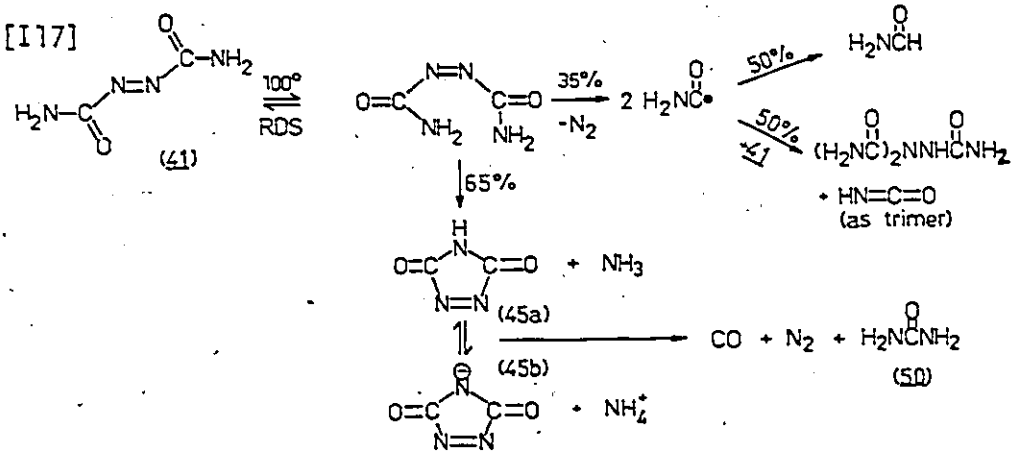

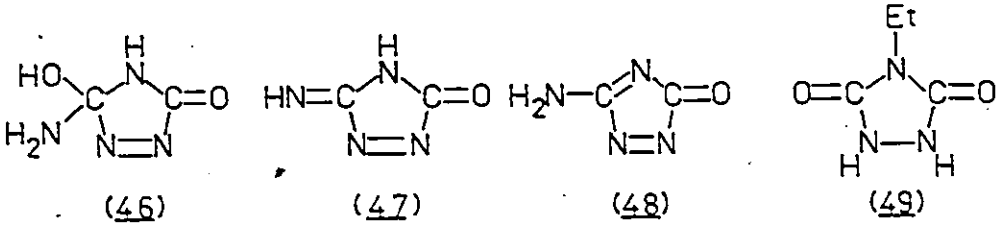

equally well lose CO and N_2. All of 45 to 48 require subsequent reaction to get to urea (50). It will later be shown that 46 resembles very active intermediates in oxadiazolinone hydrolysis. The evidence for cis-41 and 45a $\rightleftharpoons$ 45b is only circumstantial at best (tetramethyl-41 is stabler, and urazole 49 is obtained from N,N'-diethyl-41 in 45% yield), but intervention of cis-azocarbonyls is an

interesting possibility for these reactions.

Enormous scope exists for further study of α-carbonylazo compounds. Details of kinetic and product studies at low concentration should emerge without complicating bimolecular components. Syntheses of suspected cyclic and acyclic intermediates should be undertaken and these materials subjected to reaction conditions. It will be some time before synthetic methods are available, and even longer until reliable pictures of these transition states are available and the energy surfaces explored.

II.5 α-Hydroxydiazenes

α-Hydroxydiazenes (51) display three main types of chemistry: normal unimolecular fragmentation producing reasonably stable ketyl radicals R_2COH which would most likely disproportionate in the cage (Equation I18a); reversible dissociation to carbonyl compound plus diazene (Equation I18b); and radical chain abstraction of hydroxyl hydrogen (Equation I18c). Significantly all three mechanisms lead to the same major products, emphasising the point that product studies alone do not prove a mechanism.

Mechanism a was suggested by Southwick (1970)[159] and Nagata and Kamata (1970)[160] for the pyrazoline-like fragmentations of 52 and 53 to cyclopropanes 54 and 55, respectively (Equations I19 and I20).

Hünig (1968-71)[161-164] demonstrated the operation of mechanism b under strongly alkaline conditions where the intermediate diazene (R'—N=N—H) can lose a proton to become nucleophilic and thereby

[I18]

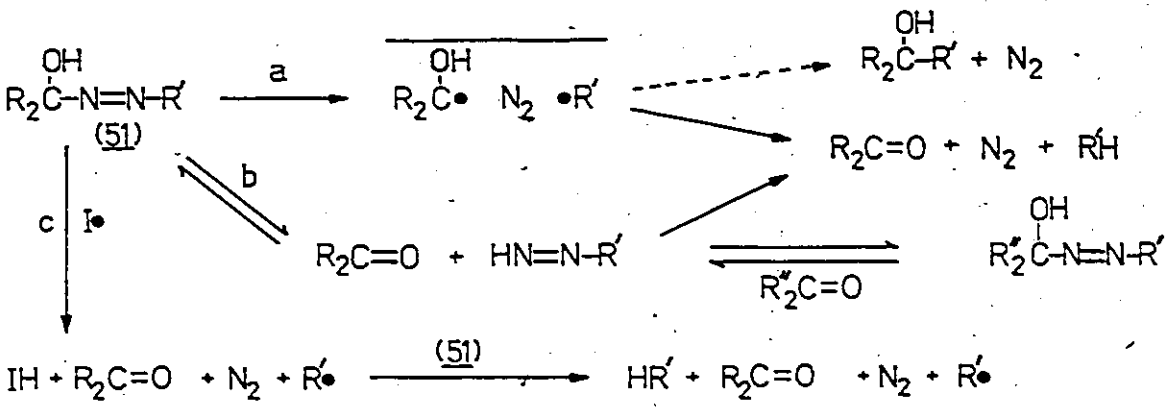

[I19]

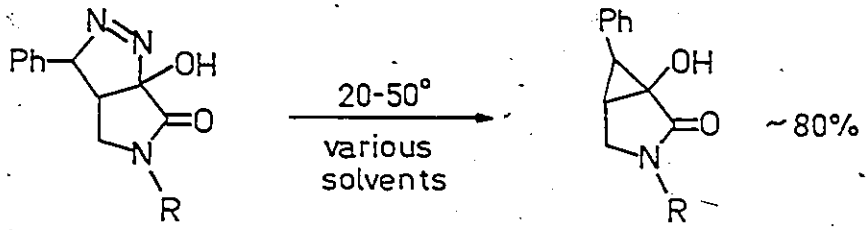

(52) (54)

[I20]

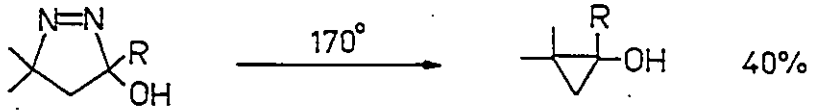

(53) (55)

exchange carbonyl groups. Freeman (1972)[165] examined 3-hydroxypyrazolines, finding them thermally stable in the absence of acid or base catalysts. Extended high temperature heating led to decomposition to ketonic products but since cyclopropanols formed by mechanism a would have decomposed to give ketonic material under these extreme conditions, any of a, b, or c is possible.

In work originating from this laboratory, Knittel and

Warkentin (1975)[166-168] first proposed and proved mechanism c. They observed some unusual features of the quantitative decomposition of 2-hydroxy-2,5,5-trimethyl-Δ^3-1,3,4-oxadiazoline (56) to isopropyl acetate. Freshly prepared solutions of the hydroxydiazene in benzene were sometimes stable and sometimes decomposed spontaneously. Once reaction had been initiated by mild heating, it could not be quenched by cooling to room temperature. A radical process was confirmed by spin-trapping 2-acetoxy-2-propyl radicals (57) using nitrosobenzene with esr detection. Olefins were converted to adducts of $CH_3CO_2\dot{C}(CH_3)_2$ and $H^{\cdot}$, and so-called inhibitors actually catalysed decomposition. On the basis of this information, the authors concluded that the radical chain mechanism was initiated and propagated by hydroxyl hydrogen atom abstraction which must be concerted with N_2 loss (Equations I21-I23). Ordinary hydroxyl hydrogen abstractions are unfavourable in solution, but the driving force of concurrent nitrogen formation makes initiation and propagation steps exothermic by some 50 kcal.[170]

This type of radical chain addition to olefins was later exploited for its synthetic value by Knittel and Warkentin (1976)[168] and Yeung and Warkentin (1976).[169,170] The latter pair employed an acyclic system (58) to generate a variety of radicals $R^{\cdot}$ which added RH across double bonds by the same radical chain mechanism (Equation I24).

Kinetic experiments conducted by Yeung and Warkentin (1976)[170] on 58 : R_2=t-Bu in CCl_4 and benzene at 35° gave irreproducible apparent

[I21] initiation:

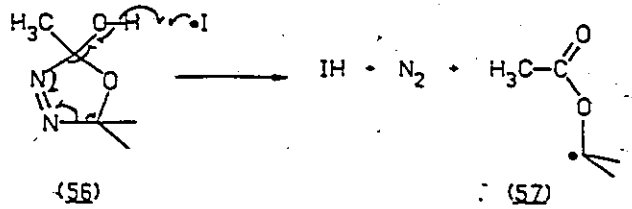

(56) (57)

[I22] propagation:

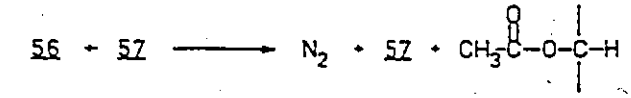

[I23] propagation by adduct formation

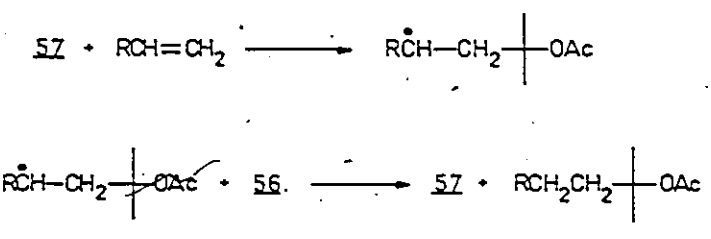

[I24]

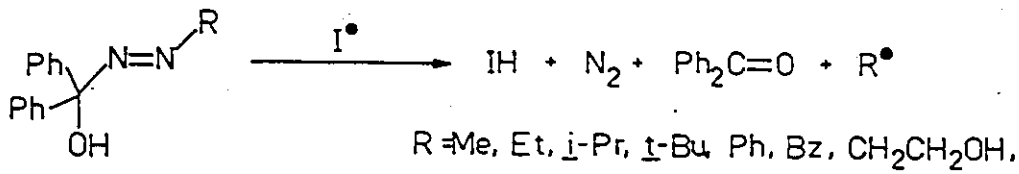

(58)

R = Me, Et, i-Pr, t-Bu, Ph, Bz, CH_2CH_2OH, allyl, cyclohexyl

first order rate constants, with air oxygen initiation increasing the rate by a factor of 100-200. Some runs were not first order. Such behaviour rules out unimolecular homolysis of 58 but is expected for a radical chain mechanism. In degassed benzene at low concentration, agreement between two kinetic runs was taken to imply a unimolecular fragmentation for that particular case.[170]

I2 Thermolysis of Cyclic cis-Diazenes

Cyclic cis-azo compounds, and Δ^1-pyrazolines in particular, have seen extensive investigation over the past 15 years, mostly from interest in the fate of biradicals generated by thermal or photochemical extrusion of nitrogen. For synthetic chemists, pyrazolines offer important routes to cyclopropanes, but variable stereospecificity and minor olefin production is a problem. Pyrolysis mechanisms for simple large ring diazenes (more than 6 to 8 atoms in the ring) are, not unexpectedly, very similar to those of corresponding acyclic cis or trans isomers. This is reflected in α-deuterium kinetic isotope effects, substituent effects (recall Table I1), solvent effects, and $\Delta V^{\ddagger}$ parameters.[108,114,171] Attention will therefore be focussed on the smaller rings which have a cis-azo function * (59 to 62).

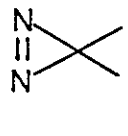

(59)

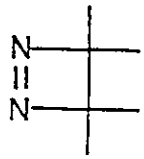

(60)

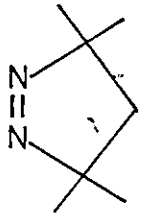

(61)

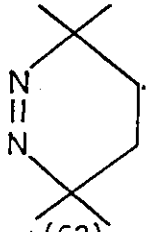

(62)

As a consequence of the small, reasonably rigid ring systems of 59 to 62, their chemistry is much different from that of their simple acyclic counterparts. In particular, appropriate substituent

---

*In 1978 Engel and Timberlake reported that irradiation of cis-62 led to detection of trans-62 at -8°C.[79] In contrast, trans-cyclohexene has never been observed.[172] The shorter NN vs CC bond length (1.25 vs 1.35 A) must contribute to stabilization of trans-62, whose only known chemistry is thermal reversion to cis.[79]

or heteroatom components increase the potential to form stable molecular fragments directly, rather than through biradicals. These more interesting cases are examined later in this Section. The background chemistry for the simple cases serves as a benchmark to compare and contrast with these other cases. Most of the emphasis in this section will be directed towards pyrazolines — reflecting greater experimentation and greater relevance to oxadiazolinones.

A lower NNC angle in 3-, 4-, and 5-membered ring diazenes reduces lone pair-lone pair interactions and stabilizes these rings relative to acyclic cases where side chain steric repulsion effects prevent attainment of the most favourable angle.[82] Thus, for example, pyrazolines decompose about 100° above cis-diisopropyldiazene (the latter at about 150°).

Pryor's viscosity test (Section II.2.3) for internal return from possible diazenyl radical intermediates cannot be applied to cyclic compounds because the diradical ends are unable to diffuse apart. Significantly, no one has detected internal return by other means (racemization, isomerization[173,174], or CIDNP).

Given the ground state polarity of cis-azo compounds noted by Rüchardt[145] and Ackermann[146], non-polar transition states corresponding to biradicals or to a concerted mechanism ought to show a decrease in the rate as solvent polarity increases. For example, a pyrolysis rate factor of 12 noted by Snyder (1978)[175] for cyclic cis-azo compounds in 96% ethanol to isooctane (5 solvents) would imply a slope of about -0.06 in a log k vs E_T plot: much the same as Rüchardt found for cis-

di-t-butyldiazene.[145] However, E_T plots are rare in this field and one must often construct one's own from reported data. When reaction rates actually increase with increasing solvent polarity, it is not unreasonable to add 0.06 to 0.07 to the observed slope to account for the ground state polarity in order to compare transition state polarity to model reactions.

Normally activation parameters and trends in product distributions can be extrapolated to the gas phase, given an E_T value of around 25-30. This makes solution and gas phase results directly comparable, strongly suggesting that the mechanism is the same.

I2.1 Diazirines

The three-membered ring diazene is unique in its ability to isomerize to a diazoalkane, which may then lose nitrogen to form a carbene (Equation I25). Great interest in these compounds stems from their ability to generate carbenes in photochemical and thermal decompositions. In principle, nitrogen extrusion could be direct or stepwise via the diazoalkane. Normally the diazoalkane would not survive the high reaction temperature, but recent detection and isolation of diazoalkanes by Liu (1976, 1977) has confirmed their intermediacy.[176,177]

[I25]

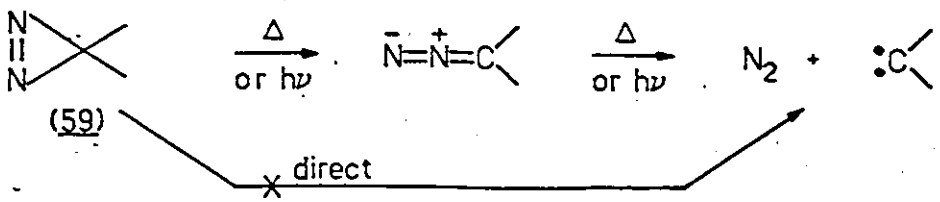

If one choses to view diazirine decomposition as a member of the general class of diazene thermolyses, the diazenyl radical formed by one-bond scission is the diazoalkane, "stabilized" by the proximity of the paired electrons. The diradical nature of diazomethane has been commented on in a theoretical paper by Harcourt and Roso (1978).[178]

I2.2 Diazetine

[I26] 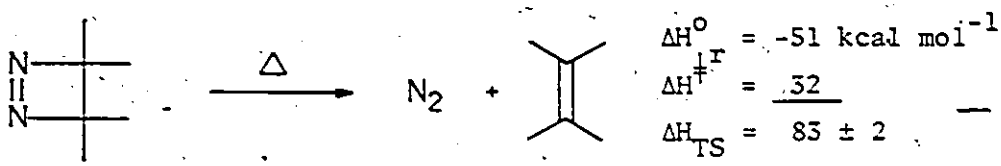

(60)

Although fragmentation to olefin plus N_2 is symmetry forbidden,[179] there is enough energy released from the transition state of the 4-membered ring diazene to populate the olefin T_1 state to permit a concerted, orbital symmetry allowed mechanism.[79]

In 1975, Greene reported the first synthesis of a monocyclic diazetine (tetramethyldiazetine, 60).[180] In 1978, Engel and Timberlake reported kinetic and thermochemical results on this molecule which are summarized in Equation I26.[79] The transition state, at 83 kcal above the products, lies above the olefin T_1 level (<75 kcal) but below the olefin S_1 (ca. 130 kcal mol^{-1} above S_0)[79,181]. Turro has now established that crossing to a T_1 state of product ketone does occur in thermolysis of tetramethyldioxetane (63, Equation I27).[182] The same might be expected, therefore for 60.

[I27]

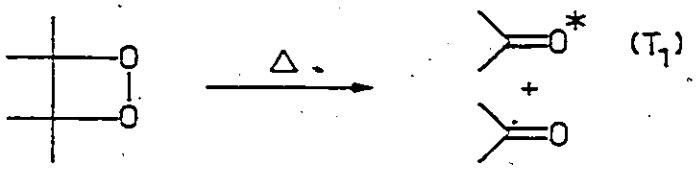

(63)

In a very lucid paper appearing in October 1978, Greene reports that the thermolysis of cis- and trans-3,4-diethyl-3,4-dimethyldiazetine (64) gives stereospecific cis-elimination of nitrogen.[181] Although stereospecificity is normally a criterion for concertedness in pericyclic reactions, and although evidence favours concerted loss of nitrogen from symmetrically substituted azoalkanes, the high stereospecificity of diazetine thermolysis (>95%) actually rules out crossover to the olefin T_1 state, because olefin triplets are known to isomerize.[183] Two bond cleavage could not give the biradical, as it would be the olefin S_1 state.

From thermochemical and kinetic data, Engel and Timberlake have calculated that, after accounting for strain energy of 60, the transition state for decomposition of 60 is 10-15 kcal higher than that for trans-di-t-butyldiazene, 61, or 62.[79] They cite three possible explanations: a higher energy concerted 2s + 2a mechanism; a possible N=N twist mechanism which would be more restricted for 60 than for 61 or 62; or the price for violating orbital symmetry rules (and fragmenting by a concerted 2s + 2s mechanism) is 10-15 kcal. A fourth unmentioned possibility is that only about half of the 25 kcal strain energy in 60 is released at the transition state.

Discounting the conceivable, but unlikely 2s (olefin) +2a (N_2) allowed alternative (which involves 90 or 180° rotation about

the C_2 axis of 60), diazenyl radical 65 emerges as an intermediate (Equation I28). If this is so, then in-plane loss of N_2 (k_d) must be very much faster than bond rotation to diazenyl radical 66 (k_{rot}).[181] Perhaps the transition state leading to 65, with eclipsed substituents and one unrelieved CNN angle, may explain the fourth possibility advanced in the previous paragraph.

[I28] 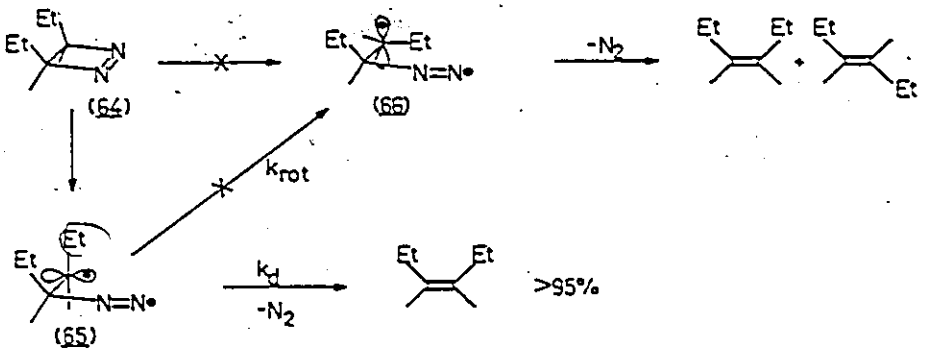

Stereospecific fragmentation of β-lactones (67)[183,184] and β-lactams (68)[185] (Equation I29), and stereospecific cycloadditions of olefins with allenes, ketenes, and isocyanates have been interpreted by Paquette (1970)[185], among others, as suggesting that cumulative π bonds can perform concerted, allowed, π2s + π2a reactions. On the other hand, cycloreversions of cyclobutanes or azetines (69) and other non-cumulenes are not stereospecific.[185] Against such a background, diazetine fragmentation appears anomalous. Some substituent effect work is in order.

[I29] 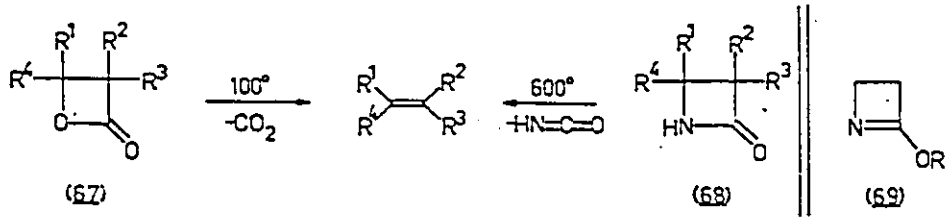

I2.3 Δ^1-Pyrazolines

I2.3.1 Alkyl or Aryl Substitution

Crawford (1966) found that successive methyl substitution at the 3 and 5 positions decreased the activation energy by roughly additive amounts (Equation I30) leading him to propose concerted two bond rupture.[186] As in acyclic analogs, $\Delta S^{\ddagger}$ is consistently around 8 ± 6 eu. This series does show a much smaller effect of methyl substitution than the trans-diazene series (for example, $\Delta\Delta G^{\ddagger}$ (25°C) = 9.8 kcal mol^{-1} between dimethyl- and di-t-butyldiazene[115]). In some series (Equation I31), methyl groups slightly discourage decomposition, and little acceleration derives from the exocyclic double bond (allylic) in the 4-position.[173,187,188] In contrast, allyl or phenyl substitution at positions 3 and 5 has a marked stabilizing effect (Equation I32). Such results would

[I30] 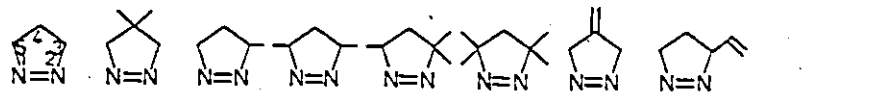

E_a 42.4 42.3 41.0 40.25 39.0 37.7 33.6 32.2 (±0.4 kcal mol^{-1} gas phase)[126,189]

[I31] 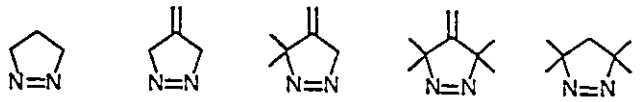

Rel. rate 1.0 315 105 5 15 (160°, gas phase)[188]

[I32] 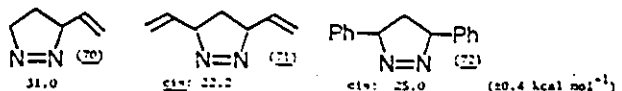

$\Delta H^{\ddagger}$ 31.0 (70); cis: 33.2, trans: 25.1 (71); cis: 25.0, trans: 27.5 (72) (±0.4 kcal mol^{-1})

Ref. 190 191 192,193

seem to indicate that, irrespective of the question of one or two bond cleavage, there must be some significant geometrical factors necessary for efficient stabilization of incipient or biradical orbitals.

Each successive allyl substitution of a pyrazoline at position 3 then 5, lowers the activation enthalpy 8-9 kcal mol^{-1} (Equation I32).[191] Furthermore, 5,5-dideutero substitution of 70 gives a normal α-D effect (k_H/k_D = 1.21 ± 0.03) indicative of extensive N1-C5 rupture in the transition state of that highly unsymmetrical pyrazoline.[190] These two facts led Crawford (1967, 1974) to conclude that, even in highly unsymmetrical pyrazolines, both CN bonds are almost completely ruptured at the transition state of a one-step nitrogen elimination.[190,191] This is in remarkable contrast to unsymmetrical acyclic diazene pyrolyses, where this same author concluded that stepwise decomposition prevails.[86] The evidence for 70 suggests that the transition state is not even asymmetric!

A 1977 stereochemical study by Bergman led to the conclusion that nitrogen was extruded in a nonlinear fashion not unlike a σ2s + σ2a pathway, and that closure of the very very short lived 1,3-biradicals to cyclopropanes was so fast that it competed with conformational changes and bond rotations.[194] Such a mechanism, with concerted nitrogen loss, could explain the confusing array of incomplete stereochemical results which had previously been used to support either one or two bond cleavage (for example, Crawford (1976)[195]).

I2.3.2 Substitution by Electronegative Groups

3-Positional substitution with electron withdrawing groups (73; X,Y = CF_3, COR, CO_2R, CN, etc.) increases the chances for 1,3- or 1,5-zwitterions in place of biradicals (Equation I33). 1,4-Zwitterions have been well characterized by Huisgen in the stepwise 2 + 2 cycloadditions of enol ethers and tetracyanoethylene.[196] Solvent polarity effects can increase these 2 + 2 rates (by a factor of 10^5 from CCl_4 to CH_3CN), providing a convenient benchmark of comparison for other reactions. In most cases, pyrazoline solvent effects are too small to account for zwitterions, but do suggest polar transition states.

[I33] 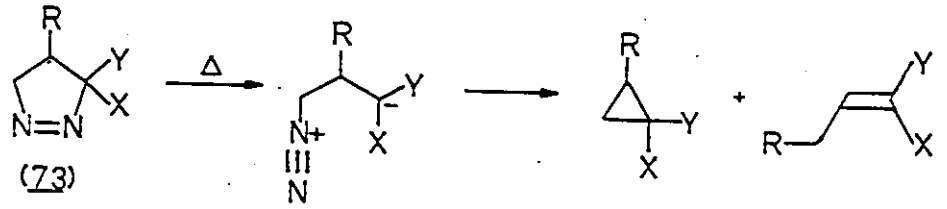

(73)

Migration of R (H or alkyl) from C4 to C5 on the way to olefin product has been taken by McGreer (1965) to be evidence of some cationic character at C5.[197] Olefin yields are always higher when electronegative groups are attached to C3. In formamide solvent the rate was 200 times faster than in ether, reversing the normal trend of solvent polarity for alkyl or aryl substituted pyrazolines, and indicative of a reasonably polar transition state.

It is interesting to compare secondary deuterium kinetic isotope effects for pyrazoline (74) and 3-carbomethoxy-3-methylpyrazoline (75). Crawford investigated the former case in 1968 (Equation I34).[198] Although the β-effect seemed quite large for 74-4,4-d_2, he considered

these results to support concerted N_2 loss. Variations in product distribution were then attributed to isotope effects in the product determining steps which followed.

[I34] 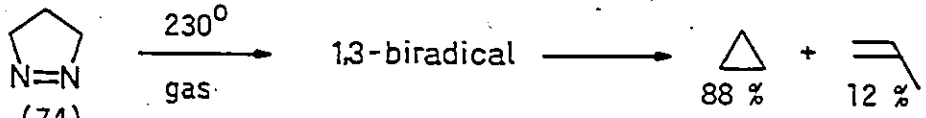

(74)

k_H/k_D(74-3,3-d_2) = 1.19 ± 0.01

k_H/k_D(74-3,3,5,5-d_4) = 1.40 ± 0.02

k_H/k_D(74-4,4-d_2) = 1.12 ± 0.01

[I35] 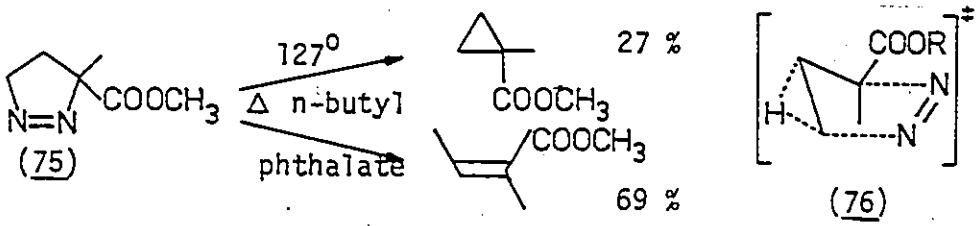

(75) (76)

k_H/k_D(75-4,4-d_2) = 1.36 ± 0.06

k_H/k_D(75-5,5-d_2) = 1.22 ± 0.05

On the other hand, McGreer (1969)[199] examined the secondary deuterium kinetic isotope effects for pyrazoline 75, and found an even greater β-effect: 1.36. Attributing the Crawford value to "hyperconjugation by the deuterium in a nitrogen free intermediate", McGreer considered his β-effect too large for similar explanation. Instead of formulating a 1,3-biradical as a common intermediate for both olefin and cyclopropane, he found it attractive to consider separate paths for olefin and cyclopropane formation. From the measured

isotope-dependent product distributions, the overall β-KIE was broken down into contributions from each route. The β-effects for olefin and cyclopropane formation were then 1.94 and 1.20, respectively. In this context, McGreer envisaged olefin formation occurring via concerted C4 to C5 hydrogen migration and nitrogen loss (76 as transition state). Polar solvents retard the overall rate slightly (but the olefin forming rate negligibly), ruling out zwitterionic intermediates. The α-effect is normal for C5-N1 rupture.[199] Although 1.94 seems a puny primary effect, it is of the magnitude of that observed in isomerization of cyclopropane to propylene.[200]

If Crawford's gas phase pyrazoline system is analysed in the context of different transition states for olefin and cyclopropane formation, the β-effects come out as 1.23 and 1.11 respectively. Even so, if C4 methyl substitution has such a small effect on the observed activation energy (recall Equation I30), why is k_H/k_D so large? For one thing, it may be necessary to break down E_a for methyl substitution to facilitate valid comparison of the methyl and k_H/k_D effects. Secondly, in their tome on pericyclic reactions, Marchand and Lehr warn of the need to critically evaluate secondary KIE data.[201] The origins of these isotope effects, when observable, can be quite complex, and the application of the data thereby obtained toward elucidating the detailed structure of transition states may be accordingly obscured by these complexities (ref. 201, p 19).

In a 1965 stereochemical study of 5-methyl-75, McGreer noted greater stereospecificity in olefin formation than in cyclopropane

formation, and a very solvent-dependent product balance. In the gas phase 90% cyclopropanes were obtained (with about 75% retention of stereochemistry), but in solution, as polarity increased, cyclopropanes declined (to 43% in formamide) and olefins were formed with > 90% stereospecificity. The rate varied only slightly.

It seems difficult to rationalize a highly ordered transition state such as 76 with an activation entropy of +7 eu.[199] More research is needed on all pyrazolines to dissect the α-effect, $\Delta H^{\ddagger}$, $\Delta S^{\ddagger}$, and solvent polarity effects into components corresponding to each of cyclopropane and olefin formation before these mechanisms can be accepted.

In 1975, Polansky thermolysed Δ^1-pyrazolines with two electronegative groups at C3, concluding that a 2-step mechanism operated in polar protonic solvents.[202,203] He also found that one equivalent of Cu^{+2} had a catalytic effect, favouring cyclopropanes. In n-butanol, for example for 77, $\Delta H^{\ddagger}$ declined from 23.3 to 12.6 kcal mol^{-1}, $\Delta S^{\ddagger}$ from -10.2 to -29.3 eu, and olefin yield at 105° from 69 to 21%, for the uncatalysed and catalysed processes, respectively. The large negative $\Delta S^{\ddagger}$ in the presence of $CuCl_2$ implicates a copper-pyrazoline complex, and the negative value in the absence of catalyst is an immediate clue that the reaction is different from heretofore discussed examples.

In fact, when Polansky's rate data are plotted against E_T for the 9 solvents used*, a slope of +0.08 is obtained. If 0.06 to 0.07

---

*Polansky actually chose to plot against the Ω polarity parameter, and obtained a much worse fit than with E_T. A number of polarity parameters are discussed by Reichardt (1965).[77]

is added to account for ground state polarity, a = 0.14 - 0.15 is inferred. Intervention of 1,4-zwitterion 79 in stepwise 2 + 2 cycloaddition has an a value of +0.29.[196] Greater resonance delocalization is expected for 79 (compare σ and σ_I for CN (0.90 and 0.56) and CO_2Me (0.68 and 0.30)[204], respectively), so 78 seems unlikely. The cyclopropane yield from 77 is very temperature sensitive (57% at 45° and 30% at 110°), but product distributions corresponding with the rate data were not given. This unfortunately leaves the question of whether 78 (with or without N_2) is an intermediate for both cyclopropane and olefin formation an unanswered one.

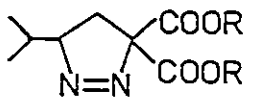

(77)

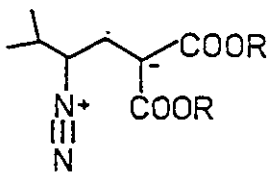

(78)

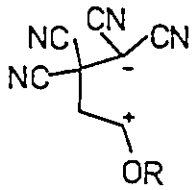

(79)

Along the line of polar intermediates, Allred and Flynn (1972) found that pyrazoline brosylate 80 decomposes 100 times faster than tetramethylpyrazoline (61), with $\Delta H^{\ddagger}$ = 32.1 kcal mol^{-1} and $\Delta S^{\ddagger}$ = 2.2 eu (Equation I36).[205] The pyrazoline acetate (possible stable product of S_N2 solvolysis) was not observed, and there was no β-D KIE in 5,5-dimethyl-d_6-80. The product proportions changed markedly on deuteration, however, and this was taken as strong evidence of a product determining intermediate after the rate determining step. Therefore 81 was a logical intermediate. In a 1979 paper, Allred[206] found that replacement of one C5 methyl in 80 with an aryl group actually reduced the rate by a factor of 3. Such a minuscule change (in the wrong direction

for radical or cation stabilization) denies rate limiting N1-C5 bond rupture and supports the intervention of 81 in Equation I36.

[I36] 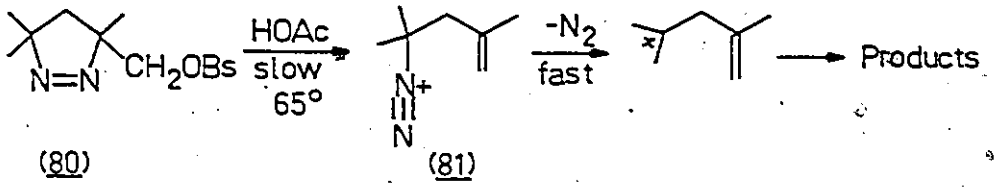

(80) (81)

[I37] 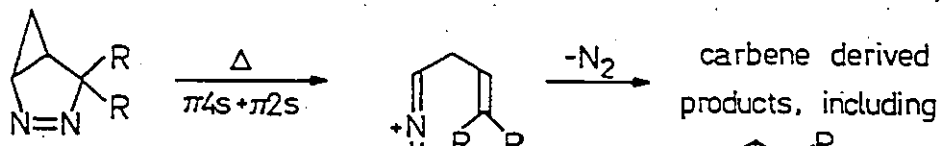

(82) (83)

Diazoalkane intermediates have recently been observed in thermolysis of bicyclopyrazolines (for example, 82, Schneider (1977),[207] Equation I37). In other bicyclic compounds, the experimental findings have been explained by a two stage (not necessarily polar) mechanism, analogous to aforementioned examples, but actual intermediates are far from unequivocally proven.[208,209] Lewis acid catalysis of cyclopropane formation from pyrazolines is known.[210] 3H-Pyrazoles (pyrazolenines; 84) containing a CC double bond are thermally stable,[211] but give cyclopropenes on photolysis[212] via diazoalkane intermediates[213] (Equation I38).

[I38] 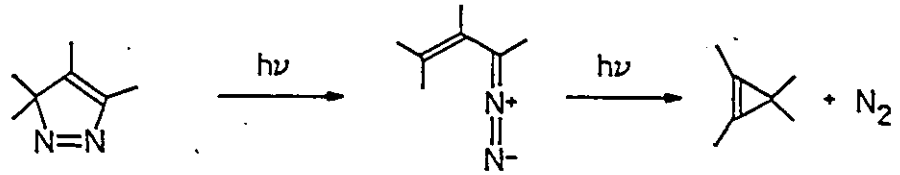

(84) (85)

I2.4 3,4,5,6-Tetrahydropyridazines

In a 1979 study which should be a model of thoroughness to researchers, Dervan compared the 1,4-biradicals formed from 86 and 87 to those generated from the corresponding cyclobutanes.[214] In so doing, he kept phase, temperature, and substitution constant, varying only the mode of 1,4-biradical generation. Carefully comparing the product distributions from the cyclobutanes and the diazenes, he concluded that excess stereospecificity in the decomposition products from 86 in the gas phase at 440°, could be accounted for with a 34% contribution from concerted 2 + 2 + 2 cycloreversion and a 66% contribution from a 1,4-diradical process (Equation I39).

Competition between concerted and biradical decomposition routes elegantly accounts for variations previously noted about the stereospecificity in tetrahydropyridazine decompositions, which declines, for example, in the series 88-90.[215,216] Berson (1974)[216] considered the symmetry and thermodynamic aspects of these fragmentations.

Conceivably, some of the difference in the stereospecificities of diazenes vs cyclobutanes could arise, not from a concerted component, but rather from the intermediacy of a 1,1-diazene (91). In a subsequent paper, Dervan showed that 91 had a somewhat higher excess stereospecificity than 86; 40 to 50% attributable to a concerted decomposition (at 125°, however).[217] Synthetic problems in the 1,1-diazene series are immense (it is not yet possible to generate them

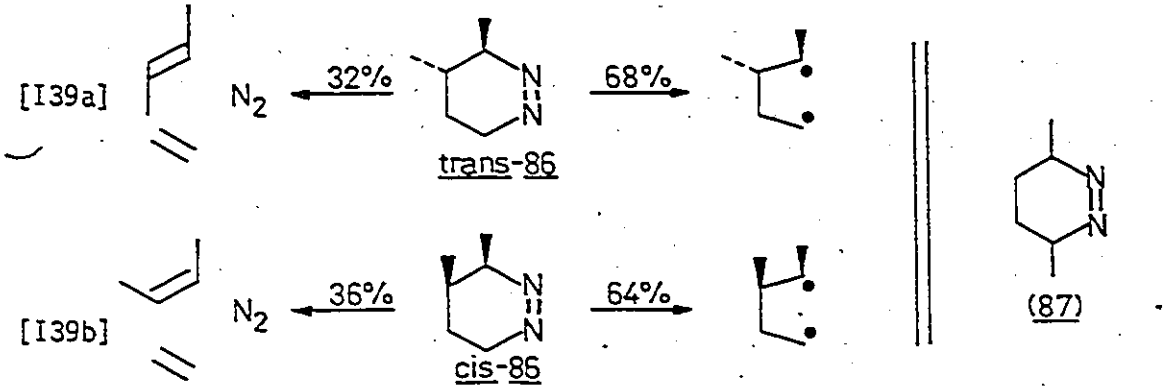
[I39a]
N_2
32%
68%
trans-86
[I39b]
N_2
36%
64%
cis-86
(87)

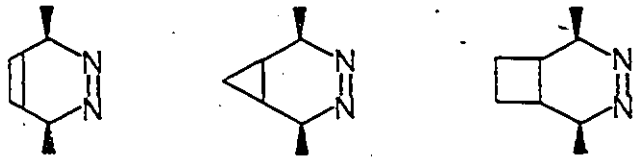
(88)
(89)
(90)

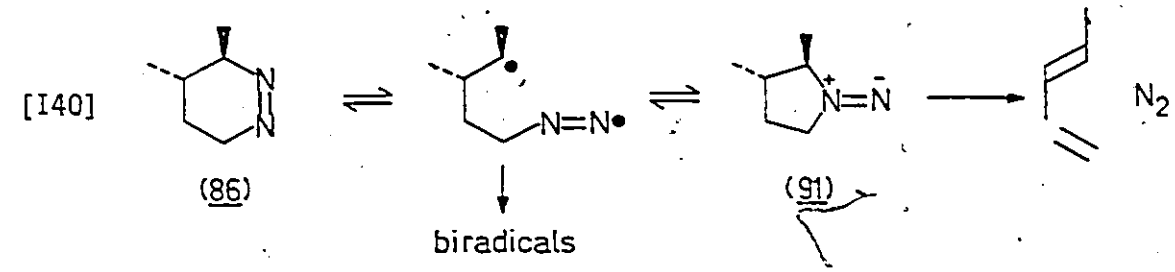
[I40]
(86)
biradicals
(91)
N_2

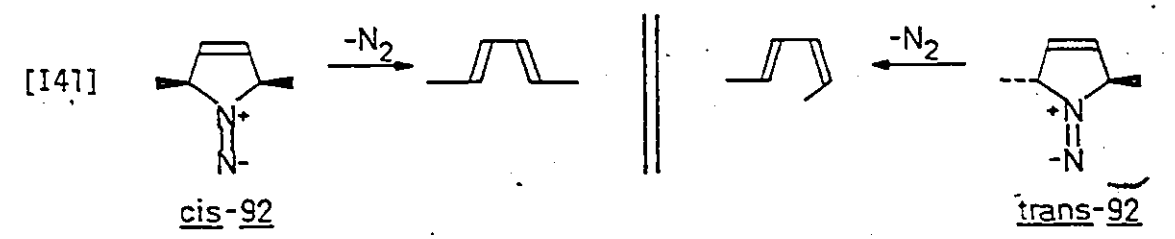
[I41]
$-N_2$
$-N_2$
cis-92
trans-92

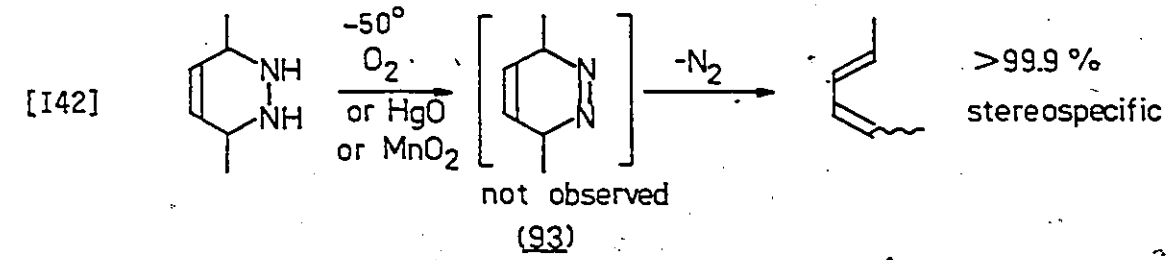
[I42]
-50°
O_2
or HgO
or MnO_2
$-N_2$
>99.9 %
stereospecific
not observed
(93)

by gas phase reactions), but it would further cement Dervan's conclusion about mechanistic duality if the possibility of Equation I40 could be ruled out. Racemization of starting material was not tested for.[214]

Lemal (1966)[218] and Berson (1969)[219] found nitrogen elimination from the isomeric diazenes 92 and 93 to be spontaneous, stereospecific, and disrotatory, as expected from the orbital symmetry rules for concerted reactions (Equations I41 and I42). Kwart and King (1968)[220] have reviewed the retro-Diels-Alder process exemplified by Equation I42 and generally considered to be a model concerted process.

I2.5 Oxadiazolines

The oxadiazoline potential energy surface may be quite complex, as Scheme II demonstrates. Δ^2-1,2,3-Oxadiazolines (94) have been proposed as intermediates in the reaction of ketones with diazoalkanes to produce epoxides or homologous ketones,[65,221] but the cyclized form is not obligatory and has yet to be observed. 1,3-Dipolar cycloaddition of ketones bearing strongly electron withdrawing groups to diazoalkanes provides the isolable Δ^3-1,3,4-isomer (95),[222] which could conceivably lead to the same products. Both the reactivity (due to the lower energy of the carbonyl LUMO) and regiospecificity (Δ^3-1,3,4- rather than Δ^2-1,2,3-isomer) are predicted by Frontier Molecular Orbital Theory for a concerted cycloaddition.[42-50]

1,3-Dipolar cycloreversion of 95 could lead to either or both of two possible pairs of ketone and diazoalkane products. If this

Scheme II

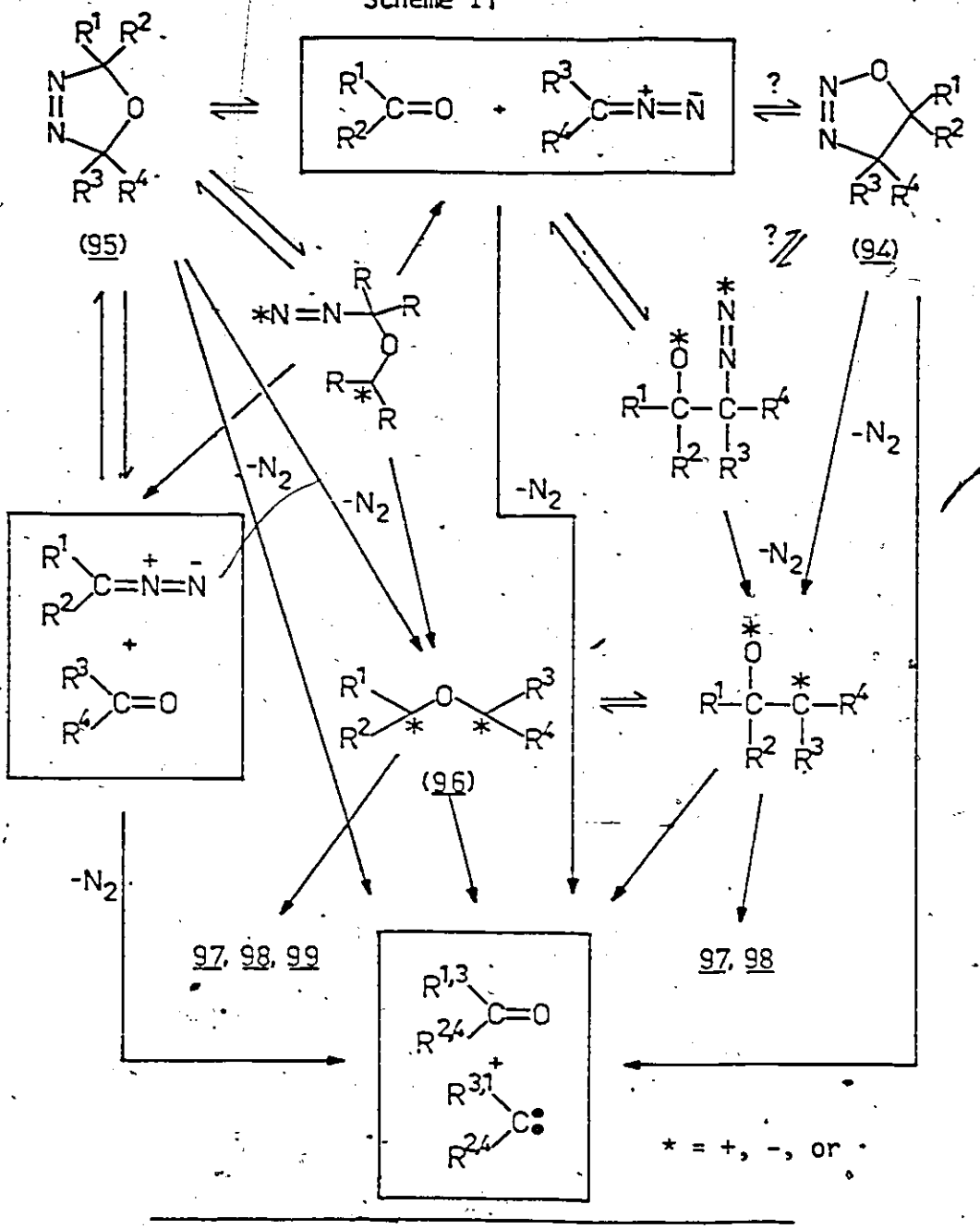

(95) (94) (96)

(97) (98) (99)

were reversible, effective carbonyl exchange could occur, as is known for the reaction between thiocarbonyls and diazoalkanes, through a Δ^3-1,3,4-thiadiazoline.[223] On the other hand, pyrazoline-like nitrogen extrusion from 95 via either a concerted or stepwise process leads to an intermediate 96 capable of forming the two types of observed carbonyl products or closing to an epoxide (Scheme II). The dipolar electron distribution in intermediate 96 will be determined by the substituents, their geometry, and perhaps the solvent. When all four R groups are identical, 96 might be a diradical. Biradicals and zwitterion intermediates are not necessarily resonance structures for the same thing if geometry is different at the terminal carbons (for example, a diradical might have pyramidal carbons whereas a zwitterion might have sp^2 carbons).

The whole issues of diradical vs zwitterionic character or stepwise mechanism vs flat concerted potential energy surface are (disappointingly) largely philosophical. This matter has been approached by, among others,[224] Salem (1972)[225], Huisgen (1977)[226], Dewar (1971-78)[227-229], and Hoffmann (1970)[230] with respect to a number of reactions. No arguments are particularly satisfying, reflecting a major weakness in the way chemists look at molecular processes, one which will likely persist until a revolutionary conceptual breakthrough.

Only meagre information is available on the Δ^3-1,3,4-oxadiazoline ring system. Although product distributions are available for thermolysis of some systems, Scheme II renders mechanistic inference from product studies unreliable because all mechanisms potentially lead to the

same products.

Hoffmann (1978)[231] found 2-acetoxyoxadiazolines (100) to be thermally unstable, forming epoxyacetates via a trappable intermediate (Equation I43). Photochemically, carbene was obtained when C5 was spirocyclohexyl, but epoxide when C5 was methyl and phenyl substituted.

[I43]

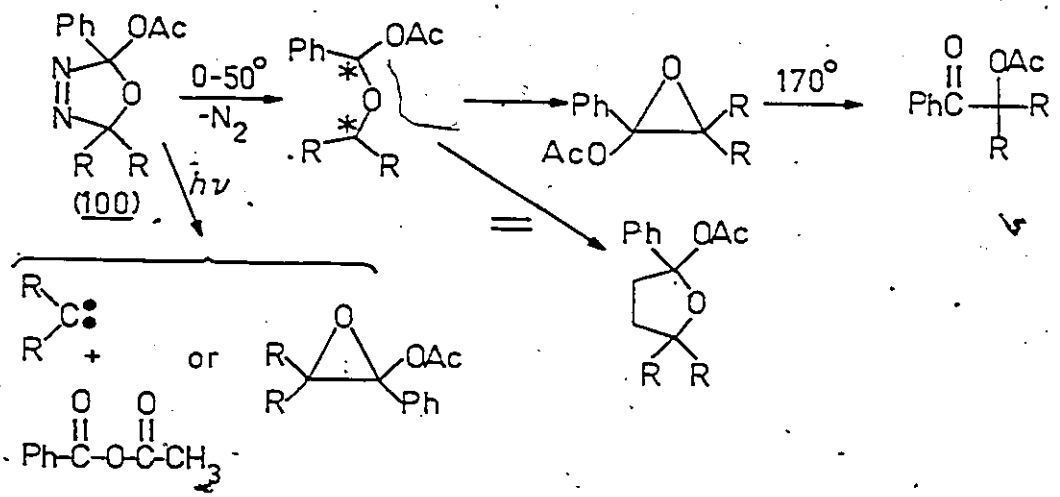

A 1972 kinetic study by Kellog[232] on symmetrically substituted Δ^3-1,3,4-thiadiazoline thermolyses to thioepoxides demonstrated that the reaction was unimolecular, with $\Delta H^{\ddagger}$ in the range 26-30 kcal mol^{-1} and $\Delta S^{\ddagger}$ = 6 ± 4 eu. The activation energy for tetramethyl-Δ^3-1,3,4-thiadiazoline was 11 kcal lower than that for the corresponding pyrazoline, reflecting significant sulfur stabilization at the transition state comparable to that of a β-sulfur atom in acyclic systems.[114] A thiocarbonyl ylide was also intercepted.

Michejda (1968)[233] found the course of thermolysis of 2-methylene-oxadiazoline (101) to proceed differently (Equation I44). In the

presence of dimethylfumarate or maleate trap, diazoalkane was converted to the cyclopropane in unmentioned yield. Other products were not determined.

[I44]

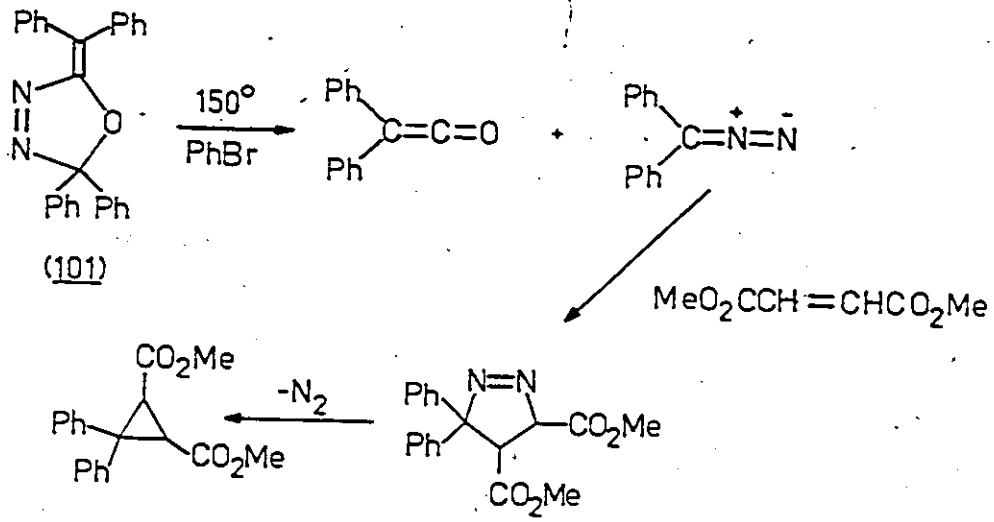

(101)

In work by Yeung, MacAlpine, and Warkentin (1978)[234] originating from this laboratory, a series of 2-acetoxy-Δ^3-1,3,4-oxadiazolines was investigated. In addition to epoxide and acetoxy ketone anticipated from Scheme II, these workers found a significant amount of enol ether (103) to be formed in some cases where intramolecular hydrogen transfer was possible (Equation I45).

[I45]

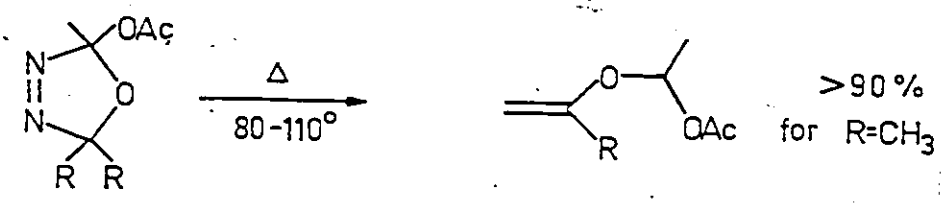

(102) (103)

To obtain similar first order decomposition rates, phenyl substitution at C2 lowered the decomposition temperature by 50° (no activation parameters determined). Only a 6.5% yield of trapping product was obtained with acrylonitrile. There was no primary

deuterium kinetic isotope effect on ether formation, ruling out an allowed concerted mechanism via a bicyclo[2.2.1] transition state. Trimethylacetoxyoxadiazoline decomposed more slowly in nitrobenzene than in benzene ($k(PhNO_2) = 0.85\ k(PhH)$; corresponding to a 2 point log k vs E_T plot with slope - 0.006), ruling out bond heterolysis. Ring size effects on thermolysis rates of 102 where R,R = 4-,5-,6-, and 8-membered ring were negligible: the rate ratios at 110° were 2:4:1:13 respectively. When these values are compared to either the cis- or trans-diazenes 104, where rate factors of 450,000 (n = 5 to 8) for the cis-isomers and 30,000 (n = 4 to 8) or 100 (n = 5 to 8) for the trans-isomers are found,[235] it would certainly appear that oxadiazolines do not rupture the N4-C5 bond in the rate limiting step.

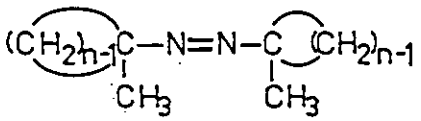

(104)

To explain these diverse observations, Warkentin proposed the mechanism of Equation I46, where competition between k_2 (ether formation) and k_3 (nitrogen loss) from a diazenyldiradical intermediate 105 accounts for the variation in product yields. Ether formation rate k_2 will depend on the ability of the abstracting site, and 105: R = CH_3 is expected to be more reactive than the relatively stable 105: R = Ph, which corresponds to a benzylic site. At the same, nitrogen loss (k_3) should be substituent insensitive, and since closure proceeds without activation, $k_4 >> k_5$, the k_3 route preferentially

[I46]

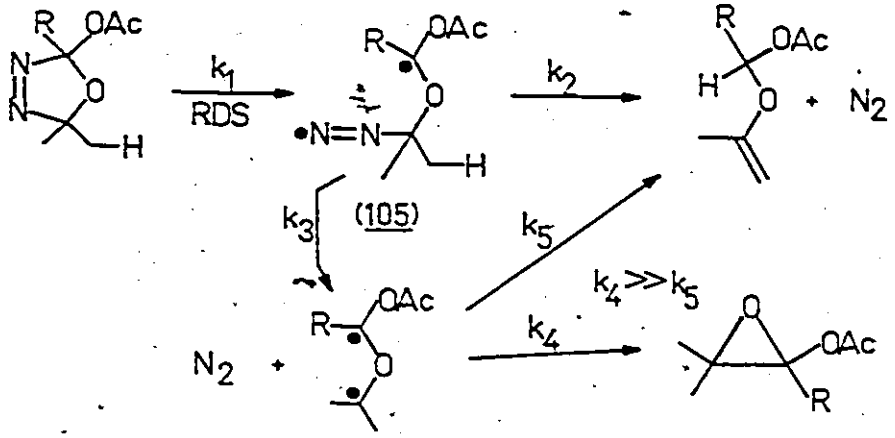

[I47]

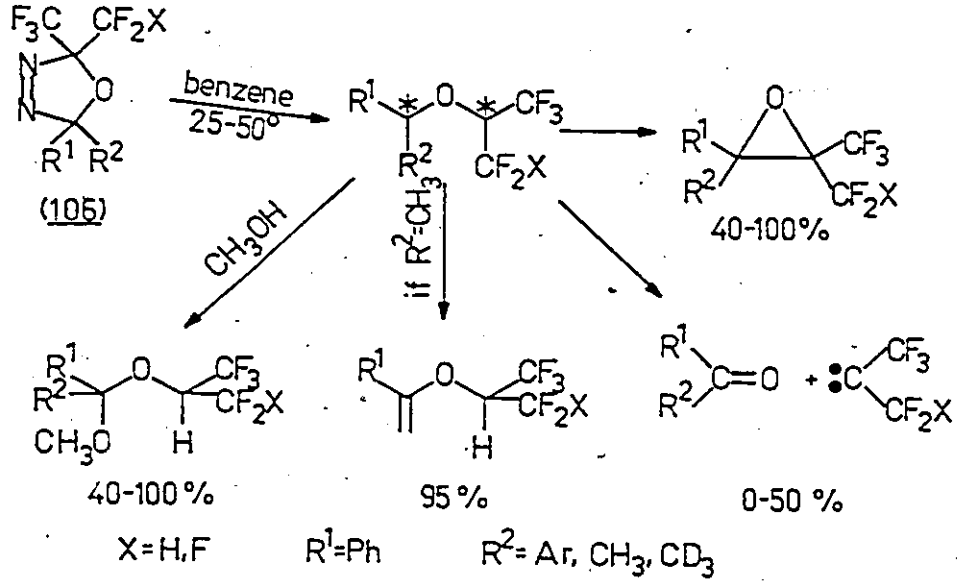

[I48]

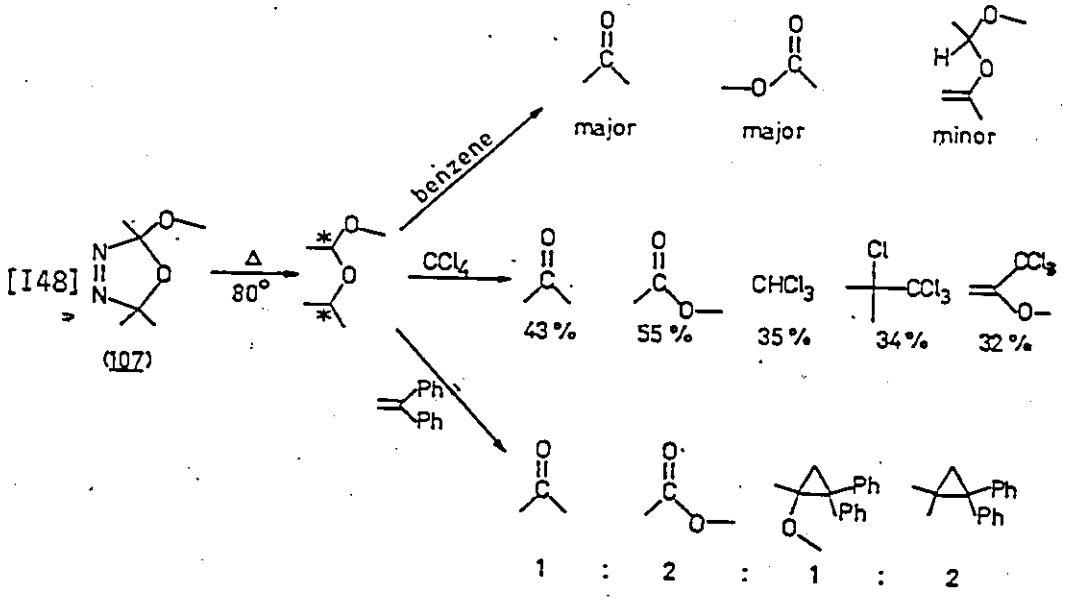

leads to epoxide. In the context of Equation I46, C2 phenyl substituted acetoxyoxadiazolines have a retarded k_2 and decompose via k_1k_3, whereas k_2 dominates for C2 methyl substituted cases.

Bartlett (1978)[222] reported the decomposition of Δ^3-1,3,4-oxadiazolines obtained by cycloaddition of diazoalkanes to highly fluorinated acetones, implicating carbonyl ylides as intermediates in epoxide, ketone, enol, and trapped products (Equation I47). For a given compound , epoxide yields were increased by 20% by lowering the decomposition temperature 25°, suggesting a common intermediate for all products. A linear Hammett plot was obtained for p-substituted 106: R_2 = Ar, with ρ = -0.50 against σ^+. For 106: $R^1 = R^2$ = Ph, solvent had little effect on the rate difference between benzene and methanol (ΔE_T = 21 kcal mol^{-1}; 3 solvents, no correlation).

The small Hammett rho and unimportant solvent effects were taken to correspond to concerted nitrogen elimination,[222] but any non-polar intermediate would be consistent with the observations. Replacing $R^2 = CH_3$ with R^2 = Ph in 106 lowers the decomposition temperature about 10-15°, rather a small effect compared to the trans-azoalkane series where a 10 kcal stabilization is typical.[114] In the fluorinated fragment, an extra fluorine atom elevates decomposition temperature by 20-25° (a destabilizing effect).

Very recent work from this laboratory by Bekhazi and Warkentin (1979)[236] on 2-methoxy-Δ^3-1,3,4-oxadiazolines (107) shows that carbonyl containing fragments predominate (Equation I48). Trapping experiments with 1,1-diphenylethylene and CCl_4 solvents implicate carbene intermediates. No epoxide or azine (bimolecular product from

diazoalkane expected at these temperatures) is observed, apparently ruling out a retro-1,3-dipolar cycloaddition mechanism.

In summary, a plethora of reasonable intermediates and identity crises amongst them with regard to their biradical, zwitterionic, dipolar, or nitrogenous character make research results in this field somewhat confusing to interpret. It is not yet clear how many unique rate-determining steps exist to convert Δ^3-1,3,4-oxadiazolines to products.

I2.6 Cyclic α-Carbonyldiazenes

The select few α-carbonyl azo compounds which have been studied are very very reactive dienophiles, and this reactivity has thwarted thermal fragmentation studies because many of these compounds self react bimolecularly. Obviously some high dilution kinetic and product studies need to be done in order to observe potential multipiece fragmentations.

Kealy (1962)[237] and Clement (1962)[238] have examined the emerald green diazaquinones 108. Even at -78° they react with dienes. In the absence of such traps, gas evolution begins around -30°, producing 109 to 111 (Equation I49). The yield of 110 increases to 85% on intentional addition of water. If the C4C5 double bond is absent, no dimer or polymer (109) is obtained, possibly suggesting that 109 arises by N_2 extrusion in a retro-Diels-Alder to a diketene (112) which is rapidly trapped by the best dienophile known: more starting material. In the dihydro case, the first step of Equation I49 corresponds to a 3-piece fragmentation to two ketenes plus nitrogen, and dimerization would be impossible.

[I49]

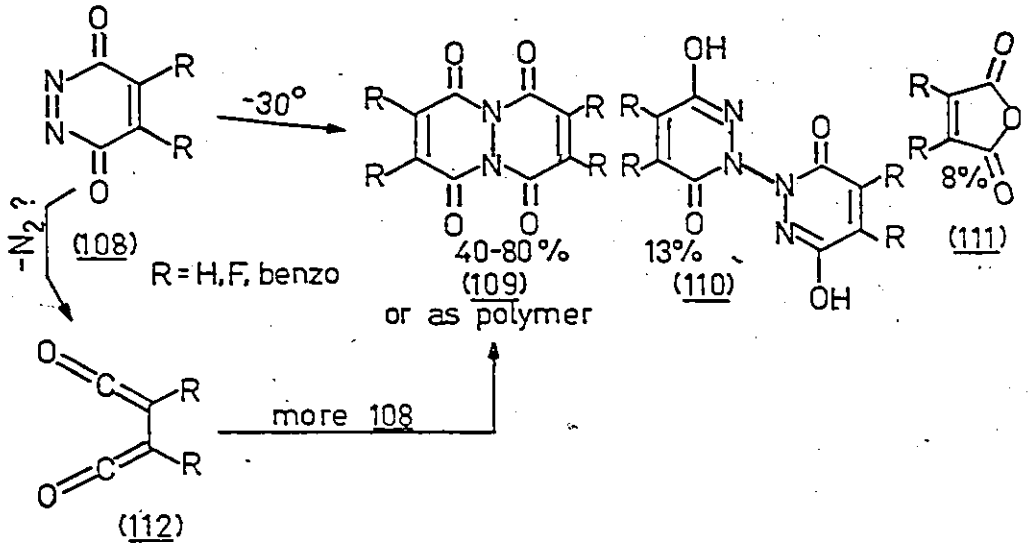

[I50]

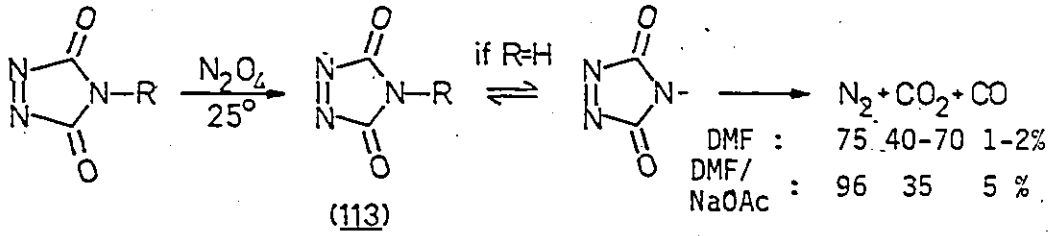

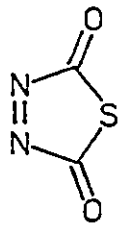

(114)

[I51]

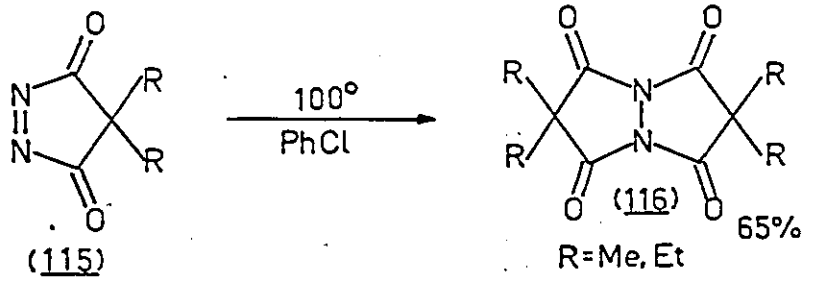

4-Phenyltriazolinedione 113: R = Ph is reasonably stable in the absence of light or water but decomposes "instantly" in alkali, but more slowly in acid, water, or alcohol.[239] The isolated carmine red solid decomposes at 160-180° but solutions containing it are unstable at room temperature (products not mentioned). This too, is a most reactive dienophile.

Other N-substituted derivatives have been prepared (and isolated) to test their dienophilic activity.[240] In the absence of dienes, unsubstituted 113 appears to show acid-base equilibrium and conditions-dependent decomposition products (Equation I50).[241] Decomposition is accelerated by water and acids — substances which are difficult to exclude in in situ preparations — making it difficult to separate thermal from hydrolytic decomposition.

Corey (1973)[242] found thiadiazolinedione 114 to be a moderately reactive dienophile which also decomposes to unnamed products. Pyrazolinedione 115 is reasonably stable in the absence of water, acids, or preparative oxidizing agent,[243,244] but gave a reasonable yield of bimolecular adduct 116 on heating in chlorobenzene.[243] The authors admitted several possible mechanisms for formation of 116, involving adventitious acid catalysis, bimolecular nucleophilic attack, or trapping of a nitrogen-free intermediate.[243] As is usual, product studies alone could not distinguish these possibilities for Equation I51.

Unsaturated monocarbonyl azocycles are also available in a few instances. For example, 117 (Equation I52) is a highly coloured transitory intermediate observed in oxidations of the corresponding

[I52] 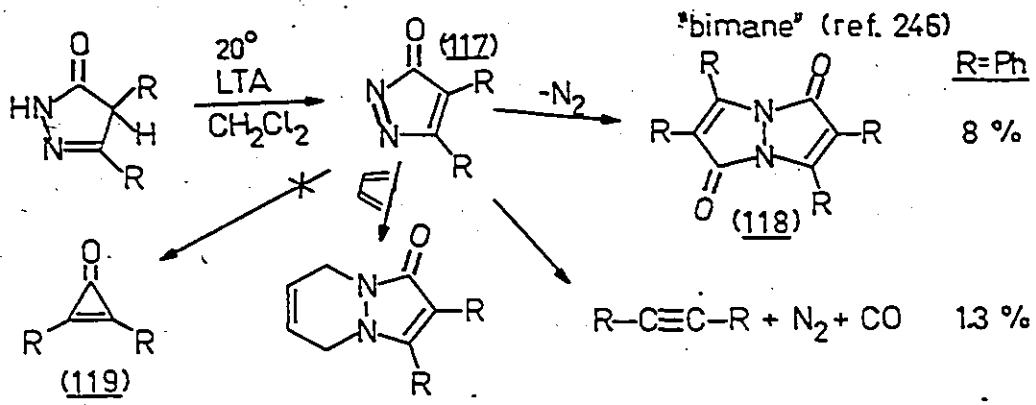

[I53] 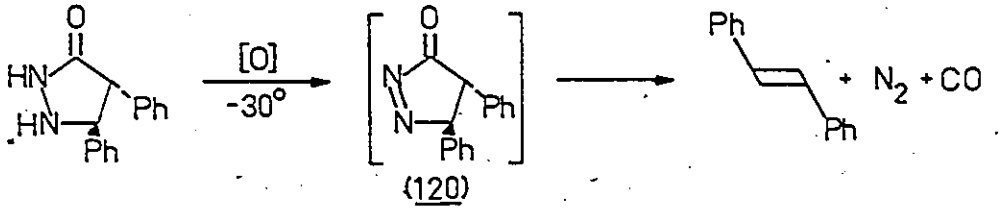

[I54] 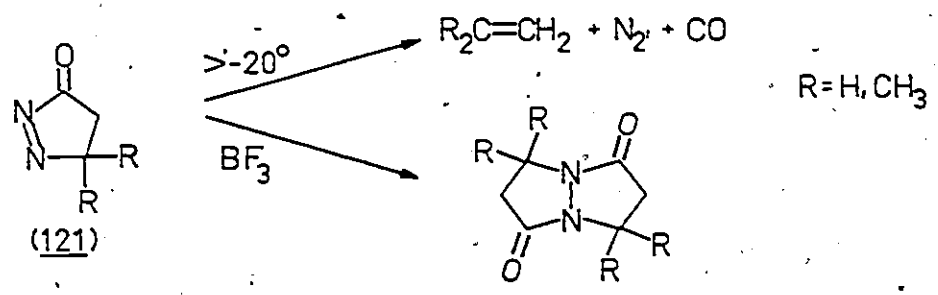

[I55] 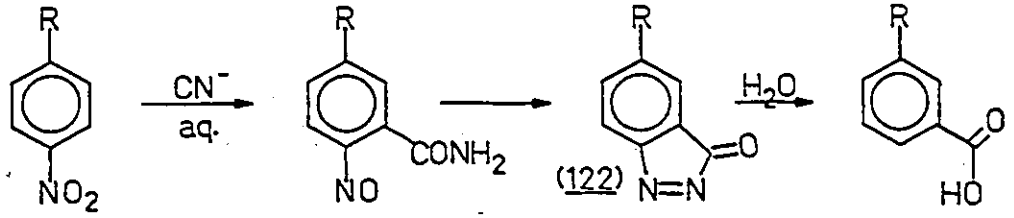

[I56] 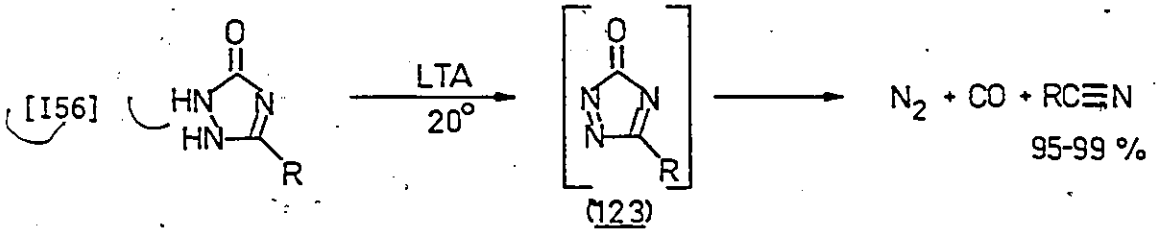

heterocycles, which reacts rapidly with dienes. Decomposition in the absence of a diene trap leads to unidentifiable solids without gas evolution.[245]

Rees (1973)[247] found that thermal decomposition of 117: R = Ph (Equation I52) at room temperature in the presence of lead tetraacetate (LTA) gave a complex product mixture of which 3-piece fragmentation accounted for 1.3% and bimane 118 formation 8%. The known-to-be-stable diphenylcyclopropenone (119) which might result from a pyrazoline-like decomposition was not detected, and control experiments showed that 119 + 117 did not give 118.

Whereas 117 is a potent dienophile, stable and observable at -10°, the carbon saturated analogue 120 is not, preferentially fragmenting stereospecifically into three stable molecules, even at -30° (Equation I53)[241,245-248]. Nagata and Kamata (1970)[160] isolated crystalline 121 at -78° and warmed to -20° to liberate nitrogen, carbon monoxide and olefin in quantitative yield, sometimes explosively. They also found BF_3 to catalyse bimolecular processes (Equation I54).

Benzopyrazolinone 122: R = H was isolated by Ullman and Bartkus (1962)[249]. It was reasonably stable, but polymerized on warming, without gas evolution. Uv irradiation also had no effect. These and other workers have shown 122 to be an intermediate in the von Richter reaction (Equation I55)[249-251].

Gillis (1971)[252] noted that triazolinones 123 underwent 3-piece fragmentation to nitrogen, carbon monoxide, and nitrile in high yields (Equation I56). Some could be trapped with dienes but others (5-methyl or 5-benzyl) fragmented too rapidly to be intercepted.

[I 57] 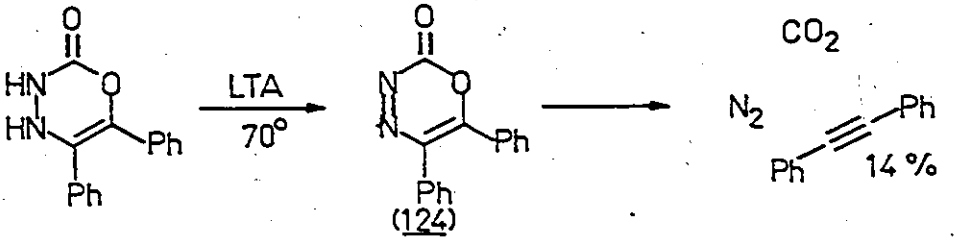

[I58] 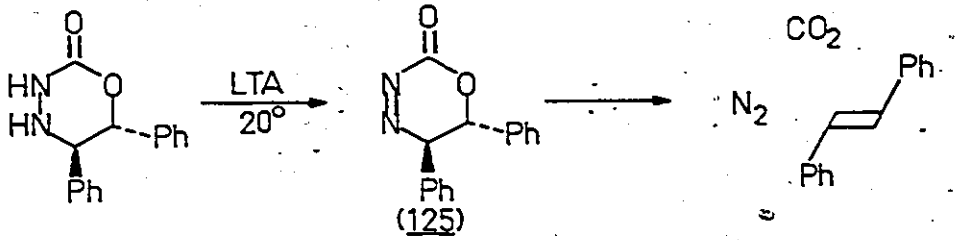

[I59] 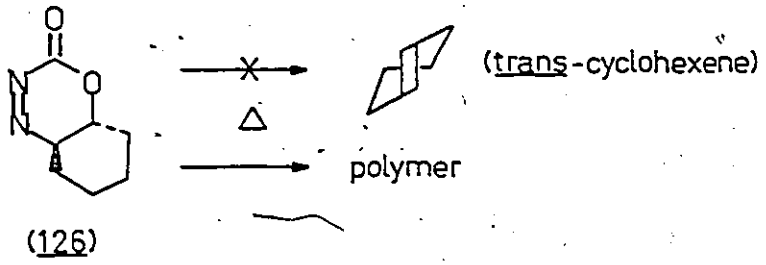

[I60] 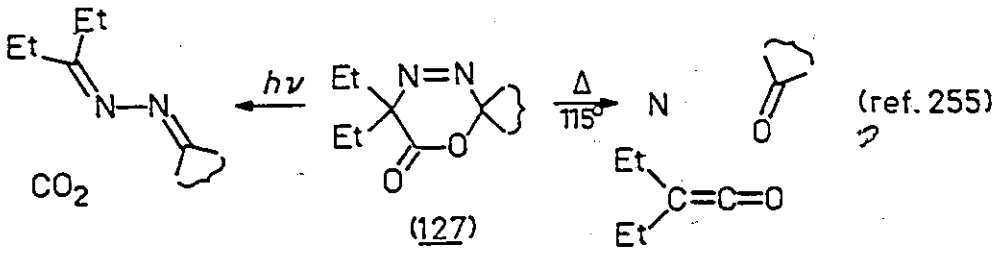

[I61] 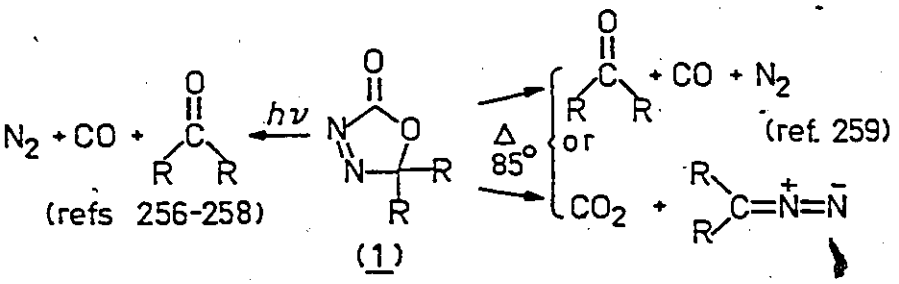

Six-membered ring azo carboxylates 124 and 125 also undergo thermal 3-piece fragmentation, retaining stereochemistry in the latter case (Equations I57 - I59).[253] The stability series 126> 124>125 reflects the stability of the organic fragment, perhaps implicating a concerted mechanism.[254]

Finally, it is interesting to compare the thermo- and photochemistry of the steroidal derivative I27 to the corresponding chemistry of Δ^3-1,3,4-oxadiazolin-2-ones (1) (Equations I60 and I61). The only other research group in the world to have published work on Δ^3-1,3,4-oxadiazolinones, Meier (1976-77)[256-258] has examined their photochemistry. Since these compounds photolyse only via 3-piece ketone formation, the photochemical reaction is of negligible significance to their synthetic potential as diazoalkane precursors.

I2.7 Molecules from the Warkentin Laboratory

From the Warkentin Laboratory, the remaining few examples complete the meagre kinetic data which was available on these 2- or 3-piece fragmentations prior to the work reported in this thesis. Even with this information, mechanistic inferences are still tenuous, and it was hoped that the present study could be more convincing.

With Warkentin, West (1967)[260,261] unravelled the competetive unimolecular thermolyses of 5,5-diaryl-2-phenylimino-Δ^3-1,3,4-oxadiazolines (128) in chlorobenzene at 104° (Equation I62). They found the 1,3-dipolar cycloreversion component, k_2, to be favoured by electron donating substituents, increasing from 15% for X = Cl to >95% for X = OMe, compared to the 3-piece fragmentation. For the former process, a ρ^+value of -1.3 ± 0.1 (using a 50/50 mixture of σ and

$\sigma^+)^*$ indicated a buildup of positive charge in the transition state. On the other hand, a rather less significant ρ value of +0.6 indicated a nonpolar transition state for the latter process. Zwitterionic intermediates were ruled out for both reactions, and, although it was obvious from the ρ values that bonds involving C5 were broken in the rate-determining step, no choice between concerted or biradical mechanisms could be made. As a consequence of the major experimental effort required to extract individual rate constants for the two processes from the complex mixture of primary and subsequent reactions, West did not investigate substituent effects across the ring in the 2-phenylimino group.

[I62]

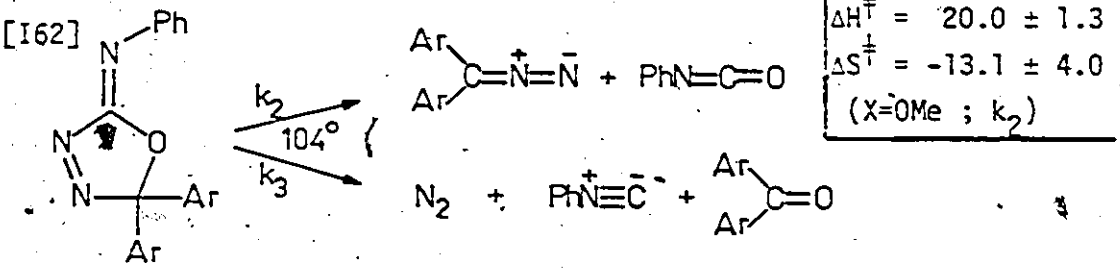

(128) Ar =  ; X = H, CH_3, Cl, OCH_3

[I63]

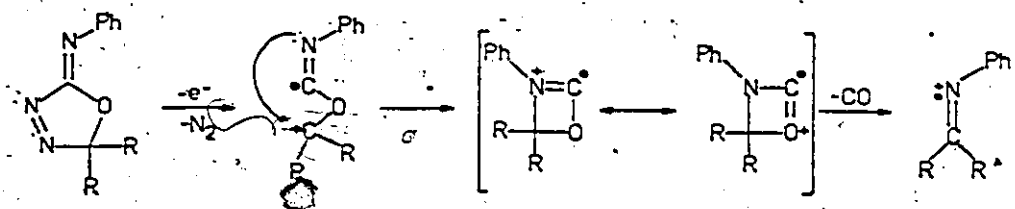

(128) M-28 M-56

*The two phenyl groups could never be coplanar, so it seems reasonable that one conjugates directly to the developing charge, while the other can only act inductively.

This work was attempted by Cameron (1972)[262]. She, however, made a very serious mistake in the kinetic analysis: "The rate constant k_2 was determined by following the production of aryl isocyanate. The rate constant [k_3] was determined by following the rate of production of benzophenone." (ref 262, p 66). In fact (as is proven in Appendix 2), the "rate constants" for appearance of each product from competitive first order reactions should be identical to each other and numerically equal to the sum $k_T = k_2 + k_3$. That Cameron did not realize this necessary identity is a testament to large and unnoticed experimental error in her single-run kinetics. Frustratingly, the original laboratory notebooks are in such disarray that it proved impossible to find all the necessary original data on which to perform a correct kinetic analysis.

Because this error was not realized until 1978, this particular research project has not been redirected toward redoing the erroneous work of Cameron. It should be reinvestigated, however, as this system offers a unique opportunity to probe bonding changes at both positions 2 and 5 and therefore to construct a reasonably complete picture of the transition states for both the 2-piece and 3-piece fragmentations.

As part of structural proofs for his novel compounds, West obtained high and low eV mass spectra. These showed major fragmentation pathways corresponding to both thermal reactions. At 11 eV ionizing voltage both molecular ion and M-28 daughter were uniquely obtained for 128; R = CH_3. These ions were absent in high voltage spectra, but M - 56 ions were prominent for all compounds at both voltages.

These ions were assigned to loss of N_2, then CO, via Equation I63. Turro (1965)[263] has noted correlations between ms processes (especially at low voltage) and photochemical decomposition.

In the same vein, Ramakrishnan, Warkentin and Fulton (1975, 1976, 1978)[264-266] reported syntheses of some interesting heterocycles (130) which were shown to arise from further reaction between the primary fragments, 2-diazopropane and an N-isocyanatoimine (129), formed by a 2-piece process in chlorobenzene at 130° (Equation I64). A single kinetic experiment (pmr) showed the reaction to be first order. No mass balance was reported. Tars were common and 3-piece fragmentation product ketone was never mentioned.

[I64]

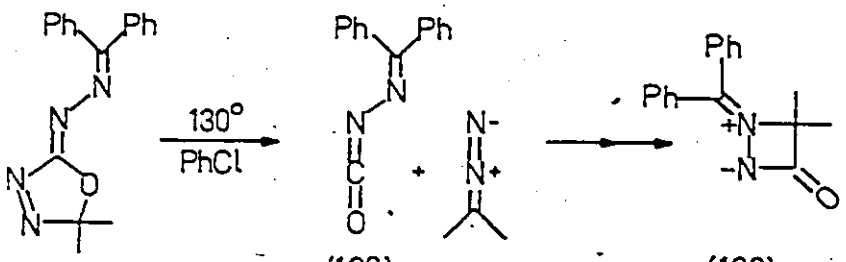

(129) (130)

In a series of beautiful kinetic studies in 1977, Cabelkova-Taguchi[267] examined 3-piece fragmentation of three triazolines 131 (Equation I65). Complementing the very precise activation parameters and solvent polarity responses appearing with Equation I65, she found the Hammett rho value to be a negligible -0.17 ± 0.02 for N4-phenyl substitution of 131: X = O. The kinetic experimental results (particularly the activation entropies) were taken to suggest that thermal decomposition of the triazolinone (131: X = O) is a stepwise process involving initial homolytic bond cleavage, most probably of the N1C5 bond, while triazoline (131: X = NPh) and triazolinethione (131: X = S)

may decompose via a concerted reaction. In support of her conclusion, she cited the presence of an N_2CO fragment in the mass spectrum of the triazolinone (calculated mass 56.0056, observed mass 56.0077), whereas the thione showed no corresponding N_2CS fragment.

[I65]

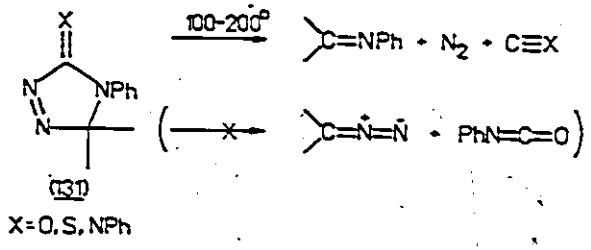

(131)

X	$\Delta H^{\ddagger}$	$\Delta S^{\ddagger}$	slope of E_T plot
O	35	6-8	-0.048
S	33	0	-0.038
NPh	28	0-2	-0.045

[I66]

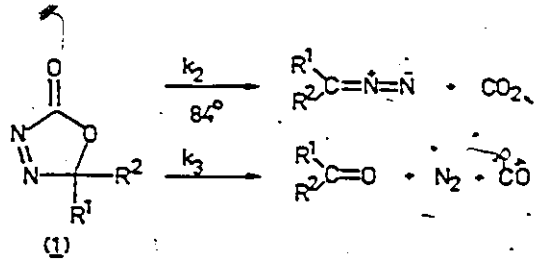

(1)

for $R^1=R^2=CH_3$

Solvent:	CCl_4	MeOH
$10^4k_2/s^{-1}$:	0.22	4.0
$10^4k_3/s^{-1}$:	0.87	0.88

The final piece of background information pertaining to thermolysis of these heterocyclic compounds is a preliminary kinetic study of the molecule of major interest in this thesis: dimethyloxadiazolinone (1-Me_2). In 1972 Lee, Cameron, and Warkentin[259] demonstrated that both 2-piece and 3-piece unimolecular fragmentation pathways are available to this molecule (Equation I66). Ketone formation (k_3) was found to proceed at the same rate in methanol and carbon tetrachloride, whereas diazoalkane formation (k_2) was accelerated by a factor of 20 in more polar methanol, suggesting a polar, if not zwitterionic, transition state for the k_2 process. At

that time, the authors mentioned the desirability of measuring the C2 carbon isotope effect for each process to determine the degree of C2—N3 or O1—C2 bond rupture at the transition state. This could most easily be done for the k_2 process which released CO_2.

I2.8 Concluding Remarks

Generalizing is far from easy. Solution and gas phase results are simultaneously very similar and widely divergent. A comprehensive mechanism covering all cyclic azo compounds is not yet available. At the very least, asymmetric transition states are implicated for unsymmetric trans-isomers, although even very unsymmetrical pyrazolines appear to have equal CN rupture at the transition state. Compelling evidence exists only for metastable phenyldiazenyl radical intermediates from aralkyldiazenes — the situation for dialkyldiazenes is more ambiguous. Thermolyses of cis and trans isomers are similar in gross features ($\Delta H^{\ddagger}$, $\Delta S^{\ddagger}$, substituent effects, CIDNP, etc.), although the former are more labile and solvent sensitive. On the other hand, aspects of azocarbonyl thermolyses suggest the possibility of multibond fragmentations. Conformational effects may be important for cyclic materials. To varying degrees, stepwise bond ruptures, bond rotations, and closure are all competitive, contributing to the intricacy.

Inconsistency is commonplace in the chemical literature and few comprehensive mechanistic investigations have been directed toward unanswered (even unposed) questions. Three potentially uniting

possibilities which allow for the high variability of experimental outcome emerge from this study. To distinguish among them by experimental means will be a most demanding task.

Following Pryor,[126] all solution reactions could proceed via a reversible multistep mechanism in which every step was very fast. Even simple bond rotations would have to be included in a kinetic scheme more complex than Equation I8 (page 15). Thus, if the steps respond unequally to changes in solvent, temperature, substituent, or isotope, the overall rate constant (represented as a complex function of individual rate constants) would not be expected to behave predictably. Reversible ring opening in the gas phase could be incorporated into this model, but further extension to acyclic diazenes in the gas phase is not so easy. A variable transition state crossing coefficient (usually assumed to be unity) could achieve the same result for the latter case. Hardly sacrosanct, perhaps transition state theory itself is at fault.

Mechanistic duality (or plurality) constitutes a second conceivable approach to unifying the data. Firestone finds concerted and biradical pathways to 1,3-dipolar cycloaddition and Diels-Alder reactions to be degenerate or nearly so, and perhaps reasonably in competition.[68-70] Dervan's work on tetrahydropyridazines[214,217] also gives credence to the notion. Perhaps both one- and two-bond cleavage do occur together in the same system, but in different amounts which depend on numerous factors.

Rather than a dissectible blend of discrete, identifiable mechanisms for two competing processes, Zimmerman[110] takes the third

view, considering the potential energy surface as a whole. A relatively flat surface in the vicinity of the transition state, which has ill-defined minima for biradical intermediates or conformations, could be anticipated when concerted and stepwise energetics were similar. Wide ranging motion over such a surface might be subject to random "leaks" to side products or enantiomeric starting material, or to products of alternate stereochemistry. The probability of each "leak" depends on the instantaneous geometry of the reactant molecule as it enters the plateau region and on its initial trajectory. In this context, any net stereochemical outcome from retention to inversion may be simply regarded as a manifestation of the type, number, and probability of molecular peregrinations on the plateau portion of the surface. Furthermore, the final outcome could be critically dependent on such rather subtle changes to the surface by solvent, substituent, isotope, or pressure. Increased temperature or photochemical reactions would increase any "leakiness" and modify trajectory momenta, possibly even favouring different trajectories.

Whereas the first two hypotheses might yield to dedicated experimentation and careful breakdown of rate constants, the last one cannot. Testing the third model is predicated on galloping advances in theoretical chemistry, but it may nonetheless function as a useful, qualitative way to accept diverse trends in apparent transition state structure for a wide variety of loosely related diazene decompositions. At the present time, all three of these uniting themes are no more than that.

I3 Hydrolysis of Diazene Carbonyls

An adjacent strongly electron withdrawing azo function activates a carbonyl group toward nucleophilic attack. Whereas azoacyls characteristically leave the NN—CO bond, ejecting R—N=N$^-$ as a reasonable leaving group (pK_a(RN=NH) is perhaps 18-20)[268], azocarboxylates preferentially shed alkoxide (pK_a(ROH) ~ 15-16)[269], retaining the azo function. Significant amounts of N-substituted products invariably accompanying hydrolytic conditions have often been ascribed to 1,4-nucleophilic attack, but this author is of the opinion that product studies alone do not discriminate amongst potential radical, radical ion, or nucleophilic mechanisms. For background on these purported cases of nucleophilic attack on azo nitrogen, interested readers are referred to the review of Fahr and Lind (1966)[270], to introductions to theses of Pechhold (1968)[171] and Knittel (1975)[166], and to the Patai monograph (1975)[272].

I3.1 Acyldiazenes

Stolle (1929)[140] reported the stoichiometry of decomposition of azodiacyls 40 in water (Equation I67). It is tempting to view this as a radical chain process where the liberated acyl radicals are trapped by the starting material which then abstracts a hydroxyl hydrogen from hydrate 132 to carry the chain.

During the 1960's, Hoffmann[273-275], and Fraenkel and Pechhold[271,276] subjected monobenzoyl diazenes 133 to alcoholic base, concluding that

[I67]

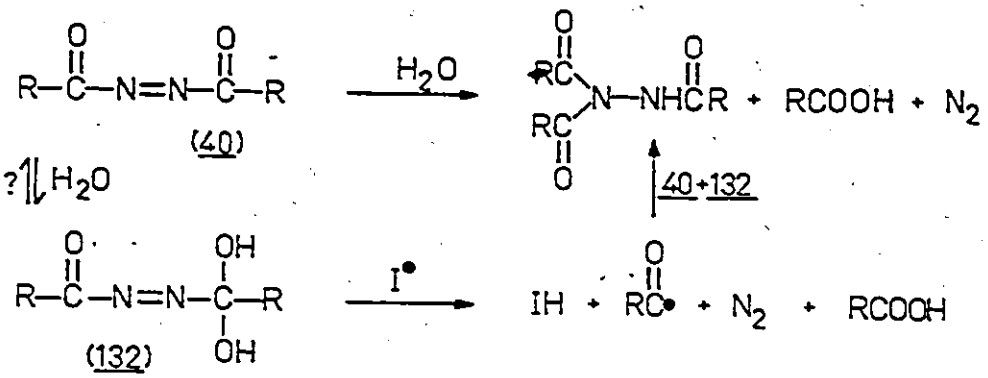

[I68]

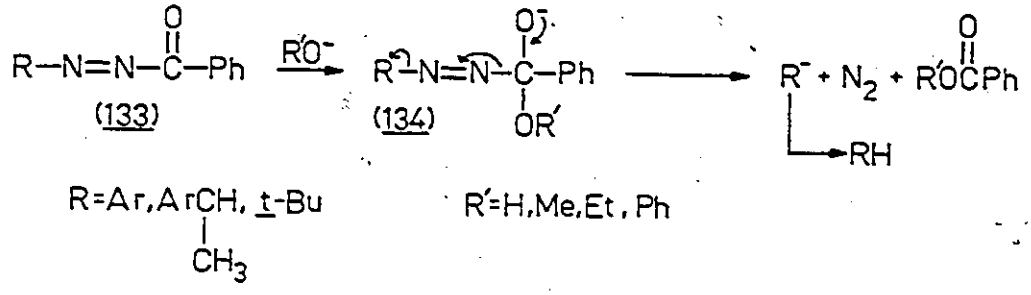

[I69]

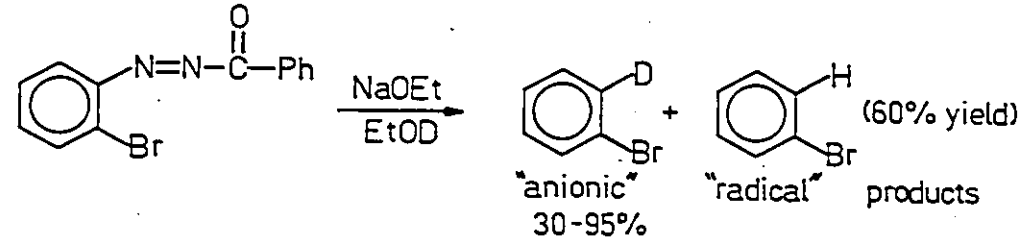

[I70]

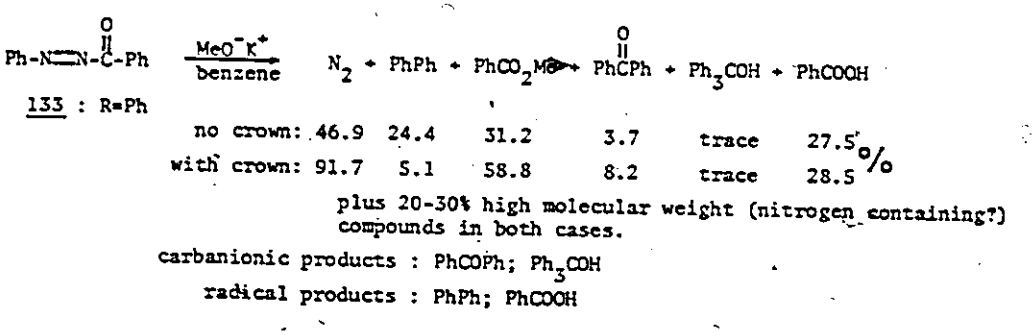

the products arose from cleavage of the tetrahedral intermediates 134 to alkyl or aryl anions (Equation I68). In support of an anionic component to this process, decompositions performed in deuterated ethanol are illuminating. Urry (1954)[277] had shown that anions accept the hydroxyl proton from alcohols whereas radicals always abstract an α-hydrogen atom. When Hoffmann decomposed alkyl- and arylbenzoyldiazenes with sodium ethoxide in OD labelled ethanol, he found an increasing proportion of deuterium incorporation in the hydrocarbon product as the base concentration was increased (Equation I69). In the light of the hydroxyl hydrogen abstraction chain reaction mechanism convincingly demonstrated by Warkentin, Knittel, and Yeung (refs. 166-170; discussed in Section II.5), and the probable intervention of RN=NH(D), the assumption that deuterated material arises only from an anionic process is tenuous.

Base catalysis in the absence of a proton source was investigated by Fraenkel and Pechhold (1968)[271,276] in benzene and benzene/crown ether (Equation I70). Formation of benzoic acid involves loss of a methyl group from the mass balance. It could be in the unidentified high molecular weight material. Benzoic acid yield increases to 60% in the presence of oxygen. While these authors maintain that nitrogen containing products arise from 1,4-nucleophilic attack, this is not necessarily so. Cohen (1965)[278] found the radical path to be preferred when oxidizing agents were present. If so, any anion could be oxidized to a radical, perhaps even by the azocarbonyl itself.

To briefly pursue this point, it is known that azobenzene and azocarboxylates even better, efficiently oxidize mercaptans, hydroxylamines, alcohols, and hydrazines (typical "nucleophiles") to the corresponding disulfides, nitroso, carbonyl, and azo compounds respectively.[272] Radical nature in these oxidations has yet to be conclusively demonstrated, however, hydrogen atom (or electron) transfers are logical processes envisaged to lead to radical (or radical ion) intermediates. Diacyldiazenes and diazenedicarboxylate esters also react thermally or photochemically with alkylbenzenes, esters, ketones, and tertiary amines to yield nitrogen substituted adducts.[270,272] In these cases, reaction is assisted by free radical initiators and products are consistent with a process whereby α-hydrogen abstraction from the substrate is followed by addition of resulting radicals to the N=N bond, and a final hydrogen abstraction.[272] The facts that azobenzene is the best radical trap found by Warkentin and Yeung[170], and that diazenecarbonyl LUMOs are so low in energy*, ought to compel one to consider charge or atom transfer mechanisms in addition to nucleophilic and unimolecular radical producing processes. Regrettably, this has not been the case. A few properly planned mechanistic investigations could have far reaching implications which would greatly clarify this matter.

---

*Compare the LUMO energies of $CH_2{=}CH_2$ (1.5 eV), $CH_3C{\equiv}CCO_2Me$ (0.8), and $MeO_2CC{\equiv}CCO_2Me$ (0.06)[59] to azobenzene (1.15), $PhN{=}NCO_2Et$ (0.78), $EtO_2CN{=}NCO_2Et$ (0.25), and $PhCON{=}NCO_2Et$ (0.16).[278]

Equations I71 to I74 illustrate other examples of azoacyl hydrolysis. Ullman and Bartkus (1962)[249] found that stable solutions of indazolone 122: R = H were instantaneously decolourized by added nucleophiles, but that nitrogen evolution was more gradual (Equation I71). This implicates a significant buildup of the tetrahedral intermediate 135. Milne and Kilday (1965)[279], Cohen (1965)[280], and Nagata and Kamata (1970)[160] reported analogous reactions I72 to I74, respectively.

The work of Cohen (Equation I73) seems to imply that $RN{=}N^-$ is ejected from the tetrahedral intermediate and is protonated in acid: the chemistry of phenyldiazene (as opposed to phenyl anion) characterizes the products in acidic methanol. For Equation I74, the use of neutral nucleophiles required warming the solution to obtain (induce?) decomposition, and in alcohol or amine solvents, nitrogen-substituted products 136 and 137 were obtained. Although Nagata and Kamata interpreted these as products of nucleophilic attack of $NuCOCH_2CR_2^-$ anion on 121, radical chain decomposition of the tetrahedral intermediate cannot be discounted, especially since system 121 so closely parallels the oxadiazoline system (56, page 31) actually studied by Knittel and Warkentin.[166-168] Again the dangers of mechanistic inference from product studies alone are obvious.

Two further examples of hydrolytic CN cleavage of diazenecarbonyls are given by Equations I75 and I76. These general types of reactions leading to olefinic carboxylates have been developed by

[I71]

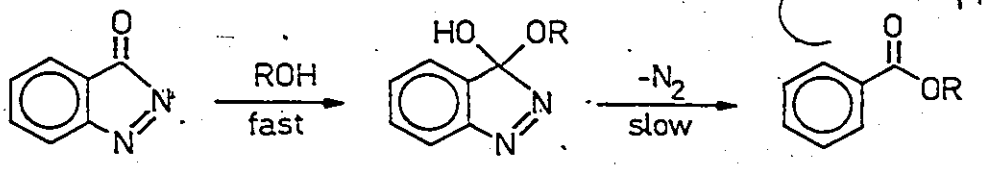

(122 : R=H) (135) R = H, Me, or CCH_3 (O)

[I72] $PhN{=}NCCH_2NHR \xrightarrow{NuH} PhH + N_2 + NuCCH_2NHR$ (O)

NuH = H_2O, EtOH, $PhNH_2$, $PhOCCH_2NH_2$ (O)

[I73] $PhN{=}N{-}C{-}Ph \xrightarrow[H^+]{MeOH} PhN{=}N{-}H + PhCOMe$ (O)

→ etc.

[I74]

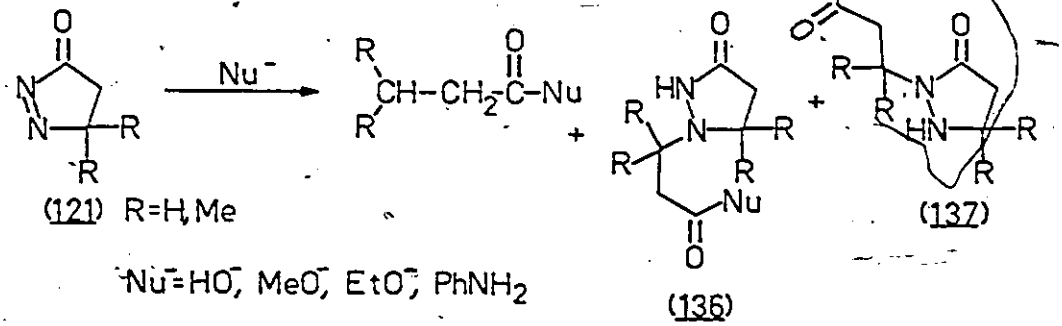

(121) R=H, Me

$Nu^- = HO^-, MeO^-, EtO^-, PhNH_2$

(136) (137)

Carpino (1969)[281] and Kocienski (1976).[282,283] The intermediate pyrazolenone 138 is trappable with dienes. Mixtures of cis and trans olefins are obtained from reaction I76 if acyclic ring substituents are used.[282] Kocienski claims that base catalyses ring opening, but that the extrusion of nitrogen from a ring-opened diazene does not lead to the vinyl anion, but rather to a vinyl radical (139), which can be intercepted with ferricyanide ion. Ferricyanide oxidizes the vinyl radical to a vinyl carbonium ion which decarboxylates, diverting the reactant to acetylene product (Equation I77). In the presence of two equivalents of ferricyanide, yields of olefinic acid declined from 70 to less than 10%, and 20-80% acetelyene was obtained.[283]

I3.2 Diazenecarboxylates

In contrast to acyldiazenes, diazenecarboxylates appear to behave as normal esters. In 1922, Diels demonstrated that primary amines convert azodicarboxylate esters to the corresponding amides (Equation I78).[284] Secondary and tertiary amines add to nitrogen,[285] but the mechanism can be argued. Bock (1966)[286] found analogous chemistry for monocarboxylates (Equation I79).

Kosower (1968)[287] studied the two step conversion of phenyl azocarboxylate esters (140) to phenyldiazene (Equation I80). He found an approximate second order rate constant for hydroxide ion attack on the ester to be 200 M^{-1} s^{-1} at 4°. This is more than 10^4 times larger than the corresponding rate constant for $PhCH{=}CHCOOCH_3$, reflecting the azo group electronegativity. In methoxide/methanol,

[I75]

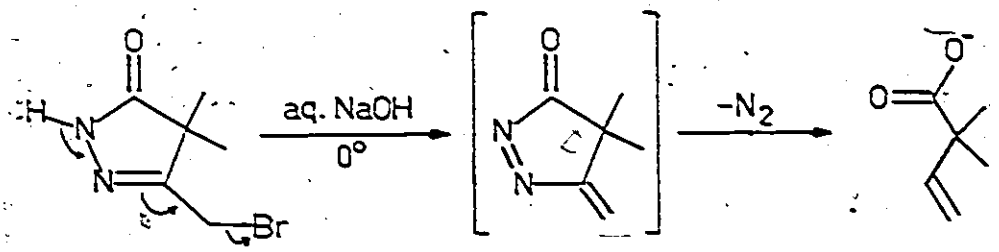

[I76]

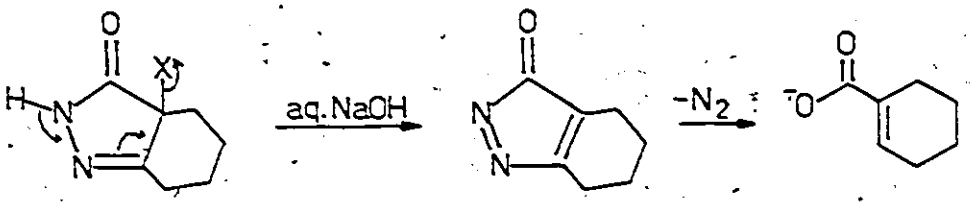

(138)

[I77]

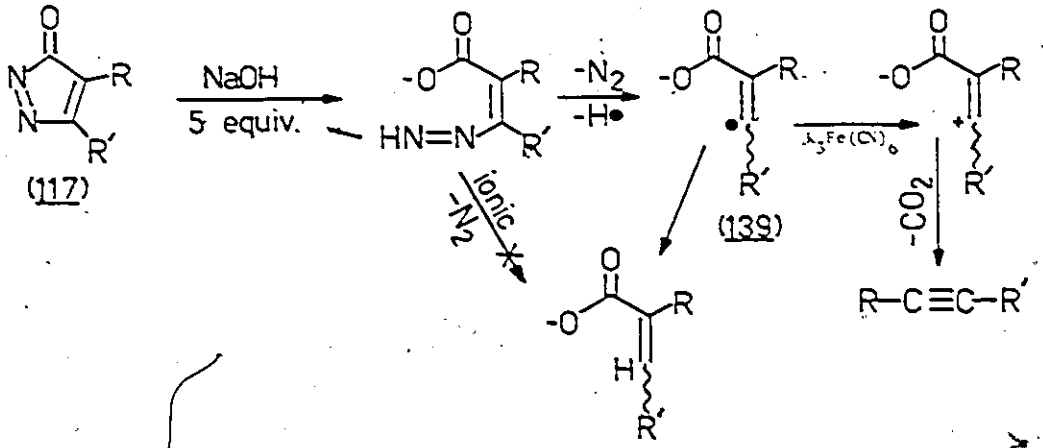

(117)

(139)

ester decomposition was 2 X 10^5 times slower than in water, reflecting the difference between the diazene and alcohol pK. Similar uv spectra in methanol and methoxide/methanol were taken to imply that the equilibrium concentration of the tetrahedral intermediate was not large.

Kosower also found decomposition of the carboxylate salt 141 was acid catalysed. Stable potassium or barium salts could be precipitated by very basic hydrolysis of the ester. Using an arduous kinetic technique involving degassed solutions to prevent oxygen catalysis of phenyldiazene decomposition, Kosower covered the pH range 10-12. To explain the acid catalysis he postulated extremely rapid decomposition ($k \sim 10^{10}$ s^{-1}) of the zwitterionic form 142, whose pK_a he estimated to be 0.5 (Equation I81). Earlier studies by King (1940, 1944)[288,289] found the decomposition of azodicarbonate ion 143 in aqueous base in the pH range 12-13 to be quite sensitive to general acid catalysis, with Bronsted $\alpha = 0.86$ (Equation I82).

In homogeneous aprotic solvent, Fraenkel and Pechhold (1968)[271,276] found potassium phenylazoformate apparently fragments to phenyl anion (Equation I83). The absence of biphenyl rules out a radical process.

It was in the context of these few available literature examples that the investigations reported in this thesis were launched, with intentional bias toward kinetic aspects which are so absent in the previous work.

[I78] $RO-\overset{O}{\overset{\|}{C}}-N=N-\overset{O}{\overset{\|}{C}}-OR \xrightarrow{R'NH_2} R'NH-\overset{O}{\overset{\|}{C}}-N=N-\overset{O}{\overset{\|}{C}}-NHR' + ROH$

(39)

[I79] $Ph-N=N-\overset{O}{\overset{\|}{C}}-OCH_3 \xrightarrow{RNH_2} Ph-N=N-\overset{O}{\overset{\|}{C}}-NHR$

(140)

[I80] $\xrightarrow{HO^-} Ph-N=N-COO^-$

(141)

$\xrightarrow[-CO_2]{} Ph-N=N-H$

[I81] $Ph-N=N-COO^- \rightleftharpoons Ph-N=N^+(H)-COO^- \xrightarrow[k]{-CO_2} Ph-N=N-H$

$pK_a \sim 0.5$; $pK_a \sim 0.3$

$Ph-N=N-COOH \rightleftharpoons Ph-N=N^+(H)-COO^-$

(142)

[I82] $^-OOC-N=N-COO^- \longrightarrow H-N=N-H \longrightarrow N_2,\ H_2N-NH_2$

(143)

$2\,CO_2 \longrightarrow HCO_3^-,\ CO_3^{-2}$

[I83] $PhN=N-COO^-K^+ \xrightarrow[\text{crown}\ 80^\circ]{THF} PhCOOH + PhH + \underbrace{CO_2 + N_2}_{22\ l/mol\ \text{total}}$ no PhPh

17% 47%

METHODS, RESULTS, AND DISCUSSION

The following material partitions naturally to three chapters. First, Chapter R1 describes the results of CNDO/2 calculations and the photoelectron spectrum of dimethyloxadiazolinone (1-Me_2). These results offer a useful vantage point from which to discuss many aspects of oxadiazolinone chemistry — both in this thesis and in future work. Chapter R2 details the results of the thermolysis mechanistic studies and attempts to unify the highly varied chemistry of 5-membered ring diazenes. Whereas the studies reported in Chapter R2 are fairly conclusive, the hydrolysis work, presented in R3, is less so.

R1 SCF Molecular Orbitals and the Photoelectron Spectrum of 5,5-Dimethyl-Δ^3-1,3,4-oxadiazolin-2-one.

Frontier Molecular Orbital (FMO) Theory has had considerable success in providing insight into the problems of transition state structure, mechanism, stereo-, regio-, and periselectivity, as well as into relative reactivity of substrates in a variety of thermal, photochemical, nucleophilic, and electrophilic reactions.[42-70] As one of many probes of the present mechanistic studies of the thermal, photochemical, and acid- and base-catalysed decomposition of oxadiazolinones we sought to determine the FMOs of the system.

The CNDO/2 method[40] was used to compute molecular orbital densities, ionization potentials and electronic transition energies for dimethyloxadiazolinone (1-Me_2) and the 5,5-diprotio (1-H_2) and 5,5-difluoro (1-F_2) analogs, to establish the effect of substituents

on the frontier MOs. To check the validity of the theoretical MOs, the photoelectron spectrum of 1-Me_2 was obtained (Experimental E1.5) and the assigned IPs compared to the IPs computed by application of Koopmans' Theorem.[290] Expensive energy minimization calculations were avoided because accurate values for bond lengths and angles could be inferred from a previous crystal structure of the closely related compound 2-p-bromophenylimino-5,5-dimethyl-Δ^3-1,3,4-oxadiazoline (144; Figure R1).

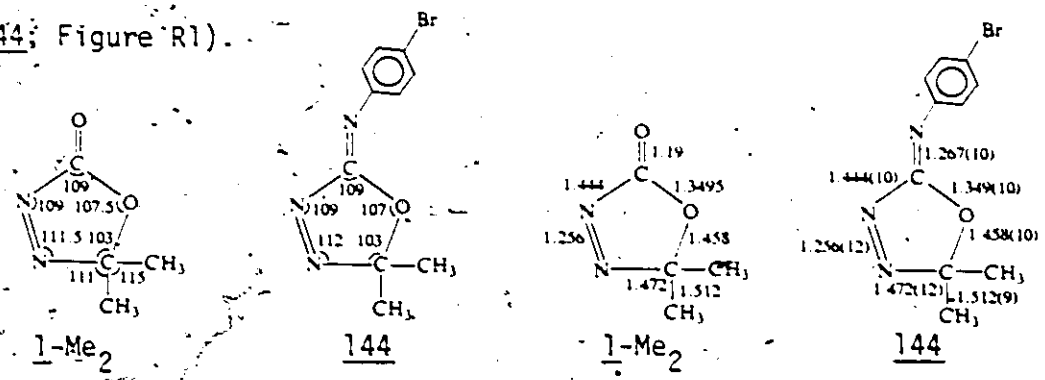

Figure R1. Bond lengths and angles in dimethyloxadiazolinone compared to those from the crystal structure of 144. Estimated standard deviations for the X-ray parameters are ±1° and ±0.01 Å.

R1.1 Estimation of Bond Lengths and Angles

Oxadiazolinone ring bond lengths and angles were set equal to those reported[291] for the X-ray crystal structure of 144, in Figure R1. Since the methyl groups in that structure were not perfectly tetrahedral (presumably because of constraints of the crystal phase and/or limitations in the structure solution) these standard parameters were used for the methyl groups[292]: R_{CH} = 1.09 Å, ∠HCH = 109.45°. Calculations performed on the 5,5-diprotio compound (1-H_2) also assumed the standard R_{CH} bond length. In the case of 1-F_2, the CF bond contraction owing to the electron withdrawing azo function was set

equal to the difference between a paraffinic CC bond length (1.541 ± 0.003 Å)[292] and R_{C-CH_3} = 1.512 ± 0.009 Å in 144. When applied to the $R_{CF}(CH_2F_2)$ = 1.360 ± 0.005 Å[292], this correction yielded the value R_{CF} = 1.331 ± 0.011 Å for 1-F_2. Although some shortening of the N4-C5 bond may also be expected on fluorine substitution, the oxadiazolinone ring parameters were not modified.

The parameter requiring the greatest attention was the carbonyl bond length. Lack of data on azocarbonyl bond lengths hampers estimation of a reasonable value for the oxadiazolinones. For simple carbonyl compounds of the type XCOY (where X,Y = H, CH_3, CF_3, CCl_3, CN, OH, OR, NH_2, NR_2, F, Cl, Br, ..etc.) there exists a reasonable correlation between the infrared stretching frequency and bond length.[293] As the electron withdrawing power (measured by σ_I[294]) increases, an accompanying increase in the CO stretching frequency reflects a shorter bond length (Table R1).

Table R1. Change in bond length and stretching frequency of the carbonyl group as a function of substituent.

	R_{CO} (Å)[a]	ν_{CO} (gas, cm^{-1})[a]	σ_I[b]
CH_3COCH_3	1.22	1737	0.00
CH_3COOCH_3	1.200	1770	0.25
CH_3COCl	1.192	1882	0.47
CH_3COF	1.181	1869	0.52

[a] Ref. 293

[b] Ref. 294

Fixing a carbonyl group in a five-membered ring usually raises the stretching frequency by 35 ± 10 cm^{-1} (ref. 295). Correction of the observed CO stretching frequency of 1-Me_2 (1835 cm^{-1} in CCl_4) for the ring size effect implies that the adjacent azo nitrogens of oxadiazolinone have an effective σ_I between those of the methoxy and chloro groups, in qualitative agreement with the value of σ_I (0.25) for the phenylazo group.[294]

It may also be useful to compare the change in $R_{C=X}$ for X = N—C_6H_4Br-p and X = O. Bond lengths in the imino group of 144 (1.267 ± 0.012 Å) and that in the p-bromoanil of benzaldehyde (1.281 ± 0.010 Å)[296] differ by 0.014 ± 0.018 Å. Since the benzaldehyde CO bond length is 1.211 Å[297], one might infer an oxadiazolinone CO bond length of 1.197 ± 0.018 Å by difference.

Since the oxadiazolinone carbonyl is flanked by both an azo nitrogen and an ester oxygen, these criteria combine to suggest a reasonable value of 1.19 Å for this bond length. This value was used in the computations, and the effect of the actual choice of R_{CO} on the calculated IPs of the 1-H_2 parent is examined in section R1.6. For a summary of the parameters employed in the calculation on 1-Me_2, see Figure R1.

R1.2 Calculation

Details of the CNDO/2 method and actual parameters have been fully discussed elsewhere.[40,298,299] Calculations were performed on an HP 3000 computer using a FORTRAN program developed by Professor D.P. Santry of this department. Electronic excitation energies

$\Delta E_{i\to j}$ were also calculated, using K_{ij} and J_{ij} obtained from the CNDO LCAO expansion coefficients (C matrix) and the CNDO atomic electron repulsion integrals γ_{AB}[40], according to Equations R1 to R4:

[R1] $$\Delta E_{i\to j} = \varepsilon_j - \varepsilon_i - J_{ij} + 2K_{ij}$$

[R2] $$J_{ij} = \iint \psi_i^*(1)\psi_j^*(2)\frac{1}{r_{12}}\psi_i(1)\psi_j(2)d\tau_1 d\tau_2$$

$$= \sum_{A=1}^{NA}\sum_{B=1}^{NA}\sum_{\mu=1}^{NBA}\sum_{\nu=1}^{NBB} C_{\mu i}^2 C_{\nu j}^2 \gamma_{AB}$$

[R3] $$K_{ij} = \iint \psi_i^*(1)\psi_j^*(2)\frac{1}{r_{12}}\psi_j(1)\psi_i(2)d\tau_1 d\tau_2$$

$$= \sum_{A}^{NA}\sum_{B}^{NA}\sum_{\mu}^{NBA}\sum_{\nu}^{NBB} C_{\mu i}C_{\mu j}C_{\nu i}C_{\nu j}\gamma_{AB}$$

where NA = number of atoms

NBA = number of basis functions on atom A

and

[R4] $$\gamma_{AB} = \iint S_A^2(1)\frac{1}{r_{12}}S_B^2(2)d\tau_1 d\tau_2^*$$

R1.3 Results and Discussion

Based on analogy with the ring of oxadiazoline 144, the oxadiazolinone ring is planar, and symmetrical substitution at C5 produces a plane of symmetry. Under C_s symmetry, any orbital transforming as a" is a π orbital, and any as a' is a σ orbital. Since the

---

* γ_{AB} is the average coulomb integral between valence S orbitals on atoms A and B. In the CNDO formalism, however, all basis orbitals are spherically symmetric, or S.

trivial designation as π or σ is meaningful in these cases we adopt it, even when there is no true plane of symmetry (as in 1-Me_2 with staggered methyl groups).

CNDO/2 LCAO solution for 1-H_2 gives 26 molecular orbitals, of which 10 are vacant. Of the 16 filled MOs, 6 are "nonbonding", containing the so-called lone pairs (1 on each nitrogen, 2 per oxygen), and 10 are "bonding" MOs. In all, 7 of the 26 orbitals have π symmetry (see Figure R2). These result from the combinations of five obvious $2p_z$ AOs on O1, C2, N3, N4, and O6 plus two symmetry orbitals on the CH_2 moiety, designated π_{CH}(145) and π_{CH}^*(146). These can be viewed as arising from the two possible antisymmetric combinations of hydrogen 1s symmetry orbitals with the $2p_z$ AO of C5. Thus the π_{CH} is of correct symmetry to interact with the other π orbitals of the molecule and four highly delocalized, filled π MOs result. Buried in each of these are contributions from π_{NN}, π_{CO}, π_O (lone pair on O1, as in carboxylates) and π_{CH}.

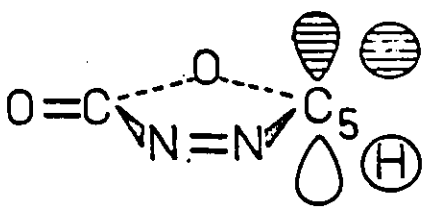

(145) π_{CH}

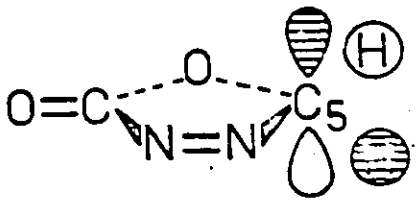

(146) π_{CH}^*

For dimethyloxadiazolinone, a "staggered" conformation of the methyl groups was assumed for the computation. Although this has the effect of destroying the symmetry plane of the diprotio and difluoro analogs, the orbital assignments of symmetry can nonetheless

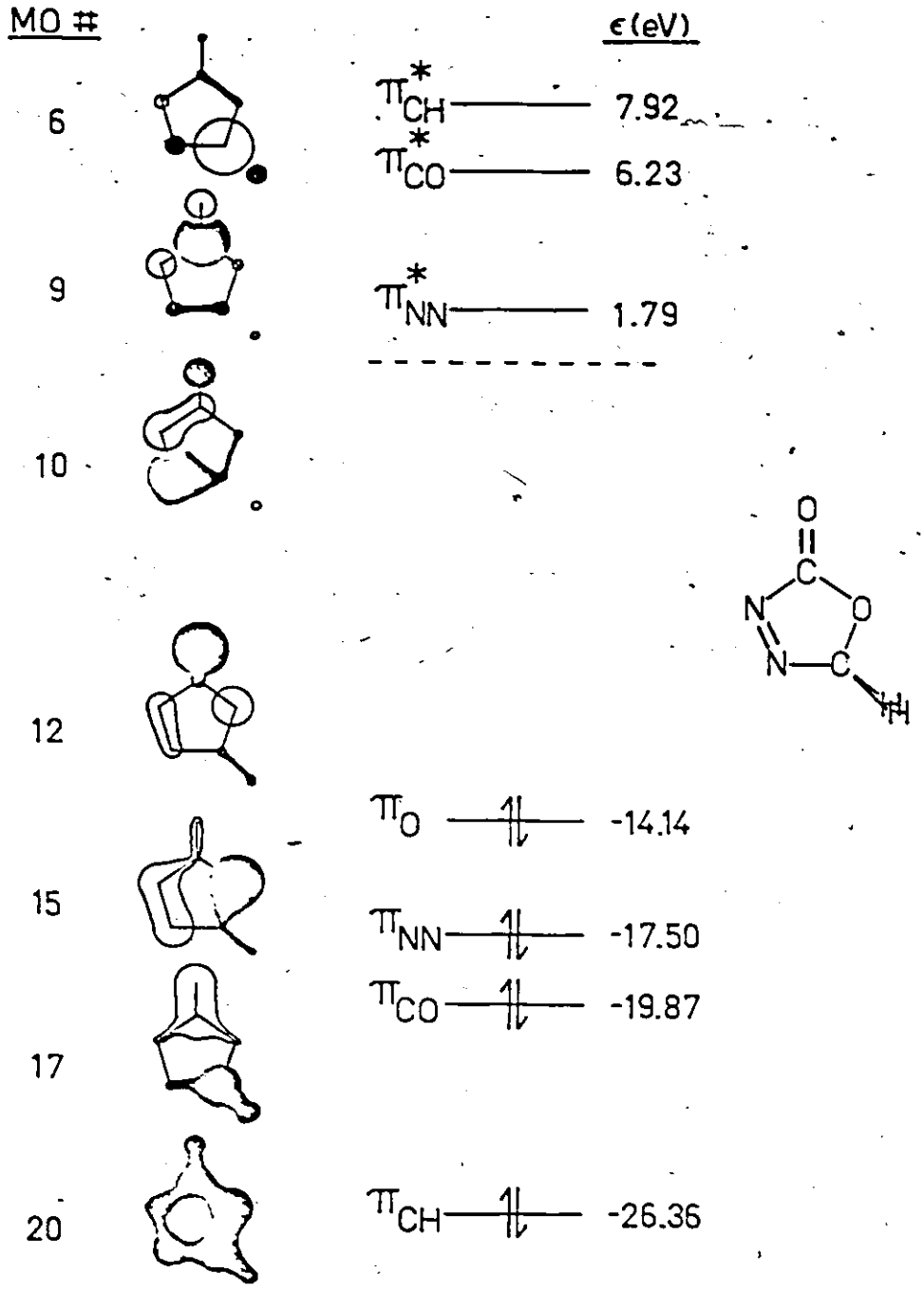

Figure R2. π MOs of oxadiazolinone 1-H_2.

be made by comparison to 1-H_2.

Computed valence energy levels for 1-Me_2, 1-H_2, and 1-F_2 are compared to the experimental IPs for 1-Me_2 in Figure R3. The electron withdrawing fluorine atoms at C5 lower all the orbital energies, and increase the calculated gaps between the first few IPs.

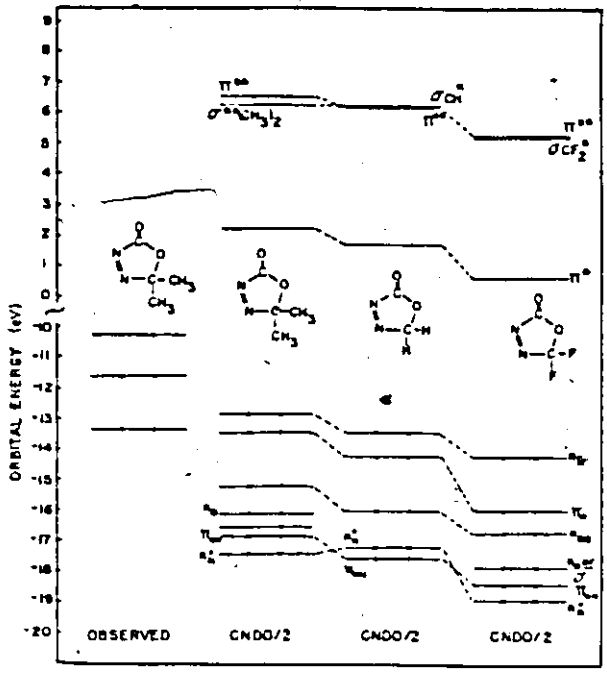

Figure R3. Calculated and observed energy levels of oxadiazolinones.

According to FMO theory,[42-46] nucleophilic and electrophilic attack are favoured at the site of greatest orbital density of the LUMO and HOMO, respectively. Klopman,[47,55] Salem,[300] and others, however, recognize the extremes of a continuum from frontier controlled to charge controlled reaction. Although examination of the LUMO of

oxadiazolinone (Table R2) suggests the possibility of nucleophilic attack on nitrogen, the fact that both nitrogens are formally negative in overall charge, as indicated in Figure R4, may mitigate against attack by negatively charged nucleophiles via the LUMO. Reduction, by acceptance of an electron from a neutral species (for example, a thiol), could easily involve the LUMO because coulombic repulsions would be considerably less important near the N atoms. On the other hand, attack by charged nucleophiles at C2 via the next lowest unoccupied orbital (NLUMO) is encouraged by the half-unit total positive charge and enormous frontier density predicted by the calculations. These two cases correspond to orbital control and charge control respectively.

Likewise, electrophilic attack (e.g., protonation) on nitrogen via the HOMO (lone pair attack) or on carbonyl oxygen or ring oxygen (NHOMO, π attack) is possible. Both the greater negative overall charge (-0.131 vs -0.029 units) and the greater HOMO frontier density (0.312 vs 0.185) on N3 compared to N4, would seem to predict N3 protonation.

The roles played by frontier orbitals in thermolysis and hydrolysis reactions of oxadiazolinones will be discussed in appropriate upcoming Results and Discussion sections. Valence orbital parameters for 1-H_2 and 1-F_2 are found in Appendix 3 in Table A3.1 and A3.2, respectively.

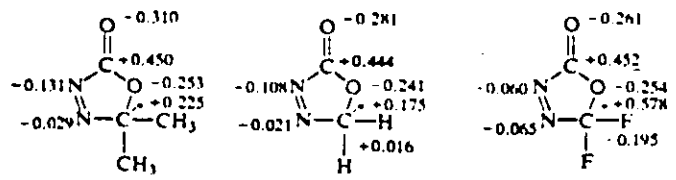

1-Me_2 1-H_2 1-F_2

Figure R4. CNDO/2 net charge densities.

Table R2. Valence orbital parameters for dimethyloxadiazolin-2-one.

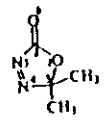

Assignment		Sym-metry[a]	Orbital energy (eV)[b] Obs.	Calcd.	Orbital densities[c] O1	C2	N3	N4	$C(Me)_2$	O6
Unoccupied ABMO	π^{**}	π		6.59	0.038	0.453	0.193	0.066	0.070	0.191
	$\sigma^* C(Me)_2$	σ		6.31	0.182	0.032	0.014	0.043	0.718	0.013
	π^*	π		2.32	0.019	0.129	0.250	0.429	0.049	0.125
Doubly occupied BMO and NBMO	n_N^-	σ	-10.20	-12.81	0.052	0.092	0.312	0.185	0.143	0.215
	π_O	π	-11.52	-13.37	0.229	0.014	0.110	0.060	0.318	0.268
	n_{CO}	σ	-13.26	-15.15	0.172	0.039	0.066	0.171	0.207	0.345
	n_O	σ		-16.07	0.436	0.009	0.089	0.108	0.313	0.046
	$C(Me)_2$ symmetry	π		-16.48	0.133	0.043	0.011	0.000	0.668	0.145
	π_{NN}	π		-16.79	0.285	0.005	0.277	0.280	0.145	0.008
	n_N^+	σ		-17.35	0.083	0.075	0.225	0.284	0.144	0.189

[a] Symmetry assignment assumes a mirror plane

[b] Orbital energies assume Koopmans' Theorem[290]

[c] Orbital density on atom A in orbital $i = \sum_{\mu}^{\text{on A}} C_{\mu i}^2$.

R1.4 The Photoelectron Spectrum of Dimethyloxadiazolinone

Only the three resolved low energy bands of the photoelectron spectrum of 1-Me_2 (Figure R5) are readily assigned by comparison to suitable models. The ordering of the IPs is verified by reference to the CNDO/2 orbital densities in Table R2. In all cases, the following discussion quotes only vertical IPs.

In cis-azoalkanes, the highest energy orbital, at 8-9eV, is typically the n_N^-, or antisymmetric combination of nitrogen lone pair orbitals. Most frequently, the π_{NN}MO is next highest (10.15 - 11.5 eV), followed by the n_N^+ symmetric combination of nitrogen lone pairs at 11-12 eV.[34-38] Photoelectron spectra of oxadiazolinones are further complicated by the presence of the conjugated ester functional group. Oxygen lone pairs are usually of lower energy than nitrogen lone pairs, owing to the increase in effective nuclear charge on going across the first row from C, N, O, to F. For example, n_{CO} and π_OIPs for ketones and esters range between 9.5 and 10.5 eV.[301] Based on these and the following considerations, the first three resolved bands for 1-Me_2 have been assigned to n_N^- (10.20 eV), π_O (11.52 eV), and n_{CO} (13.26 eV) (see Table R2).

For the purposes of the assignment, the correlation diagram for valence IPs (Figure R6) features γ-butyrolactone (147), γ-crotonolactone (148), and 3,3,5,5-tetramethylpyrazoline (61) as suitable models. There are not really any more complex heterocyclic models appropriate for 1-Me_2 in the PES Literature.* CNDO/2 calculations

*It has been suggested that 2-oxazolidinone (149) might be a useful model, but this has been resisted because the lactam

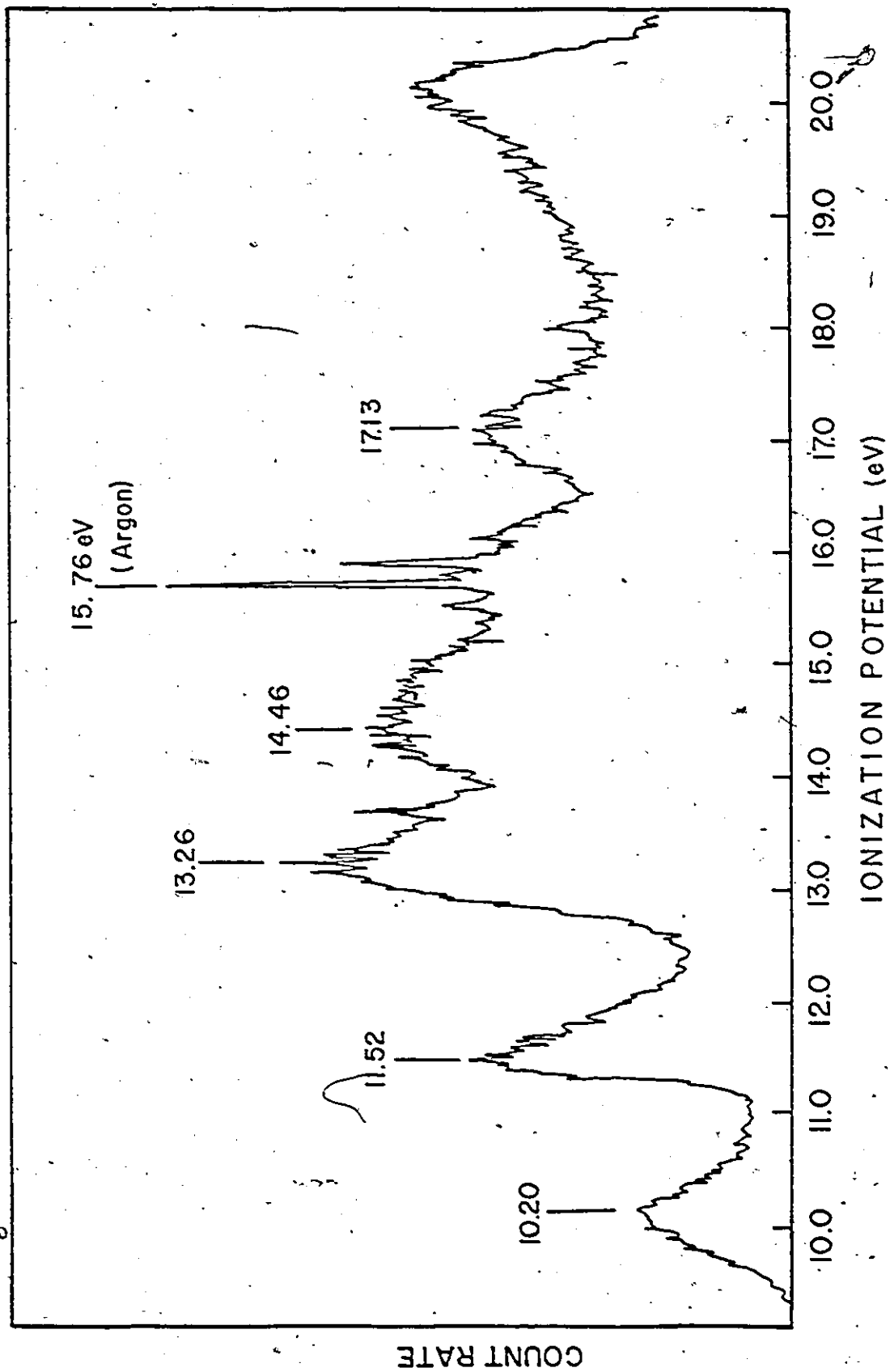

Figure R5. The photoelectron spectrum of dimethyloxadiazol1none.

and PES of lactones 147 and 148 have been reported.[302]

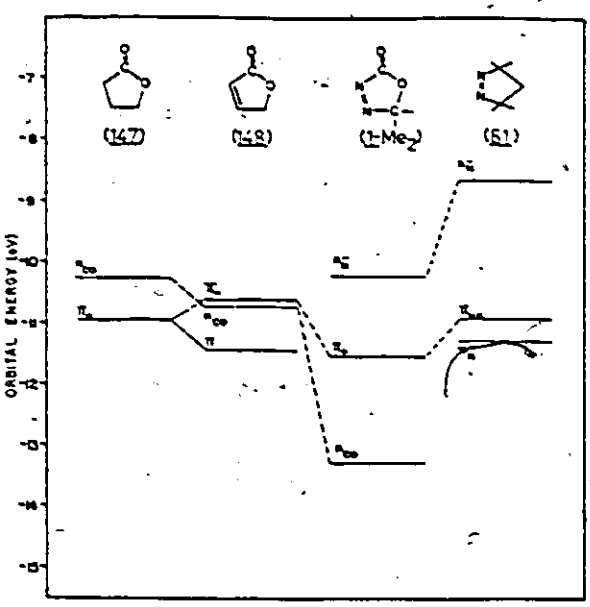

Figure R6. Correlation diagram using measured valence IPs.

The highest occupied π-type orbital in each of 147 and 148 contains a significant contribution from the $2p_z$ AO on the ring oxygen, and correlates more strongly with the HO-π in 1-Me_2 than does the π_{NN} of 61. In recognition of this fact, the label π_O has

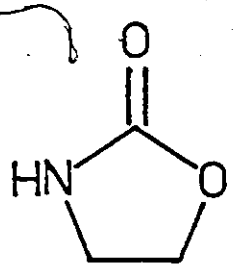

(149)

nitrogen in 149 is electron donating by virtue of the fact that its lone pair has π symmetry, and is strongly mixed with the carbonyl π bond and ring oxygen lone pair of π symmetry. In contrast, lone pairs on the electron withdrawing azo nitrogens of 1 are in the plane of the molecule (σ symmetry). Furthermore, the carbonyl stretching frequencies of 147, 148, 149 and 1 occur at 1740[303a], 1785 and 1750 (a doublet in the unsaturated lactone[304]), 1750[303b], and 1835 cm^{-1}, respectively, indicating that there is no profit in using the lactam nitrogen to model the effect of the azo group on the carbonyl IPs of 1-Me_2.

been used to describe the electron distribution in this MO. Mixing among π_O, π_{NN}, and π_{CO} levels ought to raise the HO-π level by resonance, but lower it inductively for a net stabilization. At 11.52 eV, the second IP is 0.6 eV lower than the π_O IP of 147 or 148, or π_{NN} of 61.

Excluding the π-mixed lone pair orbital on the ring oxygen, four heteroatom lone pair IPs are anticipated. Since they are on adjacent atoms, the nitrogen lone pairs interact the most, with carbonyl and ring oxygen lone pairs intermediate in energy, anticipating the sequence $n_N^- > n_O, n_{CO} > n_N^+$, where n_O refers to the in-plane lone pair orbital on O1 with σ-symmetry. Interaction of the azo nitrogen symmetry orbitals with the other lone pair orbitals of σ symmetry results in a widening of the n_N^-/n_N^+ energy gap (a resonance effect) and a lowering of the energy levels (a stabilizing inductive effect). The magnitude of the net result may be seen by comparing the IPs of dimethyloxadiazolinone and 3,3,5,5-tetramethylpyrazoline (61)[36] (Figure R6).

Because the 13.26 eV ionization has been assigned to the carbonyl oxygen lone pair (see next paragraph), the n_N^+ orbital must have an IP higher than 13.3 eV. Thus, the interaction energy $\Delta(n_N^-/n_N^+)$ has to exceed 3.1 eV, which is indeed greater than the value of 2.63 eV for the pyrazoline. The CNDO/2 calculations predict $\Delta(n_N^-/n_N^+)$ to be 4.54 eV.

The observed carbonyl oxygen lone pair ionization for 1-Me_2, assigned at 13.26 eV, is much larger than the values of 10.25 eV for γ-crotonolactone (148)[302], and well outside the normal range for

ketones and esters (9.5 - 10.5 eV).[301] The effect of the double bonds in 148 and 1-Me_2 can only be inductive, and the effect of N=N in this regard is much greater than that of C=C (compare the carbonyl stretching frequencies in the footnote on page 90 of this section, to the 0.5 and 3.0 eV stabilization of n_{CO} in 148 and 1-Me_2, with respect to 147). Additionally, interaction of lone pair orbitals in 147 and 148 is of the n_{CO}/n_O type and acts to raise the n_{CO} level (the higher energy one) in these compounds, whereas σ mixing in 1-Me_2 is more complex, but should raise n_N^-, lower n_O, and might not affect n_{CO} too much. The n_N^- orbital of 1-Me_2 is stabilized 1.6 eV with respect to that of 61, with an IP (10.20 eV) well above the usual value of 8-9 eV.[36] Without the oppositely acting destablizing σ interactions anticipated for the n_N^-, the n_{CO} orbital might well be stabilized by more than this amount. CNDO/2 calculated IPs adequately predict a dramatic stabilization: 12.83, 13.74, and 15.15 eV for n_{CO} in 147, 148, and 1-Me_2.

Also salient to this discussion are the effects of substitution at C5, as in 1-H_2 and 1-F_2, on the calculated IPs. Successive substitution of hydrogen, then fluorine for methyl reduces the electron density on the carbonyl oxygen (O6) by 9 and 16% respectively (Figure R4), and this is reflected in 1 to 2 eV stabilizations of all three valence orbitals in 1-F_2 with respect to those in 1-Me_2 (Figure R3). In spite of their physical remoteness, fluorines at C5 are able to transmit their effect to the carbonyl oxygen because the CF_2 moiety contributes π-type symmetry orbitals, strongly attracting π electron density to reduce the net charge densities,

even at O6. In a qualitative sense, these MO calculations fortify attributing the large stabilization of n_{CO} to a generalized inductive effect of the strongly electron withdrawing azo function adjacent to the carbonyl.

Consistent then with carbonyl stretching frequency data, the three model compounds, and the MO calculations on the three oxadiazolinones, 13.26 eV seems to be the most reasonable assignment of the n_{CO} band. Significantly, then, this enormously stablized carbonyl oxygen lone pair should be very much harder to protonate, and the CO-protonated conjugate acid is predicted to possess a pKa much lower than expected for a normal ketone or ester (ca-7 or -8[305]). This point is further considered in Section R3: Hydrolysis.

As usual, the CNDO/2 calculation has over-estimated the ionization potentials, in this case by some 1.5 to 2.5 eV (compared to the usual figure of about 4 eV[302,306,307]), and has correctly reproduced the ordering of the first few highest occupied MOs. Hence, the assigned photoelectron spectrum does seem to validate the initial choice of structural parameters, and in fact, the choice of the CNDO/2 method.

R1.5 Electronic Transition Energies

The uv-visible spectrum of 1-Me_2 in hexane (Figure R7) exhibits two bands: one at 372 nm (ϵ_{max} = 348 M^{-1} cm^{-1}) whose structure collapses in more polar solvents; and another at 214 nm (ϵ_{max} = 2880 M^{-1} cm^{-1}). Even for simple azoalkanes, electronic transition assignments of all but $n_N^- \rightarrow \pi^*$ have frequently been disputed.[36,308,309] In this case, the CNDO/2 method predicts five possible transitions (Table R3) which

might be responsible for the observed higher energy transitions, often casually assigned as $\pi \rightarrow \pi^*$. Of these five, the single $\pi \rightarrow \pi^*$ candidate ought to be the most intense ($\varepsilon_{max} > 10000$). Any of the $n \rightarrow \pi^*$ type should have an $\varepsilon_{max} \sim 100$, similar to that observed for α,β-unsaturated esters.[310] However, the observed intensity is intermediate. It is not beyond the realm of possibility that an ε_{max} of 2880 M^{-1} cm^{-1} reflects a fortuitous combination of several nearly degenerate $n \rightarrow \pi^*$ transitions, perhaps on the low energy tail of a $\pi \rightarrow \pi^*$ band. Further speculation on this matter would be inappropriate here.*

Table R3. Calculated and observed excitation energies for dimethyloxadiazolin-2-one (1-Me_2)[a]

Transition	J_{ij}	K_{ij}	$\Delta E_{i \rightarrow j}$	Observed
$n_N^- \rightarrow \pi^*$	9.95	0.00	5.2	3.24
$\pi_O \rightarrow \pi^*$	7.83	1.21	10.3	
$n_{CO} \rightarrow \pi^*$	8.52	0.01	9.0	
$n_O \rightarrow \pi^*$	7.85	0.01	10.6	5.80
$n_N^+ \rightarrow \pi^*$	9.80	0.03	9.9	
$n_N^- \rightarrow \pi^{**}$	9.57	0.00	9.8	

[a]All energies in eV.

*M.B. Robin, who (by virtue of his years of research and several books on spectroscopy) ought to know, says of the location of the $\pi \rightarrow \pi^*$ band of simple azo compounds: "Where then is the $\pi \rightarrow \pi^*$ transition of the azo group? This must remain as one of the more interesting unanswered questions of molecular spectroscopy, for there are no compelling arguments for its assignment to any of the observed bands". (ref. 80 (1975), Part 1, p 13).

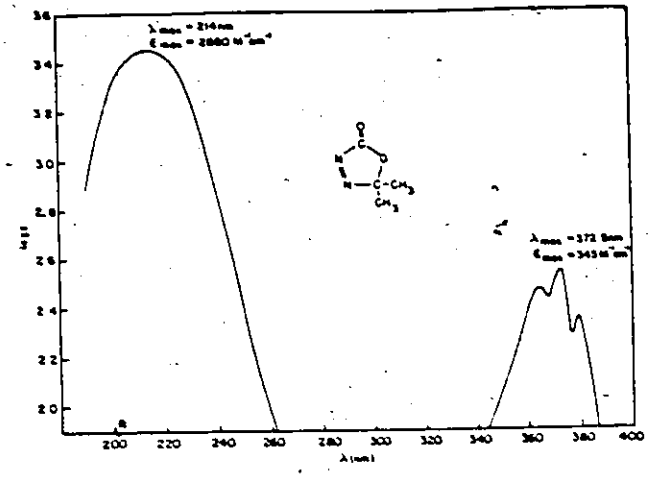

Figure R7. Absorption Spectrum of dimethyloxadiazolinone (hexane).

R1.6 Effects of Variation in R_{CO}

The carbonyl bond length turns out to be one of the key parameters in the entire set of calculations, and as such deserves some attention. Computations on the oxadiazolinone 1-H_2 with R_{CO} = 1.16, 1.19, 1.21, 1.24, 1.27 and 1.29 Å found a CNDO/2 total energy minimum at the rather large value of 1.261 Å (see Table A3.3 in Appendix 3). Although CNDO bond lengths are known to be unreliable[40] and nothing can be inferred from this particular value, it is significant, however, that the calculated energy gap between first and second IPs is a strong function of the selected bond length: declining from 0.97 eV at 1.16 Å to 0.04 eV at 1.29 Å (Figure R8). That a gap of 1.32 eV is observed for 1-Me_2 strongly supports the choice of a relatively short carbonyl distance, and may well indicate the possibility R_{CO} < 1.19 Å.

Smoothly monotonic against decreasing R_{CO}, frontier orbital densities change as expected for increasing electronegativity of

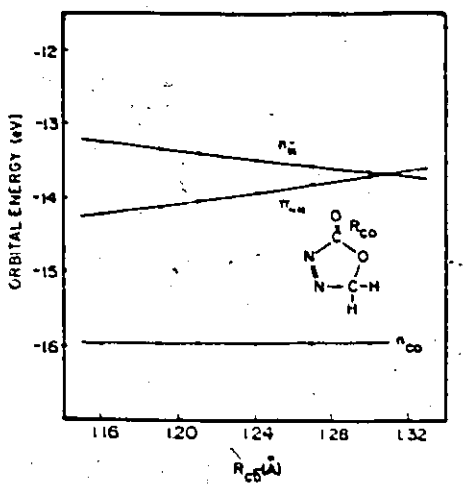

Figure R8. Valence orbital energy depends on choice of R_{CO} for 1-H_2.

the CO moiety but are not significantly altered. Shrinking the CO bond increases the electrophilicity of C3, N4, and N5 in both the charge- and frontier-controlled senses, thereby rationalizing the high reactivity of oxadiazolinones toward nucleophiles.

As a final note on the bond dimension issue, an apparently minor change in heteroatom; that is replacement of ring oxygen by nitrogen (for example, in a Δ^1-1,2,4-triazolin-3-one) would result in a substantially longer equilibrium bond length (cf. R_{CO} = 1.26 Å in diazenedicarboxamide (41)[292]), and also much different chemistry. In particular, triazolinones are less susceptible to aqueous hydrolysis than oxadiazolinones.

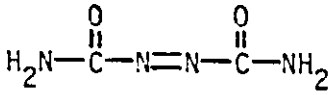

(41)

A1.7 CNDO/2 MOs for Carbon Dioxide and Diazomethane

For the discussion in the thermolysis section (R2), frontier MOs for CO_2 and CH_2N_2 were computed. The following structural parameters were used: CO_2[311], R_{CO} = 1.162 Å; diazomethane[312], R_{CH} = 1.08, R_{CN_1} = 1.32, $R_{N_1N_2}$ = 1.12, all Å, and ∠HCH = 127°.

Eight of twelve CNDO/2 LCAO orbitals for CO_2 are occupied,

giving rise to zero order net charge densities of +0.536 and -0.268 on the carbon and each oxygen, respectively. A pair of degenerate HOMOs with π symmetry at -15.70 eV have a node on carbon and coefficients of $\pm$0.707 on the oxygens. The LUMO is also a degenerate π pair at 5.14 eV, each with coefficients: C(+0.795), O(-0.429).

In the case of diazomethane, eight of fourteen LCAO orbitals are occupied, and net charge densities were computed to be: H(+0.045), C(-0.261), N_1(+0.306), N_2(-0.136). At -11.05eV, the HOMO has π symmetry, with orbital coefficients: C(-0.780), N_1(-0.125), N_2 (+0.613). The LUMO, at 4.35 eV, has σ symmetry, but the π-type NLUMO at 4.45 eV has orbital coefficients: C(+0.506), N_1(-0.704) N_2(+0.499). In cycloaddition reactions, the regiochemistry is very often controlled by the HOMO-LUMO interaction of smallest energy gap[42-49], which would be HOMO (CH_2N_2)-LUMO (CO_2), at 16.19 eV. The calculations predict the HOMO (CO_2) - NLUMO (CH_2N_2) gap to be 20.15 eV.

R1.8 Concluding Remarks

The choice of an alternate theoretical procedure is unlikely to effect a metamorphosis of the electron distributions reported herein. Even though this work shows that the CNDO/2 computational method gives a reasonable picture of Δ^3-1,3,4-oxadiazolin-2-ones, it is obvious from the orbital densities in Table R2 that the classification or assignment of orbitals as n_N, n_{CO}, n_O, π_{CO}, π_{NN}, etc., is unrealistic and over simplified. It is extremely difficult

to identify orbital mixing patterns for such a complex molecule, in spite of its low symmetry. For example, "π_{NN}" contains about a third of the electron density on O1, as well as on each of N3 and N4; because the C-H bonds in $\underline{1}$-H_2 transform with π symmetry, they are mixed into every π orbital (see Figure R2); in the orbitals designated as n_N^- and n_N^+, only half the σ electron density is found on the nitrogens; and the third-highest occupied MO, n_{CO}, has only a third of the electron density on the oxygen. Under circumstances such as these, the significance of the terms "lone pair" and two-electron "bond" crumbles.

R2. Thermolysis of Δ^3-1,3,4-Oxadiazolin-2-ones

Δ^3-1,3,4-Oxadiazolin-2-ones (1, Equation R5) are the most reactive of a series of heterocyclic compounds of general structure 150 under study in this laboratory. The ring system 150 is characterized by two possible thermolysis modes — one generating $R_1R_2C{=}Y$, together with N_2 and $:C{=}X$; and another producing a diazoalkane $(R_1R_2C{=}\overset{+}{N}{=}\overset{-}{N})$ concomitant with $X{=}C{=}Y$. The review of Introduction I2.6 and I2.7 has enumerated the few heretofore known cases and demonstrated the need for some comprehensive mechanistic studies in this area. Generation of diazoalkanes bestows synthetic utility upon the two piece fragmentation, and thermolyses of oxadiazolinones (1) as well as phenyliminooxadiazolines (150; X=NPh, Y=0) have recently been exploited, the first as a good alternative method for the conversion of α,β-epoxyketones to acetylenic carbonyl compounds[313] and the second as an alternative route to oxindoles, hydantoins, and related heterocycles[264-266].

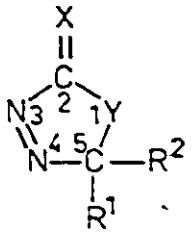

(150; X,Y=O, S, NR)

The title oxadiazolinones are easily prepared from ketone semicarbazones by oxidative cyclization with lead tetraacetate (LTA), followed by acid hydrolysis (Equation R5).[314] When both R groups are alkyl, isolated yields of oxadiazolinones are near 80%, based on semicarbazone, but if aldehyde semicarbazones are used, tautomerization of the intermediate iminooxadiazoline 151 prevents the desired

reaction[166].

[R5] 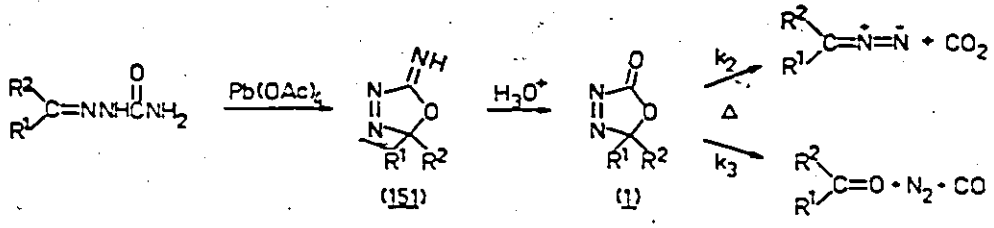

The oxadiazolinone ring system undergoes competing unimolecular fragmentations at modest temperatures (less than 100°C). One of these produces diazoalkane by carbon dioxide loss; the other ketone by carbon monoxide and nitrogen extrusion (k_2 and k_3, respectively in Equation R5).[259]

A preliminary kinetic study suggested that the balance between the two decomposition modes is dependent on solvent polarity, for the yield of diazoalkane increased on changing solvent from carbon tetrachloride to methanol.[259] Solvent effects on the individual rate constants were qualitatively assessed in terms of a nonpolar ketone-forming transition state and a polar diazoalkane-forming transition state. This thesis now reports the results of more detailed mechanistic studies which provide considerable insight on the transition state structures for these reactions. By exposing the underlying factors controlling the balance between the rates of these competing reactions, comprehensive mechanistic information permits partial control of the diazoalkane-forming reaction for synthetic purposes. In addition, it illuminates one example of a relatively rare chemical phenomenon — a three piece fragmentation to stable molecules.

R2.1 Beginnings

This thermolysis study began with an attempt to measure the C2 ^{13}C kinetic isotope effects for 2- and 3-piece fragmentation, initially concentrating on diazoalkane formation because CO_2 can be isolated from N_2 and CO by condensation at liquid nitrogen temperature on a vacuum line. To perform this experiment in the absence of a potential complicating isotope effect from concurrent ketone formation, it was essential to find a solvent sufficiently polar to accelerate the diazoalkane forming process, and eventually, trifluoroacetic acid (TFA) was found to completely suppress ketone formation. Significantly, this solvent appeared to behave normally, without any evidence for an acid catalysed decomposition component ($k_{CF_3COOH}/k_{CF_3COOD} = 1.13 \pm 0.01$ at 51.6°C; an inverse effect is expected for an acid catalysed reaction since CF_3COOD is a stronger acid[315]).

However, numerous problems were encountered with this solvent. It is vital to have a complete C2 mass balance, but CO_2 could not be recovered reproducibly from TFA. Even quintuply distilled CO_2 gas had a major impurity (later shown to be propene by ir and Br_2 trapping*) which upset the accuracy of isotope ratio mass spectrometry.

---

*Propene most likely arises from protonation of the primary product 2-diazopropane (152), followed by loss of nitrogen to form 2-propyl cation (153) which can be trapped by solvent or can eliminate a proton to generate propene (Equation R6). Mass balance shortfalls ascribed to propene formation were only observed in protonating solvents TFA and acetic acid. Although propene can be observed by pmr in CCl_4[236], it is insufficiently soluble in TFA to be detected by this method.

The work was not further pursued.

From the present investigations of solvent, substituent, and temperature effects on both processes, it is now possible to choose conditions which would give greater than 99% selectivity to each path, and avoid TFA solvent. For example, 1-Me,CH_2OMe should decompose by 99% 3-piece fragmentation in toluene at 85°C and 1-i-Pr,i-Pr should give > 99.9% diazoalkane in trifluoroethanol at 85°. It may also be possible to assay both the CO_2 and CO formed in a competitive system by isolating the CO_2 then oxidising the CO to CO_2 for analyses. Knowing the isotopic composition, and relative amounts of these fragment gases as a function of time could permit one to computer simulate, or curve fit, the observables to the complex kinetic equation describing the system. Thereby, the two isotope effects could be obtained as adjustable parameters. This is a non-trivial project, and was not attempted here: it is to be hoped that the other results in this thesis make such a painstaking experiment unnecessary.

R2.2 Mechanistic Alternatives

There are several, a priori, mechanistic alternatives for these thermolyses. Either one or both reactions could be completely concerted, for both thermal reactions are symmetry allowed. Diazo-

---

[R6] 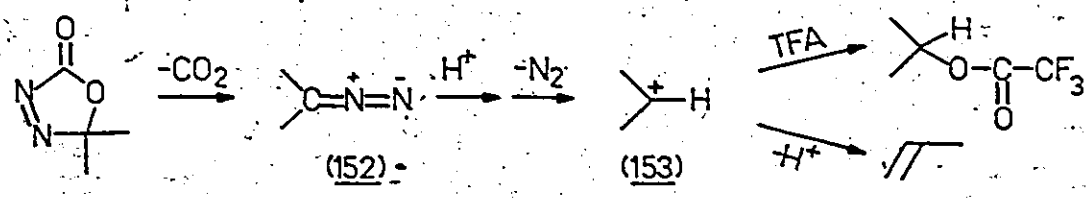

(152) (153)

alkane and carbon dioxide are produced by what is formally a 1,3-dipolar cycloreversion, while ketone, carbon monoxide, and nitrogen arise from a σ2s + σ2s + σ2s cycloreversion. Among stepwise alternatives, there exists a plethora of possibilities because either of the two bonds broken during diazoalkane formation could be broken in the rate-determining step, while any one or two of three bonds broken in the ketone formation might be broken in the slow step. The possible alternatives may be grouped according to the type of intermediate involved. As typical examples these might include zwitterions (such as 154 from O1-C5 bond heterolysis) or biradicals (for example, 155 from homolysis of the N4-C5 bond) or even closed-shell molecules (such as the α-lactone 156). It is important to remember that these two competing decomposition modes each have several possible intermediates of each of the three types from which a choice must be made: those structures below are only a few reasonable examples.

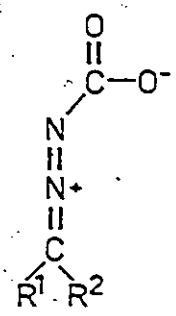

(154)

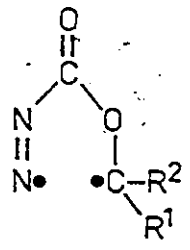

(155)

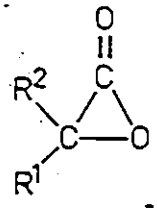

(156)

The kinetic analysis of this reacting system is straightforward.* From the disappearance of the starting oxadiazolinone, as

*More detail is provided in Appendix 2: Kinetic Methods.

monitored by its uv absorption at 360 nm (azo n → π*) or its ir carbonyl stretch at 1835 cm^{-1}, excellent concentration-independent, first order plots for the total rate constant, $k_T = k_2 + k_3$, are obtained. To dissect this further into the two individual rate constants, the product distribution is required. Since the diazoalkane formed on thermolysis is usually subject to several different fates (none of which ultimately produce, or consume, ketone at the low concentrations used in kinetic and product studies) only the time infinity ketone yield was quantitatively analysed by calibrated gas chromatography or infrared spectroscopy (see Experimental E2.3). From the fraction of ketone formed (f_{CO}), k_3 is easily calculated ($k_3 = k_T \cdot f_{CO}$), and hence k_2 by difference ($k_2 = k_T - k_3$).

That only two primary processes occur can be verified by trapping the diazoalkane with a few per cent trifluoroacetic acid (TFA). In these experiments, monitored by nmr, only ketone and trifluoroacetic acid ester are observed, indicating that the other (often unidentified) products formed in the absence of TFA, arose from subsequent reactions of diazoalkane, usually with itself or with solvent. Furthermore, even though only ketone was quantitatively assayed, better linear-free energy relationship correlations (vide infra) were always obtained for diazoalkane formation. Had an unknown third process been operative, large systematic errors would have surfaced in the diazoalkane correlations.

R2.3 Product Distributions

Relevant to the synthetic potential of oxadiazolinones as

diazoalkane precursors are the data pictorialized in Figure R9. The solid curve (computed from the points in Figure R11) shows in a quantitative way how the delicate balance between the two competing decomposition routes is affected by solvent polarity. To facilitate comparison to current literature on cycloaddition and cycloreversion reactions, the polarity parameter used here is Dimroth's E_T value (see ref. 77 for an excellent review of solvent polarity parameters).

For the 5,5-dimethyl compound, the diazoalkane yield increases from about 20% in toluene, up through chlorobenzene, 1,2-dimethoxyethane (DME), 1,2-dichloroethane (DCE), nitrobenzene, dimethylformamide (DMF), nitromethane, acetonitrile, acetic acid and 1,1,1-

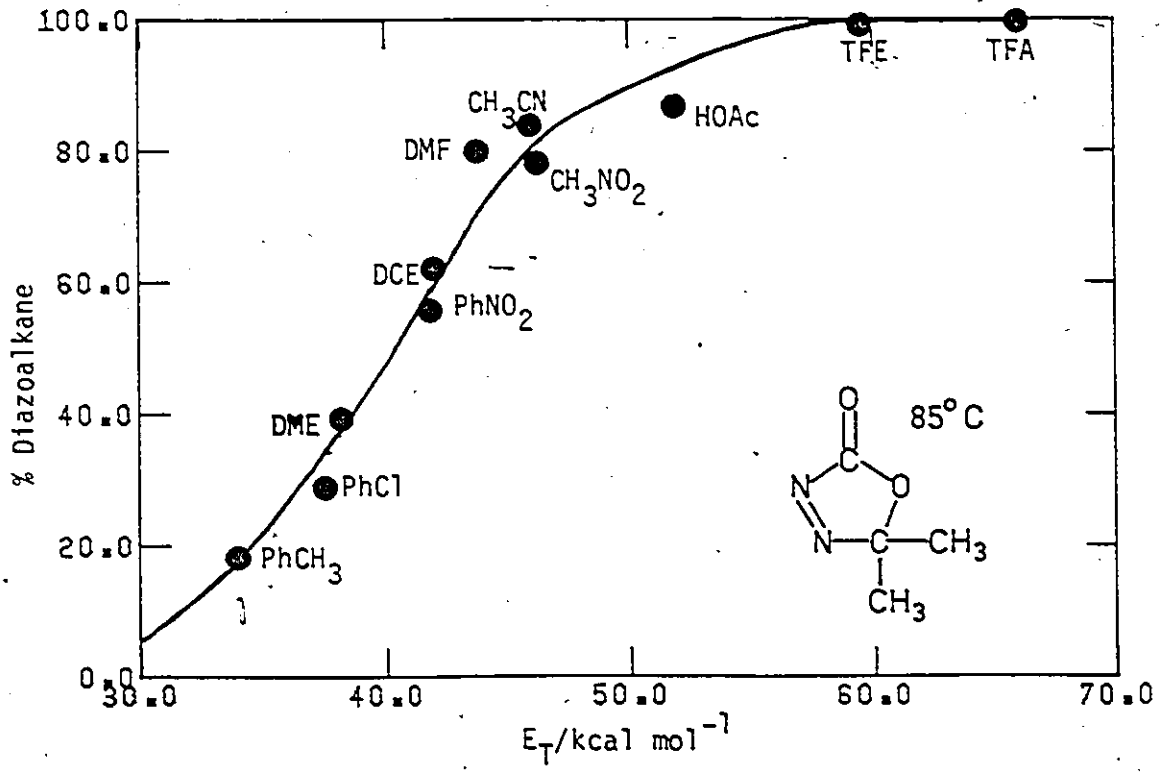

Figure R9. Product distribution as a function of solvent polarity for thermolysis of 1-Me_2 (solid curve computed from results of Figure R11).

trifluoroethanol (TFE) to TFA where one obtains diazoalkane exclusively.

The effect of substituent polarity, as measured by the Hammett σ parameter, on the product distribution from para-substituted 5-phenyl-5-methyloxadiazolinones, is shown in Figure R10. Even weak electron donors such as methyl and phenyl strongly favour the diazoalkane route, although a relatively polar solvent, acetonitrile, was used to obtain these data. Note also that these compounds were thermolysed at 50° compared to 85° for the 5,5-dialkyl oxadiazolinones. These are unstable compounds indeed, and many could only be purified by column chromatography at Dry Ice temperatures (Experimental E2.2).

Substituted acetophenone semicarbazones, in which the para-substituent is strongly electron withdrawing (NO_2, CN or CF_3) would not cyclize under normal oxidation conditions (LTA in methylene chloride at room temperature, 2 hr). For these compounds and for other semicarbazones especially insoluble in methylene chloride (e.g., p-C_6H_5), addition of five equivalents of trifluoroacetic acid boosted the oxidative capability and a rapid reaction occurred at lower temperatures. This mixed oxidizing system gave unique results not observed with lead tetratrifluoroacetate itself. For details see Experimental E1.2.

R2.4 Kinetic Investigations

R2.4.1 Solvent Effects (Table A3.4)

The degree of charge separation at the transition state, as

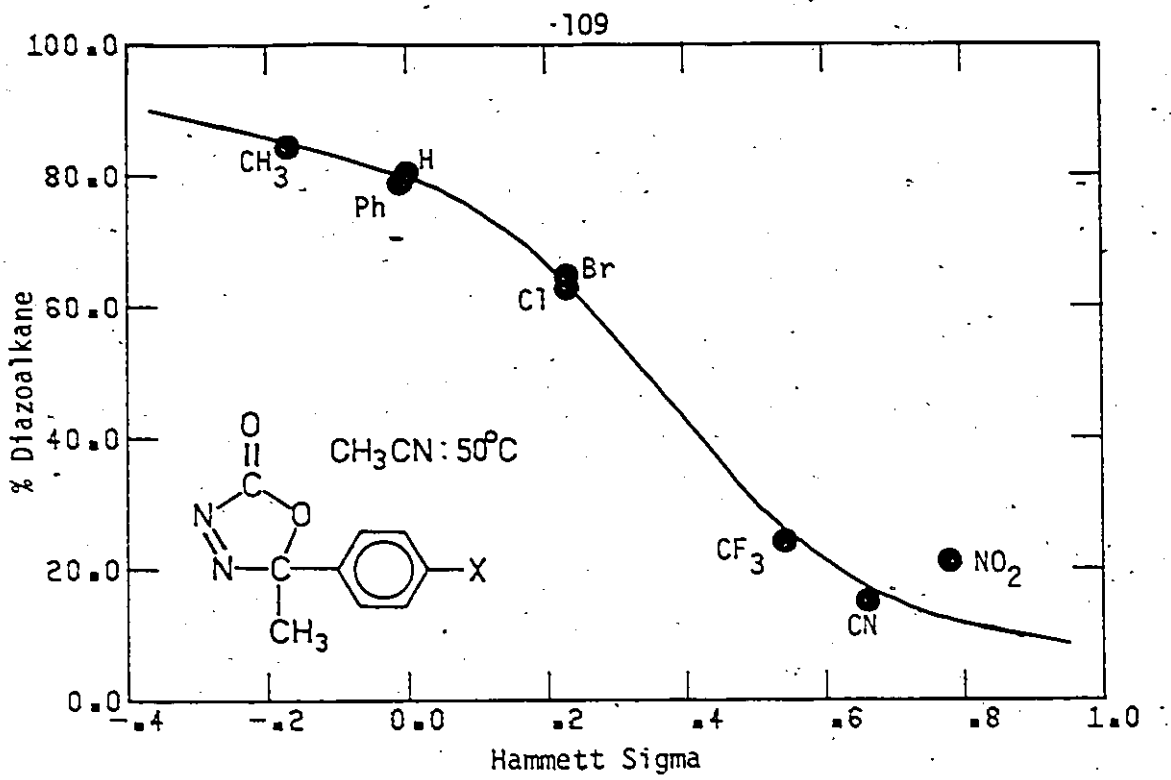

Figure R10. Product distribution as a function of substituent for thermolysis of 1-Me,Ar.

Figure R11. Effect of solvent polarity on rates of 2-diazopropane (k_2) and acetone (k_3) formation from 1-Me_2 (solvents correspond to Figure R9 and Table A3.4).

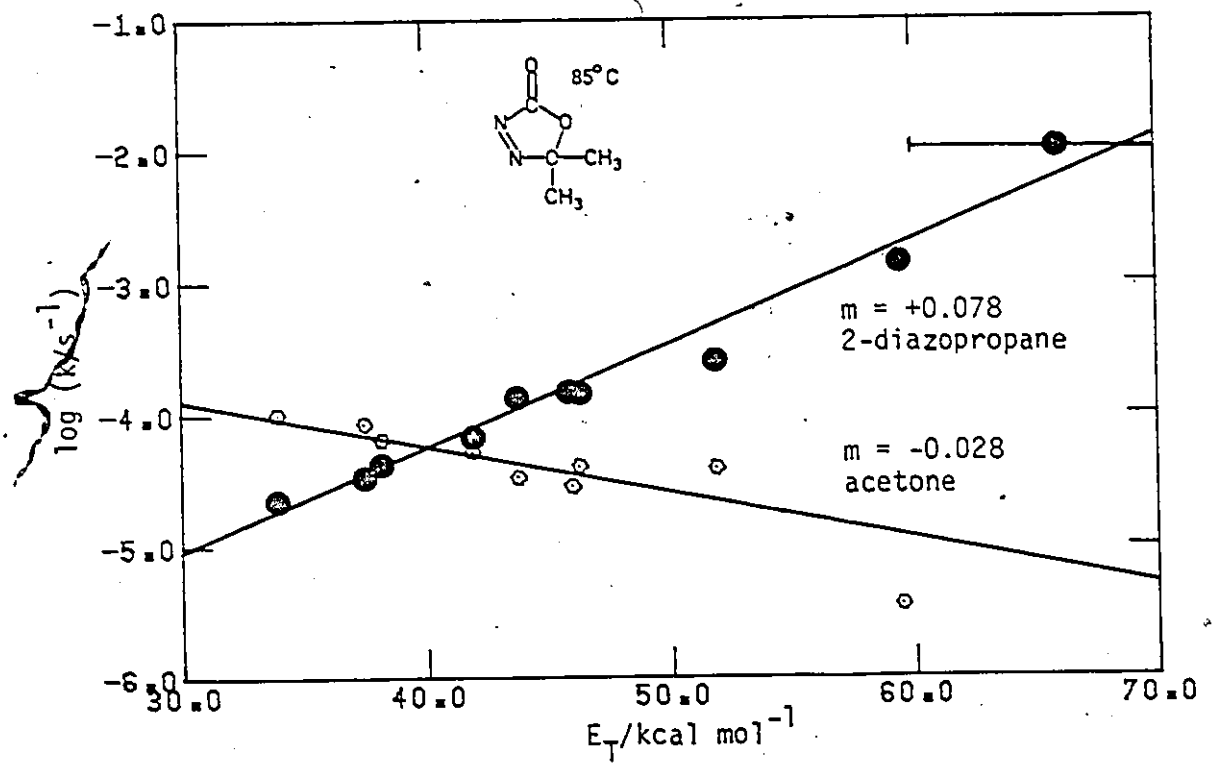

reflected in solvent effects on the reaction rate, is a particularly useful mechanistic probe. In Figure R11, the log of an individual rate constant for diazopropane or acetone formation, from 5,5-dimethyloxadiazolinone, is plotted against the E_T parameter for the same solvents found in Figure R9. Toluene is on the low E_T end and TFE and TFA are on the high E_T end. It is noteworthy that a similar plot of log k_T (the total rate constant) is not at all linear, but shows an overall U-shape. That the dissection of k_T into two competing processes gives linear correlations, supports the contention that these are independent primary processes: both products do not originate from a common intermediate, produced in the rate determining step, whose subsequent product determining steps are solvent sensitive.

The slopes of the solvent correlation lines are small. The sign of the slope means that the transition state for diazopropane formation is more polar than starting material, while that for ketone is less polar. The actual respective values of 0.08 and -0.03 mol $kcal^{-1}$ may be compared to the very much larger value of +0.29 observed by Huisgen for a known stepwise 2 + 2 cycloaddition: that of tetracyanoethylene to butyl vinyl ether which proceeds via zwitterionic intermediate 79 (Equation R7)[196].

[R7] 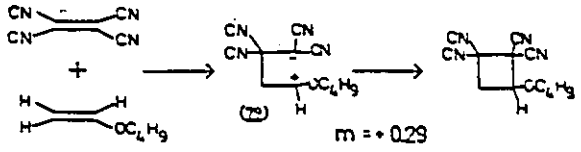

From the data in Figure R11, oxadiazolinone decomposition in either mode via zwitterionic intermediates is ruled out.

R2.4.2 Thermochemistry and Activation Parameters (Tables R4 and R5)

A brief look at the thermochemistry of these two processes is in order inasmuch as it relates to the position of the transition state on the reaction coordinate and is germane to discussion of the activation parameters. The heat of combustion of 5,5-dimethyloxadiazolinone was measured and used to calculate its heat of formation in the gas phase at room temperature (see Experimental E2.4.1). With a crude estimate for the entropy, data from standard tables, and the additivity principles of Benson[100-102], changes in the thermodynamic variables were calculated for each process. These are summarized in Table R4. From the lower part of the Table, it is plain that the thermodynamic entropy changes, $\Delta S°$, are quite large; about +26 and +58 entropy units for the two and three piece fragmentations, respectively. The calculated free energy changes of -7 and -48 kcal mol^{-1} differ by 41 kcal. This may be contrasted with the difference in the free energies of activation — a difference of about 1 kcal mol^{-1} in the nonpolar solvent, toluene (Table R5).

A further consequence of the thermodynamic estimates from Table R4 is that, exothermic as it is, fragmentation to the three very stable products — acetone, carbon monoxide, and nitrogen — is not sufficiently exothermic to populate excited states of any products. The lowest available electronically excited state would be the acetone $n\pi^*$, with respective singlet and triplet energies of 85 and 78 kcal mol^{-1} above the ground state.[182] Dioxetane thermolysis produces triplet acetone (with a few per cent singlet)

Table R4. Gas phase thermochemistry of 5,5-dimethyl-Δ^3-1,3,4-oxadiazolin-2-one.[a]

	$Me_2\overset{+-}{C}NN$	+	CO_2	⟵	1-Me_2	⟶	N_2	+	CO	+	Me_2CO
ΔH_f° (gas)	47 ± 5[b]		-94.1		-48 ± 2		0		-26.4		-51.7
S_{298}°	75[c]		51.1		ca 100 ± 10[d]		45.8		42.2		70.5

ΔH°	1 ± 7	-30 ± 2
ΔS°	26 ± 10	58 ± 10
ΔG_{298}°	-7 ± 10	-48 ± 5
ΔG_{358}°	-9 ± 11	-51 ± 6
ΔH_{max}[e]	-26 ± 7	-61 ± 2
ΔG_{max}[e]	-38 ± 12	-79 ± 7

[a] Data for acetone, CO, N_2, and CO_2 from ref. 316. Units are kcal mol^{-1} (ΔH, ΔG) or cal mol^{-1} K^{-1} (ΔS, S) throughout.

[b] $\Delta H_f^\circ(Me_2CNN) = \Delta H_f^\circ(H_2CNN) + \Delta H_f^\circ(Me_2CO) - \Delta H_f^\circ(H_2CO) = 71 \pm 5 - 51.7 + 27.7 = 47.0 \pm 5$ kcal mol^{-1} (ref. 101).

[c] Analogous to footnote b, for $S_{298}^\circ = 58.1 + 70.5 - 53.7 = 74.9$ cal mol^{-1} K^{-1} (ref. 101).

[d] Compare to S_{298}°(cyclopentane) = 70.0, (1,1-dimethylcyclopentane) = 85.4, and (cyclopentene) = 69.2 cal $mol^{-1}K^{-1}$ (ref. 101).

[e] Energy difference between transition state and products at 85°C, assuming $\Delta H^\ddagger$ and $\Delta G^\ddagger$ for toluene (Table R5) apply to the gas phase.

Table R5. Activation parameters for thermolysis of 5,5-dimethyloxadiazolinone over the temperature range 50-95°C.[a]

Solvent	Diazopropane Formation		Acetone Formation	
	$\Delta H^{\ddagger}$	$\Delta S^{\ddagger}$	$\Delta H^{\ddagger}$	$\Delta S^{\ddagger}$
Toluene	27.1 ± 0.4	-4.7 ± 1.0	30.3 ± 0.3	7.4 ± 0.9
Acetonitrile	25.1 ± 1.0	-6.3 ± 2.7	29.3 ± 1.7	1.8 ± 4.7
Trifluoroethanol	23.4 ± 0.15	-6.6 ± 0.4	32.3 ± 1.5	8.5 ± 4.3
Trifluoroacetic acid	20.8 ± 0.5	-9.9 ± 1.4	---	---

[a]Crude data found in Table A3.5, Appendix 3. All errors are those returned by linear least squares analysis. Units are kcal mol^{-1} and cal mol^{-1} K^{-1} for ΔH and ΔS, respectively. Correlation coefficients were all better than -0.993, averaging -0.998.

whose phosphorescence (and minor fluorescence) can be observed in degassed samples.[182] However, using a single photon counting apparatus, chemiluminescence could not be detected during thermolysis of 1-Me_2. Based on that experiment, an upper limit to the yield of excited state acetone was set at 10^{-7} to 10^{-8} percent (see Experimental E2.4.2 for details).

Historically, activation parameters have often been employed as a guide to the mechanism of similar unimolecular fragmentations[43,220]. It is not uncommon for concerted cycloreversions (for example, the retro-Diels-Alder reaction) to show small or even negative entropies of activation as the cycle is still complete at the transition state. For ketone formation, very little of the large positive thermodynamic entropy change of +58 entropy units is realized at the transition state: $\Delta S^{\ddagger}$ varies from +2 to +10 eu (Table R5). Although the entropy of activation is expected to be positive if the reaction proceeds through a floppy biradical intermediate, it should not be as large as the $\Delta S°$ for the whole fragmentation process. It is impossible to say, a priori, where, in the range $0 < \Delta S^{\ddagger} < +58$ eu, the borderline between a concerted mechanism and a stepwise alternative, via a biradical intermediate, would lie. For this reason, other types of evidence were sought.

For diazoalkane formation, the activation entropies (-5 to -10 eu) have neither the sign nor magnitude of the thermodynamic value of +28 eu. Here, the increasingly negative values of $\Delta S^{\ddagger}$, as solvent polarity increases, could be interpreted as arising from increased ordering of the solvent shell around the moderately polar

transition state for this process. In this case, biradicals could not account for the trend.

R2.4.3 Secondary Deuterium Kinetic Isotope Effects (Table A3.6)

The β-deuterium kinetic isotope effects measured for 1-$(CD_3)_2$ were 2.1 ± 0.3 and 1.3 ± 0.4 per cent per deuterium for diazopropane-d_6 and acetone-d_6 formation, respectively. Although small, these values are significant[94-98] and imply that a bond involving C5 is broken in the rate-determining step of each process. These would be the O1-C5 and N4-C5 bonds, respectively. There are no reasonable transition states which do not involve rupture of a bond to C5 but which could account for this isotope effect. Steric or ponderal effects of isotopic substitution are ruled out by the absence of an alkyl steric effect on either process (vide infra).

I2.4.4 Alkyl Substituent Effects (Table A3.7)

There is no correlation of rate constants for nine 5,5-dialkyl substituted oxadiazolinones with Taft steric parameters, E_S[315] for either ketone formation or diazoalkane formation. The reason for the scatter plots obtained is that the data are much better fitted by inductive parameters, σ*, for the alkyl substituents. For diazoalkane formation, $\rho^* = -1.27 \pm 0.06$ ($r = -0.993$), but there is no significant correlation of the rate of ketone formation with σ* — much like the Hammett plot for that reaction shown in Figure R12.

I2.4.5. Aryl Substituent Effects (Table A3.8, Figures R12 and R13)

For the seven para substituted 5-aryl-5-methyloxadiazolinones

(1-Me,Ar) studied, both electron withdrawing and electron donating substituents mildly accelerate ketone formation. The range of rate is only a factor of two, and the rho value is not significantly different from zero: -0.13 ± 0.12 (r = -0.402) (see Figure R12). This erratic behaviour is not unlike that observed for bis(aryl-methyl)diazene (20) fragmentation to benzyl radicals, or trans-3,5-diphenylpyrazoline (18) decomposition[114] (see Table I2, page 14) and could be interpreted as suggesting that ketone formation involves rate determining creation of a radical centre at C5*. On the other hand, scatter plots are to be expected from ketone formation if the isokinetic temperature lies in the range studied (50-85°C).

In complete contrast, diazoalkane formation gives an excellent fit to inductive parameters. A rho value of -1.93 is obtained with log k plotted against a 50/50 mixture of sigma and sigma plus (Figure R13). The utility of blending the sigma parameters in cases where a full positive charge is not achieved in the products has been discussed elsewhere.[315,317]

R2.5 Mechanism of Diazoalkane Formation

At first sight, a build-up of positive charge at C5 of the transition state is quite difficult to rationalize as CNDO calculations (see Methods, Results and Discussion R1) confirm that

*Interestingly, the relative rates of all five β-aryldiazene systems found in Table I2 are in identical temperature independent orders: Ph>Cl(1.92)>CH_3O(1.48)>CH_3(1.38)>H(1.0) (where the bracketted numbers refer to pyrazoline 18 ratios at 80° — the best model for oxadiazolinone aryl substituent effects), whereas oxadiazolinone relative k_3 at 50° are in a different order: CH_3(2.04)>Ph(1.94)>Cl(1.27)>H(1.0), with values different from those of the model. This may be a subtle clue that a different mechanism operates in the ketone forming reaction than in radical forming reactions.

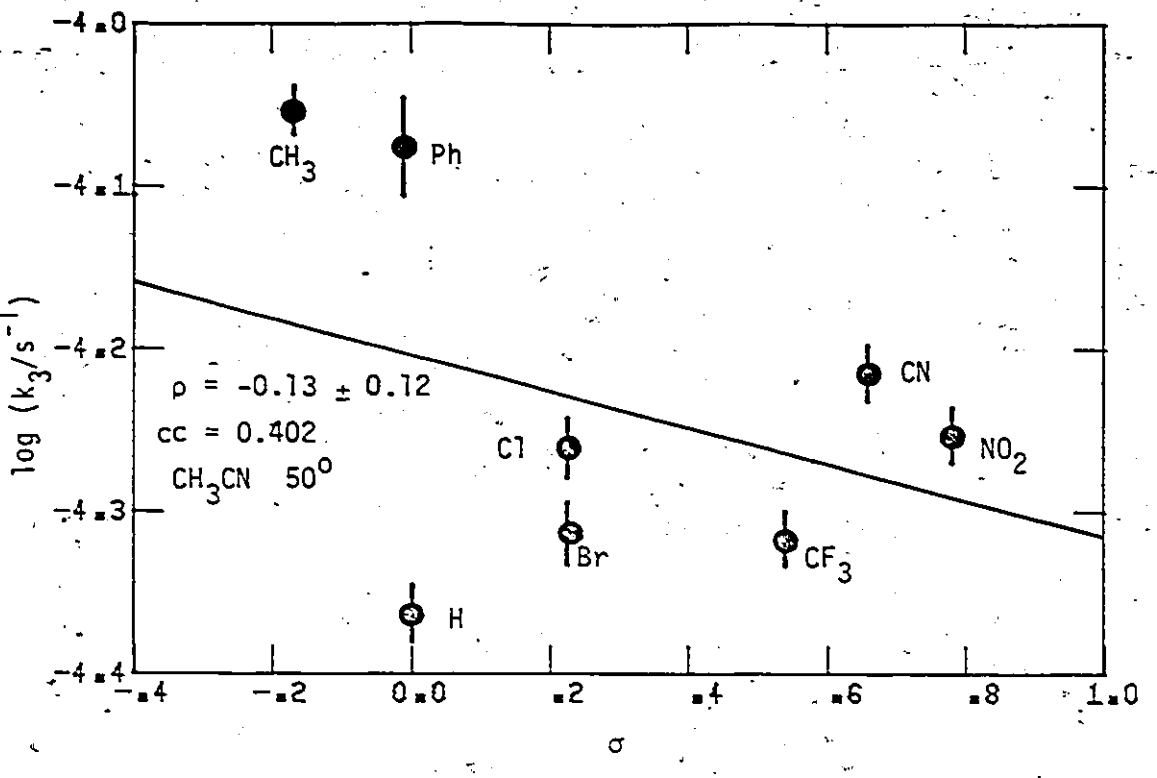

Figure R12. Hammett plot for ketone formation from 1-Me,Ar.

Figure R13. Hammett plot for diazoalkane formation from 1-Me,Ar.

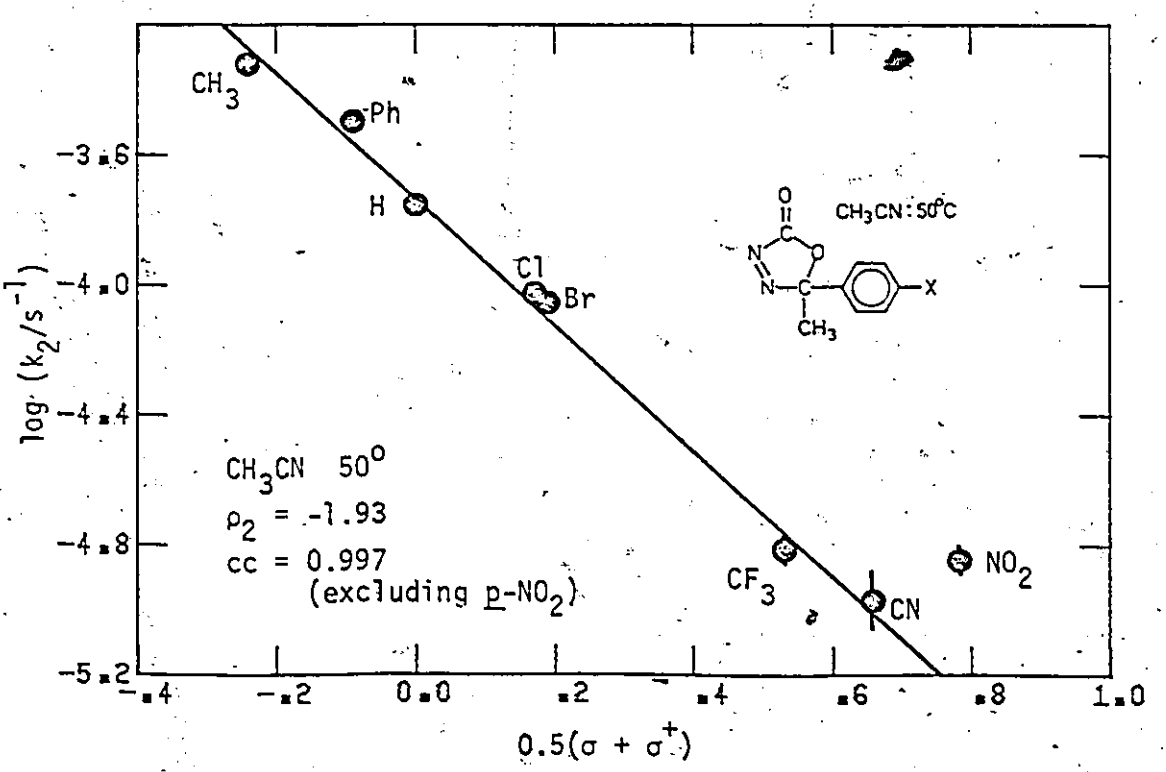

the corresponding carbon of the diazoalkane is most definitely negative in net charge density relative to C5 of the oxadiazolinone. For the hypothetical 1-H_2 in Figure R14, the calculations give a net charge density of +0.17 at C5 while in diazomethane, the same carbon is -0.26 in net charge. Notwithstanding the fact that the calculations only refer to gas phase molecules, a rho value of -1.93 measured in acetonitrile must surely mean that the net charge on C5 increases and passes through a value greater than +0.17 at the transition state. This is only consistent with some degree of O1-C5 bond heterolysis at the transition state. Both the solvent effects and the intermediate size of this Hammett rho rule out a zwitterionic intermediate sporting a full positive charge at C5. The reaction must therefore be concerted with more O1-C5 than C2-N3 cleavage at the transition state (Figure R14).

Consideration of the reverse of fragmentation, cycloaddition, tends to confirm this deduction. Fragmentation to give carbon dioxide and diazoalkane is formally a retro-1,3-dipolar cycloaddition. Thanks to the work of Fukui[42,46,48,54], Houk[59,60,63,64] and Huisgen[65-67], the stereoselectivity of the cycloaddition reaction is understandable in terms of Frontier Molecular Orbital (FMO) Theory and a concerted mechanism.

Examination of the frontier orbitals of CO_2 and diazomethane shown in Figure R14 predicts that their major cyclization product (path a) would be the wrong regioisomer 157 resulting from the largest orbital extension between the two biggest lobes — on the

carbon atoms. However, by the Principle of Microscopic Reversibility,[315] the fragmentation in question must share the same transition state as the cyclization to give that regioisomer (path ~~b~~). Now the greatest frontier density is found between the CO_2 carbon and the terminal nitrogen — predicting a transition state with more C2-N3 than O1-C5 bond formation, in precise agreement with the experimental deduction of transition state structure. One then concludes therefore, that diazoalkane formation occurs via a non-synchronous but concerted mechanism.

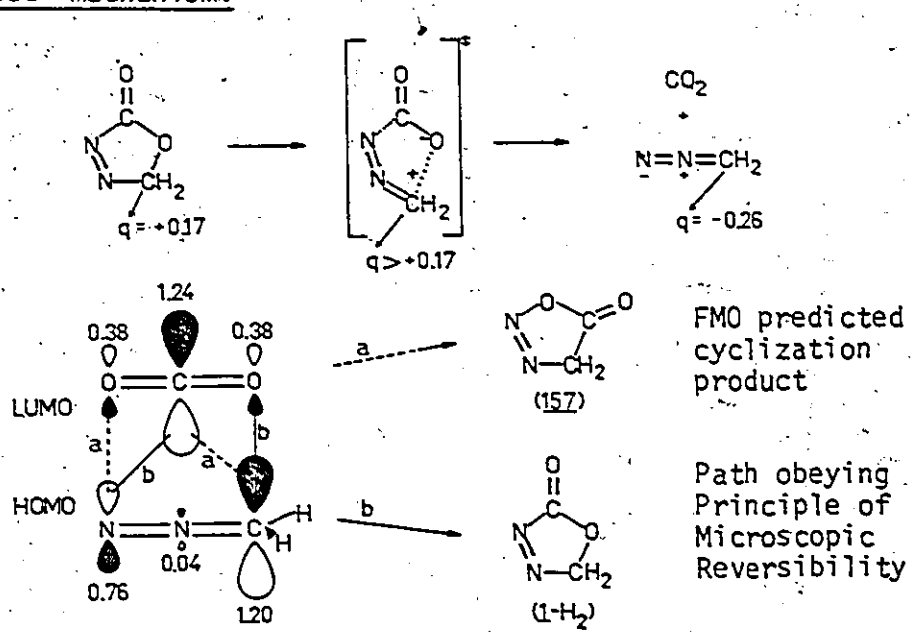

Figure R14. Charge densities (q) and frontier MOs for cycloaddition.

R2.6 Mechanism of Ketone Formation

A large number of possible mechanisms are still consistent with the information presented so far. A few reasonable alternatives to a fully concerted mechanism are: prior loss of one of the three stable fragments to give either a biradical or a closed shell species which rapidly decays to products; or a pre-equilibrium one bond

scission to give a biradical.

Even at ambient temperature (ca. 50°C) and low ionizing voltages (ca. 10 eV), the mass spectrum of 1-Me_2 shows no evidence for fragment ions at P-28 (loss of N_2 or CO), nor any metastables for P → P-28. A parent ion is also not observed. Like the parent ion, if such intermediates occur, their lifetimes must be of the order of a microsecond[318]. If they do not occur for ionized oxadiazolinone at 10^{-5} torr in the gas phase, it seems unlikely they could be significant in the solution thermolysis of oxadiazolinones.

Both a stepwise process via reasonable biradicals like 155 or 158 or a concerted mechanism, would be consistent with the observed solvent effects and β-deuterium kinetic isotope effect.

(155) 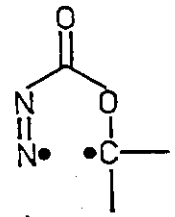 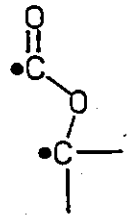 (158)

The Hammett plot (mis)behaviour possibly favours a biradical, while the low activation entropies tend to favour a concerted mechanism. No esr signals attributable to intermediate radicals or biradicals were observed when 1-Me_2 was thermolysed in the presence or absence of nitrosobenzene. Furthermore, chemically induced dynamic nuclear polarization (CIDNP) effects were not observed in the cmr of decomposing solutions of 1-Me_2 which was 90% labelled at C5 with ^{13}C (Experimental E2.4.3 and E2.4.4).

The observation of CIDNP in the products of a reaction is a diagnostic test for participation of a radical pathway[10-20].

CIDNP from 1,5-biradicals is quite rare because, in most cases, the ends of the biradical cannot get far enough apart to reduce their electron exchange coupling, $<|2J|>$, to the order of the Zeeman energy, $g\beta H_o$[21]. Furthermore, diradicals must usually be born in the triplet state in order that a net intersystem crossing to singlet (concomitant with nuclear spin coupling effects) occur prior to formation of diamagnetic products.[22,23]

Most reasonably, any diradical formed in thermolysis would be born singlet, and would, therefore, have to intersystem cross and then fragment to triplet products for CIDNP to be observed. In the fifteen year history of the phenomenon, CIDNP from 1,5-biradicals has only been reported for biradicals born as triplets[10-23]. However, the singlet 1,5-biradical 155 has unusual potential to display CIDNP effects by intersystem crossing and fragmentation, because one of the products (ketone) has a low-lying triplet state. When both C5 substituents are methyl, the thermochemistry suggests that there is actually insufficient energy for formation of triplet ketone. Nevertheless, other heterocyclic ring systems which do show chemiluminescence might be a source for this, as yet unrecognized, type of CIDNP from thermally generated biradicals. There may well be a solvent effect on the CIDNP intensity from biradicals which is perhaps due to alterations is $<|2J|>$[22], but neither chlorobenzene nor methylene iodide solvent (heavy atoms are expected to enhance singlet-triplet mixing) gave rise to any enhanced absorption or emission in ^{13}C spectra obtained during decomposition, even of the labelled substrate, which is expected

to be more sensitive. Photo-CIDNP, on the other hand, may be more likely if 1,5-biradicals are intermediates in the photodecomposition of these compounds.

Penultimately, if the biradical 155 were reversibly formed, racemization might occur during decomposition of starting material optically active at C5. To this end, the two oxadiazolinones, 159 (Scheme R1), were prepared from the semicarbazone of d-camphor. Their stereochemistry was assigned on the basis of a large downfield shift of the signal corresponding to the syn methyl group at C7 of the exo-azo isomer 159a. Models show that these protons spend time in the deshielding region of the azo pi bond and so absorb at an extra 0.5 ppm downfield from the analogous protons in the endo-azo isomer 159b (see Experimental E2.4.5). If biradicals were formed reversibly and if bond rotation (and inversion, for a non-planar radical centre) competed with decomposition, interconversion of exo-azo and endo-azo isomers could occur during decomposition (Scheme R1). Such interconversion was not observed by pmr during thermolysis of the pure exo-azo isomer, suggesting that rotation/inversion with return does not occur, although either rotation/inversion or return might occur.

A wide variety of experiments, including attempted trapping, esr, CIDNP, and racemization, have failed to detect or infer the existence of a biradical intermediate in the three bond fragmentation of oxadiazolinones.

Finally, the effect of phenyl stabilization on k_3 provides the most definitive result obtained. From the activation parameter

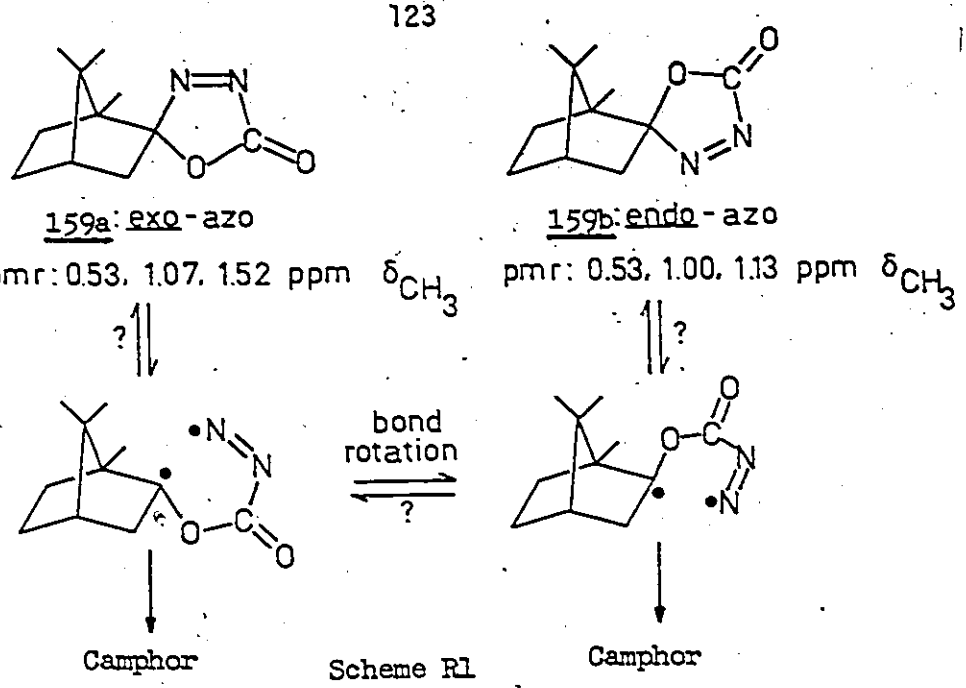

Scheme R1

data found in Table R5, the ketone forming rate constant for 1-Me_2 in acetonitrile at 50° is computed to be 2.54 X 10^{-7} s^{-1}. Thus, k_3(1-Me,Ph)/k_3(1-Me_2) = 170, corresponding to $\Delta\Delta G^{\ddagger}$ = -3.3 kcal mol^{-1}. Table R6 lists the corresponding information for three models (2 acyclic diazenes and one pyrazoline) which most certainly generate at least one radical centre at a phenyl-bearing carbon in the rate determining step.

If thermolyses of these three models are assumed to involve concerted nitrogen loss (as seems likely — see Introduction), then the $\Delta\Delta G^{\ddagger}$ per phenyl group in the models is twice as large as in oxadiazolinone. If the model nitrogen extrusions were stepwise, then the oxadiazolinone effect would be even more discrepant!

It could be argued that the ring oxygen is somehow responsible for this difference. Regrettably, similar data is not yet available for oxadiazolines. However, since the $\Delta\Delta G^{\ddagger}$ per acetyl group in the trans-azoalkane pair 36 and 160 is a negligibly

Table R6. Phenyl stabilizations of $\Delta G^{\ddagger}$ for several diazene systems.[a]

System	R	Solvent	$\Delta H^{\ddagger}$	$\Delta S^{\ddagger}$	Ref.[b]	$\Delta G^{\ddagger}$	$\Delta\Delta G^{\ddagger}$ per Ph
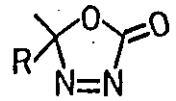	CH_3	CH_3CN	29.3	1.8	this work	28.7	-3.3[c]
	Ph	CH_3CN			this work	25.4	
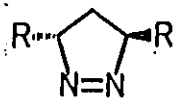	CH_3	(gas)	39.4	5.6	186	37.5	-5.8
	Ph	not given	27.0	3.5	193	25.9	
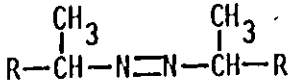	CH_3	(gas)	46.9	14.4	319	42.3	-6.3
	Ph	PhEt	31.8	6.7	320[d]	29.6	
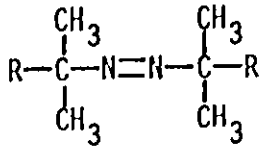	CH_3	Ph_2O	42.2	16.2	321	37.0	-5.8
	Ph	toluene	29.1	11.3	322	25.4	

[a]Units of $\Delta H^{\ddagger}$ and $\Delta G^{\ddagger}$ are kcal mol^{-1}, of $\Delta S^{\ddagger}$ cal mol^{-1} K^{-1}. All $\Delta G^{\ddagger}$ evaluated at 50°C.

[b]Activation parameters computed from original data using ln (k/T) vs 1/T (see Appendix 2).

[c]Refers to ketone formation, k_3.

[d]Data available for only two temperatures: 100.4° and 110.3°.

small +0.1 kcal[114], it would be most surprising if the adjacent lactonyl group in oxadiazolinones very greatly upset the expected phenyl stabilization for a radical centre at C5.

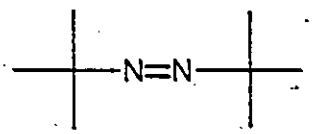

(36)

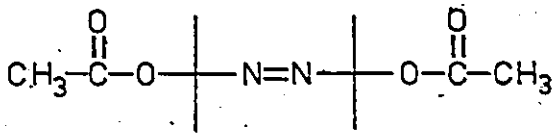

(160)

If a radical or charge centre is not developed at C5, but the N4-C5 bond is ruptured in the rate limiting step, why does a C5 phenyl group lower the reaction barrier? In a concerted ketone forming reaction, the C5 phenyl should lower the activation energy by some fraction of the several kcal by which the reaction is more exothermic due to phenyl-carbonyl resonance stabilization in the product ketone.

Concerted formation of α-lactone 156 is most unlikely, given the lack of stereospecificity of cyclopropane formation from pyrazolines, which is indicative of intervening 1,3-biradicals (see Introduction I2.3). Such lactones are known to polymerize at low temperature, and are quantitatively ring opened by nucleophilic solvents (Equation R8).[233] No methoxyacid analogous to 161 was observed when dimethyloxadiazolinone was thermolysed in methanol[259] (18% ketone formation observed).

[R8]

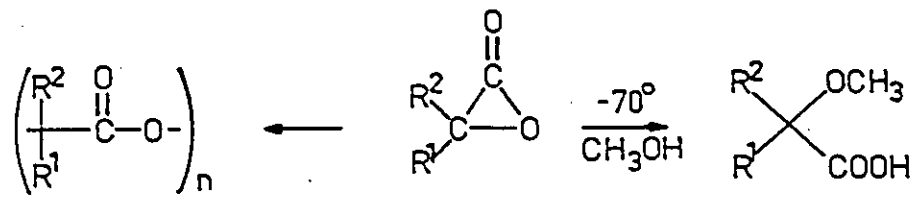

polymer (156) (161)

Therefore, after eliminating all other mechanistic alternatives to ketone formation, one must conclude that the three body fragmentation of oxadiazolinones is concerted. At the present time there is insufficient information to detail the precise transition state structure beyond this statement — nonsynchroneity will have to be assessed by ring heavy atom kinetic isotope effects. The evidence presented in this chapter is the most compelling evidence to date relating to the mechanism of three-piece fragmentations of five-membered ring diazenes. Of the available examples of such reactions enumerated in the I2.6 and I2.7 Introductions, only three cases could be said to be of mechanistic import. Rees (1973)[247] noted that 3-piece fragmentation of 120 was stereospecific (Equation I53, page 59), but reported no kinetics. West (1967)[260,261] found a rho value for 3-piece fragmentation of 128 to be +0.6 (3 substituents, Equation I62, page 63), and conceded that his study was inconclusive. Most recently, Cakelkova-Taguchi (1977)[267] assigned mechanisms for 3 body decomposition of systems 131 entirely on the basis of solvent effects and $\Delta S^{\ddagger}$ values (Equation I65, page 66). How general the

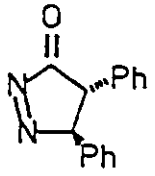

(120)

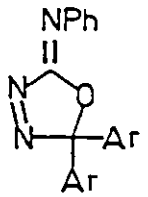

(128)

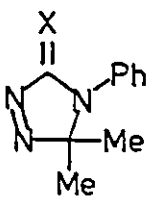

(131; X = O, S, NPh)

concerted mechanism is remains to be tested, but these systems are not all that different from one another.

R2.7 On the Variety of Product Types From Thermolyses of 5-Membered Ring Diazenes

In the series of 5-membered ring diazenes, many different reaction types have been observed (specific references may be found in Introduction I2). Δ^1-Pyrazolines, most Δ^3-1,3,4-oxadiazolines, and some thiadiazolines give products (3-membered rings in particular) which are consistent with intervention of biradicals. Some Δ^3-1,3,4-thiadiazolines as well as 2-methylene-Δ^3-1,3,4-oxadiazolines undergo 1,3-dipolar cycloreversion, retaining the nitrogen atoms in a diazoalkane product formed concurrently with a thiocarbonyl or carbonyl compound, respectively. Although Δ^1-pyrazolines are synthesized by 1,3-dipolar cycloaddition between diazoalkanes and olefins these reactions are never reversible. West found 2-phenylimino-Δ^3-1,3,4-oxadiazoline (128) to exhibit diazoalkane formation in competition with a three piece fragmentation,[260,261] similar to oxadiazolinones. All three systems studied by Cabelkova-Taguchi (Δ^1-1,2,4-triazolin-3-one and -3-thione, and 3-phenylimino-Δ^1-1,2,4-triazoline: 131)[267], together with 120 and its 4,5-dehydro derivative 117 (Equation I52, page 59) show only three-piece fragmentation. Why is this? What factors influence the direction of fragmentation from molecule to molecule (this thesis has already examined the factors such as temperature, solvent, and substitution within one particular molecular type)? Can useful predictions be made for as yet unseen cases? This section addresses these issues from a thermodynamic standpoint.

It is extremely enlightening to consider the thermochemistry of competetive 2-and 3-piece fragmentations in related cyclic diazenes. To do this is not simple: unfortunately, only two heats of formation of 5-membered ring diazenes have been measured: 3,3,5,5-tetramethylpyrazoline (61) by Engel (1976)[82] and 1-Me_2 as reported earlier in Section R2.4.2 of this discussion. Consequently, group equivalents for use in thermodynamic additivity schemes are very few in number. To overcome this obstacle, the present discussion will be founded upon two homemade sets of relative extrusibilities for various molecular fragments (Table R7) and conjugative interactions between functional groups (Table R8). These numbers can be manipulated with the scarce available data and data for appropriate model compounds to estimate thermodynamic quantities of interest for diazenes and their reactions. The reliability of the method will be established by suitable tests.

R2.7.1 A Relative Extrusibility Scale From Group Values

The thermodynamic additivity concepts of Benson[100-102], and particularly the group values found in his 1976 text[102], together with heat of formation data in his 1969 paper,[100] provide a reasonable basis from which to estimate changes in thermodynamic parameters for a number of similar reactions. Group values are not intrinsic properties: Benson's scales are anchored by numerous assigned values, making it virtually impossible to estimate values for missing groups. For a consistent set of these very interdependent values, only the 1976 compilation will be used, and in cases where

absent group equivalents prohibit a certain calculation, the fact will be noted. All unreferenced heats of formation used in the following discussion are available from the Benson references, either directly measured, or reliably computed from group equivalents. Space limitations prohibit including the detail of any straightforward computations. Units are universally assumed to be kcal mol^{-1} for G and H and cal mol^{-1} K^{-1} (eu) for S, and will not always be explicitly carried.

Consider Equation R9 to describe a general extrusion reaction which releases a fragment X (which could be N_2, CO_2, CO, a ketene, a carbene, or any of a host of mono- or multinuclear fragments). The driving force for the extrusion is the free energy change $\Delta G°$,

[R9] $$R—X—R' \rightarrow R + X + R'$$

but if various X are to be compared for constant R and R', <u>entropy changes will be approximately independent of X</u>, making differences between $\Delta G°$ and $\Delta H°$ very similar. It is both convenient and instructive to establish as the model process, Equation R9, where R=R'=C-CH_2-, a carbon fragment whose group equivalents [C-(X)(C)$(H)_2$] are readily available.

Now, the model reaction is represented by Equation R10, and Equation R11 arbitrarily defines a <u>relative</u> scale of extrusibilities: $\Delta H°_{ex}(X)$, in which the constant contribution of the co-fragments to the heat of reaction may be ignored. Importantly, <u>162</u> is not a molecule in this formalism, but rather a generalized molecular fragment (GMF), whose heat of formation $\Delta H°_f$(GMF) can be calculated

by summing the group equivalents for two $[C\text{-}(X)(C)(H)_2]$ and one $[X\text{-}(C)_2]$ (see examples below next paragraph).

[R10] $$C-CH_2-X-CH_2-C \longrightarrow C-CH_2\cdot + X + \cdot CH_2-C$$
$$\underline{162}\ \text{GMF(X)}$$

[R11] $$\Delta H^\circ_{ex}(X) = \Delta H^\circ_f(X) - \Delta H^\circ_f(\text{GMF})$$

The advantage of a relative enthalpy scale for a related set of reactions is that enthalpy contributions from ring strain, gauche interactions, eclipsed groups, or other factors are all approximately constant and cancel when two extrusions are compared. Under the assumption that similar extrusions occur by a concerted mechanism, differences in ΔH°_{ex} may be used to predict or explain differences in $\Delta H^{\ddagger}_{obs}$, using the Hammond Postulate[324], thereby achieving a bridge between thermodynamics and kinetics. Even if the extrusion mechanisms are not concerted or are not even the same, the relative extrusion scale may still be anchored using one known $\Delta H^\circ_{r(eaction)}$, and approximate ΔH°_r computed for other cases. If, in so doing, ΔH°_r is found to be excessively endothermic, the relative extrusion scale will have predicted that the corresponding reaction cannot occur.

As examples of ΔH°_{ex}, consider the cases for $X=N_2$ and $CH\equiv CH$ below:

-X-:	$-N\equiv N-$	$-CH\equiv CH-$
GMF:	$C-CH_2-N\equiv N-CH_2-C$	$C-CH_2-CH\equiv CH-CH_2-C$

groups	ΔH°_f		ΔH°_f
$2[N_A\text{-}C]$	27.0 X 2	$2[C\text{-}(C_d)(C)(H)_2]$	-4.76 X 2
$2[C\text{-}(N_A)(C)(H_2)]$	-6.0 X 2	$2[C_d\text{-}(C)(H)]$	8.59 X 2
	$\Delta H^\circ_f(GMF) = 42.0$		$\Delta H^\circ_f(GMF) = 7.66$
	$\Delta H^\circ_f(N_2) = 0.0$		$\Delta H^\circ_f(CH{\equiv}CH) = 54.19$
$\Delta H^\circ_{ex}(N_2) = \Delta H^\circ_f(N_2) - \Delta H^\circ_f(GMF)$			$\Delta H^\circ_{ex}(CH{\equiv}CH) = 46.53$
$= -42.0$			

Thus, extrusion of molecular nitrogen is 88.5 kcal more exothermic than extrusion of acetylene from the olefinic analogue (all other factors being equal). Note that this energy difference is greater than the 54.2 kcal mol^{-1} difference between the stabilities of the products: both $\Delta H^\circ_f(GMF)$ and $\Delta H^\circ_f(X)$ are important to ΔH°_{ex}. Twenty-two such extrusions spanning 150 kcal have been compiled in Table R7. These ΔH°_{ex} data do not correlate at all with the heat of formation of the fragment. The last two columns of the Table show the effect of methyl or phenyl substitution on ΔH°_{ex}, which usually lowers ΔH°_{ex} by stabilizing the products through resonance. Such correlations are reasonably important for the upcoming analysis of diazene fragmentations, but are not available for some key cases. In those instances, very rough estimates for $\delta\Delta H$ are needed, and the error in the result is necessarily higher.

In their 1967 tome on extrusion reactions, Duke and Stark approximately ranked the ease of extrusion of inorganic molecules as $N_2 > CO_2 > CO > SO > SO_2 > O_2 > S > O$, provided the mechanisms remain comparable[325]. In reasonable agreement, Table R7 quantifies

Table R7. Relative heats of extrusion ($\Delta H°_{ex}$) of various molecular fragments.

Case	-X- in GMF[a]	$\Delta H°_f$(GMF:X)	X	$\Delta H°_f(X)_{obs}$	$\Delta H°_{ex}$	$\delta\Delta H_{Me}$[b]	$\delta\Delta H_{Ph}$[c]
a		42.0		0	-42.0		
b		-16.76		-27.90[d]	-11.15		—
c		-91.5		-94.05	-2.55		
d		-90.43		-90.5	-0.1		—
e		-85.93		-83.6	2.3	-2.4	—
f		-145.33		-137.9	7.4		
g		-63.23		-51.7	11.5		
h		18.53		32.3	13.8		
i		-85.10		-70.9	14.2		
j		-41.8		-26.4	15.4		
k		-26.97		-11.4	15.6		—
l		-44.33		-26.0	18.3	-3.4	-12.7
m		-49.0		-27.90[d]	21.1		
n		11.92		35.9	(24.0)[e]		
o		-25.2		0.0	25.2[f]		
p		-2.73		22.6[g]	25.3	N:-4.0 C:+0.9	-10.4
q		-29.85		1.5	31.4		
r		-19.72		12.50	32.2	+0.8	-3.2
s		37.07		71	33.9		
t		-46.73		-11.4	35.3		
u		7.66		54.19	46.5		
v		-14.79		86±3	100.8[h]		-13.5

[a] See text for definitions and discussion. All units are kcal mol^{-1}.

[b] The effect of methyl substitution on $\Delta H°_{ex}$.

[c] The effect of phenyl substitution on $\Delta H°_{ex}$. In cases where missing group equivalents prevent calculation a dash is found.

[d] Reference 316.

[e] Due to lack of available data for unsubstituted compounds, this X contains a methyl group.

[f] $\Delta H°_{ex}(^1O_2) = \Delta H°_{ex}(^3O_2)$ + 22 kcal mol^{-1} (ref. 326).

[g] Calculated from group equivalents.[102]

[h] $\Delta H°_{ex}(^1CH_2) = \Delta H°_{ex}(^3CH_2)$ + 8 kcal mol^{-1} (ref. 327).

their qualitative observations.

It is also interesting to note that olefin extrusion (case r) is 13.3 kcal more favourable than acetylene extrusion, thereby accounting for the much more rapid decomposition of 120 and 121 compared to 117 and 122 in the pyrazolinone series (see Introduction I2.6, pages 59 to 60).

Another important factor which must be considered when attempting thermodynamic estimates is the effect of intergroup interaction, ΔH°_{int} (Table R8). This correction factor comes into play when the extruded fragment is not bound to two CH_2 groups (as defined in the GMF), but rather is adjacent to another functional group. Intergroup interactions may either stabilize or destabilize a molecule. For example, if two adjacent functional groups X and Y are both -CH=CH-, then a resonance interaction will lower the energy of R—X—Y—R, increasing $\Delta H^\circ_{ex}(X)$ or $\Delta H^\circ_{ex}(Y)$. In peroxides (X = Y = O) and hydrazines (X = Y = NR) adjacency is destabilizing, and ΔH°_{int} is positive (Table R8).

Interfragment interaction corrections (ΔH°_{int}; sometimes called conjugative interactions in this discussion) are computed from the difference between heats of formation of GMFs containing the same groups in different arrangements. For example, ΔH°_{int} (C=O/O) = ΔH°_f(163)-ΔH°_f(164)= -91.5 + 67.9 = -23.6 (Equation R12; row 1 column 4 in Table R8).

[R12] 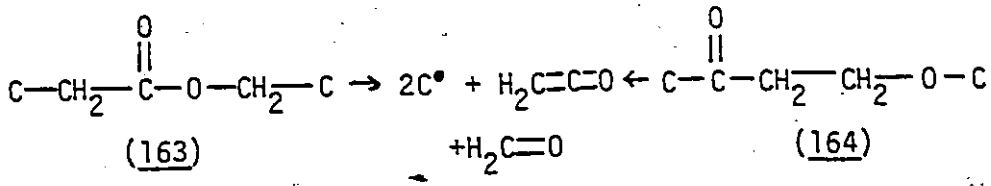

System 163 (which contains the same number of atoms as 164) is stabilized by 23.6 kcal due to the interaction (resonance) between carbonyl and oxygen groups. Both 163 and 164 may (in principle) decompose to the same products by eliminating one ketone plus one formaldehyde molecule in a multiextrusion reaction, but decomposition of 164 will be 23.6 kcal mol^{-1} less endothermic (or more exothermic) than decomposition of 163, the difference being due to $\Delta H°_{int}$ between CO and O. Significantly, $\Delta H°_{int}$ is only taken into consideration of $\Delta H°_{ex}$ when the bond between X and Y in R—X—Y—R is broken in any given reaction.

Table R8. Conjugative interactions ($\Delta H°_{int}$) in R—X—Y—R.[a]

X \ Y	-O-	-NH-	(-C≡N)[b] -C≡C-	C=O	O ‖ X—C—O-	O ‖ -C—O—X
-O-	37.4	——	-7.3	-23.6	-17.6	42.8
-NH-		11.0	——(7)[c]	-21.2[d]	——	——
-C≡C- (-C≡N)[b]			-3.6	-8.8	-3.4	-2.1
>C=O				4.4	5.1	-7.1
O ‖ Y—C—O-					5.8	-1.1
O ‖ -C—O—Y						48.2

[a] See text for defintions. All values kcal mol^{-1}. Dash lines indicate unavailable group values. Negative numbers are stabilizing interactions which raise $\Delta H°_{ex}$.

[b] Equality of resonance interactions between C≡C and C≡N bonds arises from assumptions in the additivity method that C_I and C_d equivalents are the same.[100-102]

[c]Estimated from the trends in the table.
[d]$\Delta H°_{int}(NPh/C{=}O) \approx -16.4$.

R2.7.2 Testing the Method

From Tables R7 and R8, heats of formation and reaction may now be calculated for diazenes using appropriate models. Direct calculation is impossible and measurements are unreported. Estimating the heat of formation of dimethyloxadiazolinone constitutes a very tough challenge. Table R9 demonstrates that 8 very different 5-membered ring models yield an average $\Delta H°_f(\underline{1}\text{-}Me_2)_{est} = -50 \pm 3$. The roundabout method summarized in the Table has reproduced the observed heat of formation (-48 ± 2; see Table R4) within experimental error, and with a maximum error of only about 5 kcal! Fortunately, even in cases where two fragments of a model are replaced, not much accuracy is sacrificed. Nevertheless, it is desirable to emphasize results from models which require only one fragment switch to achieve a molecule of interest.

R2.7.3 2-and 3-Piece Fragmentations in Oxadiazolines

Having established in the preceding section that a relative scale of extrusions from generalized molecular fragments and a table of interfragment interactions can reproduce thermodynamic enthalpies to better than 5 kcal mol^{-1}, these concepts will now be applied to the various oxadiazoline systems whose studied chemistry is so perplexingly varied. The overall heat of reaction for 2- and 3-piece fragmentations of $\underline{1}\text{-}Me_2$ are about 1 and -30 kcal mol^{-1}, respectively, in the gas phase (Equation R13; Table R4, page 112).

Table R9. Models of the heat of formation of dimethyloxadiazolinone

Model	ΔH°_f(Model)	ΔH°_f(1-Me_2)	
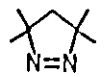	9.4	= ΔH°_f(Model) + ΔH°_f(GMF:X = CO_2) - ΔH°_f(GMF:X = $(CH_3)_2C{=}CH_2$) + ΔH°_{int} ($N{=}N/CO_2$)[a] = 9.4 - 91.5 + 34.69 - 3.4	= -50.8
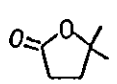	-111.43	= ΔH°_f(Model) + ΔH°_f(GMF:X = N_2) - ΔH°_f(GMF:X = CH_2CH_2) + ΔH°_{int}($N{=}N/CO_2$)[a] = -111.43 + 42.0 + 19.72 - 3.4	= - 53.1
	-62.90	= ΔH°_f(Model) + ΔH°_f(GMF:X = N_2) - ΔH°_f(GMF:X = CH_2CH_2) + ΔH°_f(GMF:X = CO_2) -ΔH°_f(GMF:X = H_2CO) + ΔH°_{int}($N{=}N/CO_2$)[a] = -62.90 + 42 + 19.72 - 91.5 + 44.33 - 3.4	= - 51.7
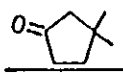	-60.47	= ΔH°_f(Model) + ΔH°_f(GMF:X = N_2) - ΔH°_f(GMF:X = CH_2CH_2) + ΔH°_f(GMF:X = $(CH_3)_2CO$) -ΔH°_f(GMF:X = $(CH_3)_2C{=}CH_2$) + ΔH°_{int}($N{=}N/CO_2$)[a] + ΔH°_{int}($C{=}O/O$)[b] = -60.47 + 42 + 19.72 - 63.23 + 34.69 - 3.4 - 23.6	= -54.3
	-46.52	= ΔH°_f(Model) + ΔH°_f(GMF:X = N_2) - ΔH°_f(GMF:X = CH_2CH_2) + ΔH°_f(GMF:X = CO_2) -ΔH°_f(GMF:X = $(CH_3)_2C{=}CH_2$) + ΔH°_{int}($N{=}N/CO_2$)[a] = -46.52 + 42 + 19.72 - 91.5 + 34.69 - 3.4	= -45.0
	-19.29	= ΔH°_f(Model) + ΔH°_f(GMF:X = N_2) - ΔH°_f(GMF:X = $CH{=}CH$) + ΔH°_f(GMF:X = CO_2) -ΔH°_f(GMF:X = $(CH_3)_2C{=}CH_2$) + ΔH°_{int}($N{=}N/CO_2$)[a] = -19.29 + 42.0 - 7.66 - 91.5 + 34.69 - 3.4	= -45.2
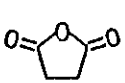	-122.6	= ΔH°_f(Model) + ΔH°_f(GMF:X = N_2) - ΔH°_f(GMF:X = CH_2CH_2) + ΔH°_f(GMF:X = C-Me_2) -ΔH°_f(GMF:X = CO) + ΔH°_{int}($N{=}N/CO_2$)[a] - ΔH°_{int}(CO/O_2C)[c] = -122.6 + 42.0 + 19.72 + 41.8 - 29.76 - 3.4 + 7.1	= -45.1
	-81.61	= ΔH°_f(Model) + ΔH°_f(GMF:X = N_2) - ΔH°_f(GMF:X = $CH{=}CH$) = -81.61 + 42.0 - 7.66	= -47.3

[a] $\Delta H^\circ_{int}(N{=}N/CO_2) \equiv \Delta H^\circ_{int}(C{=}C/CO_2)$ assumed. Found in row 3, column 5 of Table R8.

[b] See row 1, column 4, Table R8.

[c] See row 4, column 6 in Table R8.

AVG = -50±3
OBS = -48±2

[R13]

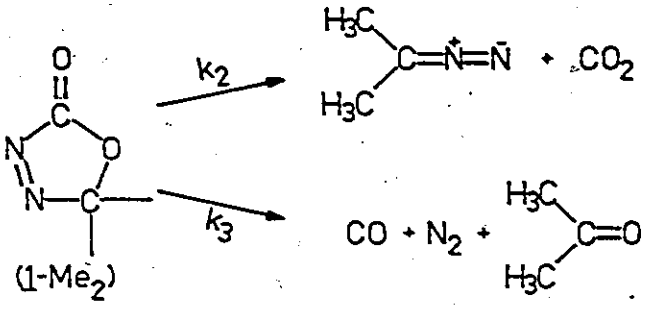

$H_2^\circ = 1 \pm 7$ (observed)

$H_3^\circ = -30 \pm 2$

[R14]

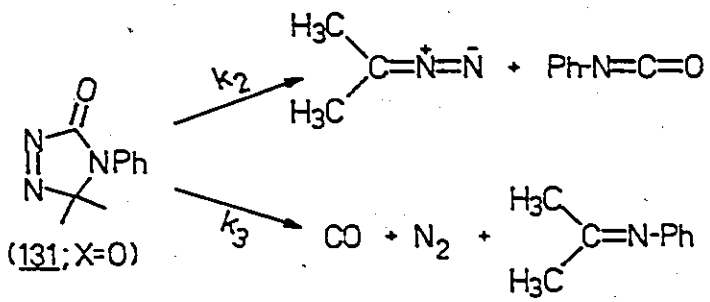

$\Delta H_2^\circ = 13.1$ (estimates)

$\Delta H_3^\circ = -22.4$

These values may now be used to estimate the corresponding values for triazolinone 131:X=O (Equations R15 to R16). Note that because the N1-C2 bond is only broken in the three body fragmentation, ΔH°_{int} corrections are needed for ΔH°_3 but not for ΔH°_2.

[R15] $\Delta H^\circ_3(\underline{131}:X=O)_{est} = \Delta H^\circ_3(\underline{1}\text{-}Me_2)_{obs} - \Delta H^\circ_{ex}(Me_2C{=}O) + \Delta H^\circ_{ex}(HN{=}CH_2) + \delta\Delta H_{Ph}$ (on N in $RN{=}CH_2$) + $2\delta\Delta H_{Me}$ (on C in $HN{=}CR_2$) + $\Delta H^\circ_{int}(C{=}O/O) - \Delta H^\circ_{int}(C{=}O/NPh) = -30 - 11.5 + 25.3 - 10.4 + 1.8 - 23.6 + 16.4 = -22.4$

[R16] $\Delta H^\circ_2(\underline{131}:X=O)_{est} = \Delta H^\circ_2(\underline{1}\text{-}Me_2)_{obs} - \Delta H^\circ_{ex}(CO_2) + \Delta H^\circ_{ex}(HN{=}C{=}O) + \delta\Delta H_{Ph}$ (in $RN{=}C{=}O$; estimated to be -6.8 from Table R8) $= 1 + 2.6 + 21.1 - 6.8 = 13.1$

Analogous calculations for the other entries in Table R10 are compiled in Appendix 3 A3.9. Many of these values of ΔH°_2 and ΔH°_3 are extremely crude (perhaps in error by more than ±5 kcal), but their differences are much greater, and the gross trends in

Table R10 are most informative.

The data in Table R10 clearly show that 2-piece fragmentation (diazoalkane formation) is only observed in cases where ΔH°_2 is less than about 5 kcal mol^{-1}, and 3-piece fragmentation is only observed when $\Delta H^\circ_3 < -20$ kcal mol^{-1}. When both conditions are satisfied, both routes compete. Unfortunately, the enthalpy estimates in Table R10 are too imprecise to attempt rate-enthalpy correlations at this time. When good heat of formation data is available, and ΔH°_3 and ΔH°_2 are known more accurately, the existence of linear free energy relationships between log k_2 and ΔH°_2 and between log k_3 and ΔH°_3 would be convincing evidence for concertedness of the corresponding fragmentations and generality, or continuousness of mechanism, even for such a variety of substrates.

By identifying processes which are too endothermic to be reasonable, the reaction enthalpy estimates are able to account for the gross features of competetive fragmentations in the series in Table R10. Such consideration, permit a qualitative a priori calculation for untried systems (where at least a few group equivalents are available) to determine if, for example, diazoalkane formation is feasible.

Consider Equation R17, for which ΔH°_2 may be calculated with considerable confidence from measured data. Not surprisingly, unobserved very endothermic diazoalkane formation is reflected in $\Delta H^\circ_2 >> 5$ kcal mol^{-1}. Pyrazoline 61 provides an excellent model for oxadiazolines. For example, ΔH°_f(107) may be estimated reliably

Table R10. Thermodynamic estimates and kinetic data for potential 2- and 3-piece fragmentations of selected pyrazoline derivatives.

Compound	ΔH° of Fragmentation[a]		Relative Rates at 100°C[b]		Reference
	2-Piece	3-Piece	2-Piece	3-Piece	
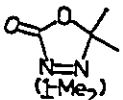 (1-Me$_2$)	(1)	(-30)	20 X 10^3	66 X 10^3	this work
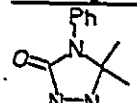 (131:X=O)	13	(-22)		62	267
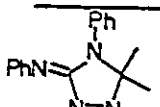 (131:X=NPh)	16	(-36)		18 X 10^3	267
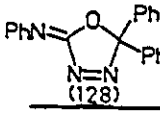 (128)	(-17)	(-45)	65 X 10^3	65 X 10^3	260
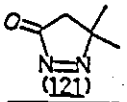 (121)	39	(-31)			160
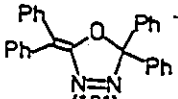 (101)	(1)	certainly >0			233
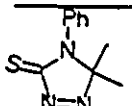 (131:X=S)				28	267[c]

[a]Estimates refer to gas phase (kcal mol^{-1}). Circles values correspond to observed products.
[b]Solvent chlorobenzene, relative to 3,3,5,5-tetramethylpyrazoline (61) at 1.0 ($k \sim 1.3$ X 10^{-8} s^{-1}; ref. 186)
[c]Group values for C=S not available.

by Equation R18. Analogous cycles produce the equally creditable estimates in the series R19. In all cases the potential co-fragment heat of formation is known.[100] Based on these thermodynamic estimates, diazoalkane formation is endothermic and therefore seems unlikely from any of these systems.

[R17] 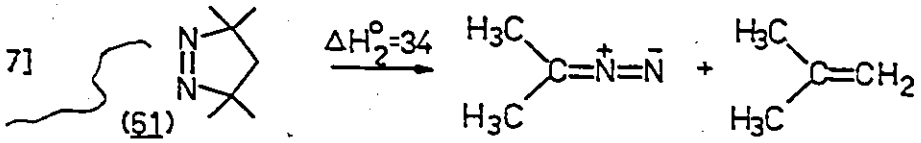

(61)

ΔH_f°: 9.4 ± 0.4 47 ± 5* -4.0

[R18] $\Delta H_f^\circ(\underline{107}) = \Delta H^\circ_f(\underline{61}) - \Delta H^\circ_f$(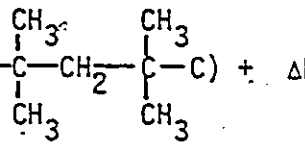) + ΔH°_f(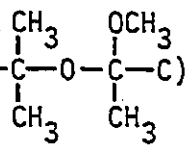)

= 9.4 + 44.9 − 112.3 = −58.0 + 2

[R19] 

(61) (95) (102) (107)

ΔH_f°: 9.4 -22.9 -106.4 -58.0

ΔH_2°: 34 18 16 7

R2.8 Concluding Remarks

Critical examination of the two competing thermolysis modes of Δ^3-1,3,4-oxadiazolin-2-ones, especially with regard to possible intermediates on the reaction surfaces, has lead to the conclusion

*Due to the constant diazopropane product in all 2-piece fragmentations in this discussion, any error in its heat of formation will not affect the difference between 2-piece reactions (the trends upon which conclusions are based).

that both ketone and diazoalkane formation are concerted processes. The diazoalkane formation proceeds through a more polar transition state featuring O1-C5 heterolysis character. Effects on the balance between the two competing routes arise from effects on the rate of the latter process, since the rate of ketone formation is fairly insensitive to either solvent or substituent. Diazoalkane formation is favoured by polar solvents and/or electron-donating substituents.

Consideration of the thermodynamics of 2- and 3-piece fragmentations in the series of competetive systems examined to date has rationalized the types of products which have been obtained. It cannot, however, explain why the transition states for diazoalkane formation and for ketone formation from oxadiazolinones are nearly degenerate in spite of an enormous difference in ΔH°_r of 30 kcal mol^{-1}.

R3 Dimethyloxadiazolinone Hydrolysis Mechanisms

This hydrolysis study was undertaken to attempt to explore some peculiar results mentioned in Knittel's thesis: "The reason why cyanide [ion] enhances the rate of decomposition of [oxadiazolinones], normally very slow at room temperature in water or methanol, remains a mystery....A similar violent reaction was observed when [1-Me_2] was treated with semicarbazide hydrochloride under normal conditions for semicarbazone formation. Instead of the expected oxadiazolinone semicarbazone, acetone semicarbazone was isolated". (ref. 166, p.120-121 (1975)).

During present investigation, dimethyloxadiazolinone was found to decompose spontaneously in water at 20.0°C at a rate 1800 times faster than expected for thermolysis, based on an E_T value of 63.1 for water.[77] Furthermore, diazopropane-derived products are not obtained in water, whereas the solvent polarity correlations reported in the previous chapter (see Results R2.3, page 106) lead one to anticipate >99% diazoalkane formation. Clearly, aqueous decomposition differs from either thermolysis route.

By way of organization, this chapter has been partitioned to correspond to the neutral and acid catalysed aqueous decomposition of oxadiazolinones. In this context, the term "neutral" refers to the reaction uncatalysed by specific acid or specific base (that is, protons or hydroxide ion, respectively). Although this study spans 30 orders of magnitude in proton activity* (from H_0 = -16

in fluorosulfuric acid[328] to pH = 14 in 1M NaOH), only two distinctly different mechanisms seem to be operable for dimethyloxadiazolinone. The distinction between these two processes is obvious from both the products and the kinetics: in solutions less acidic than H_o = -6, the only organic product is acetone, but as the reaction rate increases in more acidic media, 2-propanol is obtained exclusively.

R3.1 Neutral (and Base Catalysed) Hydrolysis

R3.1.1 Product Distributions (see Experimental E3.1)

Neutral hydrolysis occurs over the acidity range* H_o > -6 and pH <14, initially generating acetone, diazene (H—N=N—H), and CO_2 (Equation R20), although the final products are somewhat variable, depending on the concentration and solvent. In aqueous buffers of 2 < pH < 14, the equilibrium product mixture from 0.1M oxadiazolinone consists of a 30% yield of acetone and a 70% yeeld of acetone azine (165), but in aqueous sulfuric acid, the final pmr exhibits only acetone, accompanied by a precipitate of hydrazine sulfate. Gas evolution experiments could account for 1.4 to 1.6 moles of gas per mole of oxadiazolinone. When azine nitrogen is added to the gas evolved, a mass balance of 87-97% is achieved: the balance is likely hydrazine (see below), which is undetectable in pmr spectra of aqueous solutions.

---

*Spatial requirements necessitate assuming readers have a working knowledge of acidity functions.[329] The H_o acidity function is used almost exclusively here because it is the most well established, and because all acidity functions seem to be linear in H_o (ref. 330). Cox and Yates (1978) have proposed a method which eliminates the need for a different acidity function for each base,[331] and this "excess acidity" (X) method will be used later.

[R20] 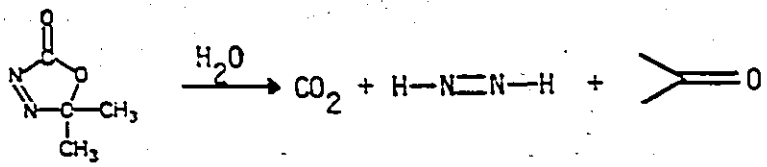

[R21] $CH_2{=}CHCOOH + H{-}N{=}N{-}H \longrightarrow CH_3CH_2COOH + N_2$

[R22] $2\ H{-}N{=}N{-}H \longrightarrow N_2 + H_2NNH_2$

[R23] 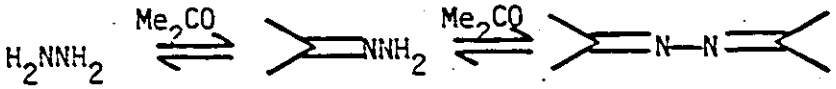

[R24] 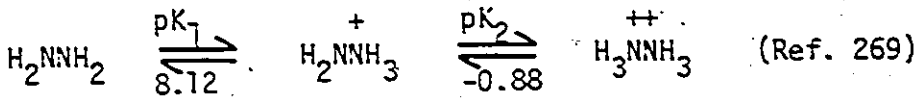 (Ref. 269)

The intermediacy of diazene was proven by trapping with acrylic acid (Equation R21). When oxadiazolinone was hydrolysed in a homogeneous solution of 10% acrylic acid in water, the pmr unmistakably showed a 40-50% yield of propionic acid. Interestingly, the two phase system water/cyclohexene could not trap diazene *in situ*. Presumably solubility was the limiting factor in this latter case.

Carbon dioxide was identified by Fourier transform ir spectroscopy of gc effluent using the characteristic sharp band at 667 cm^{-1} and the broader, structured peak at 2360 cm^{-1}.

Although acetone azine was a major (but by no means exclusive) end product of thermolytically generated diazopropane (see Results R2 and Experimental E2), diazopropane intermediacy in hydrolysis is denied by the absence of 2-propanol (or 2-propyl containing products) which ought to arise by very rapid protonation. For example, the second order rate constant for protonation of diazomethane in aqueous THF is *ca* $10^8 M^{-1}s^{-1}$ (ref. 332). Vpc analysis of hydrolysates

from 1-$PhCH_2$,Me demonstrated the absence of likely diazoalkane products: β-methylstyrene and α-phenylethanol.

One possible explanation for the observed product distributions lies in Equations R22-24. Disproportionation of diazene to nitrogen plus hydrazine creates the hydrazine essential for the ketone/azine equilibria (to which acetone hydrazone does not contribute significantly). As a consequence of the R22 disproportionation, the ketone/hydrazine ratio should be 2:1 prior to equilibration. In fact, blank experiments using standardized acetone and hydrazine solutions reproduced the observed time infinity pmr spectra (30% ketone, 70% azine) only when a 2:1 ratio was employed. This equilibrium composition leaves a 15% yield of hydrazine — an amount which completes the C2, N3, N4 mass balance: total gas + azine + hydrazine = 95 - 105%.

In media at a pH less than, or near, pK_2 for hydrazine (Equation R24), the diprotonation equilibrium shifts the ketone/azine equilibrium to replace azine with hydrazinium dication, thereby explaining why acetone is exclusively observed in the pmr from acidic decompositions. Apparently, neutral and monoprotonated hydrazine are equally effective in ketone/azine equilibria, since the ultimate product distribution from oxadiazolinone decomposition (and the composition of ketone/hydrazine blank mixtures) is reasonably independent of pH over the range $2 < pH < 14$.

R3.1.2 Kinetic Studies (see Experimental E3.2)

Aqueous decompositions were monitored at ca 1mM substrate

concentration in a thermostatted uv cell of 5 cm path length, employing the decline of the 360 nm $n\pi^*$ band (ϵ_{max} < 200 M^{-1} cm^{-1} in water) in preference to the 214 nm band which was sometimes obscured by solvent, catalysts, or products. The long path length cell greatly alleviated difficulties caused by gas evolution and also permitted efficient thermal jacketting. Usually excellent pseudo first order rate constants were obtained from weighted least squares Guggenheim plots using 40-1000 data points covering 4-7 half lives (see Appendix 2).

R3.1.2.1 Bronsted β and pH Profile

Hydrolysis of 1-Me_2 was found to be catalysed by general bases, with the observed rate constants obtained in buffer solutions at constant ionic strength (μ = 0.200) obeying Equation R25. The second order buffer catalytic constants, k_b, for six buffers were

[R25] $k_{obs} = k_o + k_b[\text{buffer base}]$; $k_o = k_{H_2O} + k_{OH}[OH^-]$

combined with $k_{H_2O}/[H_2O]$ in the Bronsted plot of Figure R15 to find a β value of 0.34 ± 0.04 (after correcting for statistical factors*). The data for Figure R15 are summarized in Table A3.10 and Figures A3.1 to A3.7 in Appendix 3. That a general correlation is obtained

*Confusion exists over the proper way to make these corrections. (see refs 333-337) More recent symmetry number corrections require an assumption about the transition state structure during proton transfer.[336,337] That is seldom known, particularly for these reactions, so Bronsted's original 1928 formulation[333] has been retained here. Practically speaking, the statistical factors seldom make much difference, but they can contribute to scatter if incorrect.

in Figure R15 from such a wide variety of base types, indicates that these catalysts act as proton transfer agents, and not as nucleophilic catalysts.[339] An intermediate value of β which is constant over a wide range of catalyst pK_a (here the linear portion is defined over 10 pK units) is considered indicative of some other process — bond breaking, rearrangement, or nucleophilic attack — occurring simultaneously with proton transfer.[340,341]

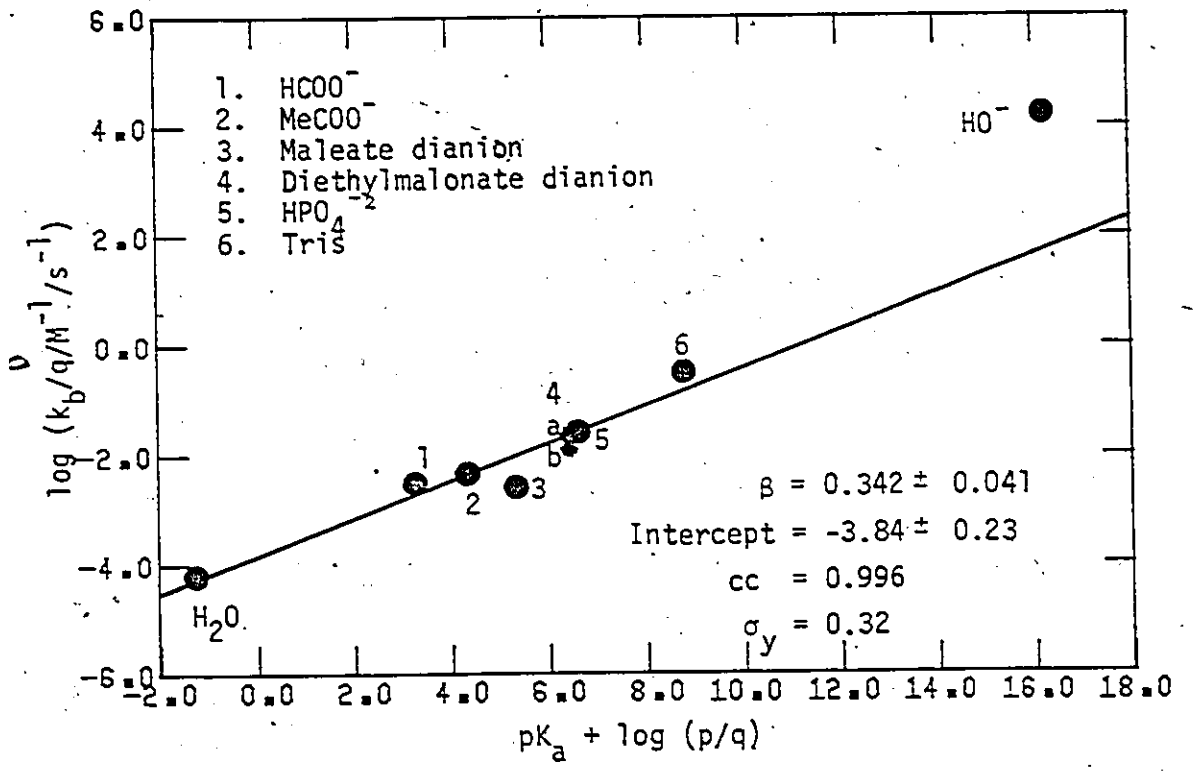

Figure R15. A Bronsted plot for neutral hydrolysis of 1-Me_2.

Significantly, the value for k_{OH} lies about 2.5 log units above the Bronsted correlation line, suggesting that either direct nucleophilic attack by hydroxide ion is much more important than its effect as a general base, or that specific base catalysis (faster reaction through a substrate anion) is possible.

Figure R16 depicts the dependence of log k_o (the observed rate constant corrected for catalysis by added buffer) on medium acidity, as measured by either the H_o acidity function in aqueous H_2SO_4 or the pH in aqueous buffers. Above pH = 6 the slope approaches unity for hydroxide catalysis. To distinguish between specific base catalysis and direct hydroxide attack, the curve would have to be extended to higher pH using stopped-flow kinetics (a technique not available at McMaster during the period of this research). A limiting, or plateau, rate in base would suggest specific base catalysis.

The neutral reaction spans a remarkably wide range of acidity, including the plateau region from pH = 0-6 and the sulfuric acid region from H_o = -6 to 0. The rate falls off in aqueous sulfuric acid because the reaction is second order in water and the water concentration is declining (see following section). Somewhere in the central portion of the neutral region lies the 0.200 M HCl solvent in which substituent effects, order in water, and k_{H_2O}/k_{D_2O} (2.52 ± 0.02) were measured. Appendix Table A3.12 contains the measured rate constants in aqueous H_2SO_4 at 20.0°.

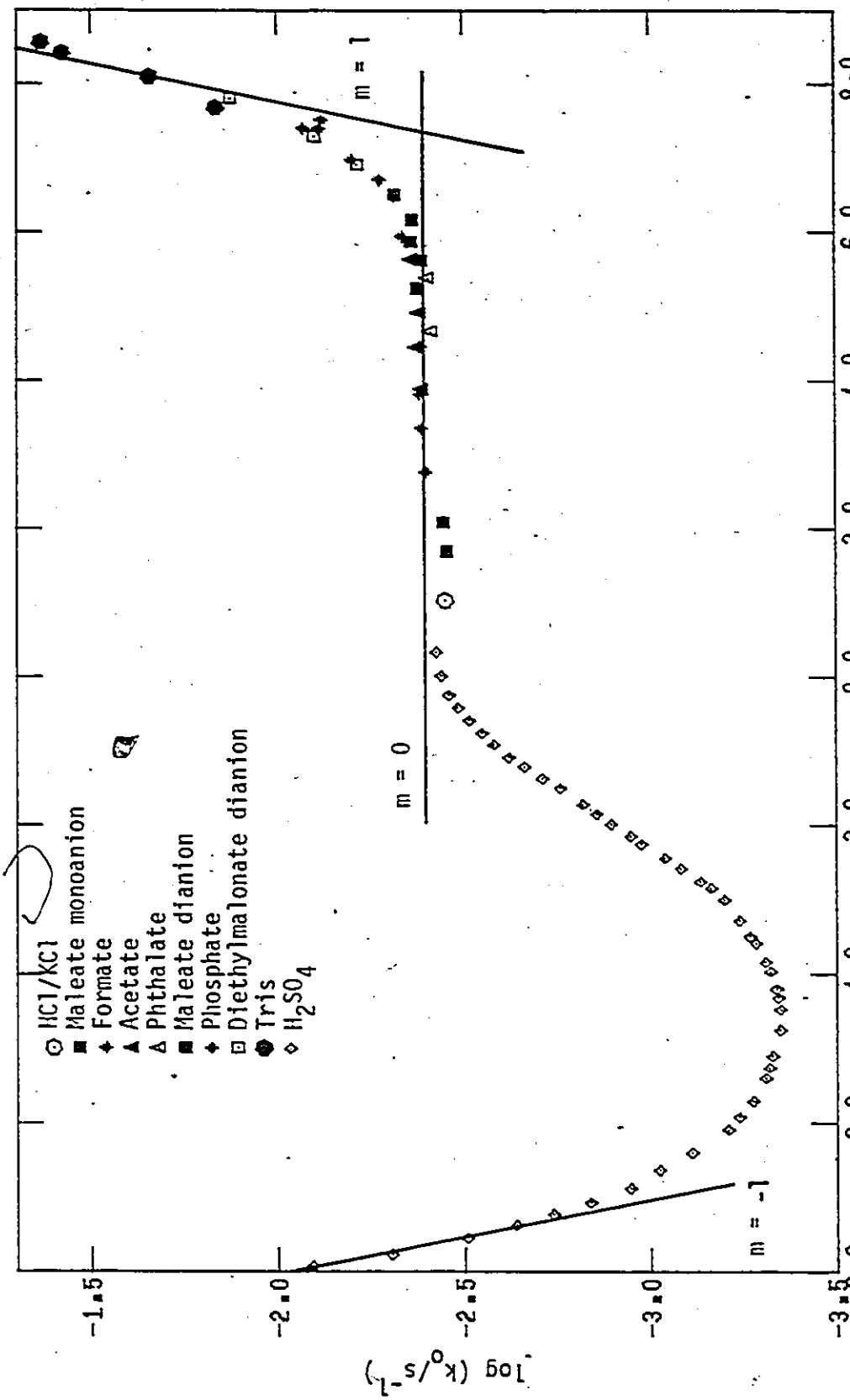

Figure R16. Acidity dependence of the solvent catalysed rate.

R3.1.2.2 Order in Water

When organic cosolvents were added, the observed pseudo first order rate constants in 0.200 M HCl were found to be almost exactly second order in water concentration for the polar cosolvents formamide (56.6), methanol (55.5), or DMF (43.8) (E_T values[77] in parentheses). These data are tabulated in Table A3.11 and visualized in Figure R17. When the much less polar 1,4-dioxane (36.0) is used, a greater apparent (nonlinear) order in water may reflect additional rate retardation in non polar media (that is to imply that hydrolysis is a polar reaction.)

Given that neutral hydrolysis in 0.200 M HCl is second order in water concentration, it is quite reasonable to ascribe the initial decline in rate as sulfuric acid is added to water to the effect of diminishing water concentration. Both dilution and medium acidity increase with the proportion of acid, and Figure R17 recommends that water concentration not activity is the properly consistent solvent property to use. Because of complicated protonation equilibria in aqueous acids, this is a quantity obtained with considerable uncertainty.

There are presently but two methods available to obtain water concentrations in aqueous H_2SO_4. In one, the activity (a_w, available from vapour pressure or emf measurements) can be used to generate "activity coefficient corrected water concentrations", C_w', from the stoichiometric concentrations C_w^S and C_A^S (Equation R26). At the very least, such an operation implicitly assumes the

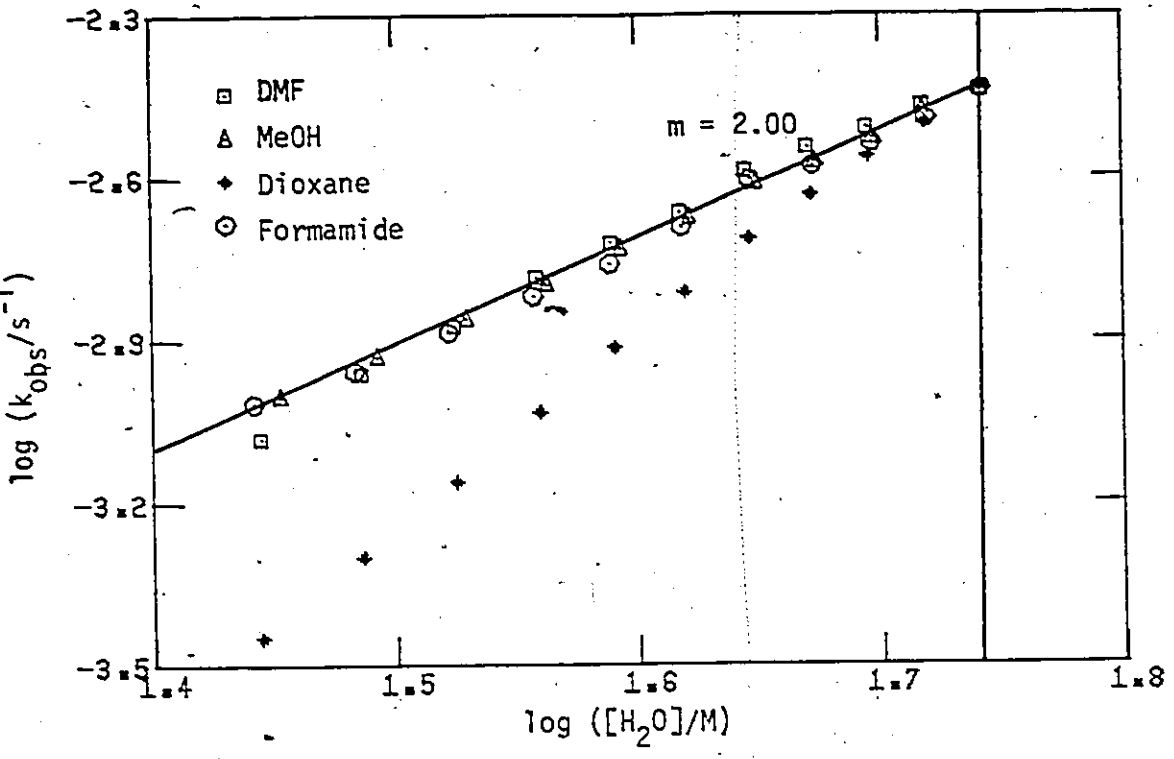

Figure R17. Order in water in 0.200 M HCl.

Figure R18. Apparent order in water in aqueous sulfuric acid (see text for explanation of symbols; interpolated data — see Table A3.13).

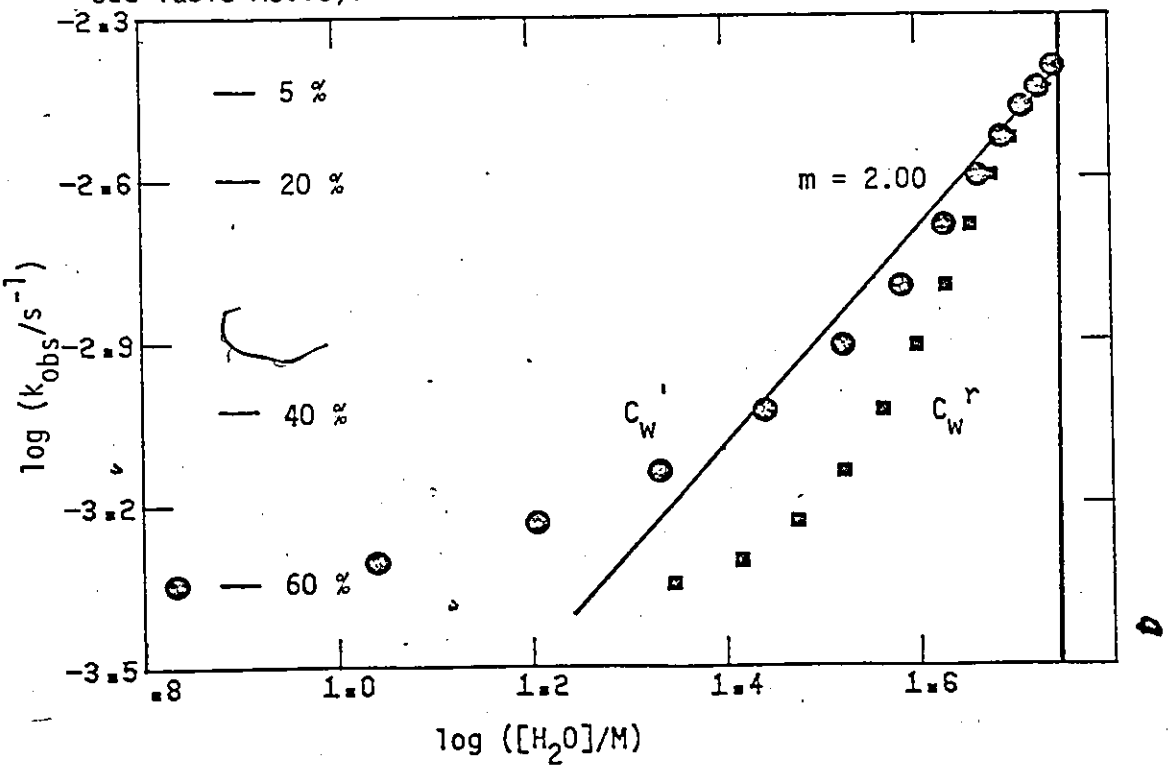

[R26] $C_W' = \frac{a_W}{X} C_W^S = a_W(C_W^S + C_A^S)$; where X = stoichiometric mole fraction

total number of species does not change on mixing (only $H_3SO_4^+$, H_2SO_4, HSO_3^-, $SO_4^=$, H_3O^+, and H_2O are permitted: $H^+(H_2O)_n$ species where n > 1 are not allowed), and that Raoult's Law is obeyed by the resulting binary solution. Given that only non polar geometric isomers form such ideal solutions, the certain failure of the second assumption renders this method dubious, at best.

A second method exploits the integrated Raman intensities of the 981 cm^{-1} line of $SO_4^=$ (Irish (1971)[345]) measured over 0-14 M (80% H_2SO_4). Under the assumption that $[H_2SO_4]$ is negligible over that composition range, water concentrations may be computed from the measured sulfate ion concentrations using Equations R27 and R28.

[R27] $$[HSO_3^-] = C_A^S - [SO_4^=]$$

[R28] $$[H_2O] = C_W^r = C_W^S - 2[SO_4^=] - [HSO_4^-]$$
$$= C_W^S - C_A^S - [SO_4^=]$$

In principle, nuclear magnetic resonance could provide a third independent measure of the actual water concentration. Gutowsky (1953)[346] found the pmr to require too many parameters ($\delta_{H_2SO_4}$, $\delta_{HSO_4^-}$, $\delta_{H_3O^+}$, δ_{H_2O}) to deconvolute the observed proton shifts in sulfuric acid mixtures. In contrast, ^{17}O nmr should circumvent this problem because oxygen exchange between H_2SO_4 and H_2O is slow on the nmr time scale. Thus, only two parameters

(δ_{H_2O} and $\delta_{H_3O^+}$ in the simple approach) are required to describe the position of the $^{17}OH_2$ signal. At present, no such study has been published.

Figure R18 is a log rate - log C_W plot, analogous to Figure R17, to determine the order in water for the neutral reaction in aqueous sulfuric acid using the two water concentration scales. Clearly, the two scales are quite different, and the ideal slope of 2.0 is not achieved. The somewhat greater slopes may hint at an acidic retardation of rate. Considerable effort was expended in fruitless attempts to curve fit the log k_{obs} vs H_o and C_W data to a variety of conceivable models for the neutral reaction in combination with an acid catalysed component to account for the rate upswing in the most acidic media. Particularly irksome was the extended rate plateau between 50 and 70% acid (Figure R19), which no model could account for (see the example accompanying the nonlinear least squares program in Appendix 2). Any possibility that these are polar media and the plateau corresponds to thermolysis, seems to be rejected by the absence of the expected diazoalkane product (2-propanol) in the plateau region.

In a very qualitative sense, general base catalysis by sulfate and/or bisulfate ions, whose raman-derived concentration profiles also appear in Figure R19, could account for the plateau. In 62.7% acid the solvent kinetic isotope effect (KIE) has sunk to 1.27 ± 0.02 (well below 2.52 in 0.200 M HCl), but the decrease in k_H/k_D cannot be ascribed to concurrent neutral ketone forming and acid catalysed, isopropanol forming, processes (an inverse KIE

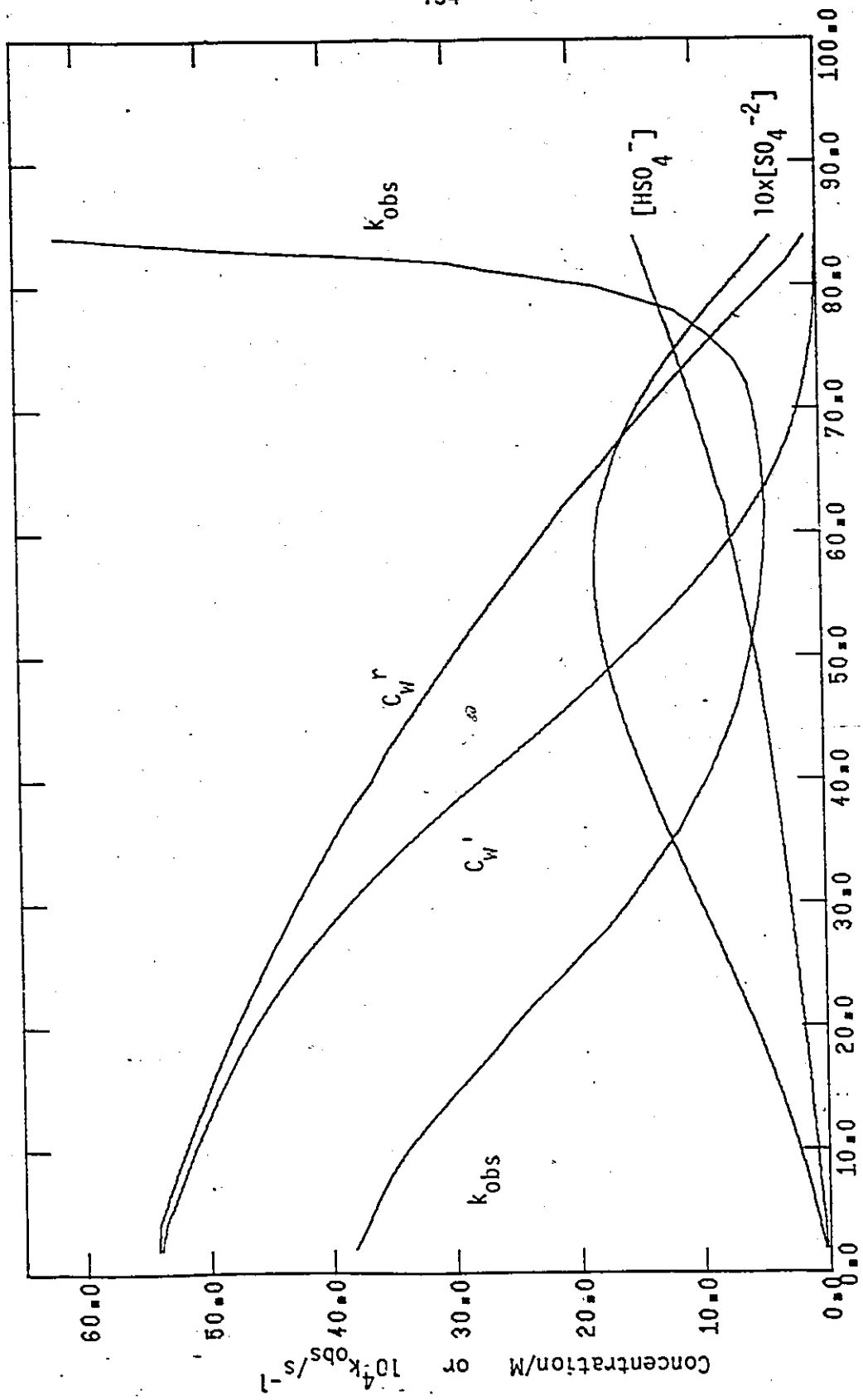

Figure R19. Concentration and rate profiles in aqueous sulfuric acid.

is anticipated for the latter), because only 8% isopropanol is formed in this solvent.

At the present time it is impossible to extend deliberation of the decomposition in 0-70% sulfuric acid. The products, acetone plus hydrazine sulfate plus 1.44 moles of gas (from 30% acid), combined with the crude order in water, are consistent with the extension of the neutral hydrolysis reaction into this region.

R3.1.3 Building a Model

General base catalysis and a large solvent KIE obviously demand a proton transfer in the rate limiting step. Such a transferable proton does not exist in the starting material ($\underline{1}$-Me_2), so its hydrate, the tetrahedral intermediate resulting from the addition of a water molecule to the carbonyl group, is implicated. This intermediate is analogous to the tetrahedral intermediates involved in ester hydrolysis, and in fact, the combined facts of general base catalysis, order in water, and solvent KIE are all suspiciously similar to those observed in ester hydrolyses[305,339,350]. This parallel confirms the contention from FMO principles and the MOs calculated in Results R1, that hard nucleophiles like water and hydroxide ion do attack the carbonyl group of oxadiazolinone in preference to the N4 azo nitrogen.

The hydrolysis of typical esters is usually catalysed by both specific acid and specific base, with $k_{obs} = k_o + k_H [H^+] + k_{OH}[OH^-]$, where the acid and base catalysed reactions usually swamp

the neutral process, k_o. This results in a pH dependence like curve A in Figure R20, for ethyl acetate (for which, at the rate minimum, k_o is believed to account for only 27% of k_{obs}[351]). More reactive esters, like phenyl acetate, show a brief plateau corresponding to a limited region of neutral dominance (curve B), and the extent of the plateau increases as reactivity increases (for example, 2,4-dinitrophenyl acetate, curve C). For very reactive esters there is characteristically a substantial pH region dominated by a fast neutral hydrolysis,with inefficient acid catalysis because they are so weakly basic. Oxadiazolinones have a strongly electron withdrawing azo group which activates the carbonyl to nucleophilic attack, resulting in rapid hydrolysis and a pH profile typical of reactive esters. This reinforces the developing suspicion that this reaction is analogous to ester hydrolysis.

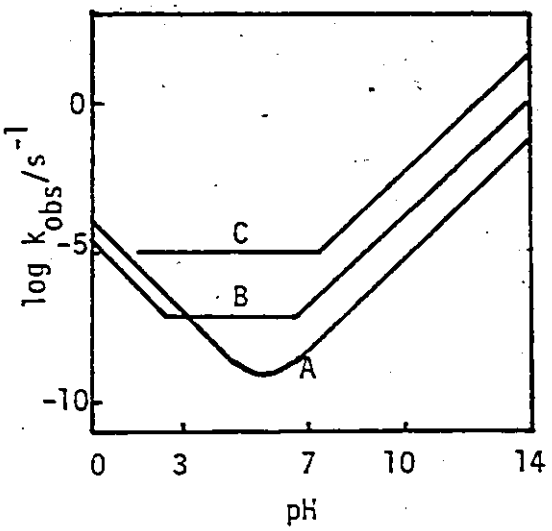

Figure R20. Limiting types of ester hydrolysis (ref. 351 p. 153).

Given such a parallel, a closer look at the model is most appropriate. Reversible formation of the tetrahedral intermediate (Equation R29) involves attack of one water molecule on the carbonyl

group of the ester, catalysed by a general base (a second water

[R29] 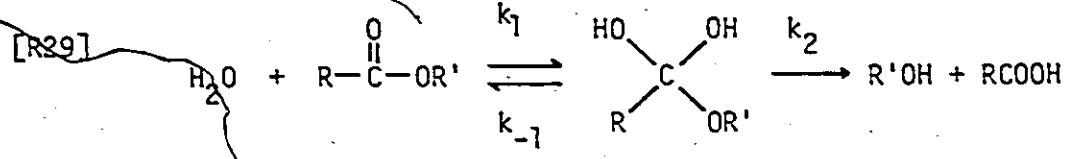

molecule in 0.200 M HCl) to make the k_1 step second order in water concentration. The tetrahedral intermediate may break down to products via a k_2 step or return to the ester via k_{-1}. In neutral ester hydrolyses, these are likely also general base catalysed. In principle (and in experience), either formation (k_1) or decomposition (k_2) of the tetrahedral intermediate may be rate determining, and it is possible to have a compromise situation where the rate expression contains all the rate constants. For example, assuming a steady state concentration of the tetrahedral species, $k_{obs} = k_1k_2/(k_{-1} + k_2)$.

When these ideas are translated to the oxadiazolinone system, Equation R30 obtains, in which one must pause to consider what the k_2 step leads to. The equation depicts the ring opened

[R30] 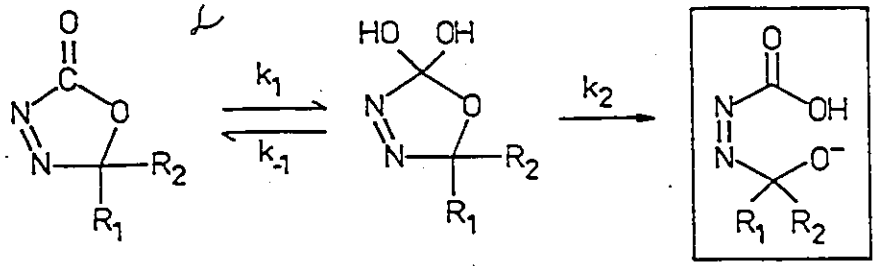

(166) (167)

alkoxide ion intermediate 167. In principle, 166 could ring open in the other direction, cleaving the C2N3 bond, but (as was discussed in Introduction I3, page 70) the better leaving group is the alkoxide

over the diazenyl anion 168 by 3-5 pK units. If 166 ring opened by cleaving the CN bond and lost nitrogen simultaneously, resulting carbanion 169 would almost certainly be rapidly protonated

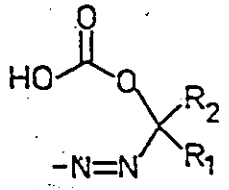

(168)

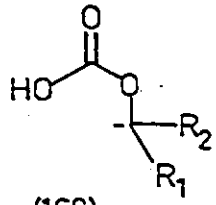

(169)

and ultimately generate 2-propanol (which is definately not observed), rather than acetone (which is the only C5 product initially formed). Ring opened alkoxide ion 167 has been drawn as the anion because general base catalysis accounts for the removal of one proton to form the carbonyl, and general acid catalysis was not observed. Naturally, 167 will be rapidly protonated, but it is a logical immediate product of the k_2 step.

R3.1.4 Substituent Effects

In an attempt to gain some insight into the balance between the two steps in Equation R30, the effect of substituent variation on k_{obs} in 0.200 M HCl was determined for 10 compounds (see Figure R21). These rate constants were extremely reproducible and the circles drawn in the figure represent about a 5σ error, with the exception of the 1-$(PhCH_2)_2$ point which has a large error (1σ shown) arising from a very long extrapolation from aqueous organic solvents to water, in which it was insoluble. In contrast to 1-Me_2, the order in water plot for that system

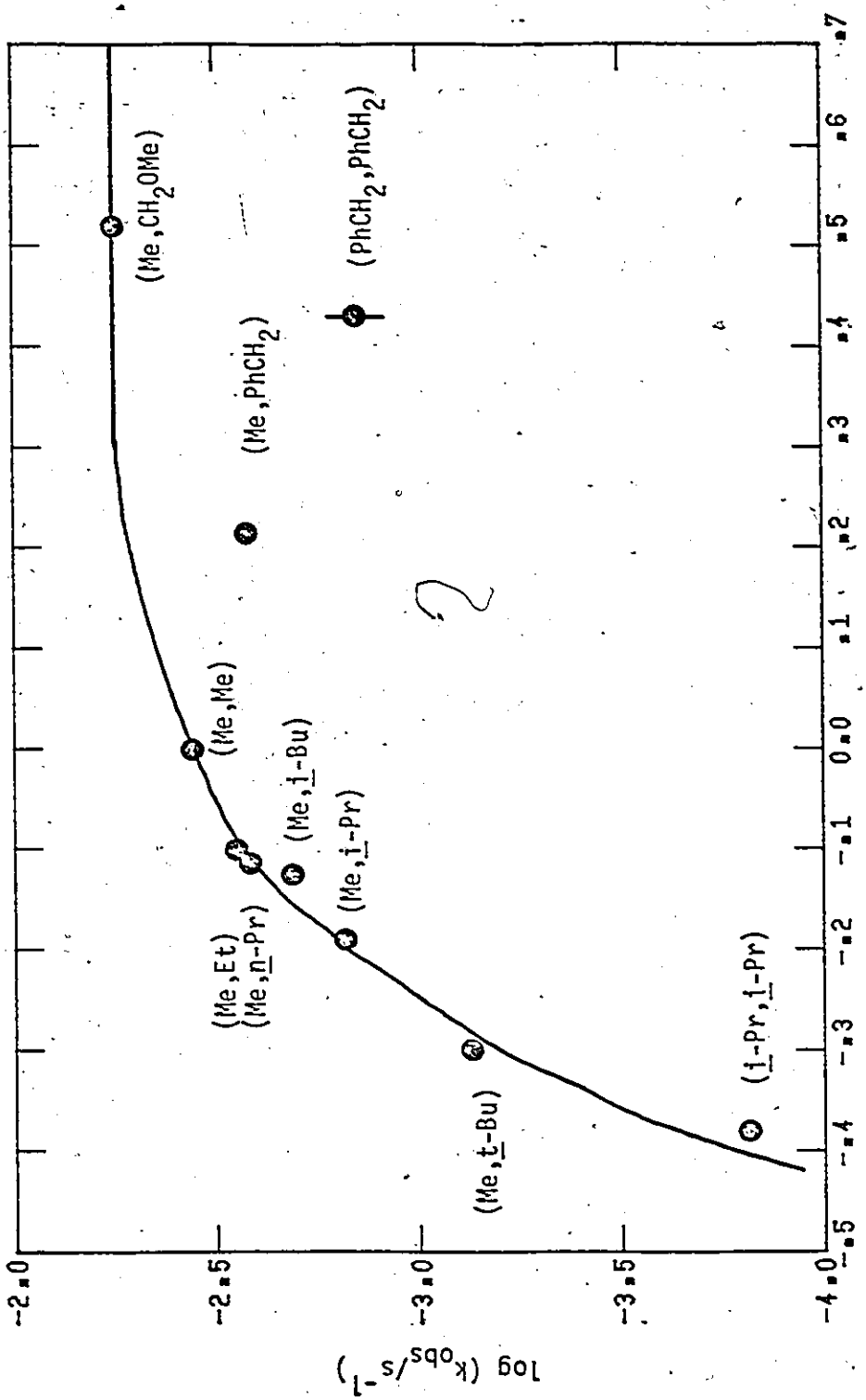

Figure R21. Alkyl substituent electronic effects in 0.200 M HCl.

was not simple (see Figure A3.8, Appendix 3).

Figure R21 is a Hammett-type plot: log k_{obs} *vs* the sum of the substituent inductive parameters, σ^*, for the two C5 substituents. Charton (1979)[352] and others[353,354] have criticized the σ^* inductive parameter, but the use of an alternative inductive parameter (σ_I)[353] leads to the same general appearance.

As a correlation, Figure R21 looks quite horrible, but all of the points can be reasonably accounted for by including some kind of steric contribution, using the E_s steric parameter. For example, the points for systems containing isopropyl, *t*-butyl, or benzyl groups all lie below the others. Possibly there is some curvature (as suggested by the arbitrary curve drawn on the plot) which is indicative of a change in the rate limiting step with substituent. Although more substituents of positive σ^* would have been desirable, all attempts to cyclize semicarbazones of 1-chloroacetone and 1,3-dichloroacetone with LTA, LTA/TFA, or even LTTFA were unsuccessful. The data for Figure R21 are found in Table A3.14, Appendix 3.

To quantify the correlation of log rate with σ^* and E_s is not straightforward in this system. All attempts to analyse the data lead to reasonably large terms for both steric and inductive contributions, but complexities arise because of a statistical problem: there are two faces to attack the planar oxadiazolinone, and when it is unsymmetrically substituted, the steric requirements are different for each face. Furthermore, k_{obs} is likely a function of rate constants (recall $k_{obs} = k_1k_2/$

$(k_{-1} + k_2)$), and each individual rate constant will respond in its own way to steric and inductive parameters, including the statistical factors.

Even in multiparameter nonlinear fits designed to take account of these complications (up to 5 independent parameters were tried), only rough or qualitative correlations were obtained. They were much better than simpler correlations, but still left something to be desired in view of the accuracy of the rate constants. Typically, these fits had $\sigma_{\log k}$ of ca 0.1 (corresponding to about 25% deviation), which was too large to discriminate amongst possible models, so no details can be afforded here. The available literature on neutral hydrolysis is scanty. (because of overwhelming acid and base catalysed reaction), but does not lead to very good correlations with σ^* either (see Table A3.15 in Appendix 3).[350] The cyclic nature of oxadiazolinones introduces 1,3-steric interactions which are likely absent in these acyclic models.

Although it proved impossible to quantify the substituent effects, all analyses returned somewhat similar results. Generally speaking, the overall response to C5 substituents is that the reaction is accelerated by electron withdrawers (yielding an approximate ρ^* in the vicinity of plus 1 to 2), and retarded by bulky substituents. The fact that there is any electronic effect whatsoever (a ρ^* of 1-2 is enormous here) demands that k_1 not be rate limiting, since substituents are hardly likely to have any electronic effect on the addition of water to a carbonyl group 3 atoms removed.

On the other hand, the sign and magnitude of the approximate ρ^*, indicating a buildup of considerable negative charge, are consistent with a ring opening k_2 step forming an alkoxide centre (167). The pK_as of a series of alcohols with substituents one carbon removed from the oxygen atom give a rough correlation against σ^* with a ρ^* of 1.6 (Equation R31).

[R31] $RCH_2OH \rightleftharpoons RCH_2O^- + H^+$ R = H, Me, CH_2Cl, $CHCl_2$, CCl_3 (pKs from ref. 269)

Concerted formation of acetone plus diazenyl anion from 166 is also inconsistent with the large substituent electronic effects. Furthermore, the secondary β-deuterium KIE (k_H/k_D (1-$(CD_3)_2$) is insignificant (0.15 ± 0.1% per D) in 0.2 M HCl, thereby denying rate limiting rehybridization of C5 in hydrolysis. This extremely low value may be contrasted with the substantial β-effects in thermolysis (ca 2%, page 115).

Thus, the outcome of the substituent effect studies is the inference that k_2 is involved in the rate expression and therefore that formation of the tetrahedral intermediate is a rapid preequilibrium (or more generally, $k_{obs} = k_1k_2/(k_{-1} + k_2)$). In either event, k_{-1} is non-negligible and one might anticipate carbonyl oxygen isotope exchange for these systems.

R3.1.5 Carbonyl Oxygen Isotope Exchange

Classically, carbonyl oxygen isotope exchange has been a key tool in ester hydrolysis mechanistic studies to determine the

partioning of the tetrahedral intermediate between return to starting material (k_{-1}) and decomposition (k_2; see Equation R32). Whereas previous studies have employed ^{18}O labelled water and mass spectral examination of recovered starting material[339,356,357], such an analytical method is impossible without an oxadiazolinone parention (recall Results R2.6, page 119). Instead, ^{17}O nmr was selected for these studies.[358-361] Modern FT spectrometers and reasonably available isotopic water ($^{17}OH_2$, 20% enriched; Merck, Sharpe and Dohme Ltd : $170.00 per g) have encouraged recent ^{17}O exchange studies on ketones.[359,361]

[R32]

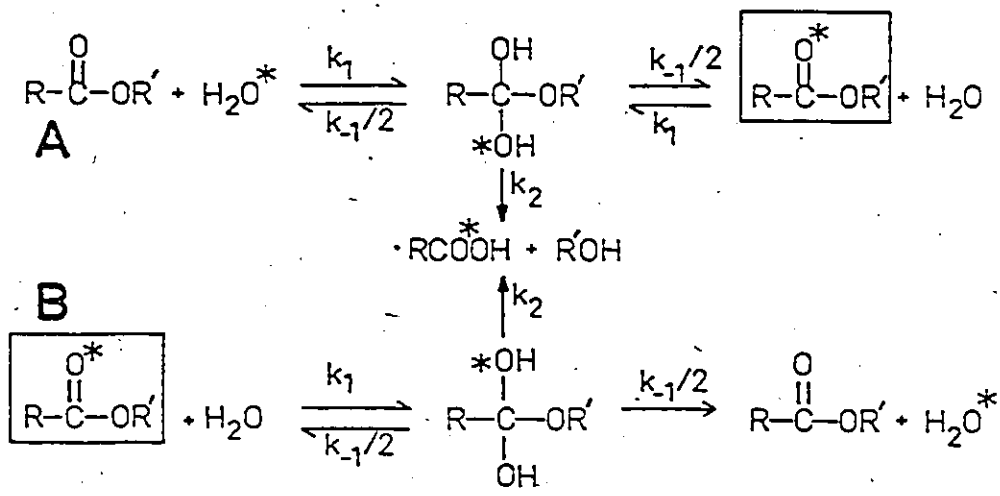

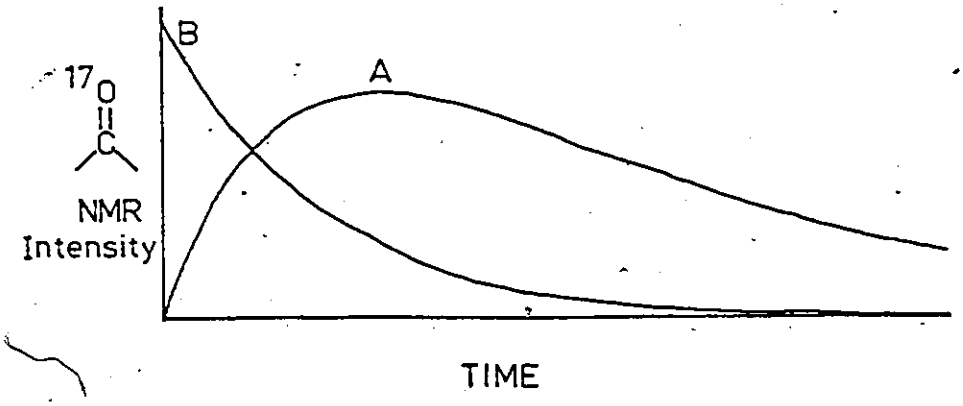

Figure R22. Hypothetical intensity vs time curves for two oxygen isotope exchange experiments.

In principle, there are two kinds of exchange experiment: exchange in or exchange out, as represented by curves A and B respectively. The easier of the two, method A, involves hydrolysing the ester in the presence of labelled solvent. The tetrahedral intermediate in Equation R32 is formed by k_1, but if it contains equivalent OH groups, there is a 50% chance that return to starting material will incorporate label, and a 50% chance that return will reject label. If return (k_{-1}) competes with decomposition (k_2), then the label may accumulate in the starting material, and be detected. During an A-type experiment the ^{17}O nmr signal will increase and then decay with time (rise/fall kinetics) corresponding to exchange in, then decomposition, as exemplified by Figure R22. If the data are good enough, the curve could be fit to a double exponential by nonlinear least squares to evaluate the rate constants. Even with poor data, this ^{17}O nmr experiment is an exceedingly simple qualitative test for return.

The second, more tedious method B involves synthesizing labelled ester and decomposing it in unlabelled water. By comparing the first order rate of loss of ^{17}O (k_0) with, say, the uv rate (k_{uv}), return is implicated when $k_0 > k_{uv}$, and the ratio k_{-1}/k_2 may be evaluated (Equation R33).

$$[R33] \qquad k_{uv} = \frac{k_1 k_2}{k_{-1}+k_2} \; ; \; k_0 = \frac{k_1(k_2+k_{-1}/2)}{k_{-1}+k_2} \; ; \; \frac{k_0}{k_{uv}} = \frac{k_2+k_{-1}/2}{k_2}$$

When the method A approach was applied to the hydrolysis of 1-Me_2 or 1-Me,t-Bu, no incorporation of label into oxadiazolinone carbonyl group was observed, but the rather high detection limit

in those ^{17}O nmr experiments merely limits exchange to certainly less than 10%.

After some difficulties, 5-15% carbonyl ^{17}O enriched oxadiazolinones were prepared, but they proved to be unsuitable for ^{17}O kinetics by method B because: (a) they were difficult to purify and the remaining semicarbazone, or other impurities, could act as catalysts; (b) they were insufficiently soluble, even in 50% methanol, for good S/N in the spectra; and (c) ^{17}O kinetics at 30 mM concentration may not relate to uv kinetics in more dilute solution. The resulting rather crude ratios k_O/k_{uv} of 1.2-2 (Table E5,page 229) were implicating far more return than permitted by the preceding method A results, and in fact, the uncertainty of the ^{17}O rate constants exceeds the maximum permissible amount of exchange (<10%).

The overall conclusion which emerges from these limited exchange studies is that <u>significant exchange does not occur</u>. How can it be that the preequilibrium formation of the tetrahedral intermediate (demanded by the dominance of k_2 in the rate expression) apparently shows insignificant exchange?

The most likely possibility focuses on the implicit assumption made in exchange studies (and in Equation R32) that the two hydroxyl groups in the tetrahedral intermediate are identical, so return to labelled or unlabelled ester is statistical — one half each way. <u>But</u>, suppose for one reason or another, that the OH groups were sufficiently different that the so-called statistical factor was not one half each way, as suggested by Equation R32, but

more like all one way, and none the other. For the oxadiazolinone case, the absence of exchange means that the tetrahedral intermediate must always eject only the attacking OH group in exclusion to the other. What could cause such a gargantuan difference?

R3.1.6 Stereoelectronic Control in the Cleavage of the Tetrahedral Intermediate

In the oxadiazolinone case, the tetrahedral intermediates do not have identical hydroxyl groups because, in general, R^1 and R^2 are different, and the ring is no longer planar (see 170 and 171 in Equation R34). Like all 5-membered rings, there are pseudo-axial and pseudo-equatorial positions for the R and OH groups which, in principle, could undergo axial/equatorial exchange via ring inversion with a presumably low energy barrier (1-3 kcal mol^{-1} for 5-membered rings),[362] as shown in the top line of Equation R34.

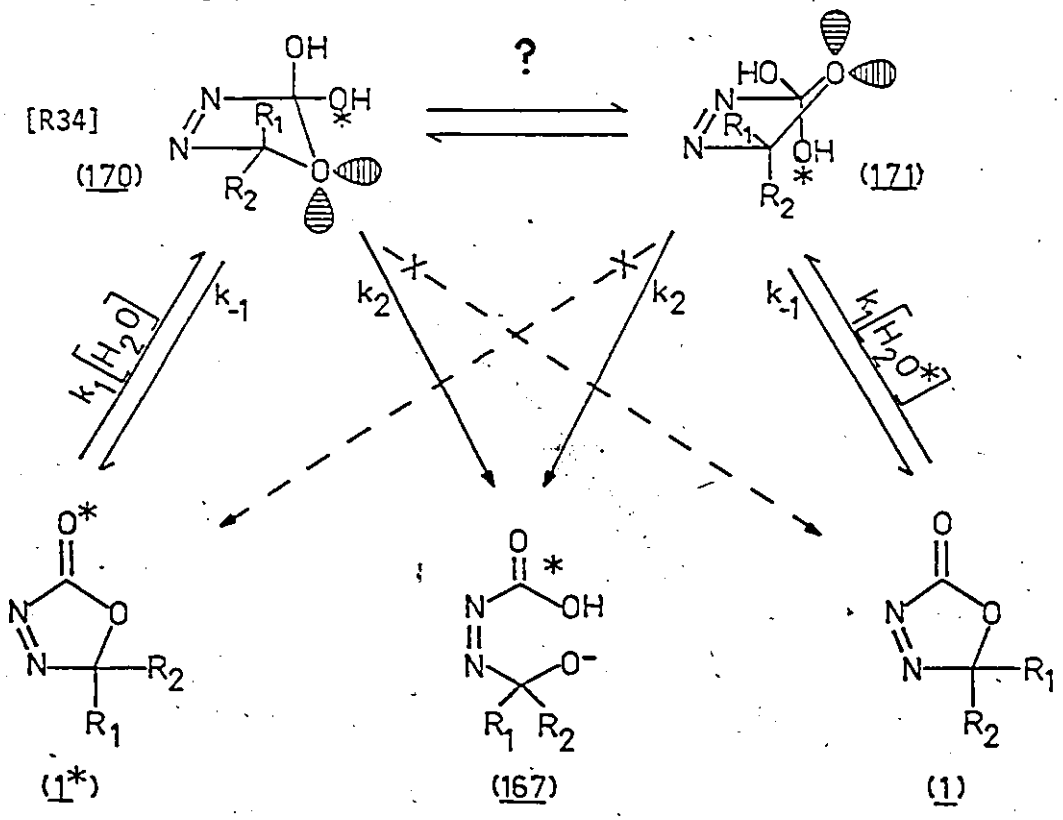

Now, the interesting aspect of such tetrahedral species is that Deslongchamps (1975) has proposed that two heteroatom lone pairs must be lined up trans antiperiplanar to a C-X bond in a tetrahedral intermediate before that C-X bond will easily cleave to either reform staring material, or to form products.[363] Hydroxy groups are able to freely rotate and may therefore always line up an orbital any way that is desired. Thus, the two hydroxyls at C2 can easily arrange their lone pair orbitals to eject the ring oxygen as a leaving group in the k_2 step, forming 167 from either 170 or 171.

However, when it comes to ejecting a hydroxide ion in the k_{-1} step, only one of the necessary two orbitals is provided by the other hydroxyl group, and the other must come from the ring oxygen. Because of the envelope conformation of the 5-membered rings, 170 and 171, one of the ring oxygen lone pairs is lined up trans antiperiplanar to the pseudo-axial C2-OH bond. The other ring oxygen lone pair is not in a position to push out the pseudo-equatorial hydroxyl: to do this; the ring must first invert to put that group in the pseudo-axial position. Thus, Deslongchamps' theory leads to the conclusion that in any conformation, only the pseudo-axial hydroxyl group can be ejected to reform starting material, and this will compete with ring opening.

Least motion principles[364] dictate that, for example, the reaction between carbonyl labelled oxadiazolinone (1*) and unlabelled water (left hand side of Equation R34) proceeds to an initial conformation with the attacking group in the pseudo-

axial position. If ring inversion cannot compete with k_{-1} and k_2, then reversible formation of 170 will not be detectable by carbonyl oxygen isotope exchange. This conforms exactly to the experimental observations; whereas the influence of substituents on k_{obs} pleads for a reversible hydration step, the absence of exchange implies very preferential ejection of the attacking nucleophile.

If the steric requirements of R_1 and R_2 are different (say R_2 is the larger group), then the incoming water molecule will favour the least hindered (R_1) face and the bulky R_2 group will initially be in a pseudo-equatorial position. Such a conformation (170) is stabler than the one with the bulky R_2 group in a pseudo-axial position (for example, by 1 kcal mol^{-1} for an ethyl, and by 5 kcal for a tert-butyl group in cyclohexane[335]); so the ring inversion barrier for 170 → 171 will be at least as great as the thermodynamic energy difference between these conformations. This will further reduce the likelihood of isotope exchange.

In an attempt to estimate the magnitude of a possible inversion barrier in the tetrahedral intermediate, low temperature pmr spectra of 107 in CCl_2F_2 were examined to determine if conformations with pseudo-equatorial and pseudo-axial methoxy groups would be prevented from rapid interconversion. The sample froze at -160° without such evidence, leading to an estimated barrier height of less than 5 kcal mol^{-1} for this model (see Experimental E3.2.3.3).

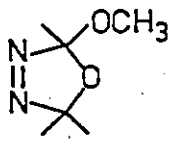

(107)

Thus, decomposition of the tetrahedral species in neutral oxadiazolinone hydrolysis is under stereoelectronic orbital control and occurs faster than ring inversion. This is exactly analogous to Deslongchamps' reasoning to explain why lactones do not exchange during hydrolysis.[363] The operation of these concepts has been supported by theoretical calculations[365,366] and further support stems from the following observations.

First, if one of the hydroxyl groups in the hypothetical tetrahedral intermediate is replaced by a methyl substituent (compare 170 to 56) it becomes impossible to line up two heteroatom lone pair orbitals to ring open this system, and a rather stable salt is obtained (Equation R35). Even when protonated in water, this compound does not ring open unimolecularly, but rather undergoes an unrelated radical chain decomposition to isopropyl acetate (discussed in Section II.5, page 31).* With two heteroatom lone pair orbitals orientable to eject hydroxide or to ring open, 170 or 171 has but a fleeting existence (a lifetime shorter than that for ring inversion — ca. 10^{-6}s). With only one, 56 is stable.

Providing a second case is the aqueous acid hydrolysis of iminooxadiazolines (151; Equation R36), which is used to complete the oxadiazolinone synthesis sequence (recall Equation R5, page 102). This reaction normally occurs with very little decomposition and Deslongchamps' ideas can account for the chemistry. Water attack on

*Even if there were an ionic component to the formation of isopropyl acetate, the stereoelectronic theory would predict ring opening with C2N3 cleavage (2 available oxygen lone pairs) in preference to the C2O1 bond (for which only one properly oriented lone pair is available), and therefore predict the observed products.

[R35]

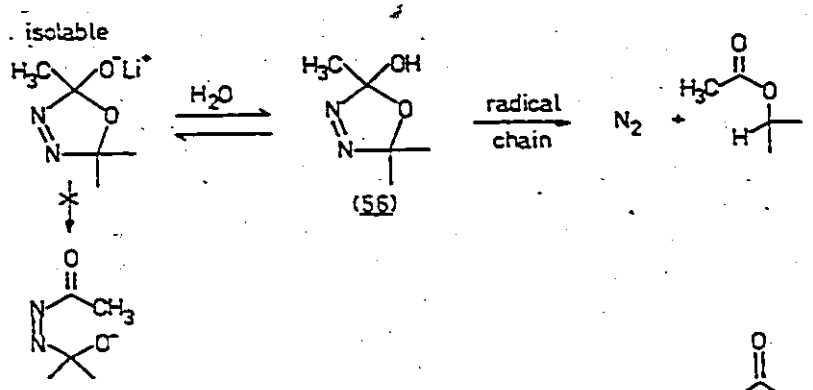

[R36]

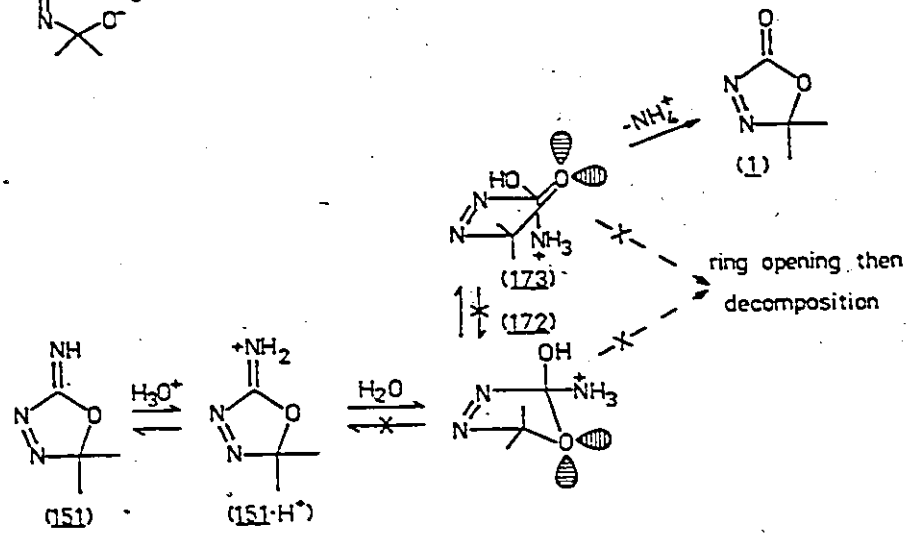

immonium ion 151·H^+ (Equation R36) and rapid nitrogen protonation leads initially to conformer 172 of the appropriate tetrahedral intermediate. Because the ammonium group has no lone pair orbitals, 172 is unable to eject hydroxide or to ring open to begin decomposition. In this context, the $\overset{+}{N}H_3$ group acts like the CH_3 in 56. Conformational inversion of 172 to 173 eventually occurs, but 173 may only eject pseudo-axial ammonium to form products, and may not ring open. Again, with two C2 hydroxyls, ring opening decomposition is very favourable, but with only one, decomposition is negligible.

It is also reassuring to compare the relative reactivity of 53 to 117 and 121. Whereas 53 is extremely stable to very hot, strong base,[165] 117 and 121 are extremely unstable in water (refs

160,241,245-249),

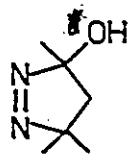
(53)

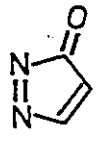
(117)

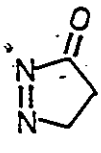
(121)

because their tetrahedral intermediates possess the necessary two lone pairs to ring open by cleaving the CN bond (for example, in Equation R37). In the latter cases, ring cleavage ejects the better leaving group; diazenyl over carbon anion. The formation of bimanes can be envisioned to be analogous to the fate of diazene in oxadiazolinone hydrolysis; except, instead of reduction, bimolecular reaction leads to an intermediate which will obviously cyclize.

[R37]

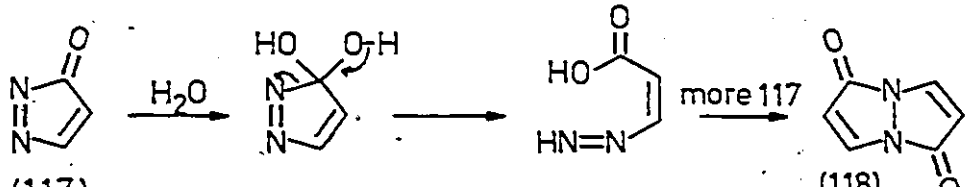
(117) (118) bimane

Although it would likely be illuminating to compare oxadiazolinone hydrolysis kinetics to the hydrolysis of model lactones 147 and 148, their neutral reaction (if it is even

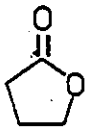
(147)

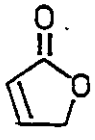
(148)

separable from acid or base catalysed reaction) has not been reported. A few authors[367-371] have examined the alkaline hydrolysis of 147, with Bender (1961) concluding that carbonyl oxygen isotope exchange does not occur to an appreciable extent ($k_{hyd}/k_{ex} > 30$).[371] No work has been reported on 148. One big unknown is the effect of C5 substitution on the basic hydrolysis of 147, apparently because most authors view the lack of exchange as proving rate limiting hydroxide attack (k_1). Deslongchamps' stereoelectronic theory appeared in 1975, subsequent to most of this lactone work, and the results obtained in oxadiazolinone hydrolysis serve to cast doubt on the presupposition about exchange. The case of lactone hydrolysis needs to be reopened, and in this context, the present kinetic studies can provide a comparatively complete and consistent model for these other, less well explored systems.

R3.1.7 Completing the Conversion to Products

Up to this point in section R3.1, discussion has been restricted to interpreting the rate limiting events in the neutral hydrolysis of oxadiazolinones — those steps inside the box of Equation R38. Presumably alkoxide ion 167 will be rapidly protonated to give the highly reactive cis-azo compound 174. From the work of Hünig[161-164], King[288,289], and Kosower[88,287] (as discussed in Introduction I1.5 and I3.2), the most logical products from such an intermediate are ketone, diazene, and carbon dioxide. Fortunately, in the end, both kinetic and product studies

are consistent with these three products.[R38]

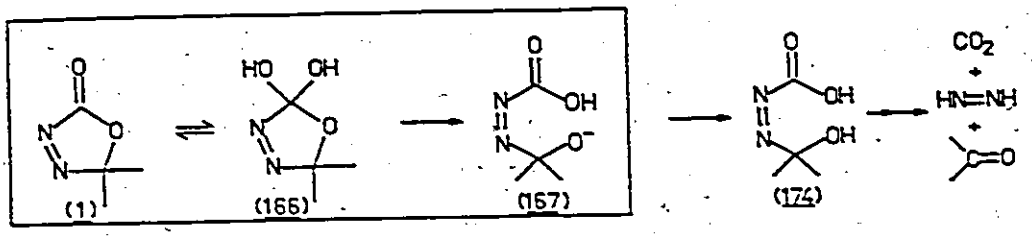

In a very beautiful way, these results now permit rationalization of the two preliminary observations by Knittel (1975)[166], with which Chapter R3 opened. He found that treatment of 1-Me_2 with a 1M solution of semicarbazide at pH 4 gave a quantitative yield of acetone semicarbazone. However, in aqueous or alcoholic media containing cyanide ion, a high yield of hydrazobis(isobutyronitrile) (175) was isolated after a very rapid reaction.

The former case likely involved general base catalysed decomposition to an equilibrium mixture of acetone and acetone azine which was pulled entirely over to the ketone side by irreversible semicarbazonation. In the latter experiment, the rapid reaction rate was due to specific base catalysis in the alkaline cyanide solutions, followed by the known, synthetically useful, reaction of ketone, hydrazine, and cyanide to form 175 (Equation R39)[372], presumably via the intermediacy of the azine.

[R39] $2\ \text{>=O} + H_4N_2 + 2HCN \rightarrow$ 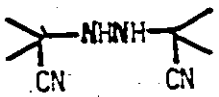 $+ 2H_2O$

175

If stereoelectronic orbital control of the cleavage of tetrahedral intermediates is valid, then cyanide ion cannot catalyse the decomposition by direct nucleophilic attack at the carbonyl group because the lone pair requirements only permit cyanide ejection and do not allow 176 to ring open. This hypothesis can be tested by measuring the buffer catalytic constant, k_b, for cyanide ion and comparing it to the value expected on the basis of the pK_a of HCN from the Bronsted plot. Anomalous acceleration could imply nucleophilic catalysis.

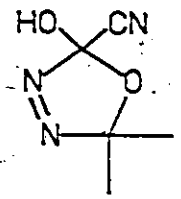

(176)

Throughout the foregoing discussion it has been convenient to explicitly assume that diazene disproportionates to hydrazine plus nitrogen via a bimolecular process involving 2 molecules of diazene. However, since diazenes rapidly reduce double bonds, and azo compounds particularly well, and since starting material is always present in considerably greater concentration than diazene itself, reduction of oxadiazolinone is possible.

Fascinatingly, such a self-trapping reaction leads to a short lived intermediate (177; Equation R40) which would release CO_2 rapidly to form acetone hydrazone. Provided that the steps after diazene formation are all fast, the overall effect is to convert

[R40]

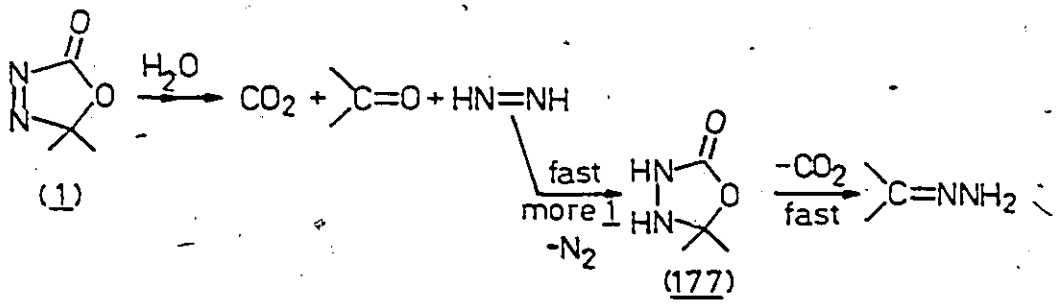

(1) (177)

two molecules of oxadiazolinone into 2 molecules each of CO_2 and acetone plus one of hydrazine and one of nitrogen — exactly the same stoichiometry as prevails from assuming diazene disproportionation! BUT, in the case of self-trapping, the observed pseudo first order rate constant is twice the rate constant for formation of diazene. In order to distinguish between self-trapping and diazene disproportionation, kinetics ought to be performed in the presence of an efficient diazene trap. Should the rate decline in the presence of an alternate trap, Equation R40 holds, but if the rate is unaffected by the trap, diazene cannot be attacking starting material. In an intermediate situation where diazene is captured both by starting material and by disproportionation, the observed rate should not be first order, and the rate will not describe the hydrolysis of the starting material, but will rather be too large, by up to a factor of 2. This may be germane to the ill-behaved substituent effect correlations discussed in R3.1.4, as well as to the small rate accelerations in 30 mM ^{17}O kinetic studies when compared to 1 mM uv kinetics, and to the failure of the water order in aqueous H_2SO_4, where diimide might be protonated.

This is an extremely complicated system indeed, but the present work represents the first detailed kinetic examination of the hydrolysis of diazenyl esters. Some of the present conclusions may need additional corroboration, but the gross features of the reaction are undisputable. In the light of this work, it becomes possible to understand other reactions of azo-

carbonyl compounds in nucleophilic media, and the direction of further studies in this general arena may be modelled on the successful experiments performed on oxadiazolinones. Work in this area must obviously continue.

R3.2 Acid Catalysed Decompositions at 20°C

Results presented on the thermolysis and neutral hydrolysis of oxadiazolinones have been sufficiently detailed to permit development of satisfying and congruent mechanisms for those reactions. In contrast, hereunder reported exploration of acid catalysed decompositions can only be considered preliminary, and many persisting uncertainties must await future work for clarification. Detailed discussion of this material is unwarranted at present.

R3.2.1 The Basicity of Dimethyloxadiazolinone

All four heteroatoms in the oxadiazolinone ring system are potentially basic. Azo compounds (only azobenzenes have been studied) are half protonated in the range 5-10 M H_2SO_4,[373] and esters over the range 12-18 M,[377] so the azo group may be considered more basic in the media of interest. It is tempting to think that electron withdrawl by the adjacent carbonyl group should make the azo group of 1 less basic, but the electron withdrawing azo group should also make the carbonyl oxygen less basic. If both groups are withdrawing electron density, where are the electrons?

Uv-visible spectroscopic evidence (see Experimental E3.1.8)

suggests that 1-Me_2 is not significantly protonated up to 85% H_2SO_4 (15M, H_o=-8). Likewise, a model azoester, diethylazodicarboxylate, is unprotonated up to 60% H_2SO_4 in ethanol (9M, H_o unknown, but likely much less than H_o in water at that molarity (ca -4.5), given that H_o in 20% ethanol is -6.5 at 9M)[373].

For weakly basic acid catalysed systems, Equations R41 to R43 hold.

[R41] $$Oxa + H^+ \underset{}{\overset{K_{BH^+}^{-1}}{\rightleftharpoons}} Oxa{\cdot}H^+ \xrightarrow{k_d} \text{Products}$$

[R42] $$k_{obs} = \frac{k_d[Oxa{\cdot}H^+]}{[Oxa]} \quad ; \quad K_{BH^+} \equiv \frac{a_{oxa}a_{H^+}}{a_{oxa{\cdot}H^+}}$$

[R43] $$\log k_{obs} - \log C_{H^+} = \log k_d + pK_{BH^+} + m^*X$$

$$y = \quad b \quad + m^*X$$

The observed rate constant contains concentrations which are converted to activities (a) to include pK_{BH^+}, and the excess acidity, X, recently defined by Cox and Yates (1978)[331] is proportional to the leftover activity coefficients, with slope parameter m* emerging as the proportionality constant. Advantages of the X method are detailed in the original reference.

To estimate a pK_{BH^+} for dimethyloxadiazolinone from Equation R43, this compound was protonated in FSO_3H (H_o =-16)[328] at -78° and the resulting stable cation was analysed by ^{13}C mr and pmr at -60°. The site of protonation will be discussed in the next section. Warming to -25° initiated decomposition to 2-propyl

cation, and rates obtained over a 20° temperature range were used to compute the activation parameters $\Delta H^{\ddagger}$ = 19.5 ± 0.5 kcal mol^{-1} and $\Delta S^{\ddagger}$ = 5 ± 2 cal mol^{-1} k^{-1} (see Experimental E3.1.6 and E3.2.2.1). From these values a $k_{20°C}$ = 0.233 s^{-1} (± 3%) was determined. The solvent kinetic isotope effect (KIE) k_{FSO_3H}/k_{FSO_3D} was 1.0 ± 0.1, consistent with rate limiting unimolecular decomposition of a fully protonated (presumably monocationic) oxadiazolinone, and so k_d in aqueous sulfuric acid at 20° was assigned the value extrapolated from the fluorosulfuric acid kinetics.

Now, assuming a negligible solvent effect, Equation R43 was fitted to the observed rate data in aqueous sulfuric acid (Figure R23). A linear plot was only obtained after subtracting out the plateau rate (k_{plat} = 44.50 X 10^{-5} s^{-1}) which precedes the onset of the acid catalysed component. Equation R44 then permits computation of the basicity of 1-Me_2 to be -9.06,

$$[R44] \quad pK_{BH^+} = b + \log k_d = -8.43 \pm 0.08 - (0.63 \pm 0.01) = -9.06 \pm 0.08$$

exceedingly weakly basic. Using this pK value, the ionization ratio in 84% H_2SO_4 is 10^{-3} (logI = -2.95). (Data used for Figure R23 may be found in Table A3.17, Appendix 3).

The m* value of 0.72 may be compared to those for 13 benzophenones (m* = 0.75 ± 0.24; pK_{BH^+} = -3.6 to -4.8) and 14 amides (0.60 ± 0.11, presumably O-protonated) examined by Cox and Yates.[331] They found anthraquinone (178; pK_{BH^+} = -7.7; m* = 0.89) and thymine (179; pK_{BH^+} = -9.8; m* = 0.90) to be the

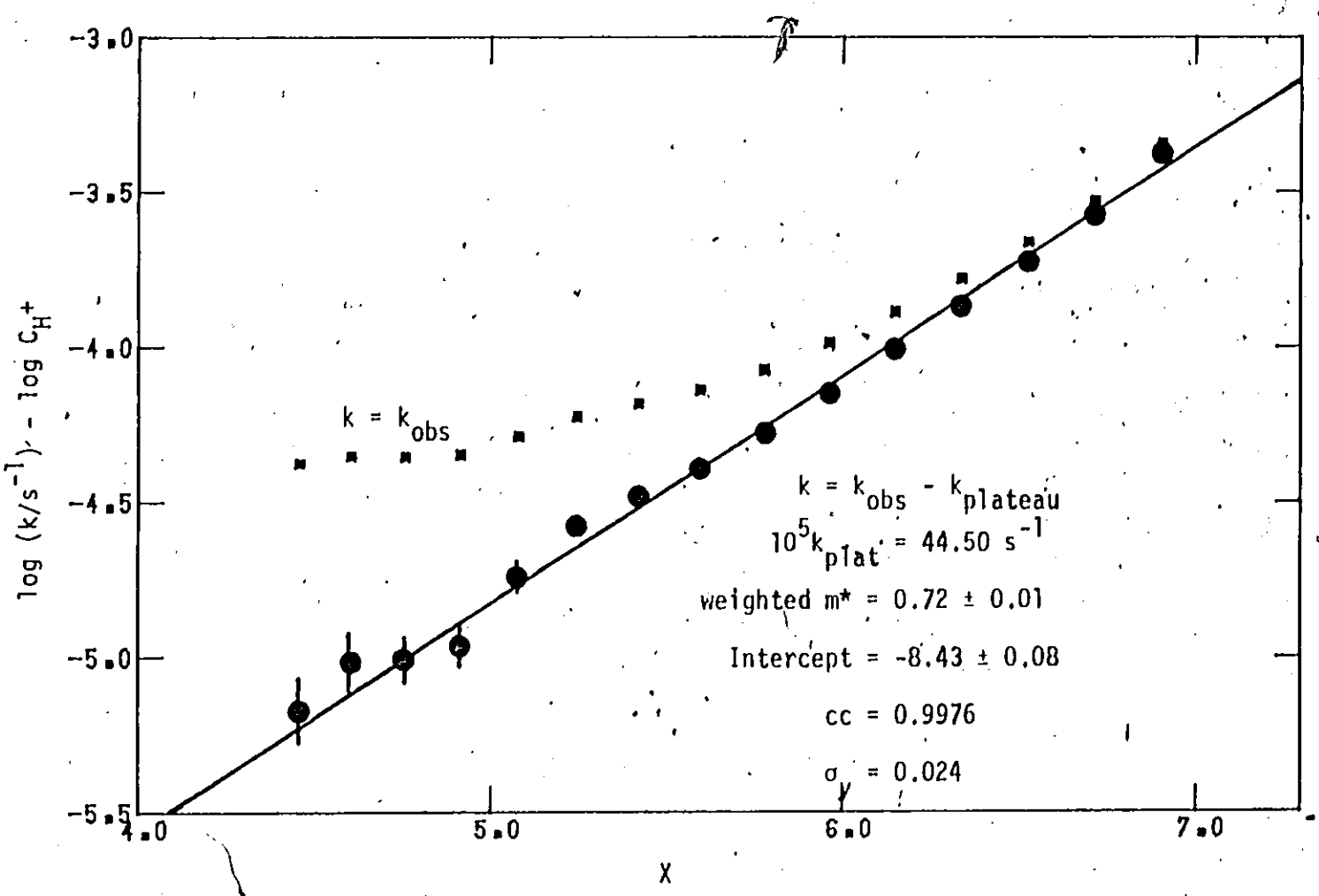

Figure R23. Application of the X-method to the acid catalysed decomposition of 1-Me_2 (interpolated rate constants, see Table A3.18).

least basic of the carbonyl compounds they looked at. Ethyl benzoate had a pK_{BH^+} of -6.0 (0.72) and 2-cyclopentenone (180) -3.2 (0.50) (m* values in parentheses). Eleven azobenzenes in

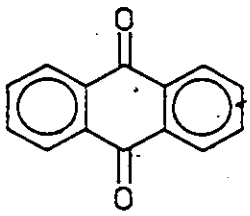

(178)

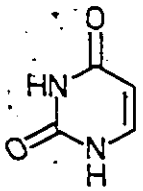

(179)

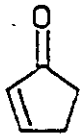

(180)

$HClO_4$ had higher m* values (1.26 ± 0.12) and pKs in the range -0.8 to -4.2.[331]

E3.2.2 Site of Protonation

The preceding section presented evidence to suggest that the acid catalysed decomposition of oxadiazolinones to 2-propanol occurs via some protonated form of the molecule. In this section the location of that proton will be considered.

Nmr spectra of the stable (at -60°) cation of 1-Me_2 in fluorosulfuric acid strongly suggest that N4 is protonated (see Table R11). The two C5 methyl protons and corresponding methyl carbons are all shifted downfield about 0.5 ppm upon protonation. Ring atom C5 experiences a 3.7 ppm downfield shift as a result of closer proximity to the charge. Startlingly, the carbonyl carbon is shifted 15.9 ppm upfield in the cation. Any adjacent charge (on O6 or N3) would have been expected to move it downfield by 30 ppm.[375] In conjugated systems, the second atom from the charge centre can show an upfield shift on protonation which is predictable by theoretical calculation. For

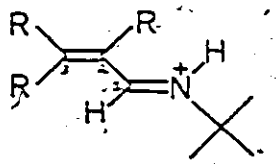

(181)

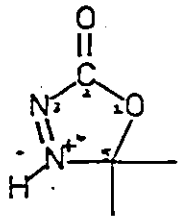

(1·H_{N4}^+)

example, the t-butylimines of α,β-unsaturated aldehydes (181) each show a 6 to 9 ppm upfield shift of their C2 carbon in FSO_3H.[376] By a very crude analogy, C2 in 1-Me_2 could move upfield on N4 protonation.

Table R11. NMR shifts of 1-Me_2 in acetone-d_6 and FSO_3H at -60°[a]

Group	δPMR[b]	δCMR[c]
CH_3	1.67(2.10)	21.4(21.9)
C5		118.8(122.5)
C2		160.5(144.6)

[a]Bracketed values refer to FSO_3H.

[b]Referenced to internal CH_2Cl_2 (δ = 5.28 ppm).

[c]Referenced to acetone-d_6 (external for FSO_3H).

To advance from N4-protonated material to 2-propanol is difficult to visualize. Rupture of the N4C5 bond would be likely, yet yields an intermediate or transition state similar to that for thermal ketone formation (Equation R45).

[R45]

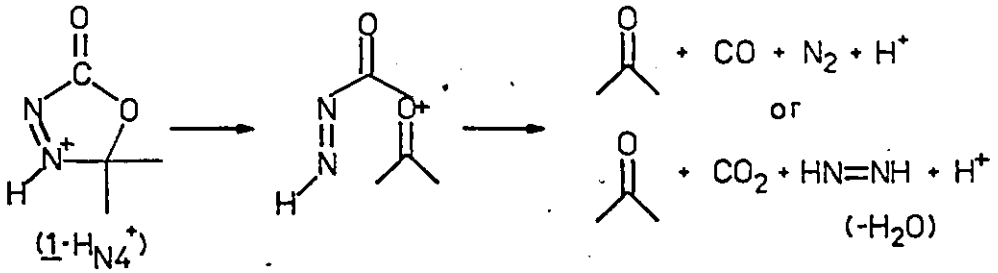

(1·H_{N4}^+)

O6 protonation could activate the carbonyl group to nucleophilic attack by scarce water molecules (Equation R46a) but this would also likely lead to (unobserved) acetone via catalysis of the neutral reaction. Because such a good correlation of log (k_{obs}-k_{plat}) was obtained with X in the previous section, the involvement of water molecules in the transition-state is unlikely. Also, nucleophilic attack on the carbonyl is not the rate limiting step in the neutral hydrolysis (the breakdown of the tetrahedral intermediate is), so to catalyse it ought not to affect the overall rate. The O6 protonated species is capable of a unimolecular ring opening process (Equation R46b), analagous to thermal diazoalkane formation, which would lead to the observed products. Such a reaction parallels the well known Lewis acid catalysis of cycloaddition reactions, and could be stepwise or concerted, but avoids forming protonated CO_2 by occuring in steps. There are known cases of two step Diels-Alder cycloaddition reactions where intermediates are stabilized

[R46]

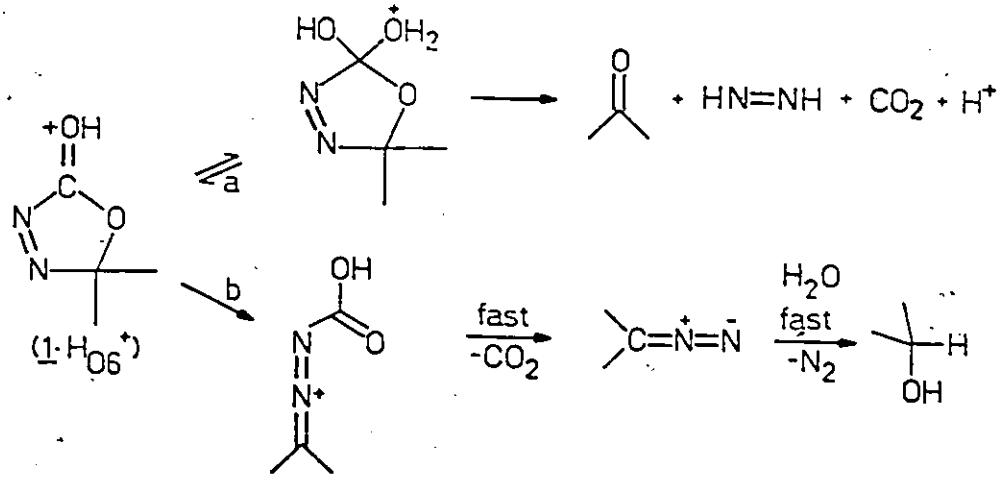

by Lewis acid coordination,[385,386] In others, Lewis acid catalysis occurs via a concerted but very nonsynchronous mechanism.[201]

N3 protonation can also reasonably lead to diazoalkane formation (Equation R47).

[R47] 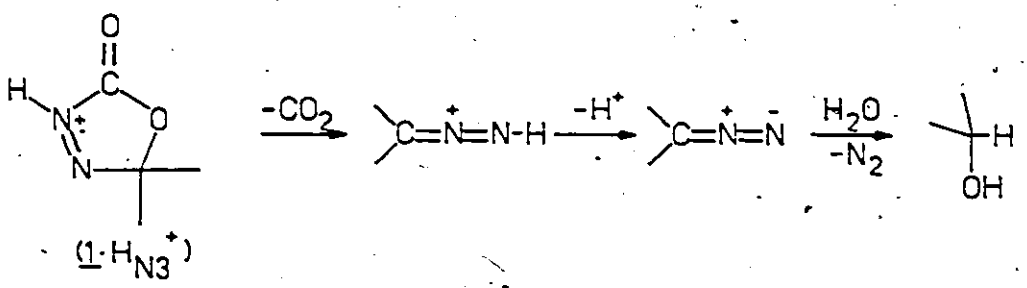

We thus arrive at a dilemma: the most likely protonated form of oxadiazolinone (N4 protonated) seems the least reasonable precursor of the observed products. It might be tempting to account for this quandary by postulating a nonclassical cation with the proton equally shared between nitrogens. Such a structure was proposed by Jaffe (1958-64) for cis and trans-azobenzenes[377-380], but Heilbronner (1962) and Haselbach (1970,1973) very effectively refuted the arguments, with nmr and pK data, particularly of ortho substituted compounds.[381-383] Frontier MO Theory, supported by more detailed calculations, corroborates the likelihood of classical azonium ions: the HOMO is the antisymmetric lone pair combination n_N^-, and therefore cannot create a 3 centre 2 electron bonding MO with an incoming proton because the net overlap between azo n_N- (HOMO) and the proton 1s (LUMO), in a symmetrical arrangement, is zero. Rehybridization changes (principle of least motion[364]) rule out π protonation in the presence of a lone pair.

It is not actually necessary for the acid catalysed reaction to proceed via the thermodynamically most stable cation. Some other, less favourable cation, present in only minor proportion at equilibrium, may be much more reactive. The absence of a solvent KIE in FSO_3H cannot clarify this point: even though FSO_3D is a stronger acid than FSO_3H, the proportion of thermodynamic (observed) cation to nonthermodynamic (kinetically active) cation is independent of acidity because both are protonated forms. For the pK_{BH^+} estimated in the previous section to correspond to the thermodynamic cation (that is for it to have any meaning at all), m* for both thermodynamic and kinetic cation must be identical. The observed m* corresponds to that for the kinetically active protonation.

Clearly, the situation is complex!

3.2.3 Other Substituents

Up to this point, a wealth of kinetic, thermodynamic and product information has been weaving a tapestry depicting dimethyloxadiazolinone hydrolysis. Just when almost everything seems to be under control, complications arise. Replacement of one C5 methyl with a bulky t-butyl group leads to different chemistry. One hint might be an anomalously high solvent kinetic isotope effect in 0.200 M HCl. Whereas k_{H_2O}/k_{D_2O} for 1-Me,CH_2OMe, 1-Me_2, and 1-Me,$PhCH_2$ are all similar (2.52 - 2.63; see Table A3.14), the corresponding value for 1-Me,t-Bu is 3.21 ± 0.03. However, the products — ketone only — are as expected for neutral hydrolysis (see Experimental E3.1.4).

A second hint emerges from the decomposition of 1-Me,t-Bu in TFA — a reaction which proceeds at room temperature to yield a number of non-ketonic products which are bereft of t-butyl groups and coupling in the pmr. Only about 15% of the expected thermolysis product tetramethylethylene is obtained. (Equation R48).

[R48]

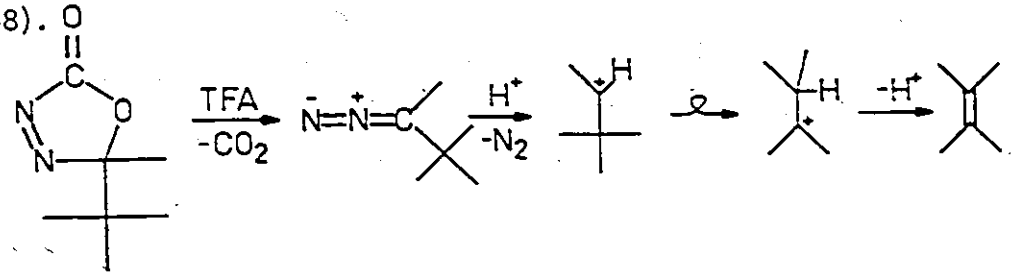

(1-Me t-Bu)

In aqueous sulfuric acid, both 1-Me,t-Bu and 1-Me,$PhCH_2$ exhibit strong acid catalysis in the region $-6 < H_o < -4$ (Table A3.18, Appendix 3), considerably earlier than does 1-Me_2 (see Figure R24). The X method of Cox and Yates generates much higher m* values for these processes (1.20 ± 0.05 and 1.32 ± 0.02 vs 0.72 ± 0.01, respectively), but all three have quite similar intercepts (-8.14 ± 0.20, -8.38 ± 0.06, -8.43 ± 0.08, respectively). Products of the acid catalysed process in this region are complicated, but contain no ketone (see Experimental E3.1.4). Possibly the TFA catalysis is analogous to the sulfuric acid catalysed process for 1-Me,t-Bu (H_o(TFA) = -2.8).[384]

Attempts to study the protonated methyl-t-butyl oxadiazolinone at -78° in FSO_3H were unsuccessful because it apparently decomposed too rapidly to a number of products among which t-butyl cation and an ethyl group (added ethanol reproduced the absorptions) were the main pmr features. Acid catalysed dealkylations are

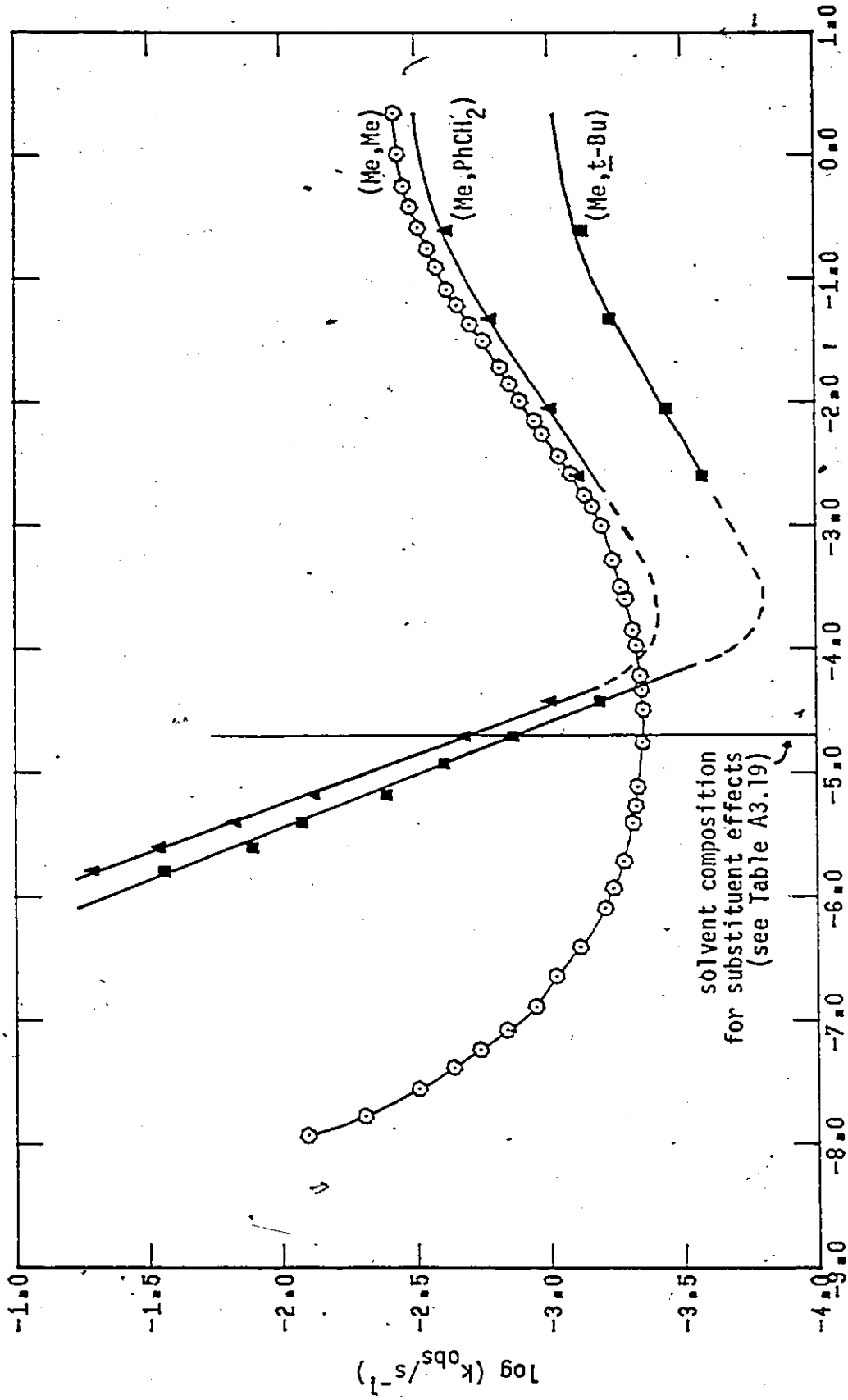

Figure R24. Rate profiles for 1-Me_2, 1-Me,t-Bu, and 1-Me,$PhCH_2$ in aqueous sulfuric acid (measured data).

known, and if the t-btuyl cation were replaced by reversing the process with a proton, methyloxadiazolinone (1-Me,H) would be formed. This could be expected to decompose to ethanol (perhaps not at -79°, however) by analogy to 1-Me_2 giving 2-propanol.

That a cation is formed in the acid catalysed processes is indicated by substituent effects and solvent KIE in 63% H_2SO_4, where primary and secondary R groups have a low rate (< 60 X 10^{-5} s^{-1}) and a near-unity KIE (1.02 - 1.27), but benzyl or t-butyl containing cations decompose much faster, with inverse isotope effects (0.62 - 0.65; see Table A3.19, Appendix 3). Again N3 or O6 protonation is better able to account for dealkylation than N4 protonation (for example, Equation R49).

[R49] 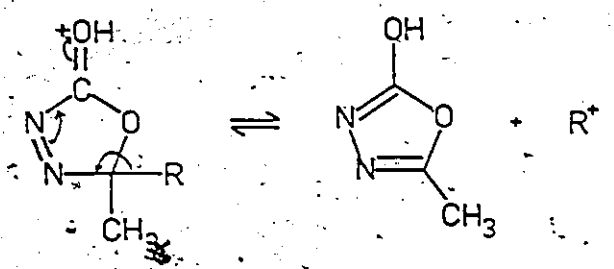

The work reported in this section is of a very preliminary nature and serves only to demonstrate the need for additional detailed kinetic and product studies in aqueous H_2SO_4. Further comment on these sparse observations would be reckless: to fully elucidate these mechanisms defines the experimental challenge of a major project in this area.

R3.3 Concluding Remarks

Two separate mechanisms for dimethyloxadiazolinone

hydrolysis over the acidity range H_o = -16 to pH = 14 have been identified and characterized. First, the neutral and base catalysed reactions share many features with ordinary ester hydrolysis — a model which predicts an intermediate which can successfully account for the observed products: diazene, CO_2, and acetone. Analysis of substituent effects indicated that decomposition of the tetrahedral intermediate was rate limiting (in contrast to most esters, where k_1 is rate determining[350]), but carbonyl oxygen isotope exchange was not observed. This was interpreted in terms of stereoelectronic orbital control of cleavage of the intermediate.

The second, an acid catalysed mechanism, produces 2-propanol (presumably with CO_2 and N_2). Preliminary evidence was presented to develop the working hypothesis that dimethyloxadiazolinone is fully protonated on N4 in FSO_3H, but that decomposition may proceed via either N3 or O6 protonated species present in minor proportion. If that were true, the estimated pK_{BH^+} for 1-Me_2 (-9.06) would be meaningless. Oxadiazolinones containing R groups capable of forming reasonably stable R^+ ions decompose with greater acid sensitivity than other oxadiazolinones, perhaps by a route involving loss of R^+.

More information is needed to progress further in this arena. Gas evolution, mass balance, substituent effect, solvent KIE, and product balance should all be carefully scrutinized in these media. These acid catalysed reactions are not intractible and can be expected to yield to detailed study similar to that

performed for neutral hydrolysis and for thermolysis. The present results might provide a framework from which to plan and launch further studies on this very interesting topic.

EXPERIMENTAL

Melting points were determined on a Thomas Hoover capillary melting point apparatus and are uncorrected. Infrared (ir) spectra (CCl_4 solutions unless otherwise noted) were obtained on a Perkin-Elmer model 283 spectrophotometer. Pmr and cmr spectra were taken on Varian EM-390 and Brüker WH-90 instruments, respectively, all with TMS internal reference unless otherwide indicated. Mass spectra (ms) were recorded on either a CEC-21-110B spectrometer at 70 eV or an Hitachi Perkin-Elmer RMU-6A instrument at lower ionizing voltages. Ultraviolet-visible (uv-vis) measurements were obtained from a Cary 14 instrument. Gas chromatographic (glc) analyses were performed on a column (10' X 1/4") packed with 20% Carbowax 20M on 60-80 mesh Chromosorb P, using a Varian Aerograph model 920 gas chromatograph equipped with thermal conductivity detection and model 485 digital integration. Chlorocarbon extracts were dried over anhydrous sodium sulfate and diethyl ether or light petroleum extracts over anhydrous magnesium sulfate. Light petroleum refers to the fraction boiling between 30-45°C; pentane to "Fisher Certified, IR Spectranalysed" n-pentane; hexane to "Baker Analysed" reagent, bp 68.5 - 69.3°.

Lead tetraacetate (LTA) refers to the material stabilized with 10% acetic acid, as sold by Ventron Corp.

E1 SYNTHESIS

E1.1 General Procedure for LTA Oxidation of Dialkyl Ketone Semicarbazones (Method A)

This is essentially the standard procedure employed by previous workers in this laboratory.[166,314]

LTA (10.0 g, 0.021 mol) was added in one portion to a stirred suspension of the semicarbazone (0.020 mol) in dry CH_2Cl_2 (150 mL) at 0°C. There was an immediate development of a yellow colour. The ice bath was then removed for a period of 0.5-2 h during which time the solution gradually became colourless and a white precipitate formed. The ice bath was returned and a mixture of 2.4 N HCl (50 mL) and ice (150 g) was added. After 15 min, the reaction mixture was filtered through Celite (Johns-Manville Ltd), the organic phase was separated and the aqueous phase extracted with ice cold CH_2Cl_2 (3 X 50 mL). The organic extracts were combined and washed with a cold, saturated solution of sodium bicarbonate (50 mL), and with water (3 X 50 mL). Drying and removal of the solvent under reduced pressure gave crude oxadiazolinone in about 80-90% yield.

Isotopically labelled dimethyloxadiazolinones (5-^{13}C and perdeutero-) were synthesized from the semicarbazones of acetone-2-^{13}C (90% enriched, Merck, Sharpe and Dohme Ltd) and acetone-d_6 (99+% D, Aldrich Co.). The deuterium content of the latter oxadiazolinone was taken to be identical to that measured for the semicarbazone (98.4 ± 0.2% D by ms comparison to unlabelled material).

Purification

The crude material was purified by one or more of the following three methods. Dimethyl- and methyl-t-butyloxadiazolinones were twice sublimed at 0.01 torr from 0°C to a Dry Ice/acetone cold finger. The methylbenzyl and dibenzyl compounds were recrystallized from light petroleum. All other alkyl-substituted products were distilled at 0.01 to 0.001 torr at room temperature (higher temperatures lead to decomposition) then repeatedly recrystallized from pentane at low temperature (ca -20 to -80°C) until magnified ir spectra of the carbonyl region showed less than 0.5% of ketone impurity. Overall yields at the end of the first purification step were 70 to 80%, in most cases. Table E1 lists the melting points and pmr data obtained for this series.

E1.2 LTA Oxidation of Semicarbazones of p-Substituted Acetophenones

As Table E2 summarizes, Method A was successfully used to synthesize the p-H, Br, Cl and CH_3 substituted 5-methyl-5-phenyloxadiazolinones. Although a change of oxidation solvent (to light petroleum) permitted ir observation of the oxadiazolinone from p-methoxyacetophenone, evaporation of the solvent was followed by rapid decomposition to the corresponding diazoalkane and subsequent products. Method B was used in cases where Method A was not successful because the semicarbazones would not cyclize at low temperature and the oxidation products were unstable if oxidation was attempted at higher temperatures.

Method B

An oxidizing mixture of 0.21 M Pb(IV) containing approximately

Table E1. Pmr data for dialkyl substituted oxadiazolinones.

R^1	R^2	M.P.	Pmr(δ)[a]
CH_3	CH_3	39.5-40.0°	1.67 (s, $2CH_3$)
CH_3	CH_2CH_3	oil	0.83 (t, J = 7.5 Hz, 3H, CH_3) 1.66 (s, 3H, CH_3) 2.11 (q, J = 7.5 Hz, 2H, CH_2)
CH_3	$CH_2CH_2CH_3$	oil	1.60 (s, 3H, CH_3) 1.8-2.2 (m, 3H, CH_3) 2.2-2.4 (m, 2H, CH_2) 3.4-3.7 (m, 2H, CH_2)
CH_3	$CH(CH_3)_2$	oil	0.94 and 1.09 (both d, J = 6.9 Hz, 6H, diastereotopic CH_3) 1.62 (s, 3H, CH_3) 2.25 (septet, J = 6.9 Hz, 1H, CH)
CH_3	$CH_2CH(CH_3)_2$	oil	0.92 and 0.98 (both d, J = 6.4 Hz, 6H, diastereotopic CH_3) 1.4-2.2 (m, 3H, CH_2CH) 1.63 (s, 3H, CH_3)
CH_3	$C(CH_3)_3$	36-36.5°	1.05 (s, 9H, t-Bu) 1.56 (s, 3H, CH_3)
CH_3	CH_2OCH_3	oil	1.65 (s, 3H, CH_3) 3.31 (s, 3H, OCH_3) 3.71 and 3.93 (2d, J = 11.3 Hz, 2H, diastereotopic AB set in ratio 2:1, CH_2)
CH_3	$CH_2C_6H_5$	108°(dec)	1.63 (s, 3H, CH_3) 3.28 (s, 2H, CH_2) 6.95-7.4 (m, 5H, aromatic H)[b]
$CH_2C_6H_5$	$CH_2C_6H_5$	105°(dec)	3.38 and 3.53 (both d, J = 15 Hz, 4H, diastereotopic AB set in ratio 4:1, $2CH_2$) 6.95-7.4 (m, 10H, aromatic H)[b]
$CH(CH_3)_2$	$CH(CH_3)_2$	oil	0.91 and 1.06 (both d, J = 6.9 Hz, 12H, diastereotopic CH_3) 2.72 (septet, J = 6.9 Hz, 2H, 2CH)

Table E1 (continued)

[a] CCl_4 solution, except were noted.

[b] $CDCl_3$ solvent.

Table E2. Synthesis of p-substituted acetophenone oxadiazolinones (1-Me,Ar)

p-Substituent	Synthetic Method[a]	Crude Yield[b]	ν_{CO}[c]	mp	f_{oxa}[d]
CH_3	A	60	1834	oil	0.866
C_6H_5	B	55	1832	68-70°	0.926
H	A	70	1835	oil	0.858
Cl	A	60	1887	oil	0.754
Br	A	60	1837	oil	0.878
CF_3	B	75	1837	oil	0.799
CN	B	55	1837	109-10°(dec)	0.844
NO_2	B	60	1840	103-4°(dec)	0.793
$CONH_2$	B	50	1836	110-11°(dec)	

[a] See text for details of methods A and B.

[b] Pmr integration prior to purification (%).

[c] Infrared in CH_3CN (cm^{-1}).

[d] Pmr assay for oxadiazolinone purity - see text. Standard deviations are 2-3%. The methyl proton resonances lie between 1.8 and 1.9 ppm.

1:1 acetate and trifluoroacetate was prepared by dissolving lead tetraacetate (90%, 102.5 g) and TFA (76mL) in dry CH_2Cl_2 (1 L). Qualitatively, this solution gave the best results: more TFA led to more decomposition, less meant incomplete cyclization. No effort was made to determine if the enhanced oxidation rate was due to increased semicarbazone solubility or to formation of a mixed acetate/trifluoroacetate Pb(IV) species of higher oxidizing power. Lead tetratrifluoroacetate (LTTFA)[387] in either CH_2Cl_2 or TFA/TFAA did not result in oxidative cyclization, even though the latter solution was completely homogeneous.

In a typical experiment, three separate solutions were cooled to -15°C for 0.5 h in an ice/salt or ice/alcohol bath: a stirred slurry of semicarbazone (0.010 mol) in dry CH_2Cl_2 (50 mL) in a stoppered flask (250 mL); oxidizing solution (50 mL, 0.0105 mol) in a stoppered flask; and 2.4 N HCl (50 mL). The oxidant was rapidly added to the semicarbazone slurry and the now-homogeneous reaction mixture stirred 3-5 min before the aqueous acid was added. Hydrolysis times of about 1 min were adequate and filtration through Celite followed by ice-cold workup was identical to that in Method A above. Pmr spectra of the crude reaction product indicated that oxadiazolinone accounted for more than 50% of this material (yields of crude products, Table E2).

Purification

For the p-NO_2, $CONH_2$, and CN compounds, the crude solid was extracted from a residue of unreacted semicarbazone with a

minimum of CH_2Cl_2, then recrystallized from $CHCl_3$. The separation of the oxadiazolinones bearing p-CH_3, C_6H_5, H, Cl, Br and CF_3 substituents from their decomposition products formed in synthesis — mostly ketone and trifluoroacetic acid ester — could only be achieved without further decomposition by low temperature column chromatography. In an evacuated, Dry Ice/acetone filled, jacketting Dewar, a column of 2.5 X 30 cm was packed with silica gel (Baker, 60-300 mesh, ca 90 g for one gram of crude material). Generally, 15-20% diethyl ether in light petroleum was used as the eluant. In spite of problems inherent in this technique — trying to keep things dry, low solubility (gumming of the sample at the top of the column) and rapid elution — magnified ir spectra of the carbonyl region for each fraction allowed selection of a small cut of reasonably clean material. In all cases but the p-C_6H_5, an oil was obtained which could not be further purified. 5-Methyl-5-p-biphenylyl-oxadiazolinone was recrystallized from diethyl ether/hexane.

Because none of the acetophenone oxadiazolinones was very pure, each was assayed by low temperature (-30°C) pmr in CCl_4 or acetone-d_6 by careful integration of the methyl group against anisole as internal standard. This information is also contained in Table E2. The assay was applied as a correction factor, f_{oxa}, when determining starting oxadiazolinone concentrations for product analysis. Fortunately, the reaction rates were independent of any impurities remaining in these samples after the above purification step. All samples (neat

or CH_3CN solution) were stored in the freezer (-25°C) prior to use, and none was kept for more than 10 days after preparation.

E1.3 LTA Oxidation of d-Camphor Semicarbazone

The crude reaction product obtained using Method A contained about 60% ketone and 40% oxadiazolinones (ir). This material was chromatographed at -20°C on silica gel (Baker, 60-300 mesh, 50 g per gram), from which it was eluted with 1% diethyl ether in light petroleum. Although the two isomeric oxadiazolinones 159a and 159b were completely separated from the ketone, they were not well separated from each other. Fractions containing more than 75% exo-azo isomer (159a; by pmr — see next paragraph) were combined and the white solid fractionally crystallized five times from pentane to give 159a (ca 0.1 g, mp 83-84°C) in 1.5% overall yield. The endo-azo isomer (159b) remained an oil and further attempts to isolate it from its contaminant (30% of 159a) were unsuccessful.

The stereochemistry in the diastereomers of d-camphor oxadiazolinones was assigned by nmr. Selective decoupling of the methyl protons at 0.53 ppm of either isomer of 159 caused collapse of the quartet at 8.6 or 9.4 ppm in the cmr spectrum (see Table E3), indicating that the upfield protons were on C10. In both isomers, these protons spend time in the shielding region above the plane of the azo pi bond and appear about 0.5 ppm upfield of their usual position at ca 1 ppm. The opposite

Table E3. Nmr assignment of stereochemistry in camphor oxadiazolinones.[a]

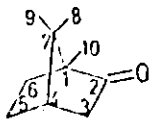
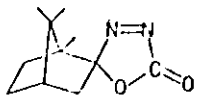
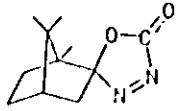
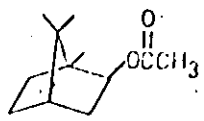
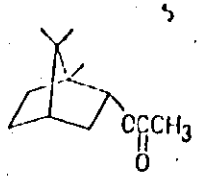

		d-camphor	159a	159b	borneol acetate	isoborneol acetate
pmr, methyls	C8	(0.85)	1.52	(1.00)	(0.83)	(0.82)
	C9	(0.92)	1.07	(1.13)	(0.90)	(0.82)
	C10	(0.97)	0.53	0.53	(0.95)	(0.96)
	reference	this work	this work	this work	388a	388b
cmr methyls	C8	(19.3)	20.5	(19.4)		
	C9	(19.0)	20.5	(19.7)		
	C10	9.5	9.4	8.6		
	reference	389	this work[b]	this work[c]		

[a]Bracketed values may not be correctly assigned. Chemical shifts are in ppm relative to internal standard TMS, in CCl_4 solvent.

[b]For the 11 carbon atoms, the following shifts were observed: 9.4, 20.5, 20.5, 26.6, 31.1, 37.9, 45.1, 50.2, 56.8, 127.3, and 159.1 ppm.

[c]For the 11 carbon atoms: 8.6, 19.4, 19.7, 27.2, 30.1, 39.9, 45.3, 50.2, 56.5, 128.0, and 159.2 ppm.

downfield shift of the C8 methyl protons to 1.52 ppm in one isomer cannot be due to the oxygen lone pairs nor to the carbonyl group since such an effect is absent in borneol and isoborneol acetates (Table E3). Models show that free rotation of the C8 methyl group of 159a permits the protons to spend time in the deshielding region in the plane of the azo pi bond. In the endo-azo isomer, this effect is not possible and the C8 methyl hydrogens appear in their usual position, at about 1 ppm.

E1.4 Synthesis of ^{17}O Carbonyl Labelled Oxadiazolinones

In these syntheses, $^{17}OH_2$ (Merck, Sharpe, and Dohme Ltd , 20.4% enriched, $170.00 per gram) was to be conserved as much as possible. The carbonyl group is introduced by aqueous acid hydrolysis of intermediate iminooxadiazoline. To avoid wasting water on hydrolysing unreacted LTA, LTA was employed as the limiting reagent, with ketone semicarbazone in excess.

In a preliminary (unlabelled) run, lead tetraacetate (1.126 g; < 2.54 mmol after accounting for excess acetic acid) was placed into a dry 25 mL flask containing a small teflon coated stirring bean, and dry CH_2Cl_2 (15 mL) was added. Acetone semicarbazone (0.303g; 2.63 mmol) was added and the flask capped with a dry serum cap and sealed with parafilm. The contents were stirred and shaken at room temperature for 30 min, during which time a clear organic layer separated from a pale brown gummy solid which stuck tenaciously to the inside walls of the flask and to the bean. Concentrated HCl (5 µL) and water (50 µL; total water

~ 3.0 mmol would have been 19% enriched if labelled*) were added through the cap and the still gummy mixture stirred and shaken for 2 days.

To monitor the progress of the hydrolysis of the iminooxadiazoline during this period, small aliquots (50 μL) of the liquid phase were withdrawn, diluted by a factor of 10 with dry CH_2Cl_2 and the ir intensity at 1835 cm^{-1} recorded in a 0.1 mm CaF_2 solution cell. The intensity of this oxadiazolinone carbonyl band rose as expected for a first or second order reaction. After 47 hours, 20% HCl (1.0 mL) was added† and the mixture was stirred at room temperature for 7 min prior to a final ir sample. At this time, the gum had been replaced by a white precipitate. Pmr of the crude material after workup showed a 90-95% yield. The ir absorbances were converted into percent reaction (normalizing to the value after the addition of 20% HCl) and plotted against hydrolysis time. From that plot, 10-12 hours was deemed sufficient for about 95% hydrolysis.

In several runs with labelled water, analogous (but unmonitored) procedures using acetone or 3,3-dimethylbutan-2-one semicarbazone gave the labelled substrates l-Me_2-^{17}O and l-Me, t-Bu-^{17}O, respectively. Some of the excess semicarbazone in the

*This figure ignores the two moles of acetic acid liberated in oxidation. Unfortunately, if the acetic acid exchanged completely with the water during hydrolysis, the enrichment would be only 1/5 of this value (and even less if $Pb(OAc)_2$ or $Pb(OAc)_4$ exchanges!) Although the carbonyl stretch of the oxadiazolinone CO^{16} and CO^{17} bands were inadequately resolved to permit calculating an enrichment, apparent asymmetry was consistent with 10±5% enrichment.

†In labelled runs this step was avoided. For the preliminary syntheses, however, it was desireable to complete the hydrolysis for yield measurement purposes.

latter crude product could be precipitated by adding pentane (1.0 mL). The overall yield of dimethyloxadiazolinone-^{17}O was sometimes lowered by decomposition (as evidenced by a bulging serum cap during hydrolysis). These products were used without further purification.

E1.5 Photoelectron and UV-Visible Spectroscopy

5,5-Dimethyl-Δ^3-1,3,4-oxadiazolin-2-one (1-Me_2) was prepared in 80% yield from the ketone semicarbazone as described in Section E1. Samples for PES were twice sublimed at 0.01 Torr from 0°C to a Dry Ice-acetone cold finger and maintained at -20°C in the dark prior to use. The photoelectron spectrum was obtained by Professor N.H. Werstiuk, of this department, using the equipment of Professor D.C. Frost at the University of British Columbia[390]: a sample pressure of 10^{-5} Torr was employed, and no evidence of any decomposition product IPs was observed during spectrum acquisition.

Hexane for the uv spectrum was purified by overnight treatment with H_2SO_4 and careful fractionation from $CaSO_4$. This material had a uv cutoff at 190 nm on a Cary Model 14 spectrophotometer.

E2 Thermolysis

E2.1 Materials

Because of the aqueous decomposition mechanism, good first order kinetics could not be obtained using wet solvents. 1,2-Dimethoxyethane (DME) and toluene were each fractionated at high reflux ratio (ca 5:1) from calcium hydride and a two-thirds centre cut stored over fresh 4 Å molecular sieves. The following solvents were fractionated from Drierite ($CaSO_4$, Hammond Co.) and the centre cut stored over molecular sieves: chlorobenzene, 1,3-dichloroethane (DCE) and trifluoroethanol (TFE); acetonitrile and nitromethane were each pretreated by passage through a column of neutral alumina (30 g L^{-1}); nitrobenzene and dimethylformamide (DMF) were fractionated at reduced pressure (10-20 torr). Trifluoroacetic acid (TFA) and acetic acid (HOAc) were each fractionated prior to use and ca 1% of the respective anhydride added to keep them dry. In all cases, glc analysis showed water to be less than 0.05%.

E2.2 Kinetics

Rate constants k_3 and k_2, respectively, for ketone and diazoalkane formation, were determined by applying the product assay for fraction of ketone formed (see below) to the total rate constant for disappearance of starting material, $k_T = k_2 + k_3$. Each value of k_T was measured in triplicate and the results averaged. The bath temperature was maintained to ± 0.10°C or better and the average k_T had

a typical standard deviation of the mean of less than 1%.

E2.2.1 UV Method

A kinetic method employing uv analysis of removed aliquots was utilized for the solvent effects (Table A3.4, Appendix 3), activation parameters (Tables A3.5 and R5), β-deuterium kinetic isotope effect (Table A3.6), and alkyl substituent effect studies (Table A3.7) in all but TFE and TFA. Solutions of oxadiazolinone were prepared at room temperature in 100 mL volumetric flasks, (3-5 mM in oxadiazolinone; ca 90 mL) which were capped and placed in the constant temperature bath. After a warming period of 20 min, aliquots of 6 mL were withdrawn by syringe and quenched in liquid N_2. Two time infinity (10 half-lives) samples were taken for each run and then all 12-14 samples were allowed to warm to room temperature for uv-vis analysis of absorption at λ_{max} of the azo n → π* transition (ca 360-380 nm, slightly solvent variable, ε_{max} ~ 200-400 M^{-1} cm^{-1}). The data were treated by a standard linear least squares procedure (see Appendix 1) and the calculated total first order rate constants (k_T) were obtained with typical correlation coefficients of 0.999 for up to 5 or more half-lives. Increasing the concentration by a factor of 20 or adding 1% aniline had no effect on the measured rate constants. TFE and TFA runs were done using 0.5 mL aliquots individually sealed in glass tubes and uv analysis was accomplished in cells of 0.1 cm path length.

The β-deuterium kinetic isotope effect, k_H/k_D, for each process was measured at 85.0°C in toluene and acetonitrile by the uv method. For labelled and unlabelled 1-Me_2, k_T was simultaneously determined,

each in duplicate to eliminate possible errors arising from minor temperature variations. Duplicate k_T's for 3 half-lives arreed within their estimated standard deviations (< 0.3%). Product analysis by calibrated glc employed acetone-d_6 in a fashion analogous to that described below. Although the total isotope effects, $k_T(H)/k_T(D)$ were nearly the same for both solvents (1.1 for all 6D), only k_H/k_D for ketone formation in toluene and for diazoalkane formation in acetonitrile are ultimately reported since the propagated error for the minor pathway in each case renders the value of k_H/k_D for that pathway unreliable (see Table A3.6).

E2.2.2 IR Method

The uv method was unsuitable for the para-substituted 5-methyl-5-phenyloxadiazolinones because a pink to red colouration develops during decomposition, presumably from the diazoalkane. Oxadiazolinone (ca 0.050 g) was carefully weighed and dissolved in dry CH_3CN (10.00 mL). Portions of about 0.2 mL were transferred by syringe to glass tubes (12 cm long by 2 mm id), filling about 45 of them to a depth of 5 cm. This amount of sample was exactly sufficient to fill a 0.5 mm CaF_2 ir solution cell. The tubes were quickly sealed and stored in the freezer at -25°C until used for either kinetics or product analysis.

In a typical kinetic run, 12 to 16 sample tubes were withdrawn from the bath at intervals calculated to give roughly equal concentration differences up to 3 to 5 half-lives. The reaction was quenched by cooling with liquid N_2. For the ir analysis, the

spectrophotometer was operated in the absorbance mode on a very slow scan speed and a large wavelength expansion setting at 1835 cm^{-1}. Calibration plots using ketones showed that measured absorbances were a linear function of concentration, and first order fits of the disappearance of ν_{CO} of oxadiazolinone gave correlation coefficients typically better than 0.9995 (see Table A3.8).

E2.3 Product Distributions

Diazoalkanes generated in oxadiazolinone thermolyses often react in a variety of ways to give several products — some incorporating solvent (pmr, glc). The addition of a few drops of TFA per mL of solvent effectively traps the diazoalkane as the trifluoroacetic acid ester; the only other product observed by pmr and glc being ketone. Under the reaction conditions employed in these thermolysis studies, neither diazopropane nor any of its subsequent reaction products (principally acetone azine) were hydrolysed or otherwise converted to the ketone. Nor, at 80-100° in dilute solution, should diazoalkane react with ketone.[1-9] This means that accurate determination of the product distribution may be inferred from quantitative assay of ketone only.

For the solvent effects (Table A3.4), activation parameters (Table A3.5), and β-deuterium kinetic isotope effects (Table A3.6) (cases where very pure starting material was available), the time infinity acetone concentration was measured by integrated glc, calibrated against internal standard 2-butanone. Typically 8-15 injections of each of several calibrant solutions and reaction mixtures were used to obtain an average of the fraction of ketone

formed in each case, f_{co}, and this result had an estimated standard deviation of the mean of about 1-2%.

Ketone measurements by ir carbonyl absorption for dialkyl and acetophenone oxadiazolinones were obtained under conditions of slow scan speed and large wavelength scale magnification. Seven to ten calibration solutions of twice recrystallized or redistilled ketone demonstrated excellent linearity between absorbance and concentration. By measuring the time infinity ketonic carbonyl absorption and correcting for any ketonic impurity at time zero, the concentration, and hence the fraction, f_{co}, of ketone formed was computed. From a knowledge of the nmr purity assay, f_{oxa} (see E1.2 above), a correction to the starting concentration of acetophenone oxadiazolinone was made:

$$f_{co} = \frac{([\text{ketone}]_{\infty} - [\text{ketone}]_{o}) \times MW_{oxa} \times Vol}{\text{weight}_{oxa} \times f_{oxa}}$$

For alkyl substituted oxadiazolinones, f_{oxa} was taken to be unity though it may have been as low as 0.95 in rare cases.

The product distribution in nitrobenzene was obtained by pmr.

For the camphor oxadiazolinones, the product ratios (ir) were obtained as a function of the exo/endo ratio (pmr) in seven mixtures. Least squares analysis gave f_{co}(exo) = 8.4 ± 0.4% and f_{co}(endo) = 26.2 ± 1.1%.

E2.4 Other Experiments

E2.4.1 Thermochemistry: $\Delta H_f°(oxa)_g$

At 25°C, the energy released by combustion of 1 gram pellets

of 5,5-dimethyloxadiazolinone was measured in a Parr Oxygen Bomb Calorimeter and found to be 526.0 ± 0.2 kcal mol^{-1}. An enthalpy of combustion was computed from the stoichiometry in Equation E1

[E1] $$C_4H_6N_2O_{2(s)} + 4\ 1/2\ O_{2(g)} \rightarrow 4CO_{2(g)} + N_{2(g)} + 3H_2O_{(l)}$$

when corrected for the ca 2% nitrogen combustion[391]. This gave $\Delta H_c° = -525.1 \pm 0.4$ and $\Delta H_f°(oxa)_s = -56.05 \pm 0.4$ kcal mol. Determination of the gaseous heat of formation necessitated approximating the heat of sublimation, $\Delta H_s°$, to a crude estimate for the heat of vaporization, $\Delta H_v°$, obtained from Benson's empirical formula (Equation E2).[101]

[E2] $$\Delta H_v°(298\ K) = 22(1.76 \times 10^{-3} \times T_b(°C) + 0.253)$$

Although the boiling point, T_b, of dimethyloxadiazolinone is unknown, it is a reasonably volatile solid of mp = 39.5 - 40.0°C, so a bracketed estimate of $40 < T_b < 100$°C generated error limits in $\Delta H_v° = 8.3 \pm 1.2$ kcal mol^{-1}. With $\Delta H_s° \approx 8.3 \pm 2.0$, $\Delta H_f°(oxa)_g = -47.7 \pm 2.0$ kcal mol^{-1}. Admittedly, several very crude assumptions are involved in the value chosen for $\Delta H_s°$, and hence $\Delta H_f°(oxa)_g$, but very generous error limits appended to the final value do reflect the uncertainty.

E2.4.2 Chemiluminescence

Attempts to observe chemiluminescence employed a single photon counting apparatus calibrated with luminol[392]. Event signals from a 14 stage Amperex 56 DUVP/03 photomultiplier tube in a PRA-510 housing operated at -1990 V were run through an ORTEC 9301 fast preamp

to an ORTEC 454 timing filter and out to a Hewlett-Packard 60 MHz frequency counter. The dark current was 13 Hz.

A solution of dimethyloxadiazolinone in hexane (0.3M) was degassed in a cylindrical quartz tube by three freeze-pump-thaw cycles and heated to 100-110°C in an oil bath for three minutes prior to transferral to the sample chamber of the single photon counting apparatus. Counting was initiated immediately. In only a few minutes, the sample had cooled to ca 50°C, but at no time was any chemiluminescence apparent. No signal above background dark current was observed. The experiment was repeated in the presence of anthracene with identical results. Another sample, 0.02 M in 5-methyl-5-(p-chlorophenyl)-Δ^3-1,3,4-oxadiazolinone, also gave no additional counts. A detection limit of a 20% increase over background counts would have meant the fraction of acetone excited states formed near 50° had been $\sim 2 \times 10^{-10}$.

E2.4.3 Electron Spin Resonance

Esr signals were not observed during thermolysis of degassed chlorobenzene solutions 0.5 M in dimethyloxadiazolinone at a temperature of 100°C in the probe of a JEOL JES-3BS-X spectrometer. When the experiment was repeated in the presence of doubly sublimed nitrosobenzene, the esr spectrum of diphenyl nitroxide was obtained (a_N = 10.0 g; a_H = 0.9 g). The same spectrum was observed from nitrosobenzene in the absence of oxadiazolinone, and the splitting parameters agree with those in the literature.[393]

E2.4.4 Chemically Induced Dynamic Nuclear Polarization

In a biradical of structure 155 (page 120), formed from

5,5-dimethyloxadiazolinone, coupling of the methyl protons to the unpaired electron at C5 might produce enhanced absorption or emission in the ^{1}H nmr during decomposition, but such effects were not observed at ca 100°C in chlorobenzene.

In some cases, ^{13}C nmr is more sensitive to CIDNP phenomena[23] but with as much as 0.25 g of sample, the carbonyl carbons of oxadiazolinone and product acetone could not be detected above baseline noise because too few scans were accumulated during the key minutes of the reaction. To overcome this problem, 90% enriched 5,5-dimethyl-Δ^{3}-1,3,4-oxadiazolin-2-one-5-^{13}C was synthesized from acetone-2-^{13}C (Merck, Sharpe and Dohme of Canada Ltd). Even though C5 and acetone carbonyl could be easily observed from 0.050 g of the labelled oxadiazolinone, the thermolysis at 100°C in either chlorobenzene or methylene iodide failed to generate emission or enhanced absorption in the cmr spectrum. The CIDNP experiment was negative.

E2.4.5 PMR Test of Interconversion of 159a and 159b

The sample of pure 159a was assayed by 90 MHz pmr to contain < 0.2% 159b. This detection limit was determined from scans of the 0.6 to 1.1 ppm region under conditions which did not saturate signals (low rf power and moderate scan speed). Excellent gaussian lineshapes were always obtained. Cut-and-weigh integration procedures established for assay of mixtures of 159a and 159b proved that a peak of 0.5% of the total intensity in this region was easily measured. Hence, a detection limit of about 40% of this level was inferred as reasonable.

Oxadiazolinone 159a (0.030 g) in dry CCl_4 (0.5 mL) was sealed

into a tube and thermolysed at 85°C for 80 min (ca 30% decomposition). The sample was cooled, transferred to an nmr tube and the pmr obtained. To the high field side of the anti-C7 methyl protons of 159a (1.07 ppm) a complex series of absorptions obscured one possible C7 methyl of the endo isomer, 159b (1.00 ppm). However, the low field side of the 159a absorption was remarkably clear and revealed no observable change in baseline attributable to the 1.13 ppm methyl in 159b. On this evidence, interconversion of 159a and 159b was ruled out.

E2.4.6 Estimation of an E_T value for TFA

Protonating solvents remove the solvatochromic absorption band of the pyridinium N-pehnolbetaine used to define the E_T scale. In order to include TFA in the reported solvent polarity correlations, an E_T value was estimated from linear correlations with other solvent polarity parameters.[77]

Solvolysis data on 2-adamantyl tosylate ($k_{2\text{-AdOTs}}$) in TFA, TFE, HCOOH, HOAc, EtOH, MeOH, and $(CF_3)_2CHOH$[394] were correlated with the solvent polarity parameter called log k_{ion}[77] to estimate a value of log k_{ion}(TFA), and then that value was used in a correlation of log k_{ion} with E_T (Equations E3-E5).

[E3] $\log k_{2\text{-AdOTs}} = (2.193 \pm 0.096) \cdot \log k_{ion} - (2.269 \pm 0.154)$ $r = 0.990$

[E4] $\log k_{ion} = (0.195 \pm 0.016) \cdot E_T - (13.17 \pm 0.75)$ $r = 0.964$

[E5] $\log k_{2\text{-AdOTs}}(TFA) = -3.05$ $\therefore E_T(TFA) = 65.7 \pm 6.6$

In spite of the necessary use of two correlations, instead of one (because log $k_{2\text{-AdOTs}}$ data are available only for very few solvents with measured E_T values), the error propagation suggests

quite reasonable confidence limits: the same procedure converts log $k_{2\text{-AdOTs}}(TFE) = -5.821$[394] to an $E_T(TFE) = 59.2 \pm 6.2$, only 0.3 units lower than the actual value.[77]

E3 Hydrolysis

E3.1 Product Distributions

Most of the product and kinetic studies focussed on the 5,5-dimethyloxadiazolinone. It is extremely difficult to obtain quantitative product composition data corresponding to the kinetics performed at about 1 mM concentration, because the products are volatile and water soluble, and because the concentrations are extremely low. Changing to higher molecular weight substituents to permit extraction and isolation for measurement is of limited relevance since substituents have an enormous effect on the course and rate of decomposition. Buffering salts, HCl, and H_2SO_4 discourage analytical vpc. For nmr analysis, water is a poor solvent, yet D_2O may obscure protons transferred from solvent, remove coupling, and exchange with acetone. Oxadiazolinone water solubilities are quite low and decrease with bulkier organic substituents, making it difficult to increase concentration for nmr experiments. Nevertheless, heterogeneous and homogeneous decompositions were performed for nmr analysis and some gas evolution experiments were conducted.

E3.1.1 PMR Product Analyses

Dimethyloxadiazolinone (ca 0.02 g) was added to various solvents (1.0 mL of 0.200 M NaOH, pH 10, 7, 4, 3 or 1 buffer, 0.200 or 1.000 M HCl, or 30, 50, 63, or 75% H_2SO_4) and the heterogeneous (insoluble solid plus liquid) mixture stirred and shaken until gas evolution subsided. Each reaction mixture was transferred to an nmr tube and time infinity spectra were recorded using the

acetone shift (arbitrarily defined as 2.0 ppm) as calibrant.

In all buffers and aqueous base, nearly identical products were obtained: about 30% acetone and 70% acetone azine (1.6 and 1.8 ppm singlets; confirmed by vpc). Similar homogeneous decompositions in unbuffered 50% v/v D_2O/CD_3CN or D_2O/CD_3OD gave very similar product proportions. Notably, in all these spectra there was absolutely no 2-propanol (1.0 ppm doublet) and no formic acid (8.0 ppm singlet). Separate experiments established that over the pH range 2-14 the final product composition could be reproduced with a 2:1 mixture of acetone and hydrazine.

When decompositions were performed in the dilute HCl solutions, the yield of acetone increased to about 50% and some unidentified material absorbing at 2.10 and 2.25 ppm appeared in the ratio 3:1. Similar absorptions were obtained when acetone azine (ca 0.02 g) was added to fresh solvent.

Heterogeneous decompositions carried out with < 55% aqueous sulfuric acid gave a white precipitate with the liquid layer containing more than an 85% yield of acetone. A similar precipitate could be obtained by adding either hydrazine or acetone azine to these solvents — the latter experiment yielding a pmr spectrum of acetone. 2-Propanol was not observed in either 30 or 50% acid, but < 8% was noted in 63% H_2SO_4, just prior to the onset of the acid catalysed region. In 75% acid, a quantitative yield of 2-propanol was obtained.

A homogeneous solution of oxadiazolinone (ca 0.001 g) was prepared in 1.0 M HCl (1.0 mL). Gated, decoupled FT pmr spectra

taken after decomposition largely eliminated the solvent signal (4.7 ppm) by irradiating it for several seconds in order to saturate it prior to the rf pulse. Collecting 100 such scans gave pmr spectra showing only acetone product (>95%) with S/N = 100. The solvent intensity was reduced by a factor of almost 5000 (1:2 compared to acetone) through the gated decoupling technique. Absolutely no (<1%) acetone azine or 2-propanol was observed in this spectrum.

E3.1.2 Gas Evolution Experiments

The gas evolved after injecting a DMF or alcohol solution of dimethyloxadiazolinone (ca 0.2 g, carefully weighed and dissolved in 2.0 mL solvent, plus 2.0 mL rinse) into various aqueous solvents (10.0 mL) was collected and its volume measured. All such mixtures were homogeneous. After correcting for the volume of added liquids and the solvent vapour pressure (but not for the gas solubility in each solvent), gas yields (moles gas/mole oxadiazolinone) were computed. Table E4 summarizes the results.

Table E4. Gas yields from hydrolyses of 1-Me_2.

Solvent	30% H_2SO_4	1.00 M HCl	50% MeOH	0.20 M NaOH
Gas Yield	1.44	1.65	1.58	0.64[a] (1.35)[b]

[a]Prior to acidification

[b]After acidification

E3.1.3 Identification of C2 Gas by GC-FT-IR

Dimethyloxadiazolinone (0.01 g) was hydrolysed in 50% v/v

methanol/water (2 mL) for one hour (more than 5 half lives) in a capped 4 mL vial at room temperature. Aliquots of this solution (5 μL) were removed and injected into a Varian 3700 gas chromatograph whose effluent was analysed with a Nicolet 7199 FT-IR fitted with a nickel transfer line and 25 cm path length light pipe. The column (4' by 1/8" stainless steel, 10% carbowax 20 M on Chromosorb W (100-120 mesh)), was temperature programmed for 30-200°, with transfer line, light pipe, injector, and gc detector base all at 250°. Nitrogen carrier gas flowed at 25 mL min^{-1}. (It is doubtful that any of these conditions are critical to the required crude separation of product gases from organic material and solvents).

The first eluted peak (20s) to show ir activity gave a spectrum featuring a strong asymmetric multiplet at 2365 cm^{-1} (position of maximum intensity) and a sharp single line at 667 cm^{-1}. An identical spectrum was obtained by injecting CO_2 in water (lit.[395] 667 and temperature sensitive 2360 cm^{-1}). Absorption bands at 2187 and 2112 cm^{-1} (resulting from a separate CO injection) were completely absent from any spectra obtained prior to the elution of the second ir active peak (acetone: 1738, 1365, and 1217 cm^{-1}).

When a methanolic solution of 1-Me_2 was injected, the (presumably very rapid) thermal decomposition in the injector port produced a first eluting peak containing both CO_2 and CO absorptions in a 2:1 area ratio. Clearly, the gases were not separable by the chromatography, but are readily identified by their ir spectra.

E3.1.4 Other Substituents

Heterogeneous hydrolysis of 1-Me,t-Bu (0.02 g) in 0.200 M

HCl (1.0 mL) gave the corresponding ketone as the only product detected by pmr. In 63% sulfuric acid, however, no ketone was obtained, but an unassigned spectrum consisting of 4 closely grouped signals at 1.42 (189), 1.40 (69), 1.39 (13), and 1.34 (11) ppm (bracketed values refer to peak height in mm) and another lower group at 2.26 (53), 2.30 (41), 2.31 (40), and 2.19 (15) ppm was observed. Added ketone resonates at 1.10 (3H) and 2.28 ppm (1H).

Heterogeneous decomposition of 1-CH_3,CH_2Ph in 1M NaOH or 1 M HCl gave >80% ketone (isolated and measured by calibrated ir spectroscopy, pmr, and vpc) and no 1-phenyl-2-propanol or β-methylstyrene (vpc).

E3.1.5 Diimide Trapping Experiments

Dimethyloxadiazolinone (ca 0.03 g) was added to either 1.0 M HCl or to pH 7.0 buffer (1.0 mL) in the presence of cyclohexene (0.1 mL). The resulting two phase system was shaken vigorously until decomposition was complete (30 min) then ether (1.0 mL) was added to the mixture. The (wet) organic layer was subjected to analytical vpc (Varian 3700 gas chromatograph with CDS 101 digital integrator, 1/8" X 1.5 m stainless steeel column of 5% OV-17 on Chromosorb W (100–120 mesh), N_2 carrier flow 15 mL min^{-1}, column temperature 30°C) to inspect for cyclohexane. Under intense magnification, < 1% yield of cyclohexane was detected (integrated against acetone and acetone azine, no calibration), but even this tiny amount was ascribed to an impurity present in the cyclohexene (< 0.1% by integration). Therefore, cyclohexene

had not been reduced to cyclohexane in these experiments.

Dimethyloxadiazolinone (ca 0.04 g) was dissolved in 10% v/v acryclic acid/water (1.0 mL). Pmr analysis an hour later clearly showed the ethyl group of propionic acid at 0.87 (triplet) and 2.17 (quartet) ppm with J = 7.5 Hz, which integrated to 40-50% of the acetone (≡2.0 ppm). The assignment was confirmed by adding more propionic acid to the solution. No azine or 2-propanol was detected. Blank experiments established a clear solvent window upfield of 2.5 ppm at identical instrument settings. A small singlet at 1.87 ppm accounted for another 5% of the product yield, but other absorptions downfield of 2.5 ppm were likely obscured by solvent. This experiment therefore gave a 40% yield of reduced olefin.

E3.1.6 Behaviour of Dimethyloxadiazolinone in FSO_3H

Dimethyloxadiazolinone (ca 0.02 g) was dissolved in FSO_3H (0.5 mL, Cationics Inc., redistilled from NaF) at -78°C and CH_2Cl_2 (1 drop) was added as internal standard (pmr 5.28 ppm). Pmr and cmr spectra of the conjugate acid (Table R11, page 181) were recorded at -60°, and decomposition began around -30° (see Experimental E3.2.3.1 for kinetic results). The sometimes complex temperature-dependent product mixtures which were obtained in FSO_3H could be duplicated by dissolving propene in FSO_3H at low temperature and warming to the decomposition temperature. Therefore, intermediate 2-propyl cation is implicated, and in fact observed: 1.52 ppm (d, 6H, CH_3) and 5.4 ppm (septet, 1H, CH) with J = 6 Hz.

E3.1.7 Behaviour of Methyl-t-butyloxadiazolinone in FSO_3H

Samples were prepared in FSO_3H at -78°C by the procedure of the preceding paragraph. Rapid decomposition precluded nmr observation of the oxadiazolinone conjugated acid at this temperature. Instead, complicated pmr spectra were obtained which indicated that the components were stable to -20° although partly reversible line broadenings and sharpenings were evident. Below -30°, the main features of the pmr were an ethyl group (quartet at 4.58 ppm, triplet at 1.56 ppm, J = 7Hz, reproduced by adding ethanol to FSO_3H at low temperature) and singlets at 1.72, 2.87 (t-butyl cation) and 3.77 ppm (broad). At -30° the relative peak heights were: 50 (quartet sum), 80 (triplet sum), 160, 215, and 20, respectively. Intensities and line widths of the 1.72 and 3.77 ppm absorptions were temperature sensitive.

E3.1.8 UV-Vis Attempts to Estimate the Basicity of 1-Me_2 in H_2SO_4

Ultraviolet-visible spectra (200-600 nm) of decomposing solutions of dimethyloxadiazolinone (0.1 to 5 mM) in aqueous sulfuric acid mixtures (< 85% acid) were obtained at room temperature. Decomposition was too fast in more acidic media. With increasing acidity , the azo $n\pi^*$ transition at ~360 nm showed a small extension of a blue shift trend established in other solvents as being due to solvent polarity (for example solvent (λ_{max} in nm): hexane (373), CH_3CN(362), 0.200 M HCl (360), 28% H_2SO_4 (357), 87% H_2SO_4 (350)). In the aqueous acid solvents the decomposition kinetics were well behaved: both 215 ($\pi\pi^*$) and 360 nm bands decayed with identical first order rate constants.

For purposes of comparison, spectra of p-phenylazoacetophenone were also obtained in the same solvents, and its conjugate acid (present in >30% H_2SO_4) was found to absorb about 100 nm to the red of the free base with an ε_{max} ~ 10-25 times as large. The spectral maxima of dimethyloxadiazolinone and this azo compound are summarized in Figure E1. There are obviously no large maxima shifts suggestive of significant protonation of dimethyloxadiazolinone in the range studied. Therefore, the half protonation point of the oxadiazolinone (wherever protonated) must be lower than H_o =-8.5.

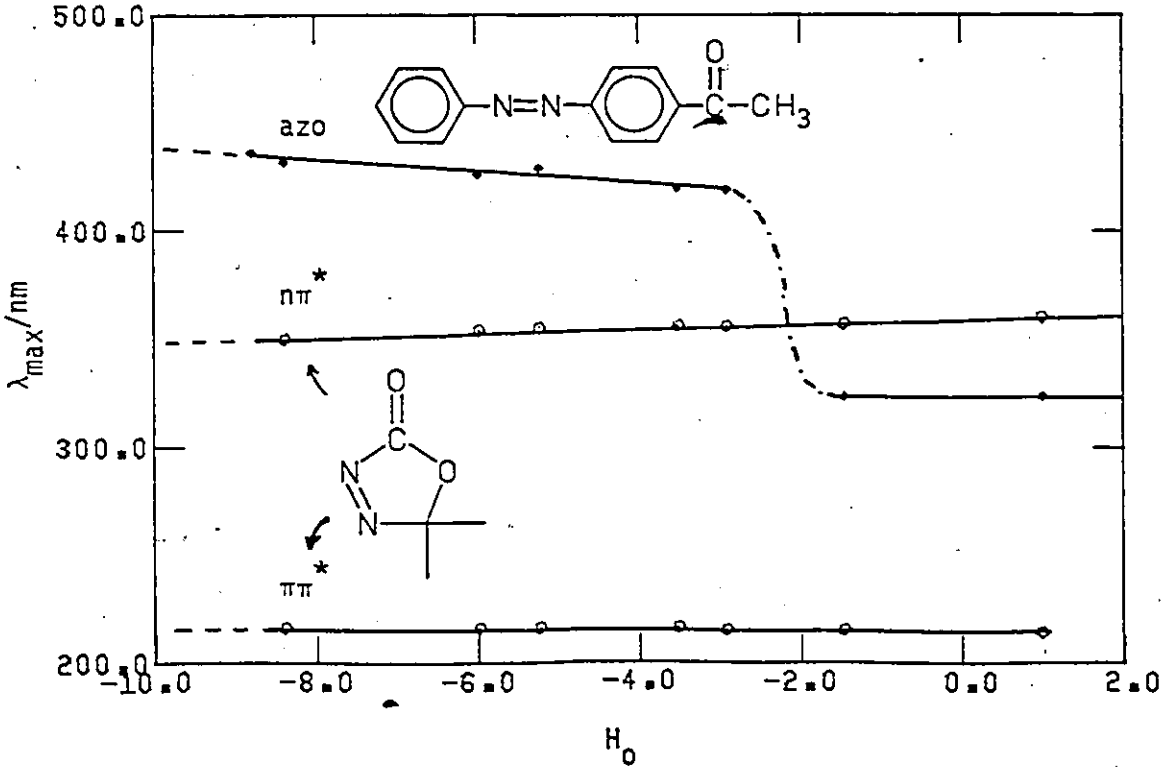

Figure E1. Position of λ_{max} as a function of acidity.

Diethylazodicarboxylate was found to have a 400 nm $n \rightarrow \pi^*$ band which disappeared by an acid catalysed process which precluded studies above 40% H_2SO_4 in water. However, some extension was possible in ethanolic H_2SO_4 (which included some water from the use of 95% H_2SO_4) where the rate was somewhat slower and the 400 nm band survived long enough to be observed in 60 wt % H_2SO_4. Significant protonation had still not occurred, but because an ethanol/H_2SO_4 acidity function is not available, a limiting pK_a cannot be estimated. In this regard, however, the behaviour of this model does parallel that of the oxadiazolinone.

E3.2 Kinetics

E3.2.1 General UV Method

In almost every case, hydrolysis kinetic experiments were monitored at 20.0 ± 0.1°C by absorption spectroscopy at 360 nm (azo $n \rightarrow \pi^*$, $\varepsilon \sim 200\ M^{-1}\ cm^{-1}$). Gas bubble formation precluded using 1 cm cuvettes, but jacketed 5 cm cells (capacity 20 mL or 4 mL) were very satisfactory.

Decay of starting material was measured by a Datex digitized Cary 14 spectrophotometer (Applied Physics Corp.) which employed an interval timer (Cramer 524 series, available from Electro Sonic Inc.) to initiate computer card punching of absorbance values at constant time intervals. Between 20 and 1000 data points were collected per run (average around 200) and analysed by appropriate least squares computer routines for first order kinetics (see Appendix 2). Points more than 3σ from the line were discarded (usually <5% of points). Correlation coefficients exceeded 0.999 in most cases.

Temperature fluctuations were smaller than ±0.05° in the controlling bath (15 L) whose contents were circulated through insulated hoses to the cell jacket at a rate of 3.5 L min^{-1} with a 1/6 horsepower pump. As a consequence of this very powerful pump and the high jacket to cell volume ratio of about 1:1, the temperature of the cell contents was measured to be identical to that of the bath (within ±0.05° over the range 10-40°, as measured with a Doric Trendicator 400 (Doric Scientific, Model 410-T-C)), even when bath temperature was changing at the rate of 0.5° min^{-1} during special kinetic runs designed to determine activation parameters from a single kinetic run.*

Solvents were pre-thermostatted in the bath at least 15 min prior to use, then a small volume was used to rinse out the cell. To initiate reaction, 20 to 50 μL of a stock solution of oxadiazolinones (ca. 0.2 M) in a suitable organic solvent (methanol, DMF, ether, THF, etc.) was blown by mouth out of the measuring pipette into the sample solvent (25 mL or 4.5 mL; dilution factor > 200; final concentration ~ 1mM). The resulting solution was mixed by a few second burst of air through the pipette (oxygen saturation or nitrogen purging did not affect the rate in 0.200 M HCl.) Within 30-40 s after mixing, the sample had been transferred to the cell and absorbance-time data acquisition activated. Reactions were monitored for three to ten half lives, and usually showed a

*This very useful kinetic method will not be detailed in this thesis because activation parameters were not evaluated in the hydrolysis studies. For background on the concept, see refs 396-403.

constant infinity absorbance. On infrequent occasions a very slow rise in A_∞ of $\sim$ 0.005 units per half life was noted. Rate constants obtained by weighted Guggenheim analysis up to 5 half lives are unaffected by such a trivial drift in A_∞ (Appendix 2).

In order to obtain consistent results, experience dictated that all pipettes and handling apparatus ought to be glass. "Plastic" (composition not specified) 30 mL syringes (Plastipak syringes; Beckton-Dickinson Co.) apparently leached into diethylmalonic acid buffers a 360 nm absorbing impurity whose absorbance decayed faster than that of oxadiazolinone — leading to biphasic kinetics. Metal syringes sometimes increased rate constants a few percent. Highly impure oxadiazolinone samples decomposed at rates identical to freshly sublimed material, but the latter was universally employed.

In testing the effects of some impurities on the rates, thiophenol was found to cause the 360 nm behaviour described in Figure E2. The reaction was not further investigated. Thiols are known to attack azo compounds at nitrogen.[270-272]

Distilled water was used as supplied throughout the department once it had established that triply distilled water gave identical rate constants in 0.200 M HCl.

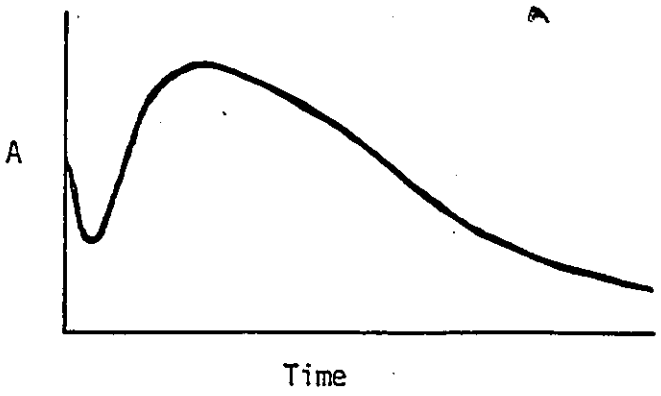

Figure E2. Absorbance-time behaviour of solutions containing thiophenol.

E3.2.1.1 Buffer Catalysis

The pH range 1 to 9 was surveyed in appropriate buffers of constant ionic strength 0.200. From a given buffer of given pH, a series of 5 to 15 solutions of differing total buffer concentration, but identical buffer ratio, was prepared by appropriate dilution with 0.200 M KCl. Observed pseudo first order rate constants were plotted against the buffer base concentration (determined by titrations against standard acid or base) to give a straight line whose intercept (k_o) and slope (k_b) were determined by least squares (Appendix 1 and Equation E6). This was repeated for several different pHs using the same buffer components in different ratios, then all values of $k_{obs} - k_o$ were plotted against [buffer base] to give the best possible

[E6] $$k_{obs} = k_o + k_b[\text{buffer base}]$$

estimate for the second order buffer catalytic constant, k_b, as the slope of a line through the origin (Figures A3.2 to A3.7 and Table A3.10 in Appendix 3). Few duplicate rate constants were obtained as more efficient averaging occurs through line drawing. For example, about 10 points determine a k_o and about 30-40 a k_b. Rate constants bore individual least square propagated errors (Appendix 1) of <0.2%, but were reproducible to only 1-5% in buffers.

E3.2.1.2 Dilution Effects in 0.200 M HCl

Four organic cosolvents were employed to examine the effect of water concentration on reaction rates in 0.200 M HCl:

dioxane, DMF, methanol, and formamide. In each case, 11 solutions from 50 to 100 volume percent water were prepared to contain 0.200 M HCl. Water concentrations were computed from measured densities and only small corrections on the order of 1-3% accounted for non-ideality. Table A3.11 and Figure A3.8 in Appendix 3 contain the relevant results.

E3.2.1.3 Alkyl Substitutent Effects in 0.200 M HCl

Triplicate hydrolysis kinetics for 5,5-dialkyloxadiazolinones were performed in 0.200 M HCl using freshly recrystallized material prepared by the methods described in E1.1. Rate constant reproducibility was excellent (~0.3%) in this solvent (results may be found in Table A3.14). Solutions containing 1-Me,CH_2Ph were initially very slightly cloudy due to insolubility, and 1-$(CH_2Ph)_2$ was insufficiently soluble for rate measurement. An estimate for the rate constant of the latter case was obtained by extrapolation from aqueous DMF, but unlike 1-Me_2, behaviour was nonlinear in water concentration (see Figure A3.8).

E3.2.1.4 Aqueous Sulfuric Acid

Solutions were prepared by mixing reagent grade H_2SO_4 (Fisher Scientific Co., ca 96%) with distilled water in an ice bath. Less pure grades of acid contained absorbing impurities. Weight percent acid was determined by titration of weighed samples, and properties of these mixtures were interpolated (Appendix 1) from literature data (Table A3.13). First order 360 nm kinetics (Table A3.12) for 5 or more half lives were noted up to 84% H_2SO_4

($H_0 \sim -8$). Above this acidity, the reaction was fast, not first order, and sometimes showed rise/fall biphasic kinetics (Appendix 2).

E3.2.2 NMR Kinetics

E3.2.2.1 PMR in FSO_3H

Dimethyloxadiazolinone (ca 0.02 g) and internal standard CH_2Cl_2 (1 drop) were dissolved in fluorosulfuric acid (0.5 mL; from Cationics Inc., and redistilled from NaF prior to use) at -78°C and transferred to an nmr tube. FSO_3D was used as supplied by Cationics Inc. Decomposition kinetics were monitored with a Brüker WH-90 FT spectrometer using 16 or 36 scans per spectrum so that 13-20 spectra covered 3.5-6 half lives. Temperatures (-5 to -30°) were measured with the Doric Trendicator 400 before and after every run, and were constant in a given run to ±0.4°C. Peak height ratios of oxadiazolinone to CH_2Cl_2 were determined from each spectrum to give good weighted first order kinetics sporting correlation coefficients in excess of 0.99. Five temperatures were used to obtain activation parameters, and two runs in FSO_3D gave $k_H/k_D = 1.0 \pm 0.1$. The results are summarized in Table A3.16, Appendix 3.

E3.2.2.2 ^{17}O NMR

^{17}O nmr spectra (12.22 MHz) were easily obtained using a Brüker WH-90 FT instrument equipped with a multinuclear probe. Short acquisition times (0.17 s per pulse) permitted rapid scanning; as few as 100 scans of D_2O (10 mm tube) gave a respectable S/N > 10. Chemical shifts are reported relative to water and lines are reasonably broad (100-300 Hz). Natural abundance spectra are

difficult to obtain, except for neat solvents because of the low natural occurrence of ^{17}O (0.037%; ref. 358) but dimethyloxadiazolinone (0.43g; 3.8 mmol) in CCl_4 (2.0 mL) scanned overnight (17h, 350,000 scans) gave a reasonable spectrum with S/N ~ 4 containing two absorptions. The 296 ppm line (half width 100 Hz) was assigned to the carbonyl oxygen and the 184 ppm line (half width 200 Hz) to the ring oxygen atom (shifts relative to external D_2O). Methanol absorbs at -20 ppm and acetone at 532 ppm in 0.200 M HCl.

To study ^{17}O carbonyl exchange in oxadiazolinone hydrolysis, two kinetic methods were tried. In the first, a solution containing $^{17}OH_2$ (0.10 mL; Merck, Sharpe, and Dohme Ltd , 20.4% enriched) and HCl (0.20 mL of a 1M solution) was added to a methanolic solution of dimethyoxadiazolinone (0.10g; 0.87 mmol, in 0.70 mL). Sets of 2111 scans (~6 min) were obtained at a regulated probe temperature of 20.0°C. Whereas rapid exchange of oxadiazolinone carbonyl oxygen should have lead to a rise/fall (exchange in/decomposition) profile of the corresponding 278 ppm absorption (compared to 296 ppm in CCl_4), no signal above background noise was obtained at that shift value. The molar ratio of water to oxadiazolinone was about 20:1, but a signal area ratio of about 300:1 could have been detected in this experiment. Therefore, certainly less than 10% of oxadiazolinone had exchanged the carbonyl oxygen with solvent.*

*As described, this experiment was designed to be of a kinetic nature, but failed. A more accurate way to assess the maximum permissible amount of exchange would be to collect only one set of scans over about 5 half lives, and then examine this (better S/N) spectrum for carbonyl intensity. If there were any, this total, integrated, intensity (relative to water) could then be related, by appropriate formulae, to an approximate value of k_{hyd}/k_{ex}.

During this experiment a sharp line at 67 ppm grew rapidly over 20 min before an approximately zero order decline over 5 hours. In this solvent, dimethyloxadiazolinone decomposes with a half life of about 30-40 min based on the solvent effects previously noted. At its maximum, this spike reached half the height of the water absorption, but with a half width only 1/25 as great, it integrated to 1:50 against water. Similar spikes varying between 67 and 80 ppm were observed in all ^{17}O nmr kinetic runs. With a half width of only 15-20 Hz, this line is anomalously narrow for ^{17}O nmr, and it was never assigned. It could be due to a gas because it could be purged with vigorous N_2 bubbling Addition of $NaHCO_3$ (0.5 ml saturated solution) generated a broad mound at 185 ppm, but no spike.

A similar experiment conducted with 1-Me,t-Bu gave very similar results, with carbonyl and spike shifts of 276 and 79 ppm respectively.

In the second type of experiment, carbonyl oxygen enriched oxadiazolinone 1-Me_2 or 1-Me,t-Bu (ca 5-15% ^{17}O; for preparation see Experimental E1.4, page 199) was decomposed in the nmr probe at 20°C and the rate compared to that determined by the UV method in the same solvent. In a typical experiment, a methanolic solution of oxadiazolinone-^{17}O (ca 0.035 g in 100 mL) was added to an HCl solution (0.4 M; 1.00 mL). Although these solutions were sometimes cloudy at first due to initial precipitate formation, they did become homogeneous before the end of the reaction. During decomposition, 6-10 spectra covering at least 3

half lives were obtained. Oxadiazolinone peak areas at 275-280 ppm were normalized to the methanol absorption area and pseudo first order rate constants were determined by weighted least squre fits to $-\ell n(A_{oxa}/A_{MeOH})$ vs time. The small number of points and large area errors due to S/N problems led to low correlation coefficients. The results are summarized in Table E5 and as a sample, Figure E3 shows a typical rate plot. Oxadiazolinones are insufficiently soluble in 63% H_2SO_4 for the experiment to be performed in that solvent.

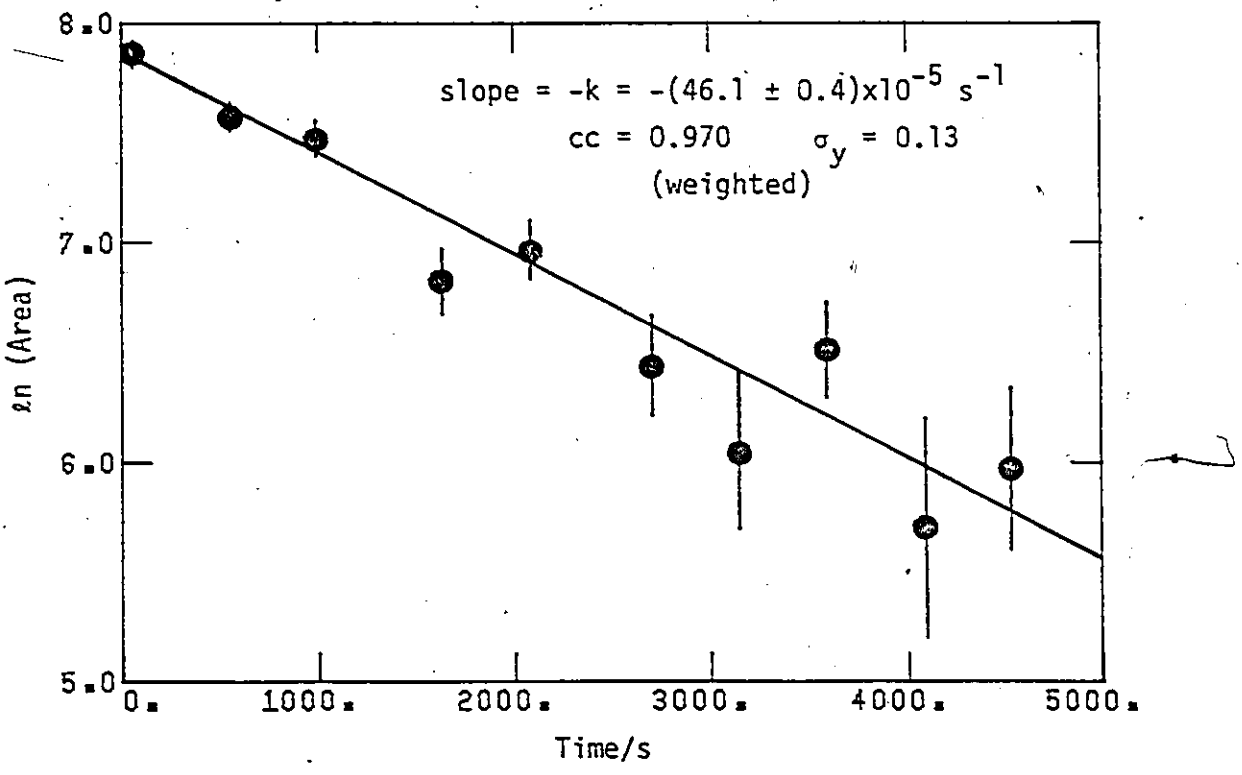

Figure E3. Sample ^{17}O nmr kinetic run: Run #1 (Table E5).

Table E5. Summary of ^{17}O nmr kinetic results in 0.200 M HCl

Run	Substrate	Solvent	Temp.[a]	scans per data pt.[b]	Number of Data Points	$10^5 \cdot k_{obs}/s^{-1}$	corr. coeff.	$10^5 \cdot k_{uv}/s^{-1}$	k_0/k_{uv}
1	1-Me_2	50% acetone	11.1	2400	10	46 ± 4	0.970	40[d]	1.2 ± 0.4
2	1-Me_2	50% acetone	11.2	2400	10	47 ± 4	0.977	40[d]	1.2 ± 0.4
3	1-Me_2	50% MeOH	20.3	1600	4	201 ± 26	0.984	99.1	2.0 ± 0.3
4	1-Me,t-Bu	50% MeOH	20.3	7000	6	25 ± 3	0.957	13.9	1.8 ± 0.2
5	1-Me,t-Bu	50% MeOH[c]	19.7	7500	5	40 ± 5	0.974		

[a] ±0.3°C, measured with Doric Trendicator 400.

[b] 0.17 seconds per scan.

[c] 0.50 M HCl.

[d] Estimated from preliminary activation parameters from a single kinetic run.

E2.3.2.3 Conformational Freeze-Out Attempt

Oxadiazoline 107 (ca 0.01 g) was dissolved in CCl_2F_2 (0.5 mL) at -78° and several FT pmr spectra were obtained at 6 temperatures between -68 and -160°, at which point the sample froze. At no time did any of the 4 methyl absorptions at 1.39, 1.51, 1.55, and 2.96 ppm (relative to external TMS) resolve into two components although slight line broadening was evident as the temperature was lowered — perhaps due to increasing viscosity. Therefore, if the exchange rate is still rapid at -160°, then it is greater than about 50 $|\nu_a - \nu_e|$[404] or >100 s^{-1} for a minimum 0.2 ppm separation between assumed equienergic "axial" and "equatorial" methoxy groups. Assuming $\Delta S^{\ddagger} = 0$, $\Delta H^{\ddagger}$ must be less than 5.4 kcal mol^{-1} (Appendix 2.3).

APPENDICES

Appendix 1. Error Analysis and Curve Fitting Procedures

Error analysis is important. In any human endeavor where conclusions must be drawn from an analysis of numbers, it is vital to know how reliable those conclusions will be. The reliability of conclusions can be no better than the least reliable of two components: the numerical results (usually generated by mathematical manipulation of the raw numbers) and some kind of interpreting theory. Responsible investigators must consider both aspects of the reliability problem. Throughout this thesis, cases of questionable interpreting theories have been identified and the conclusions drawn using them regarded with some due amount of skepticism. This appendix describes the methods, relevant to this work, which have been used to calculate and propagate experimental errors, and to manipulate data through curve fitting procedures.

A1.1 Error Propagation

If the measured raw numbers do not truly represent the system under study, then the conclusions drawn from them may be just as irrelevant, regardless of the quality of the interpreting theory. To analyse the reliability of numerical results, it is common to use the criterion of repeatability in statistical error analysis to ensure that any difference on repeating an experiment would not be so large as to alter the conclusions. However, the statistical approach can only cope with one of two types of experimental errors —

the random errors due to the finite precision of the experiment, or to small, unpredictable, fluctuations in conditions. Systematic errors (reproducible inaccuracy introduced by faulty experiment, calibration, or technique) cannot be dealt with as easily. Sometimes, if a systematic error is suspected, a probable error (the error believed to have been incurred) may be estimated, and this result propagated with the statistical theories.

The mean, $\bar{x}$, of a set of N measurements, x_i, can be associated with two kinds of standard deviation (Equation A1.1).

[A1.1] $$\sigma = \sqrt{\frac{\sum_{i=1}^{N} (x_i - \bar{x})^2}{N-1}} \qquad \sigma_m = \frac{\sigma}{\sqrt{N}}$$

The standard deviation of the sample distribution is σ, and it indicates how closely one might expect a single extra measurement to approach the mean already calculated. On the other hand, the quantity σ_m — the standard deviation of the mean — indicates how closely one can reasonably expect the mean of another set of N measurements to approach this mean. The standard deviation of the mean is used universally to describe the precision of the mean of a set of measurements — it estimates the error in the value of the mean and is the error which should be progagated when the mean is used in subsequent computations. Because errors are assumed to be normally distributed, the mean and its standard deviation express the probability that the "true" mean (for which the calculated mean is an estimate) falls in a certain range: 68% that it falls in the range $\bar{x} \pm \sigma_m$; 95.4% in $\bar{x} \pm 2\sigma_m$; 99.73% in $\bar{x} \pm 3\sigma_m$, and so on.[405-407]

When averaging a set of measurements whose individual errors, σ_i, are known, the most probable value is a weighted average in which each weight, w_i, is inversely proportional to the square of the associated error[405] (Equation A1.2).

[A1.2]
$$\bar{x} = \sqrt{\frac{\sum_{i=1}^{N} x_i w_i}{\sum_{i=1}^{N} w_i}} \qquad \sigma = \sqrt{\frac{\sum_{i=1}^{N} (x_i - \bar{x})^2 w_i}{(N-1)\sum_{i=1}^{N} w_i}}$$

where $w_i \propto \frac{1}{\sigma_i^2}$ and $\sigma_m = \frac{\sigma}{\sqrt{N}}$

For a quantity, Q, which is some function of several observables a,b,c,..., it can be shown[405] that, if Q = f(a,b,c,...), then the variance in the mean of Q is given by Equation A1.3.

[A1.3]
$$\sigma_{mQ}^2 = \left(\frac{\partial Q}{\partial a}\right)^2 \sigma_{ma}^2 + \left(\frac{\partial Q}{\partial b}\right)^2 \sigma_{mb}^2 + \cdots$$

Two simple consequences of this formula are:

1) if Q = a + b (the sum (or difference) of two numbers) then

$\sigma_{mQ} = \sqrt{\sigma_{ma}^2 + \sigma_{mb}^2}$.

For example, the <u>absolute</u> error in the mean pressure calculated from reading two arms of a manometer to ± 1 mm Hg is 1.4 mm Hg.

2) if Q = a x b (the product (or quotient) of two numbers)

then $\frac{\sigma_{mQ}}{Q} = \sqrt{\left(\frac{\sigma_{ma}}{a}\right)^2 + \left(\frac{\sigma_{mb}}{b}\right)^2}$

Here the <u>relative</u> errors obey an equation similar to Consequence 1: the percent error in Q is equal to the root of the sum of the squares

of the percent error in a and b.

For more complicated functions, it is important to write the functional form of Q as simply as possible, for unnecessary terms will inflate the value of σ_{mQ} by over counting the same error. As an extreme example, if Q = a, but one chose to write it as Q = a x a/a, then Consequence 2 would produce $\sigma_{mQ} = \sqrt{3}\ \sigma_{ma}$ instead of the correct result $\sigma_{mQ} = \sigma_{ma}$. A prime application of this point is the analysis of the competing thermolysis kinetics, where Equations A1.4 and A1.5 were used.

[A1.4] $$k_3 = f_{CO} \cdot k_T \quad ; \quad k_2 = (1 - f_{CO}) \cdot k_T$$

[A1.5]
$$\frac{\sigma_3}{k_3} = \sqrt{\left(\frac{\sigma_{CO}}{f_{CO}}\right)^2 + \left(\frac{\sigma_T}{k_T}\right)^2} \quad ; \quad \frac{\sigma_2}{k_2} = \sqrt{\left(\frac{\sigma_{CO}}{1-f_{CO}}\right)^2 + \left(\frac{\sigma_T}{k_T}\right)^2}$$

It would be wrong to calculate σ_2 using $k_2 = k_T - k_3$, because this would double count the error in k_T since k_3 is a function of k_T.

A1.2 Curve Fitting

Least squares curve fitting procedures provide a wide-ranging portfolio of powerful methods of statistically sound data analysis. The techniques relevant to this work include linear, polynomial, and non-linear functions (each with or without weighting), as well as interpolation.

In most applications of curve fitting systems, it is first assumed that a particular, well defined, analytical function of the observed independent variables (x) and desired parameters (p) describes

the observed dependent variable (y), and that any deviation from the predefined functional relationship is due to random errors in y, not x. Under these assumptions, the best possible estimates for the parameters are obtained by minimizing chi-squared (χ^2), the sum of the squares of the deviations between the observed and calculated y's, with respect to each parameter.

[A1.6] $$y = f(x_1, x_2, x_3, \ldots, p_1, p_2, p_3, \ldots)$$

[A1.7] $$y_i(\text{calc}) = f(x_{1i}, x_{2i}, x_{3i}, \ldots, p_1, p_2, p_3, \ldots)$$

[A1.8] $$\chi^2 = \sum_{i=1}^{N} w_i (y_i - y_i(\text{calc}))^2 \; ; \; w_i \propto \frac{1}{\sigma_{yi}^2}$$

[A1.9] $$\frac{\partial \chi^2}{\partial p_1} = \frac{\partial \chi^2}{\partial p_2} = \frac{\partial \chi^2}{\partial p_3} = \ldots = 0$$

When f is a power series polynomial, of any degree, in only one dependent variable, the parameters, p, may be obtained by analytical solution of the homogeneous equations implied by A1.9, usually employing matrix methods. In other cases, one of several kinds of iterative search of the χ^2 surface in parameter space must be carried out to find the minimum described by A1.9.

A1.2.1 Polynomial Functions ($y = p_0 + p_1 x + p_2 x^2 + \ldots$)

The exact solution of the normal equations is simplified by defining the following sums and normalizing the sum of the weights to N.

[A1.10] $$(X) = \sum_{i=1}^{N} w_i x_i \qquad (X^2) = \sum_{i=1}^{N} w_i x_i^2 \qquad (XY) = \sum_{i=1}^{N} w_i x_i y_i$$

[A1.11] $$\sum_{i=1}^{N} w_i = N \qquad w_i \propto \frac{1}{\sigma_{yi}^2}$$

Case I ($y = kx$). When theoretical considerations justify forcing the regression line through the origin, only a slope parameter, k, is needed to fit the data. The applicability of the theory to a particular data set may be tested by including an intercept parameter (Case II, below), in which case, the zero intercept should be reproduced within experimental error. An example of a one-parameter line fit would be the calculation of the second order buffer catalytic rate constant from data collected at several pH's. (See Figures A3.2 to A3.7). In that case, the dependent variable was the part of the rate constant due to buffer catalysis after correction for hydroxide catalysis, and the independent variable was the concentration of the base form of the buffer. The least squares equations for $y = kx$ are:

[A1.12] $$k = \frac{(YX)}{(X^2)} \qquad \sigma_k = \frac{\sigma_y}{\sqrt{(X^2)}}$$

[A1.13] $$\sigma_y = \sqrt{\frac{X^2}{N-1}} = \sqrt{\frac{(Y^2) - k(XY)}{N-1}}$$

[A1.14] $$I = r^2 = \frac{(XY)^2}{(X^2)(Y^2)} = cc^2$$

The correlation coefficient (r, square root of the index of determination, I) is a measure of the goodness of fit. Values of I fall between 0 and 1, corresponding to no correlation and perfect correlation respectively. The standard deviation of the

observed y from the line is given by σ_y, and generates σ_k by propagation through Equation A1.3.

Case II ($y = mx + b$) The most common application of least squares analysis is the two parameter straight line. If non-linear functions (for example; $y = ae^{-kx}$, $y = a/(x + b)$, $y = ax^n$, etc.) can be linearized by a simple transformation (such as taking logs or inverting, for instance), then the analytical solutions available for the linear problem are very conveniently applied. For normalized weights, the equations for the slope and intercept of $y = mx + b$ are given by Equations A1.15 to A1.17.

[A1.15] $$m = \frac{N(XY) - (X)(Y)}{\Delta_x} \quad ; \quad \sigma_m = \sqrt{\frac{N}{\Delta_x}}\,\sigma_y$$

[A1.16] $$b = \frac{(X^2)(Y) - (X)(XY)}{\Delta_x} \quad ; \quad \sigma_b = \sqrt{\frac{(X^2)}{\Delta_x}}\,\sigma_y$$

[A1.17] $$r = m\sqrt{\frac{\Delta_x}{\Delta_y}} \quad ; \quad \Delta_x = N(X^2) - (X)^2 \quad ; \quad \sigma_y = \sqrt{\frac{\chi^2}{N-2}}$$

Case III (general polynomial). Any continuous, single-valued, non-linear function can be approximated by a power series polynomial of sufficiently high order. This is advantageous for the following reasons: the coefficients are determined relatively easily by analytical solution; to improve a fit (although the physical significant of the coefficients might be negligible), higher order terms may be added until there is no significant improvement in chi-squared; a polynomial of degree n exactly fits a set of n + 1 data points (I = 1); and, if desired, values for the instantaneous

derivatives dy/dx, d^2y/dx^2, etc., are simply calculated from the coefficients and exponents.

As a typical example, the nine calculated CNDO/2 total energies, for various carbonyl bond lengths in the hypothetical unsubstituted oxadiazolinone, were fit to a third order polynomial (higher terms not really improving the fit), and the energy minimum computed by setting $dE/dR_{CO} = 0$ and solving near $R_{CO} = 1.26$ Å (Equations A1.18 to A1.23; see Results R1.6, page 97, and Table A3.3a)

[A1.18] $y = -10(E + 75.8)$ a.u. ; $-75.86 < E < 75.81$

[A1.19] $x = R_{CO} - 1$ Å ; $1.15 < R_{CO} < 1.30$

[A1.20] $y = -3.07582 + 32.6388x - 88.9522x^2 + 67.8194x^3$; $\sigma_y = 5 \times 10^{-4}$

[A1.21] $\frac{dE}{dR_{CO}} = 0$ when $\frac{dy}{dx} = 0 = 32.6388 - 177.9044x + 203.4582x^2$

at $x = x_{min}$

[A1.22] $\therefore \quad x_{min} = 0.6725$ or $0.2619 \qquad y_{min} = 0.5892$

[A1.23] and $R_{min} = 1.2619$ Å $\qquad E_{min} = -75.85892$ a.u.

The conversion of variables defined in Equations A1.18 and A1.19 is sometimes necessary to enable small computers to accurately obtain the small differences between large sums required to solve equations like A1.12 to A1.17. The second root obtained for the solution to A1.21 was rejected because it lay outside the data range used. Generally, computer library programs can be used for this analysis.

Another major use of polynomial least squares fitting is

interpolation. From a larger set of data, typically 3-6 known data points (x,y) in the vicinity of a particular desired point (x_o,y_o) are exactly fit to a polynomial which gives y_o when evaluated at x_o. Obviously, higher order interpolations are more reliable than simple linear ones, but the polynomical coefficients only apply over the range of data fit, so extrapolations can be very dangerous. The properties of aqueous sulfuric acid solvent systems were interpolated using the INTERP program found in ref. 407.

A1.2.2 Non-linear Functions

A fascinating array of approaches to the iterative search of parameter space for the minimum in chi-squared can be focussed on the problem when analytical solutions to Equations A1.9 cannot be obtained.[407] One of the most sophisticated, and fastest converging, is Marquardt's Gradient Expansion Algorithm.[408] To introduce the non-linear least squares computer program, a few salient features of the method may be noted.[407]

The m parameter, N data point problem with any number of independent variables is given by Equation A1.6 and can be symbolized by $y_i = f(\tilde{x}_i)$, where $\tilde{x}_i$ is a matrix of the values of the independent variables corresponding to the i-th point. From initial estimates of the parameter matrix, $\tilde{p}$, parameter increments ($\Delta\tilde{p}$), needed to lower chi-squared, are determined by solving the matrix Equation A1.24, where $\tilde{\beta}$, the gradient matrix, is an m element column vector, like $\tilde{p}$, $\Delta\tilde{p}$, and $\tilde{\alpha}_i$, defined in Equation A1.25, and $\tilde{\alpha}'$ is an mxm modified curvature matrix, defined from $\tilde{\alpha}$ (and Equation A1.27),whose inverse is the mxm error matrix, $\tilde{\varepsilon}'$.

[A1.24] $$\tilde{\beta} = (\tilde{\Delta p})\tilde{\alpha}' \rightarrow \tilde{\Delta p} = \tilde{\beta}(\tilde{\alpha}')^{-1} = \tilde{\beta}\tilde{\varepsilon}'$$

[A1.25] $$\beta_k = \frac{\partial \chi^2}{\partial p_k} = \sum_{i=1}^{N} w_i \left[\frac{\partial f(\tilde{x}_i)}{\partial p_k} (y_i - f(x_i))\right]$$

[A1.26] $$\alpha_{jk} = \frac{\partial^2 \chi^2}{\partial p_j \partial p_k} \simeq \sum_{i=1}^{N} w_i \left[\frac{\partial f(x_i)}{\partial p_j} * \frac{\partial f(x_i)}{\partial p_k}\right]$$

[A1.27] $$\alpha'_{jk} = \begin{cases} \alpha_{jk}\cdot(1+\lambda) & \text{if } j=k; \\ \alpha_{jk} & \text{if } j\neq k \end{cases} \quad \text{where } \lambda \sim 10^{-3} \text{ controls interpolation}$$

The parameter increments are given more explicitly by Equation A1.28 and the parameter errors estimated in Equation A1.29, setting λ to 0.

[A1.28] $$\Delta p_j = \sum_{k=1}^{m} (\beta_k \varepsilon'_{jk})$$

[A1.29] $$\sigma_{pj} = \sqrt{\frac{\varepsilon_{jj}\chi^2}{N-m}} \quad ; \quad \tilde{\varepsilon} = \tilde{\alpha}^{-1}$$

A1.2.2.1 Nonlinear Least Squares Computer Program LSQ

The FORTRAN program LSQ (listed on pages 246 - 254) is a personally modified, significantly improved, version of Bevington's CURFIT[407], consisting of the following 10 routines. As written, it

PROGRAM LSQ

SUBROUTINE SUBZ

SUBROUTINE CURFIT

FUNCTION FUNCTN

FUNCTION CHI

SUBROUTINE FDERIV

SUBROUTINE MATINV

SUBROUTINE DETAILS

SUBROUTINE LPPLOT

SUBROUTINE MINMAX

is capable of handling up to 10 independent variables, 15 parameters, and 200 data points. Options to weight data, to freeze parameters, to do either numerical or analytical differentials, and to printout details after every iteration are included. The format used to read in the data is variable and is specified during execution with an appropriate data card.

Throughout the program, the following variables are employed:

NPAR = the number of parameters ($1 \leq NPAR \leq 15$)

IFREZE = the number of frozen parameters (subscripts in IB) ($0 \leq IFREZE \leq NPAR-1$)

NDV = the number of independent variables ($1 \leq NDV \leq 10$)

NFREE = the number of degrees of freedom (N-NPAR + IFREZE)

N = the number of data points ($NFREE + 1 \leq N \leq 200$)

MAXIT = maximum number of iterations before an automatic quit

CRIT = fractional change in chi-squared necessary to terminate the fit

NUMDER = code for the type of derivative

IWT = code for weighting used

IDETA = code for printout

X = array of observed values of independent variables

Y = array of observed dependent variable

YFIT = array of calculated dependent variable

P = array of parameters

SIGP = array of parameter error estimates

DERIV = array of partial derivatives of the function at a certain point

i, with respect to each parameter.

The data cards which must be supplied for each fit are:

Card 1+2: Title and Description

Card 3: N, NPAR, IFREZE, NDV, IDETA, NUMDER, IWT, MAXIT

Card 4: Subscripts of frozen parameters (omit if none)

Card 5: Initial values for parameters

Card 6: Format to read in Y, X, WEIGHT

Card 7: Blank

Card 8: data (Y,X, WEIGHT), one set per card

The main program, LSQ, reads in the data, computes the weights (normalizing to N) and checks the input codes for possible errors in consistency. Subroutine SUBZ is called to make any required mathematical manipulations of the input arrays of X and Y, such as adding or multiplying a constant, taking logs, inverting, etc. Each iteration calls subroutine CURFIT until the fractional change in chi-squared is less than CRIT, or MAXIT is exceeded. The results are then printed and plotted in subroutine DETAILS, employing routines LPPLOT and MINMAX. These last two subroutines have quite general utility outside mere curve fitting. Subroutine MINMAX finds useful, rounded-off, bracketting values of the minimum and maximum of any input array.

In subroutine CURFIT, the $\tilde{\alpha}$ and $\tilde{\beta}$ matrices (AL and BETA, respectively) are evaluated from the derivatives using Equations A1.25 and A1.26. Matrix AR is set equal to $\tilde{\alpha}'$ (normalizing $\tilde{\alpha}$ to the diagonal elements to enhance the accuracy of the inversion), then inverted in MATINV[407]. The parameters are incremented and χ^2 re-

calculated. If the new chi-squared (CHISQR) is larger than the old one (CHISQ1), λ is increased by a factor of 10 and the modified curvature matrix recomputed, inverted again, and new parameter increments calculated. If chi-squared has decreased, the uncertainties in the parameters are evaluated and control returned to the main program.

In the function subroutine FUNCTN(I), the value of $f(x_i) \equiv$ YFIT(I) is calculated from the current values of the parameters. From the current arrays of Y and YFIT, the reduced chi-squared (χ^2/NFREE) is computed in the function subroutine CHI. SUBROUTINE FDERIV(I) calculates the derivatives of $f(x_i)$ with respect to each parameter. Depending on the value of NUMDER, these may be analytical derivatives (first part) or numerical estimates (second part). The latter approach is most useful when the function is very complicated, but can be used anytime. Derivatives with respect to omitted parameters are set equal to zero.

The sample listing of LSQ tries to fit the rate profile of dimethyloxadiazolinone in aqueous sulfuric acid using activity coefficient corrected water concentrations, C_w', and the H_o acidity function as the two independent variables in Equation A1.30. Forty-five observed pseudo first order rate constants were fit to the 3 parameter function representing two mechanisms.

[A1.30] $$10^5 \cdot k_{obs} = 10^5 \cdot k_o (C_w')^2 + 10^5 \cdot k_H \cdot h_o^n$$

The input data cards are given in Table A1.1, and the results summarized in Table A1.2. Note that blanks were read in for the weights then replaced with unit weights in the program because

IWT = 1. Weighting was not used in this particular instance because there were too few points in the acid catalysed region. Weighting drastically reduced their contribution and, because the fit was poor, the acid catalysed region was incorrectly dominated by the data from the plateau region.

Table A1.1. Input data cards for sample listing of LSQ.

Card	Contents
1	1 DECOMPOSITION OF DIMETHYLOXADIAZOLINONE IN AQUEOUS SULFURIC ACID AT 20.0 C
2	K(OBS)=KO*CW **2 + KH*HO**N P1=KO P2=KH P3=N
3	45 3 0 2 0 1 1 50
4	.15 .00005 1.0
5	(2F10.5,10X,2F10.5)
6	
7	374.83 .3406790 .981951454.1699283
col:	| | | | | | | |
	1 11 21 31 41 51 61 71

Table A1.2. Results of the LSQ fit of Equation A1.30.

Parameter	Symbol	Input Value	Final Value	% Error in Parameter
P_1	$10^5 \cdot k_0$	0.15	0.123±0.004	3.3
P_2	$10^5 \cdot k_H$	$.5X10^{-5}$	$(8.9±8.3)X10^{-5}$	93
P_3	n	1.0	0.87±0.05	6.0

For this example, the enormous estimated error in k_H is a consequence of the following factors, which can be typical of problems encountered in some fits. First, p_2 and p_3 are very strongly correlated (see the parameter correlation matrix printed

at the end of the listing).* Since the fit is more sensitive to $p_3(n)$, than $p_2(10^5 \cdot k_H)$, greater uncertainty exists in the value of p_2. Second, Equation A1.30 gives a poor overall fit to the observed data, especially in the central region, so large error estimates are expected. The standard error in $10^5 \cdot k_{obs}$ was 30.4 s^{-1}.

Freezing $p_3 = n = 0.97$ (the value determined from the linear portion of log k_{obs} vs H_o in the region $-8<H_o<-6.5$) returned an identical p_1 value, but gave $p_2=10^5 \cdot k_H=(1.57\pm1.05)X10^{-5}$. The standard error in $10^5 \cdot k_{obs}$ was slightly higher: 30.8 s^{-1}. From a sequence of futile fits like these evolved the necessity of including other contributions to k_{obs} to account for the plateau rate (see Results R3.2).

---

*Generally speaking, correlated groups of parameters strongly suggest that there is at least one too many parameters — a useless one and/or one which can be expressed as a function of others in the correlated group. For example, the parameters in $f(x) = (A+Bx)/(C+Dx^2)$ could each be multiplied by the same constant without altering $f(x)$, so this problem can only be fed three unique parameters, say in units of A: $f(x) = (1+p_1x)/(p_2+p_3x^2)$. Even then, if $p_1x>>1$ over the whole range of observed x_i, then $f(x) \sim p_1x/(p_2+p_3x^2)$ and yet another parameter would have to be omitted, fitting $f(x) \sim x/(p_1'+p_2'x^2)$. The need to write the functional dependence as simply as possible was already raised in Section A1.1, Error Propagation. Such mistakes are not obvious in Equation A1.30.

LSQ -- Program Listing (page 1 of 9)

```
      PROGRAM LSQ(INPUT,OUTPUT,TAPE5=INPUT)
C
C                    T. PAINE      1979     NONLINEAR LEAST SQUARES
C                                  BY THE MARQUARDT METHOD
C
C
      COMMON X(200,10), Y(200),YFIT(200),WEIGHT(200)
      COMMON /NON/ P(15),SIGP(15),DERIV(15),IB(15),N,NFREE,NPAR,IFREZE
     X,NUMDER
      DIMENSION FMT(9),ITITLE(16),AR(15,15)
    7 READ (5,305) (ITITLE(I),I=1,16)
      IF(EOF(5)) 9999,6
 9999 STOP
    6 READ (5,306) N,NPAR,IFREZE,NDV,IDETA,NUMDER,IWT,MAXIT
      IF(IFREZE.NE.0) READ (5,306) (IB(I),I=1,IFREZE)
      READ(5,307) (P(I),I=1,NPAR)
      READ (5,305) (FMT(I),I=1,8)
      READ (5,FMT) (Y(I),(X(I,L),L=1,NDV),WEIGHT(I),I=1,N)
   14 CONTINUE
C  IWT=0 DEFAULT WEIGHTING BY 1/Y**2
C  IWT=1 UNIT WEIGHT FOR ALL POINTS
C  IWT=ANYTHING ELSE  READ IN THE WEIGHT
C  NUMDER=1 NUMERICAL DERIVATIVES
C  NUMDER=ANYTHING ELSE   ANALYTICAL DERIVATIVES.MUST BE SUPPLIED IN SUBROUTINE
C  IDETA=0 NO DETAILS, EXCEPT AT END OF LAST ITERATION
C  IDETA=ANYTHING ELSE, DETAILS AFTER EVERY ITERATION
      IF(IWT.NE.1) GO TO 4
   13 DO 10 I=1,N
   10 WEIGHT(I)=1.0
      GO TO 3
    4 TOT=0.0
      IF(IWT.NE.0) GO TO 15
      DO 5 I=1,N
    5 WEIGHT(I)=1.0 /Y(I) **2
      IWT=1
   15 DO 2 I=1,N
    2 TOT=TOT+WEIGHT(I)
      TOT=TOT/FLOAT(N)
      DO 1 I=1,N
    1 WEIGHT(I)=WEIGHT(I)/TOT
    3 PRINT 305,(ITITLE(I),I=1,16)
      PRINT 301,N,NPAR,IFREZE,NDV,MAXIT
      IF(IDETA.NE.0) PRINT 302
      IF(NUMDER.EQ.0) PRINT 303
      IF(NUMDER.NE.0) PRINT 304
C  ENSURE THAT THE DATA FOR THIS RUN IS OK..
      IF(N.LT.NPAR) PRINT 300
      IF(N.LT.NPAR) GO TO 7
      IF(IFREZE.EQ.0) GO TO 9
      DO 8 I=1,IFREZE
    8 IF(IB(I).LT.1.OR.IB(I).GT.NPAR) GO TO 11
      GO TO 9
   11 PRINT 308,I,IB(I)
      GO TO 7
C  MAKE ANY CHANGES NECESSARY TO X OR Y IN SUBZ...
    9 CALL SUBZ(R)
      PRINT 314,(P(I),I=1,NPAR)
      NITER=0
      OLCHI=1.0E200
      CRIT=0.0001
      FLAMDA=0.001
      NFREE=N-NPAR+IFREZE
   20 CONTINUE
      CALL CURFIT(CHISQR,FLAMDA,AR)
C  DETAILS OUT HERE
      NITER=NITER+1
      PRINT 313, NITER,CHISQR,SQRT(CHISQR),FLAMDA
      PRINT 314,(P(I),I=1,NPAR)
      PRINT 315,(SIGP(I),I=1,NPAR)
      IF(IDETA.NE.0) CALL DETAILS(IWT,NDV)
      IF(NITER.GE.MAXIT) GO TO 420
      FLAMDA=FLAMDA/10.0
      BOP=(CHISQR-OLCHI)/CHISQR
      IF(BOP.LT.CRIT.AND.BOP.GT.-CRIT) GO TO 200
      OLCHI=CHISQR
      GO TO 20
C  FINAL PRINT OUT
  420 PRINT 316
  200 CALL DETAILS(IWT,NDV)
      IF(NUMDER.EQ.0) PRINT 303
      IF(NUMDER.NE.0) PRINT 304
      PRINT 310,(I,I=1,NPAR)
C  CALCULATE THE PARAMETER CORRELATION MATRIX FROM THE INVERTED CURVATURE MATRIX
      DO 400 I=1,NPAR
      DO 400 J=1,I
      IF(I.EQ.J) GO TO 400
      TEST=AR(I,I)*AR(J,J)
      IF(TEST.LT.0.0) GO TO 403
      AR(I,J)=AR(I,J)/SQRT(TEST)
      IF(TEST.EQ.0.0) AR(I,J)=0.0
      AR(J,I)=AR(I,J)
  400 CONTINUE
      DO 401 I=1,NPAR
      AR(I,I)=1.0
  401 PRINT 311,I,(AR(I,J),J=1,NPAR)
      GO TO 7
  403 PRINT 312,I,J
```

LSQ -- Program Listing (cont'd: page 2 of 9)

```
      GO TO 7
  300 FORMAT(*- TOO MANY PARAMETERS*)
  301 FORMAT(//* INPUT PARAMETERS=*I4* POINTS*5X,I2*PARAMETERS,*I2* FROZ
     XEN*5X,I2* DEPENDENT VARIABLES*5X,I3* MAXIMUM ITERATIONS*)
  302 FORMAT(* PRINTED DETAILS REQUESTED*)
  303 FORMAT(* ANALYTICAL DERIVATIVES USED*)
  304 FORMAT(* ESTIMATED DERIVATIVES USED*)
  305 FORMAT(8A10/8A10)
  306 FORMAT(16I5)
  307 FORMAT(8F10.5)
  308 FORMAT(* OMITTED INDEX TO PARAMETER*2I4* OUT OF BOUNDS*)
  310 FORMAT(*1*,15X,*PARAMETER CORRELATION MATRIX*/, 7X,15I8)
  311 FORMAT(X,I8,15F8.4)
  312 FORMAT(* NEGATIVE DIAGONAL ELEMENT*2I4)
  313 FORMAT(*-     ITERATION NUM=*I4,5X*CHI SQUARED=*E16.8,5X*STD ERROR
     XIN Y=*E16.8,5X,*LAMBDA=*E10.3/)
  314 FORMAT(*    PARAMETERS*6G19.10)
  315 FORMAT(*    STD ERRORS*6G19.10)
  316 FORMAT(*-FORCED OFF*)
      END


      SUBROUTINE SUBZ(R)
      COMMON X(200,10), Y(200),YFIT(200),WEIGHT(200)
      COMMON /NON/ P(15),SIGP(15),DERIV(15),IB(15),N,NFREE,NPAR,IFREZE
     X,NUMBER
      RETURN
      END


      SUBROUTINE CURFIT(CHISQR,FLAMDA,AR)
      COMMON X(200,10), Y(200),YFIT(200),WEIGHT(200)
      COMMON /NON/ P(15),SIGP(15),DERIV(15),IB(15),N,NFREE,NPAR,IFREZE
     X,NUMBER
      DIMENSION AL(15,15),AR(15,15),B(15),BETA(15)
      NFREE=N-NPAR+IFREZE
C  SAVE THE PARAMETERS IN B, IN CASE CHISQR INCREASES.
      DO 10 I=1,NPAR
   10 B(I)=P(I)
C  EVALUATE THE ALPHA AND BETA MATRICES...
   20 DO 34 J=1,NPAR
      BETA(J) =0.0
      DO 34 K=1,J
   34 AL(J,K)=0.0
      DO 50 I=1,N
      YFIT(I)=FUNCTN(I)
      CALL FDERIV(I)
      DO 46 J=1,NPAR
      BETA(J)=BETA(J) + WEIGHT(I)*(Y(I)-YFIT(I))*DERIV(J)
      DO 46 K=1,J
   46 AL(J,K)=AL(J,K) + WEIGHT(I)*DERIV(J)*DERIV(K)
   50 CONTINUE
      CHISQ1=CHI(R)
      DO 53 J=1,NPAR
      DO 53 K=1,J
   53 AL(K,J)=AL(J,K)
C  INVERT THE MODIFIED CURVATURE MATRIX TO FIND THE NEW PARAMETERS
   71 DO 74 J=1,NPAR
      DO 73 K=1,NPAR
      AR(J,K)=AL(J,K)
      TEST=AL(K,K)*AL(J,J)
      AR(J,K)=AL(J,K)/SQRT(TEST)
      IF(TEST.EQ.0.0) AR(J,K) =0.0
   73 CONTINUE
   74 AR(J,J)=1.0 + FLAMDA
   80 CALL MATINV(AR,NPAR,DET)
      IF(FLAMDA.EQ.0.0) GO TO 1
   81 DO 84 J=1,NPAR
      DO 84 K=1,NPAR
      TEST=AL(J,J)*AL(K,K)
      IF(TEST.LE.0.0) GO TO 84
      P(J)=P(J) + BETA(K)*AR(J,K)/SQRT(AL(J,J)*AL(K,K))
C     CHECK HERE FOR NEGATIVE PARAMETERS(OPTIONAL).
C
   84 CONTINUE
C  IF CHISQUARED INCREASED INCREASE FLAMDA AND TRY AGAIN
      DO 85 I=1,N
   85 YFIT(I)=FUNCTN(I)
      CHISQR=CHI(R)
      IF(CHISQ1.GT.CHISQR)  GO TO 101
      DO 65 I=1,NPAR
   65 P(I)=B(I)
   95 FLAMDA=10.0*FLAMDA
      GO TO 71
C  EVALUATE  THE UNCERTAINTIES IN THE PARAMETERS
  101 CONTINUE
      SAVE=FLAMDA
      FLAMDA=0.0
      GO TO 20
    1 FLAMDA=SAVE
      DO 103 J=1,NPAR
      IF(AL(J,J).EQ.0.0) SIGP(J)=0.0
      IF(AL(J,J).EQ.0.0) GO TO 103
      SIGP(J)=SQRT(AR(J,J)/AL(J,J)*CHISQ1)
  103 CONTINUE
      RETURN
      END
```

LSQ -- Program Listing (cont'd: page 3 of 9)

```
      SUBROUTINE DETAILS(IWT,NDV)
      DIMENSION RESID(100)
      COMMON X(200,10), Y(200),YFIT(200),WEIGHT(200)
      COMMON /NON/ P(15),SIGP(15),DERIV(15),IB(15),N,NFREE,NPAR,IFREZE
     X,NUMBER
      DIMENSION XP(100),YP(100),ICHAR(100),LY(50),LX(3),LP(8),ISYM(12)
      IF(IWT.NE.0) GO TO 100
      PRINT 10
   10 FORMAT(*1-     Y OBSERVED     Y CALCULATED     DIFFERENCE   INDEPEN
     XDENT VARIABLES*//)
      DO 20 I=1,N
      DIFF=Y(I)-YFIT(I)
   20 PRINT 30,Y(I),YFIT(I),DIFF,(X(I,L),L=1,NDV)
   30 FORMAT(X,F15.5,F17.7,F15.7,5F15.6,/,48X,5F15.6)
      GO TO 140
  100 PRINT 110
  110 FORMAT(*1      YOBSERVED     YCALCULATED     WEIGHTING     WT.SQ DI
     XFF   INDEPENDENT VARIABLES*//)
      DO 120 I=1,N
      DIFF=WEIGHT(I)*(Y(I)-YFIT(I))*ABS(Y(I)-YFIT(I))
  120 PRINT 130,Y(I),YFIT(I),WEIGHT(I),DIFF,(X(I,L),L=1,NDV)
  130 FORMAT(X,F15.5,F17.7,F14.6,F15.6,4F15.6,/,62X,4F15.6,/,62X,4F15.6)
C  SET UP FOR THE PLOT DONE IN LPPLOT
  140 CONTINUE
      LX(1)=10H      INDEP
      LX(2)=10HENDENT VAR
      LX(3)=10HIABLE
      DO 60 I=1,50
      IF(I.LE.8) LP(I)=10H
      IF(I.LE.12) ISYM(I)=10H
      LY(I)=1H
   60 CONTINUE
      LY(21)=LY(26)=1HO
      LY(22)=LY(24)=LY(27)=LY(38)=1HE
      LY(23)=1HP
      LY(25)=LY(28)=1HN
      LY(29)=1HT
      LY(31)=1HV
      LY(32)=LY(35)=1HA
      LY(33)=1HR
      LY(34)=1HI
      LY(36)=1HB
      LY(37)=1HL
      ISYM(4)=10HO=OBSERVED
      ISYM(6)=10H      $=OVE
      ISYM(7)=10HRLAP
      ISYM(9)=10HF=CALCULAT
      ISYM(10)=10HED
      IF(N.LE.50) GO TO 40
C  REDUCE TO 50 DATA POINTS AND 50 FIT POINTS
      ND=N/50+1
      NP=N/ND
      J=0
      DO 50 I=1,N,ND
      J=J+1
      JJJ=J+NP
      XP(J)=XP(JJJ)=X(I,1)
      YP(J)=Y(I)
      RES=YFIT(I)-Y(I)
      RESID(J)=RES*ABS(RES)*WEIGHT(I)
      ICHAR(J)=1HO
      YP(JJJ)=YFIT(I)
      ICHAR(JJJ)=1HF
   50 CONTINUE
      NP=NP*2
      CALL LPPLOT(NP,XP,YP,ICHAR,LY,LX,LP,ISYM)
      GO TO 200
   40 DO 70 I=1,N
      J=I+N
      XP(J)=XP(I)=X(I,1)
      YP(I)=Y(I)
      ICHAR(I)=1HO
      YP(J)=YFIT(I)
      RES=YFIT(I)-Y(I)
      RESID(I)=RES*ABS(RES)*WEIGHT(I)
      ICHAR(J)=1HF
   70 CONTINUE
      NP=N*2
      CALL LPPLOT(NP,XP,YP,ICHAR,LY,LX,LP,ISYM)
C  NOW DO THE RESIDUALS PLOT
  200 IF(N.LE.50) GO TO 210
      J=0
      DO 220 I=1,N,ND
      J=J+1
  220 ICHAR(J)=1HR
      GO TO 230
  210 DO 240 I=1,N
  240 ICHAR(I)=1HR
  230 CALL MINMAX(XP,NP,RMIN ,RMAX,CMIN,CMAX)
      NP=NP/2
      NUM=99-NP
      DELX=(CMAX-CMIN)/NUM
      NP=NP+1
      DO 250 I=NP,100
      XP(I)=DELX*(I-NP)+CMIN
      RESID(I)=0.0
  250 ICHAR(I)=1H-
      ISYM(4)=ISYM(6)=ISYM(7)=ISYM(9)=ISYM(10)=10H
      DO 666 K=1,50
```

LSQ -- Program Listing (cont'd: page 4 of 9)

```
100             IF(K.LE.8) LP(K)=1OH
                666 LY(K)=1H
                    LP(4)=10H RESIDUALS
                    LP(5)=10H  PLOT
                    LY(25)=1HP
105                 LY(26)=1HE
                    LY(27)=1HS
                    LY(28)=1HI
                    LY(29)=1HD
                    LY(30)=1HU
110                 LY(31)=1HA
                    LY(32)=1HL
                    LY(34)=LY(35)=LY(39)=1H*
                    LY(37)=1H2
                    LY(41)=1HW
115                 LY(42)=1HT
                    CALL LPPLOT(100,XP,RESID,ICHAP,LY,LX,LP,ISYM)
                    RETURN
                    END



                    SUBROUTINE LPPLOT(N,X,Y,IS,LY,LX,LP,ISYM)
                C  THIS PROGRAM PLOTS A SET OF DATA X,Y ON A SINGLE LINEPRINTER PAGE
                C THE INPUT PARAMETERS ARE THESE ARRAYS, PLUS THE SYMBOL DESIRED FOR EACH POINT
                C  (IN IS) -- THIS WILL ALLOW THE SIMULTANEOUS PLOTTING OF SEVERAL CURVES.
 5              C LY IS THE LABEL FOR THE Y AXIS WHICH MAY BE UP TO 50 CHARACTERS (NB-PRINTED VE
                C  RTICALLY), LX IS A 30 CHARACTER LABEL FOR THE X AXIS, LP THE PLOT TITLE
                C THIS ROUTINE USES THE MINMAX ROUTINE WICH FINDS CONVENIENT VALUES JUST ABOVE
                C  AND JUST BELOW THE MAX AND MIN.
                C
10                  DIMENSION X(100),Y(100),IS(100),XLAB(11),YLAB(11),LY(50),LX(3),
                   C LP(8),ISYM(12)
                    INTEGER BLANK,A(50,120)
                C  ZERO THE PLOT AREA
15                  BLANK=1H
                    DO 20 I=1,50
                    DO 20 J=1,120
                 20 A(I,J)=BLANK
                C  FIND THE CONVENIENT VALUES OF MINS AND MAXES
                    CALL MINMAX(X,N,AA,BB,XMIN,XMAX)
20                  CALL MINMAX(Y,N,AA,BB,YMIN,YMAX)
                    XINC=(XMAX-XMIN)/120.
                    YINC=(YMAX-YMIN)/50.
                C  FIND THE SCALE LABELS
                    DO 30 I=1,11
25                  XLAB(I)=XMIN + (I-1)*12.0*XINC
                 30 YLAB(I)=YMIN + (I-1)*5.0*YINC
                C  FIND THE COORDINATES OF THE INPUT POINTS, AND ASSIGN THE SPACE THE SYMBOL
                    DO 40 I=1,N
                    IX= IFIX((X(I)-XMIN)/XINC+0.9999999999999)
30                  IY= IFIX((Y(I)-YMIN)/YINC+0.9999999999999)
                    IY=51-IY
                    IF(A(IY,IX).NE.BLANK) GO TO 50
                    A(IY,IX)=IS(I)
                    GO TO 40
35              C  THERE IS ALREADY A POINT HERE SO USE A *
                 50 A(IY,IX)=1H$
                 40 CONTINUE
                C
                    PRINT 100,(LP(I),I=1,8)
40               100 FORMAT(1H1,34X,8A10,//,14X,12(10H**********),2H**)
                C  NOW DO THE PLOT
                    PRINT 156,1H ,YLAB(11),(ISYM(I),I=1,12)
                    DO 10 J=1,50
                    JJ=J/5
45                  RJ=FLOAT(J)/5.0
                    IF(RJ.EQ.FLOAT(JJ)) GO TO 200
                C  THIS IS AND ORDINARY LINE
                    PRINT 140,LY(J),(A(J,I),I=1,120)
                 140 FORMAT(2X,A1,T15,1H*,120A1,1H*)
50                  GO TO 10
                C  THIS IS A Y-LABELLED LINE
                 200 PRINT 150,LY(J),YLAB(11-JJ),(A(J,I),I=1,120)
                 150 FORMAT(2X,A1,X,G9.3,2H**,120A1,2H**)
                  10 CONTINUE
55              C  NOW LABEL THE BOTTOM PART
                    PRINT 119
                    PRINT 120,YMIN,YMAX,YINC
                    PRINT 310,XMIN,XMAX,XINC
                 119 FORMAT(14X,1H*,T136,1H*)
60               120 FORMAT(14X,1H*,10X,*YMIN=*G15.8,5X,*YMAX=*G15.8,5X,*YINC=*G15.8,
                   C * PER CHARACTER*,T136,1H*)
                 310 FORMAT(14X,1H*,10X,*XMIN=*G15.8,5X,*XMAX=*G15.8,5X,*XINC=*G15.8,
                   C * PER CHARACTER*,T136,1H*/,14X,1H*,T136,1H*)
                    PRINT 110
65                  PRINT 130,(XLAB(I),I=1,11),(LX(I),I=1,3)
                 110 FORMAT(14X,12(10H**********),2H**,/,15X,10(1H*,11X),1H*)
                 130 FORMAT(08X,      11(1XG11.5),//,60X,3A10)
WARNING  *    RECORD LENGTH EXCEEDS 137 COLUMNS -- MAY EXCEED I/O DEVICE
                 156 FORMAT(2X,A1,X,G9.3,2H**,12A10,2H**)
                    RETURN
70                  END
```

LSQ -- Program Listing (cont'd: page 5 of 9)

```
      SUBROUTINE MINMAX(A,N,RMIN,RMAX,CMIN,CMAX)
C  FROMAN INPUT ARRAY A, OF DIMENSION N, THE REAL MIN AND MAX ARE RMIN AND RMAX
C  USEFUL ROUNDED, BRACKETTING MIN MAX ARE CMIN AND CMAX
C  NOTE--MIN REFERS TO THE MAGNITUDE IF BOTH ARE NEGATIVE.
C
      DIMENSION A(200)
      ICODE=1
      RMIN=1E+200
      RMAX=-RMIN
      DO 10 J=1,N
      IF(RMIN.GT.A(J)) RMIN=A(J)
   10 IF(RMAX.LT.A(J)) RMAX=A(J)
      IF(RMAX.EQ.RMIN) GO TO 40
C IF RMAX IS LESS THAN 0 INTERCONVERT MIN AND MAX
      IF(RMAX.GT.0.0) GO TO 20
      ICODE=-1
      TEMP=ABS(RMAX)
      RMAX=ABS(RMIN)
      RMIN=TEMP
   20 Y=ABS(RMIN)
      X=ABS(RMAX)
      RDIF=ABS(RMAX-RMIN)
      RATIO=RDIF/ABS(RMIN)
      B=1.0/ALOG(10.0)
      IF(X.NE.0.0) NMAX=IFIX(B*ALOG(X))
      IF(Y.NE.0.0) NMIN=IFIX(B*ALOG(Y))
      IF(X.EQ.0.0) NMAX=NMIN
      IF(Y.EQ.0.0) NMIN=NMAX
      IF(X.LT.1.0) NMAX=NMAX-1
      IF(Y.LT.1.0) NMIN=NMIN-1
      IMAX=IFIX(RMAX/(10.**NMAX))
      IF(IABS(IMAX).LE.3) NMAX=NMAX-1
      IMAX=IFIX(RMAX/(10.**NMAX))
      IMIN=IFIX(RMIN/(10.**NMIN))
      IF(IABS(IMIN).LE.3) NMIN=NMIN-1
      IMIN=IFIX(RMIN/(10.**NMIN))
   30 IF(NMAX.NE.NMIN) GO TO 50
   60 IF(IMAX.NE.IMIN) GO TO 50
      NMAX=NMAX-1
      NMIN=NMAX
      TEMP=10.**NMAX
      IMAX=IFIX(RMAX/TEMP)
      IMIN=IFIX(RMIN/TEMP)
      GO TO 60
   50 IMAX=IABS(IMAX)+1
      IF(RMIN*RMAX.LT.0.0) IMIN=IMIN-1
   35 CMIN=FLOAT(IMIN)*10.**NMIN
   40 CMAX=FLOAT(IMAX)*10.**NMAX
      IF(RMIN.EQ.0.0) GO TO 75
      IF(CMIN.EQ.0.0) GO TO 95
      IF(RATIO.GT.50..OR.RATIO.LT.5.0) GO TO 75
      IF(RMIN*RMAX.LT.0.0) GO TO 75
      CMIN=0.0
      IMIN=0
      GO TO 95
   75 IF(RDIF.LT.12.*ABS(RMIN-CMIN)) GO TO 95
   70 IMIN=IMIN-1
      GO TO 35
   95 IF(RDIF.LT.12.*(CMAX-CMIN)) GO TO 93
      IMAX=IMAX+1
      GO TO 40
   93 CMIN=ICODE*CMIN
      CMAX=ICODE*CMAX
      RETURN
   80 CMIN=RMIN-1.0
      CMAX=RMAX+1.0
      RETURN
      END
```

```
      FUNCTION FUNCTN(I)
      COMMON X(200,10), Y(200),YFIT(200),WEIGHT(200)
      COMMON /NON/ P(15),SIGP(15),DERIV(15),IB(15),N,NFREE,NPAR,IFREZE
     X,NUMBER
      FUNCTN=P(1)*X(I,2)**2  +  P(2)*((10.**(-X(I,1)))**P(3))          REPLACE
      END
```

```
      FUNCTION CHI(R)
      COMMON X(200,10), Y(200),YFIT(200),WEIGHT(200)
      COMMON /NON/ P(15),SIGP(15),DERIV(15),IB(15),N,NFREE,NPAR,IFREZE
     X,NUMBER
      NFREE=N-NPAR+IFREZE
      TOT=0.0
      DO 10 J=1,N
      DIFF   =(YFIT(J)-Y(J))**2*WEIGHT(J)
   10 TOT=TOT + DIFF
      CHI=TOT/FLOAT(NFREE)
      RETURN
      END
```

LSQ -- Program Listing (cont'd: page 6 of 9)

```
      SUBROUTINE FDERIV(I)
      COMMON X(200,10), Y(200),YFIT(200),WEIGHT(200)
      COMMON /NON/ P(15),SIGP(15),DERIV(15),IB(15),N,NFREE,NPAR,IFREZE
     X,NUMBER
      IF(NUMBER.NE.0) GO TO 10
C  ANALYTICAL DERIVATIVES HERE                                          REPLACE
C
C
C  SET THE DERIVATIVES FOR THE OMITTED PARAMETERS TO ZERO
   20 IF(IFREZE.EQ.0) RETURN
      DO 30 J=1,NPAR
      DO 30 K=1,IFREZE
   30 IF(J.EQ.IB(K)) DERIV(J)=0.0
      RETURN
C  ROUTINE FOR ESTIMATED DERIVATIVES
   10 DEL=0.00001
      DO 15 K=1,NPAR
      IF(IFREZE.EQ.0) GO TO 40
      DO 50 J=1,IFREZE
      IF(IB(J).NE.K) GO TO 50
      DERIV(K)=0.0
      GO TO 15
   50 CONTINUE
   40 IF(P(K).NE.0.0) DP=P(K)*DEL
      IF(P(K).EQ.0.0) DP=DEL
      SAVE=P(K)
      P(K)=P(K) +DP
      FN=FUNCTN(I)
      P(K)=SAVE-DP
      DERIV(K)=(FN-FUNCTN(I))/2.0/DP
      P(K)=SAVE
   15 CONTINUE
      RETURN
      END


      SUBROUTINE MATINV(A,N,DET)
      DIMENSION A(15,15),IK(15),JK(15)
      DET=1.0
      DO 100 K=1,N
      AMAX=0.
   21 DO 30 I=K,N
      DO 30 J=K,N
      IF( ABS(AMAX)- ABS(A(I,J))) 24,24,30
   24 AMAX=A(I,J)
      IK(K)=I
      JK(K)=J
   30 CONTINUE
      IF(AMAX) 41,32,41
   32 DET=0.0
      RETURN
   41 I=IK(K)
      IF(I-K) 21,51,43
   43 DO 50 J=1,N
      SAVE=A(K,J)
      A(K,J)=A(I,J)
   50 A(I,J)=-SAVE
   51 J=JK(K)
      IF(J-K) 21,61,53
   53 DO 60 I=1,N
      SAVE=A(I,K)
      A(I,K)=A(I,J)
   60 A(I,J)=-SAVE
   61 DO 70 I=1,N
      IF(I-K) 63,70,63
   63 A(I,K)=-A(I,K)/AMAX
   70 CONTINUE
   71 DO 80 I=1,N
      DO 80 J=1,N
      IF(I-K) 74,80,74
   74 IF(J-K) 75,80,75
   75 A(I,J)=A(I,J)+A(I,K)*A(K,J)
   80 CONTINUE
   81 DO 90 J=1,N
      IF(J-K) 83,90,83
   83 A(K,J)=A(K,J)/AMAX
   90 CONTINUE
      A(K,K)=1.0/AMAX
  100 DET=DET*AMAX
  101 DO 130 L=1,N
      K=N-L+1
      J=IK(K)
      IF(J-K) 111,111,105
  105 DO 110 I=1,N
      SAVE=A(I,K)
      A(I,K)=-A(I,J)
  110 A(I,J)=SAVE
  111 I=JK(K)
      IF(I-K) 130,130,113
  113 DO 120 J=1,N
      SAVE=A(K,J)
      A(K,J)=-A(I,J)
  120 A(I,J)=SAVE
  130 CONTINUE
      RETURN
      END
```

```
 DECOMPOSITION OF DIMETHYLOXADIAZOLINONE IN AQUEOUS SULFURIC ACID AT 20.0 C
K(OBS)=K0*CH3**2 + KH*HO**N          P1=K0      P2=KH      P3=N

INPUT PARAMETERS=  45 POINTS      3PARAMETERS, 0 FROZEN      2 DEPENDENT VARIABLES      50 MAXIMUM ITERATIONS
ESTIMATED DERIVATIVES USED
  PARAMETERS     .1500000000          .5000000000E-04     1.000000000

    ITERATION NUM=   1      CHI SQUARED=   .3418949 5E+05      STD ERROR IN Y=   .18490402E+03     LAMBDA=  .100E-02

 PARAMETERS     .1231381037          .2859096888E-04     .9784026366
 STD ERRORS     .2241551668E-01      .8646355860E-04     .1684393371

    ITERATION NUM=   2      CHI SQUARED=   .2544420CE+04      STD ERROR IN Y=   .50492244E+02     LAMBDA=  .100E-03

 PARAMETERS     .1231114321          .3068241192E-04     .9445874632
 STD ERRORS     .6115004947E-02      .4170944562E-04     .7529341961E-01

    ITERATION NUM=   3      CHI SQUARED=   .11659189E+04      STD ERROR IN Y=   .34145554E+02     LAMBDA=  .100E-04

 PARAMETERS     .1231105446          .4865599893E-04     .9015647540
 STD ERRORS     .4139392573E-02      .5818239401E-04     .6674736987E-01

    ITERATION NUM=   4      CHI SQUARED=   .1149307 8E+04      STD ERROR IN Y=   .33901442E+02     LAMBDA=  .100E-05

 PARAMETERS     .1231096624          .7394042423E-04     .8783418102
 STD ERRORS     .4109799773E-02      .8525096122E-04     .6440397772E-01

    ITERATION NUM=   5      CHI SQUARED=   .9258943 7E+03      STD ERROR IN Y=   .30428512E+02     LAMBDA=  .100E-06

 PARAMETERS     .1231092508          .8603915153E-04     .8742273752
 STD ERRORS     .3688783979E-02      .8197298449E-04     .5273613603E-01

    ITERATION NUM=   6      CHI SQUARED=   .92378921E+03      STD ERROR IN Y=   .30393901E+02     LAMBDA=  .100E-07

 PARAMETERS     .1231091856          .8874555947E-04     .8734990101
 STD ERRORS     .3684588118E-02      .8286385663E-04     .5217791665E-01

    ITERATION NUM=   7      CHI SQUARED=   .9237 8779E+03      STD ERROR IN Y=   .30393878E+02     LAMBDA=  .100E-08

 PARAMETERS     .1231091744          .8906434074E-04     .8733092947
 STD ERRORS     .3684585290E-02      .8314733553E-04     .5215675659E-01
```

LSQ -- Sample Output (cont'd: page 8 of 9)

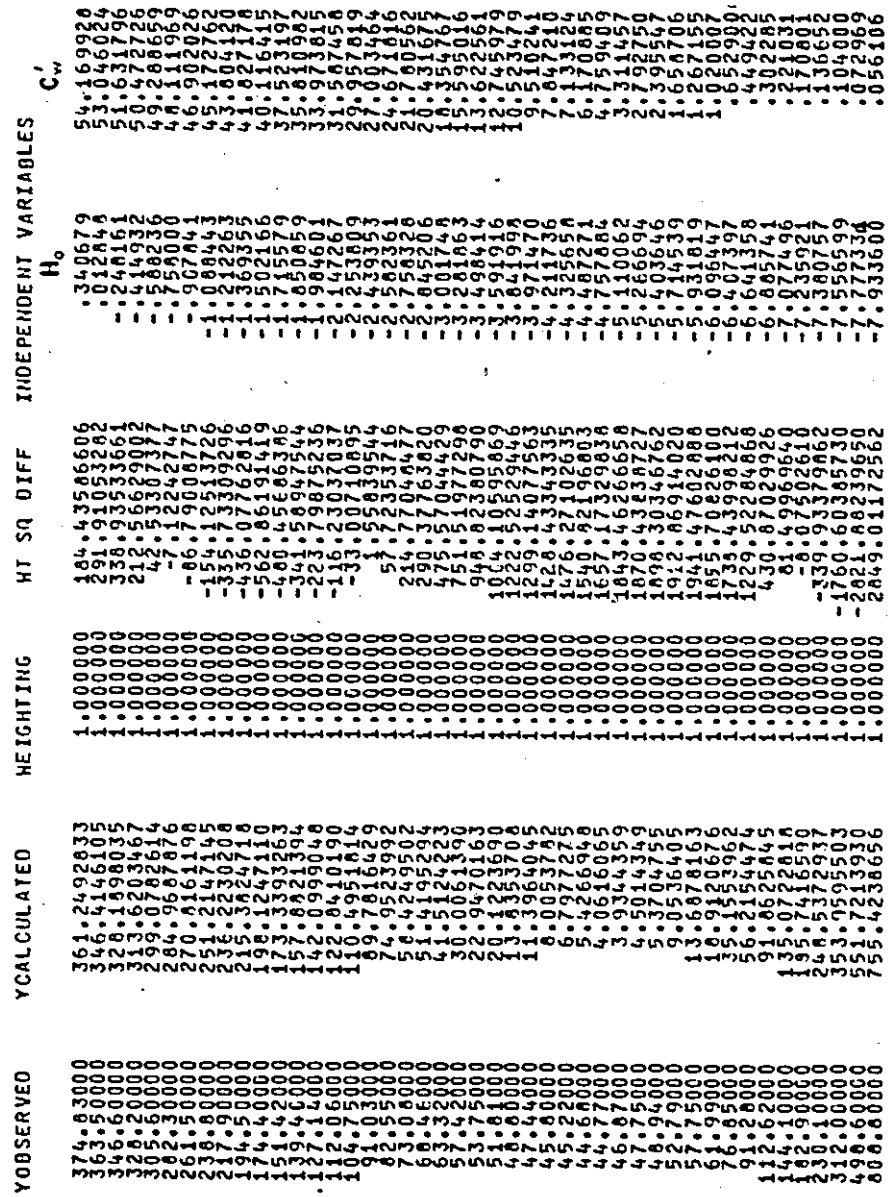

LSQ -- Sample Output (cont'd: page 9 of 9)

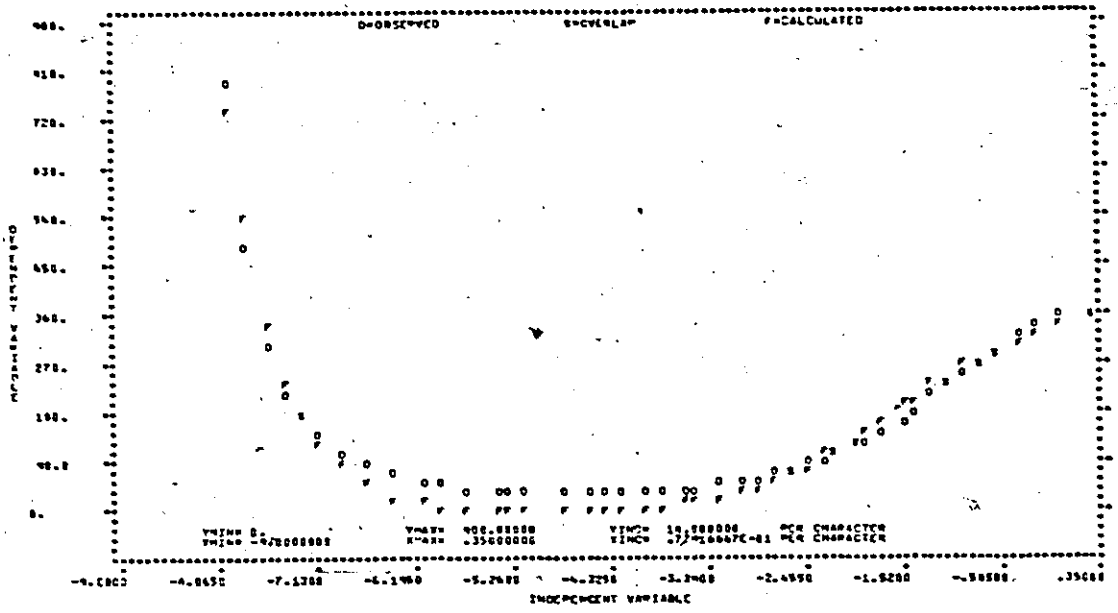

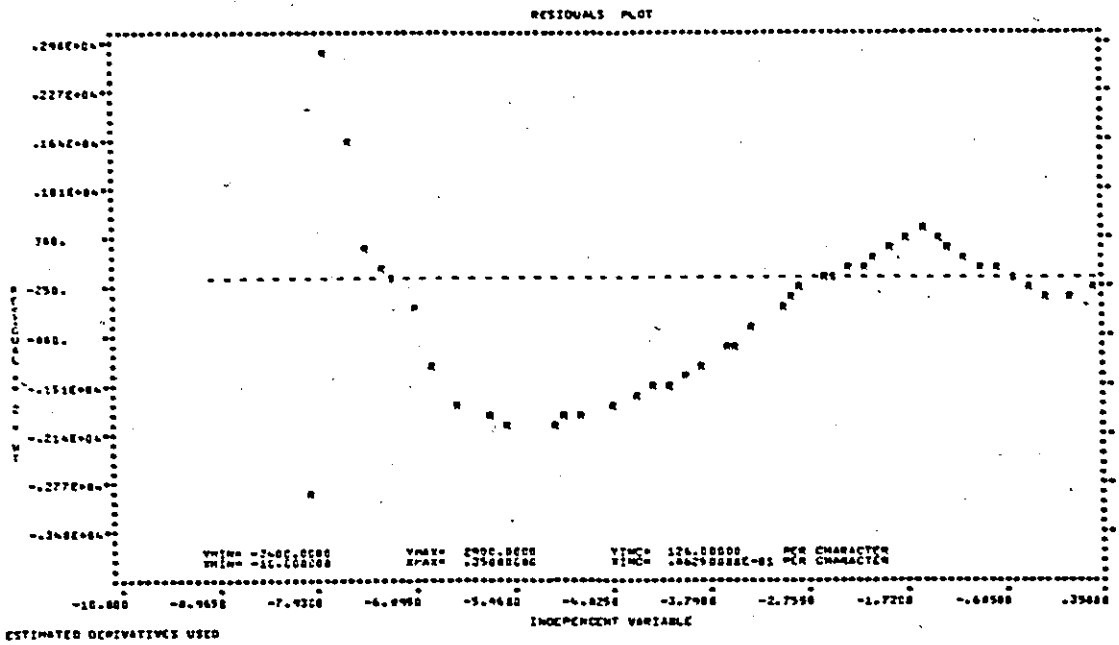

ESTIMATED DERIVATIVES USED

Appendix 2. Kinetic Methods

A2.1 Treatment of First Order Reactions

Virtually all the reactions of oxadiazolinones investigated during this research were of the first order with respect to oxadiazolinone concentration, and first order or pseudo first order overall, in thermolysis and hydrolysis, respectively. For a simple, irreversible, first order process, the rate constant, k, is given by simple integration of the rate equation[409] (Equations A2.1 and A2.2).

[A2.1] $$Oxa \xrightarrow{k} P$$

[A2.2] $$\frac{d[Oxa]}{dt} = -k[Oxa] \quad ; \quad [Oxa] = [Oxa]_o e^{-kt}$$

$$\ln[Oxa] = \ln[Oxa]_o - kt$$

Measured concentration *vs* time data may then be fit, by the methods outlined in the previous Appendix, to either the non-linear or linear forms of the integrated rate equation (A2.2). However, an obvious general property of first order rate equations is that explicit concentrations may be replaced by any variable which is proportional to concentration (for example, ir, uv-vis, or nmr absorption intensities, A). Another handy feature of first order rate equations is that the validity of the equations is independent of the arbitrary assignment of time zero.

In principle, only one parameter, k, is required to curve fit either integrated form of Equation A2.2 to a set of concentration

(or absorbance) vs time data containing time zero measurements. However, this procedure unjustifiably weights a single measurement (the one at t=0) much more than all the others, even though it is very likely to have the same uncertainty as any other data point. This objection may be overcome be defining A_o or ℓnA_o, as the case may be, as a second parameter in either fit of Equations A2.2. Furthermore, it is sometimes desireable to include A_∞, corresponding to the residual absorbance at the end of the reaction which may be due to either background absorbance or product absorbance.

Even when the product, P, absorbs at the monitoring wavelength, it can easily be shown that, as long as the starting material and product have different absorption coefficients (ε, in the case of uv-vis spectroscopy), then equations of similar form still pertain[410] (Equation A2.3).

$$[A2.3] \quad (A-A_\infty) = A_o e^{-kt} \qquad \ell n(A-A_\infty) = \ell nA_o - kt$$

In this particular case, $A_o = [Oxa]_o \cdot \ell \cdot (\varepsilon_{Oxa} - \varepsilon_p)$, which is not actually the absorbance at time zero, as it was in Equation A2.2.

A_∞ may be measured after 10 or 20 half lives ($t_{1/2} = \ell n2/k$), or in the case of the nonlinear fit, shifted to the right hand side of the equality and evaluated as a third parameter. Again, the latter course is preferred because it removes the dependence of the fit on a single measurement of A_∞. A_∞ may be removed entirely by the method of Guggenheim[411]: readings taken some time interval, Δt, apart are paired, and their difference linearized

to retain the previous form:

$$A_t = A_o e^{-kt} - A_\infty$$

$$A_{t+\Delta t} = A_o e^{-k(t+\Delta t)} - A_\infty = A_o(e^{-kt}e^{-k\Delta t}) - A_\infty$$

$$(A_t - A_{t+\Delta t}) = A_o e^{-kt}(1-e^{-k\Delta t})$$

[A2.4] $\ell n(A_t - A_{t+\Delta t}) = \ell nC - kt$; constant $C = A_o(1-e^{-k\Delta t})$

Normally, Δt is selected to be about one half life in order to minimize the accumulated error in the absorbance differences, while retaining data over a sufficiently long time to ensure a well defined slope. The Guggenheim method is particularly well suited to analyse the data generated at constant time intervals by the automated card punching apparatus used in the hydrolysis kinetics.

It is vitally important to appreciate the differences in weighting which must be applied to the linear and nonlinear curve fitting approaches. If the absorbances have an estimated error σ_A, then error propagation using Equation A1.3 gives $\sigma_{\ell nA} = \sigma_A/A$, so in fitting the linearized form of the rate equation, the absorbance data must be weighted by $1/(\sigma_{\ell nA})^2 = A^2/\sigma_A{}^2$. If σ_A is nearly constant over the range of A, then linear fits should weight data proportional to A^2, whereas nonlinear fits should employ unit weighting. In cases where σ_A is some function of A (for example, absorbance readings are "noisier" at higher absorption), the weighting should follow the propagation formula.

Because the first order rate constant is evaluated

independently of the assignment of time zero, or of starting concentrations, there are several practical tests of the applicability of first order kinetics (and, by inference, perhaps the applicability of the assumed mechanism) to a given reaction. Firstly, the calculated rate constant (that is, the least squares estimate the true rate constant) must be independent of the number of half lives for which the reaction was monitored. From the least squares Equations A1.15 to A1.17, the uncertainty in the calculated rate constant decreases as more half lives are included, with 3 to $5t_{1/2}$ (87 to 97% reaction) being optimum, since weighting decimates the impact of further data. Secondly, the rate constants evaluated by weighted linear, unweighted linear, and nonlinear procedures ought to agree within their error estimates. If they do not, sources of systematic error (such as instrumental drift, temperature fluctuations, etc.) should be examined before abandoning the first order model. Finally, when A_∞ is a included as a floating parameter, its calculated value should closely correspond to that actually measured. Except when noted throughout this thesis, these criteria were well satisifed for all oxadiazolinone kinetics.

A2.1.1 Parallel First Order Reactions

Oxadiazolinone thermolysis is an example of a competing, or parallel, set of first order reactions. In this case, the two competing processes, k_3 and k_2, generate ketone (S_3) and diazoalkane (S_2) respectively. Temporarily assuming that a time zero, $[S_2]$ =

$[S_3] = 0$, the kinetic analysis is quite similar to Equation A2.1 except now only the total rate constant, $k_T = k_2 + k_3$, may be found by monitoring the rate of dissappearance of oxadiazolinone, or the rate of appearance of either product.[412 *]

[A2.5] $$S_3 \xleftarrow{k_3} \text{Oxa} \xrightarrow{k_2} S_2$$

[A2.6] $$\frac{d[\text{Oxa}]}{dt} = -k_2[\text{Oxa}] - k_3[\text{Oxa}] = -k_T[\text{Oxa}]; \quad [\text{Oxa}] = [\text{Oxa}]_o e^{-k_T t}$$

[A2.7] $$\frac{dS_3}{dt} = k_3[\text{Oxa}] = k_3[\text{Oxa}]_o e^{-k_T t}; \quad S_3 = \frac{k_3}{k_T}[\text{Oxa}]_o(1-e^{-k_T t})$$

[A2.8] $$S_3(t=\infty) = \frac{k_3}{k_T}[\text{Oxa}]_o \quad \text{so} \quad k_3 = \frac{S_3(t=\infty)}{[\text{Oxa}]_o} \cdot k_T$$

As a consequence of Equation A2.7, and its counterpart for S_2, the ratio of product concentrations, S_3/S_2, at any time (including $t=\infty$, when they would be most conveniently measured) is equal to the ratio of their rate constants, k_3/k_2. In oxadiazolinone thermolysis, S_2 reacts further and is never measured, rather k_3 is obtained from Equation A2.8 and k_2 by difference: $k_2 = k_T - k_3$. Errors propagated in these calculations are discussed in Appendix 1, (Equations A1.4 and A1.5, page 234).

*In previous work in this laboratory, on the competing thermolysis routes of 5,5-dimethyl-2-phenylimino-Δ^3-1,3,4-oxadiazoline, Cameron[262] incorrectly assumed that the individual rate constant for each process could be obtained by monitoring only the rate of appearance of each product. In that study, single run ir kinetics generated rate constants with such large errors that the close correspondence of the two rate constants was never noticed Regrettably, the original data is in disarray, and a proper recalculation impossible.

Even in the case where some S_2 and S_3 are present at time zero, similar results pertain, using $S_i(t) \equiv [S_i]_t - [Si]_o$. Because k_T is a first-order rate constant, it is unaffected by time zero concentrations, but Equation A2.9 more explicitly represents A2.8 in this event.

$$[A2.9] \qquad k_3 = \frac{[S_3]_\infty - [S_3]_o}{[Oxa]_o} \cdot k_T$$

A2.2 First Order Two Stage Reactions

It is instructive to briefly examine the first order, two stage reaction represented by Equation A2.10, because of its wide applicability to pseudo first order reactions. From the outset, it is both appropriate to the chemistry, and greatly

$$[A2.10] \quad R + Oxa \underset{k_{-1}}{\overset{k_1}{\rightleftharpoons}} Int + R' \underset{k_{-2}}{\overset{k_2}{\rightleftharpoons}} P$$

simplifying, to assume that all the reactions are first order (or pseudo first order), that at time zero (which may no longer be arbitrary) [Int] = 0, and that, since the overall reactions of oxadiazolinones are very exothermic and irreversible, k_{-2} may be set to zero. For purely first order reactions, R and R' do not exist, whereas for the case of pseudo first order reactions, R and R' may represent nucleophiles, acid or base catalysts, or solvent, which are present in much higher concentrations than the oxadiazolinone. Once the individual pseudo first order rate constants have been found, their dependence on [R] and [R'] may be evaluated in a series of experiments where these variables are systematically manipulated.

Observed overall pseudo first order kinetics can arise from several simple limiting situations of Equation A2.10, but the observed first order rate constant, k_{obs}, will not easily reveal which of the following cases prevails:

[A2.11] $k_2, k_{-1} >> k_1$; steady state [Int], $k_{obs} = \frac{k_1 k_2}{k_{-1}+k_2}$

[A2.12] $k_1, k_{-1} >> k_2$; rapid preequilibrium, $k_{obs} = Kk_2$; $K = k_1/k_{-1}$

[A2.13] $k_2 >> k_1, k_{-1}$; k_1 rate determining, $k_{obs} = k_1$

Not absolutely every hydrolysis reaction religiously obeyed the simple first order kinetics expected from Equations A2.11 to A2.13. However, some insight into the rate problem cases is possible from examination of a more general form of the solution to Equation A2.10. Under the simplifying constraints enumerated in the first paragraph of this section, the general solutions to the first order, two stage problem are given by Equations A2.14 to A2.17[412], from which Equations A2.18 to A2.22 are derived to describe absorbance monitored kinetics, where the intermediate is also permitted to absorb at the monitoring wavelength, with $F \equiv \varepsilon_{int}/\varepsilon_{oxa}$. The product does not absorb.

[A2.14] $$[Oxa] = [Oxa]_o \frac{(\gamma_1 - k_{-1} - k_2)e^{-\gamma_1 t} - (\gamma_2 - k_{-1} - k_2)e^{-\gamma_2 t}}{\gamma_1 - \gamma_2}$$

[A2.15] $$[Int] = -k_1[Oxa]_o \frac{e^{-\gamma_1 t} - e^{-\gamma_2 t}}{\gamma_1 - \gamma_2}$$

[A2.16] $$[P] = \frac{k_1 k_2 [Oxa]_o}{\gamma_1 \gamma_2} \left[1 + \frac{\gamma_2 e^{-\gamma_1 t} - \gamma_1 e^{-\gamma_2 t}}{(\gamma_1 - \gamma_2)} \right]$$

[A2.17] $$\gamma_{1,2} = \frac{(k_1+k_{-1}+k_2)}{2}\left[1 \pm \sqrt{1 + \frac{4k_1k_2}{(k_1+k_{-1}+k_2)^2}}\right]$$

$$\gamma_1 > \gamma_2;\ \gamma_1\gamma_2 = k_1k_2$$

[A2.18] $$A_o \equiv [Oxa]_o \cdot \varepsilon_{Oxa} \cdot \ell$$

$$A = \ell([Oxa]\cdot\varepsilon_{Oxa} + [Int]\cdot\varepsilon_{int})$$

$$= A_o\left[\frac{[Oxa]}{[Oxa]_o} + \frac{F[Int]}{[Oxa]_o}\right]$$

[A2.19] $$= A_o\ \frac{(\gamma_1-k_{-1}-k_2-Fk_1)e^{-\gamma_1 t} - (\gamma_2-k_{-1}-k_2-Fk_1)e^{-\gamma_2 t}}{\gamma_1 - \gamma_2}$$

[A2.20] $$A = A_1e^{-\gamma_1 t} + A_2e^{-\gamma_2 t}$$

Equation A2.19 implies that the absorbances may be curve fit to a double exponential in 4 adjustable parameters (Equation A2.20). If A_o is known, then, in principle, the values of A_1, A_2, γ_1, and γ_2 permit evaluation of F, k_1, k_{-1}, and k_2. As first order rate constants, γ_1 and γ_2 are independent of the assignment of time zero, but A_1 and A_2 are not. Complete analysis requires all 4 values be known to obtain the individual rate constants. Comparison of the aforementioned limiting cases to the general solution shows that, since $\gamma_1 > \gamma_2$, $k_{obs} = \gamma_2$ and γ_1 describes the rapid unobserved approach to either a steady state or equilibrium condition. Thus, γ_2 corresponds to the pseudo first order rate constant measured during the tail portion of a biphasic reaction. When F>1 the absorbance rises quickly then slowly decays with time

(rise/fall biphasic kinetics), whereas when F<1 the absorbance decays, at first quickly, then settles down to follow γ_2 (fast/slow biphasic kinetics).

Both of these forms of biphasic kinetics were occasionally observed in oxadiazolinone hydrolyses, and these few cases will now be rationalized. Although the absorbance-time data could be curve fit to a double exponential, the lower proportion of data points collected during the faster initial phase lead to strongly correlated parameters with large estimated errors, particularly when γ_1 and γ_2 were within a factor of three of each other. Usually, γ_2, the desired pseudo first order rate constant corresponding to others measured in strictly simple, first order reactions, was measured by first order fits to the tail portion of the biphasic decay curve. Generally, A_1 and γ_1 values were too imprecise to break down the observed rate constants into individual rate constants, so it was not possible to positively assign mechanisms to the biphasic runs. More discussion of these observations may be found in Experimental E3.

In aqueous sulfuric acid solutions containing more than 60 or 80% acid, respectively, rise/fall biphasic first order kinetics were observed for dibenzyl- and dimethyloxadiazolinones. Since nitrogen protonation ought to remove the $n\pi^*$ absorption band used to monitor these kinetics, and since the pK_a of protonated oxadiazolinone was estimated to be near -9 (>90% acid), it is unreasonable to assign the rise component of these kinetics to observably slow protonation. These reactions were initiated by injecting 30 µl of an ethereal

oxadiazolinone solution into 5-20 ml of acid solvent, so it is possible that the small, initial rise in the 360 nm absorbance (ca 10%) corresponds to resolvation of slowly dissolving oxadiazolinone. Resolvation would shift the λ_{max} from 375 to 355-360 nm, thereby increasing the molar absorptivity, ε, at 360 nm. If this were the case, then Equation A2.21 (with $k_{-1} = 0$) might account for the observed result.

[A2.21] $$Oxa_{ether} \xrightarrow{k_1} Oxa_{H_2SO_4} \xrightarrow{k_2} P \; ; \; k_1 > k_2, \; F > 1$$

Two independently reacting absorbers present in the same solution will also give rise to a biphasic absorbance decay obeying a double exponential (Equation A2.22). For example, thermolysis of a mixture of exo-azo and endo-azo isomers of camphor oxadiazolinone (159, page 123) would have exhibited biphasic, fast/slow, kinetics, from which extraction of their individual rate constants would have been of questionable accuracy. Also, it was demonstrated that the use of plastic syringes to manipulate diethylmalonic acid buffers introduced an absorbing impurity which decomposed rapidly in solution, presumably independently of the oxadiazolinone, and fast/slow biphasic decay was observed.

$$S \xrightarrow{k} P \quad ; \quad [S] = [S]_o e^{-kt}$$

$$S' \xrightarrow{k'} P' \quad ; \quad [S'] = [S']_o e^{-k't}$$

[A2.22] $$A = \ell([S].\varepsilon + [S'].\varepsilon') = A_o e^{-kt} + A_o' e^{-k't}$$

Finally, a third, triphasic, kinetic system was observed

when oxadiazolinone was hydrolysed in the presence of thiphenol in the acid pH range. The absorption at 360 nm first dropped, then rose substantially (10-150%) prior to a very, very slow decay to zero (see Experimental E3.2, page 222). Obviously, the first order, two stage model cannot explain such an observation and a more complicated mechanism must be postulated to quantitatively analyse these kinetics. Such work would make excellent fodder for further studies on the chemistry of oxadiazolinones. Perhaps, some of the principles gleaned from two stage hydrolysis kinetics will pertain to such reactions, and future analyses of these, and other reactions may capitalize on this section.

A2.3 Activation Parameters

Transition State Theory[413] predicts the temperature dependence of the reaction rate constant to be given by Equation A2.23.

[A2.23] $$k = K \frac{kT}{h} e^{-\Delta G^{\ddagger}/RT} \quad ; \quad \Delta G^{\ddagger} = \Delta H^{\ddagger} - T\Delta S^{\ddagger}$$

k = rate constant whose time domain is seconds.

K = transmission coefficient (assumed = 1).

k = Boltzmann constant.

h = Planck constant.

T = absolute temperature.

$\Delta G^{\ddagger}$ = free energy of activation.

$\Delta H^{\ddagger}$ = activation enthalpy (assumed temperature independent).

$\Delta S^{\ddagger}$ = activation entropy (assumed temperature independent).

R = universal gas constant, determines units of $\Delta G^{\ddagger}$, $\Delta H^{\ddagger}$, $\Delta S^{\ddagger}$.

From measured rate constants obtained at various temperatures, the activation parameters $\Delta S^{\ddagger}$ and $\Delta H^{\ddagger}$ may be found by curve fitting Equation A2.23 by nonlinear least squares, or by linearizing and plotting against reciprocal temperature (Equation A2.24). As written in the latter equation, the slope and intercept of a plot of y vs 1/T are $-\Delta H^{\ddagger}$ and $\Delta S^{\ddagger}$ respectively.

[A2.24] $$R\left[\ell n\left(\frac{k}{T}\right) - \ell n\left(\frac{k}{h}\right)\right] = \frac{-\Delta H^{\ddagger}}{T} + \Delta S^{\ddagger} \; ; \; \ell n\left(\frac{k}{h}\right) = 23.75997$$

Table A3.1 Valence orbital parameters for oxadiazolinone ($\underline{1}$-H_2).

	Assignment	Symmetry	Orbital Energy[a]	Orbital Densities[b] O1	C2	N3	N4	CH_2	O6
ABMO	$\sigma^*_{CH_2}$	σ	6.23	0.165	0.046	0.002	0.019	0.751	0.017
ABMO	$\pi^{**}_{CO_2}$	π	6.23	0.043	0.465	0.174	0.042	0.071	0.205
ABMO	π^*_{NN}	π	1.79	0.012	0.116	0.266	0.402	0.079	0.125
BMO and NB MO	n_N^-	σ	-13.34	0.066	0.089	0.314	0.160	0.078	0.293
BMO and NB MO	π_O	π	-14.14	0.233	0.032	0.119	0.094	0.177	0.345
BMO and NB MO	n_{CO}	σ	-15.96	0.158	0.057	0.085	0.230	0.221	0.349
BMO and NB MO	n^+_N(or n_O)[c]	σ	-17.20	0.346	0.006	0.252	0.245	0.108	0.043
BMO and NB MO	π_{NN}	π	-17.50	0.416	0.003	0.301	0.262	0.007	0.011
BMO and NB MO	n_O(or n^+_N)[c]	σ	-18.48	0.142	0.111	0.190	0.073	0.084	0.400

[a] In eV.

[b] Orbital density on atom A in orbital i is given by $\sum_{\nu}^{\text{on A}} C_{\mu i}^2$.

[c] Assignment in these terms is arbitrary.

Table A3.2 Valence orbital parameters for difluorooxadiazolinone ($\underline{1}$-F_2).

	Assignment	Symmetry	Orbital Energy[a]	Orbital Densities[b] O1	C2	N3	N4	C5	O6	F
ABMO	$\pi^*_{CO_2}$	π	5.32	0.040	0.469	0.203	0.058	0.010	0.209	0.005
	$\sigma^*_{CF_2}$	σ	5.26	0.242	0.064	0.004	0.065	0.436	0.025	0.082
	π^*_{NN}	π	0.71	0.009	0.121	0.297	0.385	0.016	0.138	0.017
BMO and NBMO	n_N^-	σ	-14.19	0.055	0.089	0.290	0.211	0.092	0.216	0.023
	π_{CO_2}	π	-15.88	0.269	0.064	0.068	0.106	0.002	0.418	0.038
	n_{CO}	σ	-16.67	0.285	0.027	0.051	0.216	0.058	0.267	0.048
	n_O	σ	-17.79	0.306	0.026	0.139	0.023	0.102	0.198	0.103
	π_{NN}	π	-18.33	0.385	0.000	0.297	0.301	0.001	0.000	0.008
	n_N^+	σ	-18.88	0.077	0.072	0.279	0.272	0.012	0.200	0.044
	$\pi^1_{CF_2}$	π	-20.38	0.001	0.029	0.001	0.002	0.051	0.038	0.439
	σ_{CF_2}	σ	-21.16	0.050	0.037	0.114	0.142	0.022	0.169	0.232
	$\pi^2_{CF_2}$	π	-22.14	0.002	0.001	0.005	0.007	0.000	0.001	0.492

[a] eV.

[b] Orbital density on atom A in orbital i is given by $\sum_{\mu}^{\text{on A}} C_{\mu i}^2$.

Table A3.3a Effect of carbonyl bond length variations on the CNDO/2 energy levels of Δ^3-1,3,4-oxadiazolin-2-one.

R_{CO} (Å)	Total Energy (hartree)[a]	Orbital Energy (eV) Unoccupied (ABMO)			Doubly Occupied (BMO and NBMO)					
		σ^*	$\pi^*_{CO_2}$	π^*_{NN}	n_{N^-}	π_{CO_2}	n_{CO}	n_O[b]	π_{NN}	n_{N^+}[b]
1.16	-75.81470	6.39	6.45	1.94	-13.25	-14.22	-15.93	-17.01	-17.32	-18.58
1.19	-75.83795	6.23	6.23	1.79	-13.34	-14.14	-15.96	-17.20	-17.50	-18.48
1.21	-75.84831	6.17	6.08	1.69	-13.40	-14.06	-15.96	-17.23	-17.65	-18.41
1.24	-75.88716	6.07	5.86	1.54	-13.50	-13.92	-15.95	-17.32	-17.62	-18.30
1.27	-75.85869	6.07	5.68	1.40	-13.62	-13.80	-15.99	-17.28	-17.56	-18.23
1.29	-75.85626	5.99	5.55	1.29	-13.66	-13.70	-15.94	-17.35	-17.62	-18.13
Observed[c]					-10.20	-11.52	-13.26			
1.19(5,5-dimethyl)	-93.22614	6.31	6.59	2.32	-12.81	-13.37	-15.14	-16.07	-16.79	-17.35
1.19(5,5-difluoro)	-129.82776	5.26	5.32	0.71	-14.19	-15.88	-16.67	-17.79	-18.33	-18.88

[a] 1 hartree = 27.2107 eV.

[b] Assignment of n_{N^+} and n_O orbitals is arbitrary for the unsubstituted compound.

[c] Observed orbital energies for 5,5-dimethyloxadiazolinone assume Koopmans theorem.[290]

Table A3.3b Effect of carbonyl bond length variations on the CNDO/2 net charge densities of Δ^3-1,3,4-oxadiazolin-2-one.

R_{CO} (Å)	Net Charge Densities[a]						
	H,F or CH_3	O1	C2	N3	N4	C5	O6
1.16	0.0139	-0.2383	0.4598	-0.1159	-0.0210	0.1732	-0.2855
1.19	0.0161	-0.2408	0.4437	-0.1078	-0.0214	0.1747	-0.2805
1.21	0.0172	-0.2376	0.4367	-0.1049	-0.0199	0.1750	-0.2836
1.24	0.0188	-0.2334	0.4259	-0.1011	-0.0174	0.1755	-0.2871
1.27	0.0196	-0.2194	0.4249	-0.0963	-0.0166	0.1744	-0.3062
1.29	0.0209	-0.2179	0.4173	-0.0954	-0.0136	0.1748	-0.3068
1.19(5,5-dimethyl)	0.0806	-0.2533	0.4501	-0.1314	-0.0289	0.2247	-0.3102
1.19(5,5-difluoro)	-0.1949	-0.2535	0.4519	-0.0599	-0.0648	0.5773	-0.2610

[a]Net charge density on atom A = Nuclear charge - total electron density

$$= Z_A - 2 \sum_{\mu}^{\text{on A}} \sum_{i}^{\text{occ}} C_{\mu i}^2$$

Table A3.4 Solvent effects on thermolysis of dimethyloxadiazolinone at 85.0°C.[a]

Solvent	E_T[b]	$10^5 k_T$	Kinetic[c] Method	%Ketone	Analytical[d] Method	$10^5 k_3$	$10^5 k_2$
Toluene	33.9	12.23 ± 0.11	A	82.0 ± 0.5	GC	10.03 ± 0.11	2.20 ± 0.09
Chlorobenzene	37.5	11.90 ± 0.12	A	71.3 ± 0.8	GC	8.48 ± 0.13	3.42 ± 0.10
1,2-Dimethoxyethane	38.2	10.60 ± 0.11	A	60.8 ± 1.7	GC	6.44 ± 0.19	4.16 ± 0.19
1,2-Dichloroethane	41.9	11.75 ± 0.08	S	44.3 ± 0.6	IR	5.21 ± 0.08	6.54 ± 0.08
Dimethylformamide	43.8	16.60 ± 0.20	A	19.9 ± 0.2	GC	3.30 ± 0.05	13.30 ± 0.16
Acetonitrile	46.0	17.40 ± 0.17	A	16.2 ± 0.3	GC	2.82 ± 0.06	14.58 ± 0.15
Nitromethane	46.3	18.3 ± 0.3	A	21.9 ± 0.6	GC	4.01 ± 0.13	14.3 ± 0.3
Acetic Acid	51.9	28.62 ± 0.19	A	13.3 ± 0.15	GC	3.81 ± 0.05	24.81 ± 0.46
Trifluoroethanol	59.5	139.4 ± 0.6	S	0.9 ± 0.15	GC	0.35 ± 0.14	139.1 ± 0.6
Trifluoroacetic Acid	66±7[e]	1045 ± 20	S	0.4 ± 0.25	NMR	–	1041 ± 20
Nitrobenzene[f]	42.0	17.7 ± 0.5	NMR	38 ± 2	NMR	–	–

[a] Errors are standard deviations of the mean of triplicates, propagated by the formulae in Appendix 1.
[b] Rate constants are in s^{-1}.
[b] Ref. 77. (kcal mol^{-1}).
[c] A = 100 mL volumetric flask in bath; 6 mL aliquots withdrawn and quenched in liq. N_2; analysed in 1 cm uv cells near 360 nm
S = Individual sealed tubes suspended in bath; removed and quenched; analysed in 0.1 cm uv cells near 360 nm.
[d] NMR = Varian EM-390 spectrometer operated at 85 ± 2°C
GC = calibrated gas chromatography with internal standard
IR = calibrated ir spectroscopy - slow scan speed
[e] Calculated from correlations among E_T and other solvent polarity parameters. See Experimental E2.4.6
[f] A pmr experiment - meaningful only for product distribution.

Table A3.5 Temperature dependence of dimethyloxadiazolinone thermolysis.[a]

Solvent	Temperature	$10^5 k_T$	% Ketone	$10^5 k_3$	$10^5 k_2$
Toluene	94.0	35.26 ± 0.38	84.0 ± 0.8	29.62 ± 0.43	5.64 ± 0.29
	89.0	19.84 ± 0.07	82.4 ± 0.4	16.35 ± 0.10	3.49 ± 0.08
	85.0	12.23 ± 0.11	82.0 ± 0.5	10.03 ± 0.11	2.20 ± 0.09
	81.0	7.50 ± 0.04	81.1 ± 0.5	6.08 ± 0.05	1.42 ± 0.04
	77.0	4.69 ± 0.015	80.8 ± 0.5	3.79 ± 0.03	0.90 ± 0.02
Acetonitrile	89.0	24.3 ± 0.8	16.5 ± 0.3	4.01 ± 0.15	20.3 ± 0.7
	85.0	17.40 ± 0.17	16.2 ± 0.3	2.82 ± 0.06	14.58 ± 0.15
	81.0	11.01 ± 0.08	15.2 ± 0.1	1.67 ± 0.02	9.34 ± 0.07
	77.0	6.98 ± 0.03	14.0 ± 0.2	0.98 ± 0.01	6.00 ± 0.03
Trifluoroethanol	85.0	139.4 ± 0.6	0.25± 0.10	0.35 ± 0.14	139.1 ± 0.6
	70.6	34.21 ± 0.14	0.30± 0.10	0.10 ± 0.03	34.11 ± 0.14
	60.3	11.55 ± 0.06	0.40± 0.10	0.046± 0.012	11.5 ± 0.06
	51.6	4.24 ± 0.04	0.90± 0.15	0.038± 0.006	4.20 ± 0.04
Trifluoroacetic Acid	85.0	1045 ± 20	not	—	1041 ± 20
	77.15	517 ± 13	measureable	—	515 ± 13
	70.6	320 ± 5	put	—	319 ± 5
	60.3	116.5 ± 1.0	at	—	116.0 ± 1.0
	51.6	46.0 ± 0.3	0.4 ±0.25	—	45.8 ± 0.3

[a]Kinetics by uv aliquot methods, product distribution by calibrated glc. Errors are standard deviations of the mean of triplicates, propagated by the formulae in Appendix 1. Rate constants are in s^{-1}. Temperatures were measured by National Research Council calibrated thermometer (°C, ±0.1°).

Table A3.6 β-Deuterium secondary kinetic isotope effects in thermolysis of 1-Me_2 at 85.0°C.[a]

Solvent	Substrate	$10^5 k_T$[b,c]	% Ketone[c,d]	$10^5 k_3$	$10^5 k_2$	$k_3(H)/k_3(D)$[e]	$k_2(H)/k_2(D)$[e]
Toluene	1-$(CH_3)_2$	12.12 ± 0.05	80.6 ± 1.5	9.77 ± 0.19	2.35 ± 0.18	1.078 ± 0.024	1.199 ± 0.110
	1-$(CD_3)_2$	11.02 ± 0.04	82.2 ± 0.9	9.06 ± 0.10	1.96 ± 0.10	1.013 ± 0.004 perD	1.031 ± 0.018 perD
Acetonitrile	1-$(CH_3)_2$	17.4 ± 0.2	16.5 ± 0.3	2.82 ± 0.06	14.68 ± 0.18	1.041 ± 0.041	1.131 ± 0.020
	1-$(CD_3)_2$	15.6 ± 0.2	17.4 ± 0.5	2.71 ± 0.09	12.89 ± 0.17	1.007 ± 0.007 per D[f]	1.021 ± 0.003 per D

[a]For each solvent, each substrate was done in duplicate, all four runs simultaneously.

[b]Total first order rate constant, $k_T(s^{-1})$.

[c]Errors are standard deviations of the mean of duplicates.

[d]Calibrated glc with internal standard.

[e]$k(H)/k(D)$ (per D) = $(k(H)/k(D)\ (obs.))^{1/6}$.

[f]For the minor pathway, the propagated error is large (see Experimental E2.2.1) and this value may, therefore, not be reliable.

Table A3.7 Alkyl substituent effects on thermolysis of oxadiazolinones in 1,2-dichloroethane at 85.0°C.[a]

R_1	R_2	$10^5 k_T$	% Ketone	$10^5 k_3$	$10^5 k_2$	$\sum\sigma^{*b}$	$\sum E_s^{b}$
CH_3	CH_3	11.75 ± 0.08	44.3 ± 0.6	5.21 ± 0.08	6.54 ± 0.08	0.00	0.00
CH_3	$CH_3CH_2CH_2$	17.43 ± 0.17	50.9 ± 1.7	8.87 ± 0.31	8.56 ± 0.31	-0.115	-0.36
CH_3	$(CH_3)_2CH$	16.05 ± 0.19	42.4 ± 0.6	6.81 ± 0.13	9.24 ± 0.14	-0.19	-0.47
CH_3	$(CH_3)_3C$	21.02 ± 0.12	28.4 ± 0.5	5.97 ± 0.11	15.05 ± 0.14	-0.30	-1.54
CH_3	$(CH_3)_2CHCH_2$	36.6 ± 1.7	43.0 ± 1.5	15.7 ± 0.9	20.9 ± 1.1	-0.125	-0.93
CH_3	$C_6H_5CH_2$	8.39 ± 0.09	66.8 ± 1.0	5.60 ± 0.10	2.79 ± 0.09	+0.215	-0.38
CH_3	CH_3OCH_2	3.41 ± 0.01	97 ± 3	3.31 ± 0.10	0.10 ± 0.10	+0.52	-0.19
$(CH_3)_2CH$	$(CH_3)_2CH$	25.84 ± 0.22	24.7 ± 0.6	6.38 ± 0.16	19.46 ± 0.23	-0.38	-0.94
$C_6H_5CH_2$	$C_6H_5CH_2$	6.36 ± 0.10	69.9 ± 0.5	4.45 ± 0.08	1.91 ± 0.04	+0.43	-0.76

[a]Kinetics and product distributions by ir spectroscopy. Errors are standard deviations of the mean of triplicates, propagated by the formulae in Appendix 1. Rate constants in s^{-1}.

[b]Ref. 315. Correlations of log $(k_2/k_2(CH_3/CH_3)) = \sigma^*\rho^*$ and log $(k_3/k_3(CH_3/CH_3)) = \sigma^*\rho^*$ gave $\rho^* = -1.27 \pm 0.06$ ($r = -0.993$) and $\rho^* = -0.28 \pm 0.11$ ($r = -0.686$), respectively.

Table A3.8 Thermolysis of p-substituted acetophenone oxadiazolinones in acetonitrile at 50.0°C.[a]

p-Substituent	f_{oxa}[b]	$10^5 k_T$	% Ketone	$10^5 k_3$	$10^5 k_2$	σ[c]	σ^+[c]
CH_3	0.866	57.01 ± 0.17	15.5 ± 0.6	8.84 ± 0.34	48.17 ± 0.37	-0.17	-0.31
C_6H_5	0.926	39.98 ± 0.48	21.0 ± 1.6	8.40 ± 0.65	31.58 ± 0.74	-0.01	-0.17
H	0.858	21.96 ± 0.15	19.7 ± 0.8	4.33 ± 0.18	17.63 ± 0.21	0.00	0.00
Cl	0.754	14.91 ± 0.10	36.9 ± 1.5	5.49 ± 0.23	9.42 ± 0.23	0.23	0.11
Br	0.878	13.64 ± 0.15	35.6 ± 1.7	4.86 ± 0.24	8.78 ± 0.25	0.23	0.15
CF_3	0.799	6.34 ± 0.05	75.9 ± 3.0	4.81 ± 0.19	1.53 ± 0.19	0.54	0.52
CN	0.844	7.16 ± 0.02	85.1 ± 3.4	6.10 ± 0.24	1.06 ± 0.24	0.66	0.66
NO_2	0.793	6.995 ± 0.053	78.9 ± 3.2	5.59 ± 0.23	1.41 ± 0.21	0.78	0.79

[a]Errors are standard deviations of the mean of triplicates, propagated by the formulae in Appendix 1. Rate constants are in s^{-1}, product determination by ir spectroscopy.

[b]NMR purity assay prior to thermolysis - applied as a correction factor to determine product distribution (See Experimental E1.2). Standard deviations are 2-3%.

[c]Ref. 294.

Appendix A3.9 Estimations of ΔH°_2 and ΔH°_3 for systems found in Table R10 (page 139).

[A3.1]

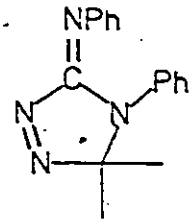

(131:X=NPh)

k_2 → Ph-N=C=N-Ph + $\rangle C{=}\overset{+}{N}{=}\bar{N}$ $\quad \Delta H^\circ_2 = 15.9$

(estimates)

k_3 → N_2 + Ph-$\overset{+}{N}\equiv\bar{C}$ + Ph-N=C$\langle$ $\quad \Delta H^\circ_3 = -35.8$

[A3.2] $\Delta H^\circ_2(\underline{131}:X=NPh) = \Delta H^\circ_2(\underline{1}\text{-}Me_2)_{obs} - \Delta H^\circ_{ex}(CO_2) + \Delta H^\circ_{ex}$ (H—N=C=N—H; assumed equal to p-ℓ+k in Table R7) $+ \delta\Delta H_{Ph}$ (ca 10?)

$= 1 + 2.6 + 22.3 - 10 = 15.9$

[A3.3] $\Delta H^\circ_3(\underline{131}:X=NPH)_{est} = \Delta H^\circ_3(\underline{131}:X=O)_{est} - \Delta H^\circ_{ex}(CO) + \Delta H^\circ_{ex}(Me-\overset{+}{N}\equiv\bar{C}) + (\delta\Delta H_{Ph} - \delta\Delta H_{Me}) + \Delta H^\circ_{int}(C{=}O/NPh) - \Delta H^\circ_{int}(C{=}C/N)$

$= -22.4 - 15.4 + 24.0 - 3 - 16.4 + 7 = -35.8$

[A3.4]

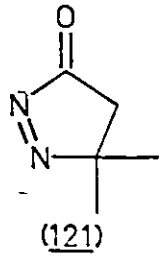

(121)

k_2 → $\rangle C{=}\overset{+}{N}{=}\bar{N}$ + $H_2C{=}C{=}O$ $\quad \Delta H^\circ_2 = 38.9$

(estimates)

k_3 → N_2 + CO + $\rangle C{=}CH_2$ $\quad \Delta H^\circ_3 = -31.3$

[A3.5] $\Delta H^\circ_2(\underline{121})_{est} = \Delta H^\circ_2(\underline{1}\text{-}Me_2)_{obs} - \Delta H^\circ_{ex}(CO_2) + \Delta H^\circ_{ex}(H_2C{=}C{=}O)$

$= 1 + 2.6 + 35.3 = 38.9$

[A3.6] $\Delta H^\circ_3(\underline{121})_{est} = \Delta H^\circ_3(\underline{1}\text{-}Me_2)_{obs} = \Delta H^\circ_{ex}(Me_2C{=}O) + \Delta H^\circ_{ex}(Me_2C{=}CH_2) - \Delta H^\circ_{int}(C{=}O/O)$

$= -30 - 11.5 + 33.8 - 23.6 = -31.3$

[A3.7]

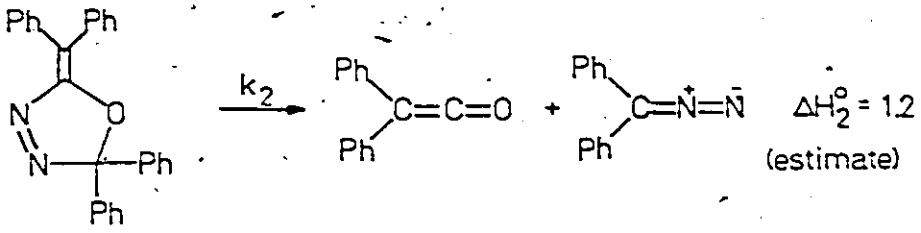

(101)

[A3.8] $\Delta H^\circ_2(\underline{101})_{est} = \Delta H^\circ_2(\underline{1}\text{-}Me_2)_{obs} - \Delta H^\circ_{ex}(CO_2) + \Delta H^\circ_{ex}(H_2C{=}C{=}O) + \delta\Delta H_{Ph}$

$= 1 + 2.6 + 15.6 - 18 = 1.2$

[A3.9]

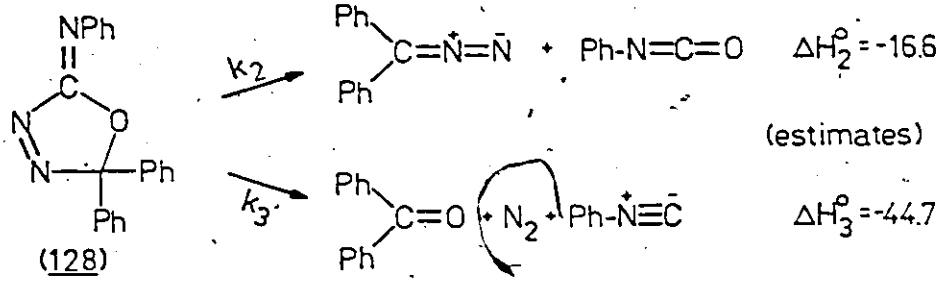

(128)

[A3.10] $\Delta H^\circ_2(\underline{128})_{est} = \Delta H^\circ_2(\underline{1}\text{-}Me_2)_{obs} - \Delta H^\circ_{ex}(CO_2) + \Delta H^\circ_{ex}(HNCO) + \delta\Delta H_{Ph}$

$= 1 + 2.6 - 11.2 - 9 = -16.6$

[A3.11] $\Delta H^\circ_3(\underline{128})_{est} = \Delta H^\circ_3(\underline{1}\text{-}Me_2)_{obs} - \Delta H^\circ_{ex}(CO) + \Delta H^\circ_{ex}(MeN{\equiv}C) + \delta\Delta H_{Ph} + \Delta H^\circ_{int}(C{=}O/O) - \Delta H^\circ_{int}(C{=}C/O)$

$= -30 - 15.4 + 24.0 - 7 + 23.6 + 7.3 = -44.7$

Table A3.10 Buffer catalysis summary for hydrolysis of 1-Me_2 in the pH range 1-9.

measured pH at 20.0°C	$10^8 \cdot [OH^-]/M$[a]	Buffer (pK,p,q)[b]	$10^5 k_o/s^{-1}$[c]	$10^5 k_b/M^{-1}s^{-1}$[d]
		H_2O/H_3O^+ (-1.74,3,1)[e]		6.56±0.04[f]
1.03		KCl/HCl	354 ± 3	
1.700		Maleic	352 ± 9	
2.087		Acid	359 ± 6	
2.767		Formic Acid	399 ± 7	635±33
3.356		(3.581,1,2)	409 ± 7	(Figure A3.7)
3.820			414 ± 8	
4.548			412 ± 6	
3.890		Acetic Acid	408 ±14	944±52
4.457		(4.644,1,2)	421 ± 5	(Figure A3.6)
4.925			414 ± 8	
5.644			435 ± 9	
4.67		Phthalic Acid	386 ± 6	
5.39			393 ± 5	
5.251		Maleic Acid	420 ± 6	1048±46
5.630		(5.937,1,4)	410 ±3	(Figure A3.5)
5.880			436 ± 7	
6.173	1.0		433 ± 3	
6.516	2.3		484 ± 5	
5.950	0.6	Phosphoric Acid	462 ± 10	
6.711	3.5	(7.21, 1,4)[h]	531 ± 24	
7.520	22.5		760 ± 15	
6.490	2.1		484 ± 23	10400±200
6.980	6.5		629 ± 14	(Figure A3.4)
7.201	10.8		772 ± 19	
7.405	17.3		850 ± 17	
6.920	5.7	Diethylmalonic	608 ±7	9300±200 (a)
7.300	13.6	Acid	793 ± 20	or 5000±300 (b)
7.815	44.5	(7.019,1,4)	1333 ±34	(Figure A3.3)
7.683	32.8	Tris(hydroxymethyl)	1458 ± 34	33500±120
8.100	85.7	aminomethane	2193 ± 59	(Figure A3.2)
8.418	178.3	(8.32,3,1)	3778 ± 42	
8.558	246.1		4313 ± 53	
		H_2O/HO^- (15.91,2,1)[g]		$(1.66\pm0.06)\times10^9$ (Figure A3.1)

[a] Assuming pK_w (20.0°C) = 14.1669 (ref. 338), used to find $k_b(HO^-)$ in Figure A3.1.

[b] pK measured from titration and pH data. p=number of equivalent protons in acid, q = number of equivalent basic sites in conjugate base.[333]

[c] Error limits returned by least squares fits of k_{obs} vs [buffer base] at given pH.

[d] Error limits returned by least squares fits of $(k_{obs}-k_o)$ vs [buffer base] efor a given buffer system (see Experimental E3.2.1.1 and Figures A3.2-A3.7).

[f] Ref. 269

[g] $k_b(H_2O)$ = k (0.200 MHCl)/$[H_2O]$ = 362/55.2

Includes water concentration to be compatible with other pKs.

[h] Ref. 269.

Table A3.11 Dilution effects on hydrolysis of 1-Me_2 at 20.0° in 0.200 M HCl.[a]

Vol % H_2O	Cosolvent Dioxane		Cosolvent DMF		Cosolvent CH_3OH		Cosolvent $HCONH_2$	
	$[H_2O]$/M	$10^5 k_{obs}$	$[H_2O]$/M	$10^5 k_{obs}$	$[H_2O]$/M	$10^5 k_{obs}$	$[H_2O]$/M	$10^5 k_{obs}$
100	55.20	368.8	55.20	363.7	55.20	362.0	55.20	363.7
95	52.30	315.7	52.19	339.8	52.20	334.0	52.37	320.3
90	49.56	274.1	49.46	309.8	49.71	295.8	49.71	289.6
85	46.93	232.6	46.76	285.2	47.09	267.6	47.02	263.6
80	44.26	192.6	44.11	257.3	44.56	244.0	44.29	247.0
75	41.63	153.5	41.46	216.3	41.83	210.5	41.55	203.1
70	38.96	121.8	38.84	190.4	39.19	185.2	38.80	174.0
65	36.27	92.71	36.17	163.9	36.53	159.1	36.06	151.6
60	33.49	68.86	33.43	133.3	33.82	137.2	33.26	129.7
55	30.67	50.04	30.64	108.9	31.10	117.3	30.46	110.3
50	27.86	35.54	27.84	83.1	28.37	99.1	27.66	96.2

[a]Water concentrations determined from measured density data. All rate constants are s^{-1}, single determination.

Table A3.12 Decomposition of 1-Me_2 in aqueous sulfuric acid at 20.0°C.

% H_2SO_4[a]	$10^5 k_{obs}/s^{-1}$[b]	% H_2SO_4[a]	$10^5 k_{obs}/s^{-1}$[b]
3.21	374.8 ± 0.3	53.21	51.81 ± 0.07
5.75	363.5 ± 0.3	55.52	48.80 ± 0.09
8.94	346.6 ± 0.3	56.66	47.44 ± 0.05
11.40	328.2 ± 0.2	58.67	45.80 ± 0.06
13.98	305.6 ± 0.2	59.60	45.22 ± 0.06
16.50	282.3 ± 0.1	60.92	44.68 ± 0.07
18.80	261.5 ± 0.1	63.09	44.77 ± 0.06
21.61	238.8 ± 0.1	65.75	46.87 ± 0.08
23.56	217.9 ± 0.2	68.88	47.75 ± 0.06
26.09	194.5 ± 0.1	67.85	48.94 ± 0.07
28.10	174.4 ± 0.1	70.01	52.79 ± 0.11
30.92	151.4 ± 0.1	71.50	57.75 ± 0.09
32.67	139.4 ± 0.3	72.63	61.99 ± 0.17
34.45	127.1 ± 0.1	73.52	60.03 ± 0.09[c]
36.63	112.1 ± 0.1	74.75	77.1 ± 0.2
38.05	104.8 ± 0.2	76.30	94.6 ± 1.3
40.52	91.03 ± 0.13	77.86	112.5 ± 0.3
42.42	82.55 ± 0.12	79.07	145.4 ± 0.4[d]
44.83	73.08 ± 0.09	80.07	182.9 ± 0.3[d]
46.02	68.46 ± 0.07	81.00	230.1 ± 0.3[d]
47.91	63.32 ± 0.06	82.13	312.0 ± 1.5[d]
50.48	57.42 ± 0.09	83.54	497 ± 4[d]
52.35	53.75 ± 0.08	84.52	809 ± 4[d]

[a]Weight percent, as determined by titration of concentrated H_2SO_4 (97.405%), and subsequent weighings.

[b]Single run only. Reproducibility is about 10 times the quoted error.

[c]Discarded.

[d]Quoted rate constant corresponds to the tail portion of a slightly biphasic run (see Appendix 2). In solutions more concentrated than 85% H_2SO_4, first order kinetics were not observed, and tail rates could not be evaluated.

Table A3.13 Properties of aqueous sulfuric acid at 20.0°C.[a]

Weight % H_2SO_4	Stoichiometric[b] $C_W^S=[H_2O]$	Stoichiometric[b] $C_A^S=[H_2SO_4]$	Activity[c] a_W	$C_W' = a_W(C_W^S+C_A^S)$ [d]	Acidity H_o [e]	Raman Derived Concentrations[f] $[SO_4^{-2}]$	$[HSO_3^-]$	$[H_3O^+]$	$[H_2O]$	$a_{H_3O^+}$ [g]
0	55.41	0.00	1.000	55.41	–	0.000	0.00	0.00	55.41	0.000
5	54.40	0.53	0.969	53.22	+0.097	0.097	0.43	0.62	53.78	0.011
10	53.26	1.09	0.942	51.19	-0.323	0.226	0.86	1.31	51.95	0.025
15	51.99	1.69	0.912	48.95	-0.658	0.387	1.30	2.07	49.92	0.040
20	50.60	2.32	0.873	46.20	-0.985	0.574	1.75	2.90	47.70	0.057
25	49.05	3.00	0.820	42.70	-1.300	0.782	2.22	3.79	45.27	0.077
30	47.34	3.73	0.752	38.39	-1.646	1.002	2.73	4.73	42.61	0.100
35	45.46	4.50	0.668	33.39	-2.025	1.223	3.27	5.72	39.74	0.126
40	43.39	5.31	0.568	27.64	-2.490	1.432	3.88	6.75	36.65	0.155
45	41.14	6.18	0.456	21.58	-2.767	1.615	4.57	7.80	33.35	0.190
50	38.72	7.11	0.352	16.11	-3.232	1.753	5.36	8.87	29.85	0.229
55	36.10	8.10	0.249	11.00	-3.783	1.826	6.28	9.93	26.17	0.275
60	33.27	9.17	0.161	6.83	-4.375	1.814	7.35	10.98	22.29	0.330
65	30.16	10.30	0.0912	3.69	-5.009	1.699	8.60	12.00	18.16	0.398
70	26.84	11.49	0.0434	1.66	-5.714	1.473	10.02	12.96	13.87	0.483
75	23.16	12.77	0.0172	0.617	-6.444	1.136	11.63	13.90	9.26	0.600
80	19.16	14.09	5.22×10^{-3}	0.174	-7.225	0.720	13.37	14.81	4.35	0.773
85	14.80	15.42	1.62×10^{-3}	-0.0490_{-3}	-8.012	0.297[h]	15.12[h]	15.71[h]	–	–
90	10.07	16.65	3.09×10^{-4}	8.26×10^{-4}	-8.837	–	–	–	–	–
95	5.09	17.76	3.4×10^{-5}	7.74×10^{-4}	-9.721	–	–	–	–	–

[a] All concentrations expressed in mol L^{-1}.

[b] Computed from density and gpL concentrations of H_2SO_4 (ref. 347).

[c] Ref. 348.

[d] Activity coefficient corrected water concentration C_W' (see Equation R26, page 152).

[e] Interpolated from the variable temperature data of Ref. 349.

[f] Based on the quantitative Raman study of sulfate concentrations over the range $0<C_A<14.2M$ (ref. 345) $[SO_4^{-2}]=0.1575x + 0.05468x^2 - 0.007474x^3 + 0.0002170x^4$, (where $x=C_A^S$) $[HSO_3^-]=C_A^S-[SO_4^{-2}]$; $[H_3O^+] = 2[SO_4^{-2}] + 2[HSO_3^-]$; $[H_2O] = C_W^S-[H_3O^+]$; $[H_2SO_4]$ assumed = 0.

[g] Fraction of water in protonated form.

[h] Extrapolation of footnote f. Some caution must be used with these values.

Table A3.14 Alkyl substituent effects on oxadiazolinone decomposition in 0.200 M HCl.

R_1	R_2	$10^5\ k_{obs}$ [a]	$\log k_{obs}$	$\sum\sigma^*$ [b]	$\sum E_s$ [b]	k_{H_2O}/k_{D_2O} [c]
CH_3	CH_3OCH_2	558.3 ± 1.6	-2.253	0.52	-0.19	2.55 ± 0.03
CH_3	CH_3	359.8 ± 0.7	-2.444	0.00	0.00	2.52 ± 0.02
CH_3	CH_3CH_2	279.8 ± 2.8	-2.553	-0.10	-0.07	
CH_3	$CH_3CH_2CH_2$	258.6 ± 1.3	-2.587	-0.115	-0.36	
CH_3	$(CH_3)_2CHCH_2$	202.3 ± 3.0	-2.694	-0.125	-0.93	
CH_3	$(CH_3)_2CH$	151.2 ± 0.8	-2.820	-0.19	-0.47	
CH_3	$(CH_3)_3C$	73.80 ± 0.25	-3.132	-0.30	-1.54	3.21 ± 0.03
$(CH_3)_2CH$	$(CH_3)_2CH$	15.25 ± 0.12 [d]	-3.817	-0.38	-0.94	
CH_3	$PhCH_2$	264.1 ± 0.6	-2.578	0.215	-0.38	2.63 ± 0.04
$PhCH_2$	$PhCH_2$	141 ± 20 [e]	-2.851	0.430	-0.76	

[a] Observed pseudo first order rate constants (s^{-1}). Errors are standard deviation of the mean of triplicates.

[b] Ref. 315.

[c] From 2-4 runs in 0.200 M DCl in D_2O.

[d] Single run only.

[e] Not soluble: this vlaue was interpolated from data in aqueous DMF (see Figure A3.8).

Table A3.15 Model neutral ester hydrolyses[a]

System	Solvent	N	ρ or ρ*	cc	$\sigma_{\log k}$
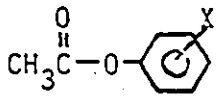	H_2O	5	1.3±0.2[b]	0.976	0.081
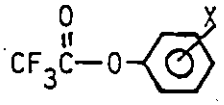	70% acetone/H_2O	3	1.7±0.7[b]	0.929	0.199
$CF_3C(=O)-O-R^c$	70% acetone/H_2O	4	9.1±0.4[d]	0.997	0.043
$CCl_3C(=O)-O-R^c$	50% dioxane/H_2O	7	1.1±0.1	0.970	0.160
$CHCl_2C(=O)-O-R^c$	H_2O	4	0.8±0.1	0.981	0.080
1[e]	0.200 M HCl	10	0.9±0.4	0.624	0.364

[a]Excepting oxadiazolinone, these results were computed from data compiled in Table 27, p. 156, ref. 350.

[b]To properly compare to the other systems in this table, these ρ values should be halved to account for an intervening carbon atom (C5 in 1).

[c]These R groups chosen so R =CHR_1R_2 to compare to C5 disubstituted oxadiazolinones.

[d]R = Et, n-Pr, n-Bu, n-C_5H_{11} gave a range of $\sum\sigma^*$ of only 0.13 - a very narrow range, but the correlation here is the best in the table!

[e]Linear correlation against ρ* only - see Figure R21.

Table A3.16 Decomposition of 1-Me_2 in FSO_3H by pmr.[a]

Solvent	°C	$10^5 k_{obs}/s^{-1}$	corr. coeff.
FSO_3H	-26.0 ± 0.5	33.5 ± 0.5	-0.999
FSO_3H	-19.85 ± 0.25	113 ± 2	-0.995
FSO_3H	-17.5 ± 0.5	160 ± 5	-0.994
FSO_3H	-14.95 ± 0.25	218 ± 4	-0.979
FSO_3H	-8.5 ± 0.25	540 ± 10	-0.998
FSO_3D	-16.6 ± 0.4	170 ± 5	-0.997
FSO_3D	-16.2 ± 0.4	188 ± 5	-0.996

[a]Activation parameters: $\Delta H^{\ddagger}$ = 19.5 ± 0.5 kcal mol^{-1}, $\Delta S^{\ddagger}$ = 5.1 ± 1.8 eu, r = -0.996. Find $k_{20°}$ = 0.233 ± 0.006 s^{-1} and k_H/k_D = 1.0 ± 0.1.

Table A3.17 Application of the X-method to acid catalysed decomposition of 1-Me_2.

$\%H_2SO_4$	X[a]	$10^5 k_{obs}$[b]	$\log C_{H^+}$[a]	$\log k_{obs} - \log C_{H^+}$	$\log(k_{obs} - k_{plat}) - \log C_{H^+}$[c]
70	4.459	52.76	1.097	-4.375	-5.180 ± 0.080
71	4.606	56.58	1.103	-4.350	-5.021 ± 0.070
72	4.759	56.94	1.108	-4.353	-5.014 ± 0.060
73	4.916	58.47	1.113	-4.346	-4.968 ± 0.050
74	5.080	67.90	1.118	-4.286	-4.749 ± 0.035
75	5.247	79.27	1.123	-4.224	-4.582 ± 0.025
76	5.421	88.39	1.128	-4.182	-4.486 ± 0.020
77	5.597	98.87	1.132	-4.137	-4.397 ± 0.015
78	5.779	115.5	1.136	-4.074	-4.285 ± 0.012
79	5.963	141.8	1.140	-3.988	-4.152 ± 0.010
80	6.150	179.8	1.143	-3.888	-4.012 ± 0.010
81	6.339	230.1	1.144	-3.782	-3.875 ± 0.010
82	6.528	301.3	1.143	-3.664	-3.733 ± 0.010
83	6.717	405.5	1.139	-3.531	-3.581 ± 0.010
84	6.906	615.5	1.133	-3.344	-3.376 ± 0.025

[a]Ref. 331.

[b]Interpolated to even wt. % H_2SO_4 values to match available data.

[c]$k_{plateau}$ = 44.50 X 10^{-5} s^{-1} subtracted from k_{obs}.

Table A3.18 Decomposition of 1-Me,t-Bu and 1-Me,$PhCH_2$ in aqueous sulfuric acid at 20.0°C.[a]

				1-Me,t-Bu		1-Me,$PhCH_3$	
$\%H_2SO_4$	$-H_o$[b]	X[c]	$\log C_{H+}$[c]	$10^5 k_{obs}/s^{-1}$	$5+\log k-\log C_{H+}$	$10^5 k_{obs}/s^{-1}$	$5+\log k-\log C_{H+}$
14.22	0.606			74.1 ± 0.3		238 ± 2	
25.38	1.324			58.5 ± 0.2		164 ± 2	
35.33	2.050			36.1 ± 0.1		97.8 ± 0.9	
42.64	2.600			26.6 ± 0.1		76.7 ± 1.2	
60.37	4.420	3.277	1.036	64.7 ± 1.5	0.775[d]	98.9 ± 0.5	0.959[e]
62.70	4.708	3.528	1.054	136.7 ± 0.3	1.082	207 ± 2	1.262
64.39	4.927	3.718	1.065	249.4 ± 2.0	1.404		
66.26	5.181	3.923	1.078	410 ± 21	1.535	766 ± 4	1.806
67.84	5.402	4.161	1.086	847 ± 42	1.842	1508 ± 10	2.092
69.23	5.602	4.355	1.093	1300 ± 50	2.021	2850 ± 50	2.362
70.56	5.795	4.526	1.110	2760 ± 100	2.341	5120 ± 100	2.609

[a] X and log C_{H+} values only given for mixtures in which acid catalysed decomposition occurs. All rate constants from single runs, except for 1-Me,t-Bu above 60%, where triplicates were averaged.

[b] At 20.0°, interpolated from data in ref. 349.

[c] Ref. 331.

[d] The data in this column give $m^* = 1.20 \pm 0.05$, $pK_{BH+} - \log k_d = -8.14 \pm 0.20$, cc = 0.996.

[e] The data in this column give $m^* = 1.32 \pm 0.02$, $pK_{BH+} - \log k_d = -8.38 \pm 0.06$, cc = 0.9997.

Table A3.19 Substituent effects in 63% sulfuric acid.

R_1	R_2	$10^5 k_{obs}/s^{-1}$ [a]	Solvent KIE [b]
CH_3	CH_3	45.0 ± 0.2	1.27 ± 0.02
CH_3	CH_3CH_2	40.3 ± 0.2	
CH_3	$CH_3CH_2CH_2$	43.3 ± 0.2 [c]	
CH_3	$(CH_3)_2CHCH_2$	53.4 ± 0.8 [c]	1.11 ± 0.02
CH_3	$(CH_3)_2CH$	34.6 ± 0.1	
$(CH_3)_2CH$	$(CH_3)_2CH$	35.24± 0.25	1.02 ± 0.02
CH_3	$PhCH_2$	207.0 ± 2.3	0.616 ± 0.010
$PhCH_2$	$PhCH_2$	213 ± 4	
CH_3	$(CH_3)_3C$	136.7 ± 0.3 [d]	0.649 ± 0.003

[a] Single run only, except where noted. Temperature = 20.0 ± 0.1°C.
[b] Ratio of $k(H_2O/H_2SO_4)/k(D_2O/D_2SO_4)$ at $[L_2SO_4]$ = 9.72 M.
[c] Average of duplicates.
[d] Average of triplicates.

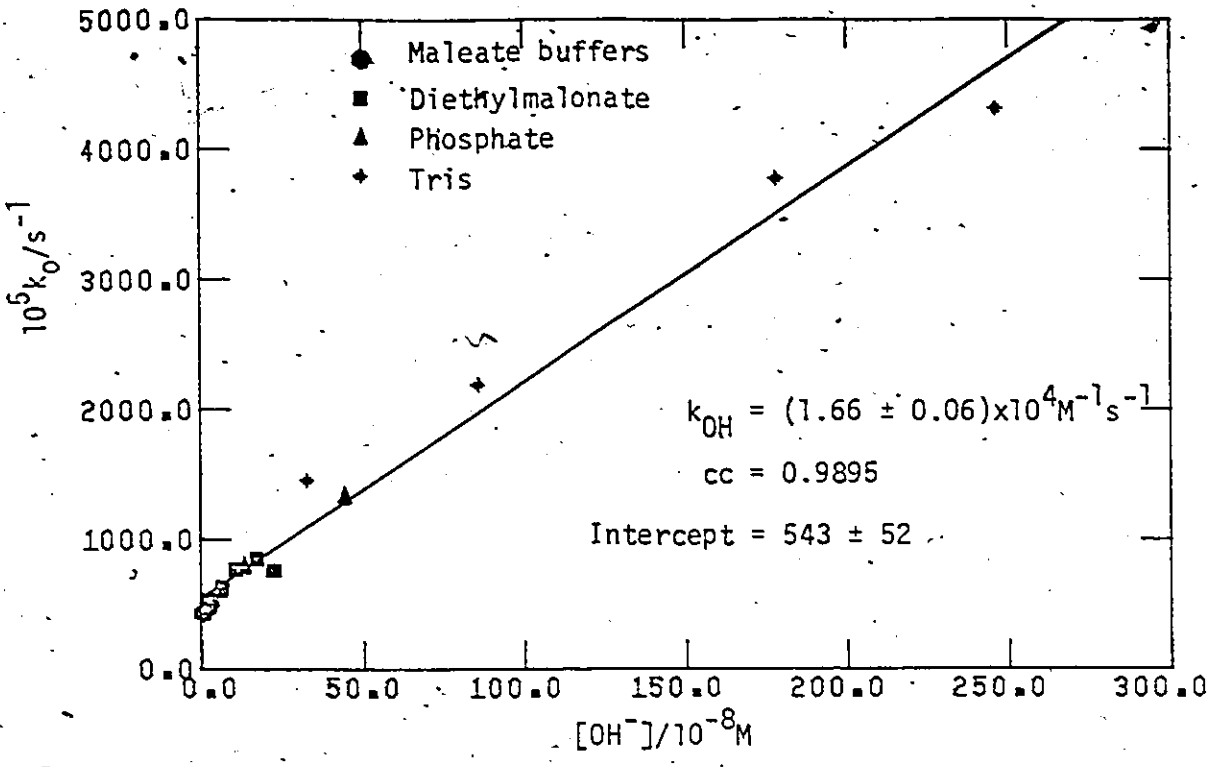

Figure A3.1 Hydroxide ion buffer catalytic constant.

Figure A3.2 Tris(hydroxymethyl)aminomethane buffer catalytic constant.

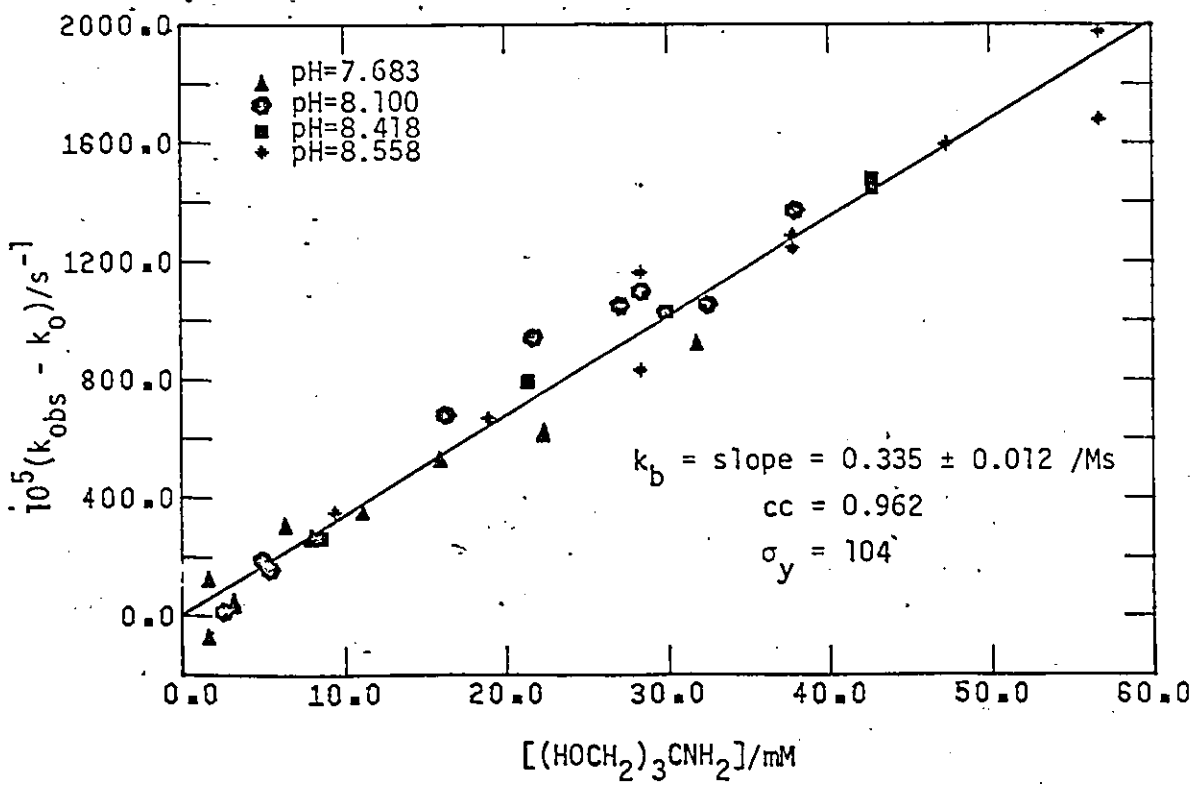

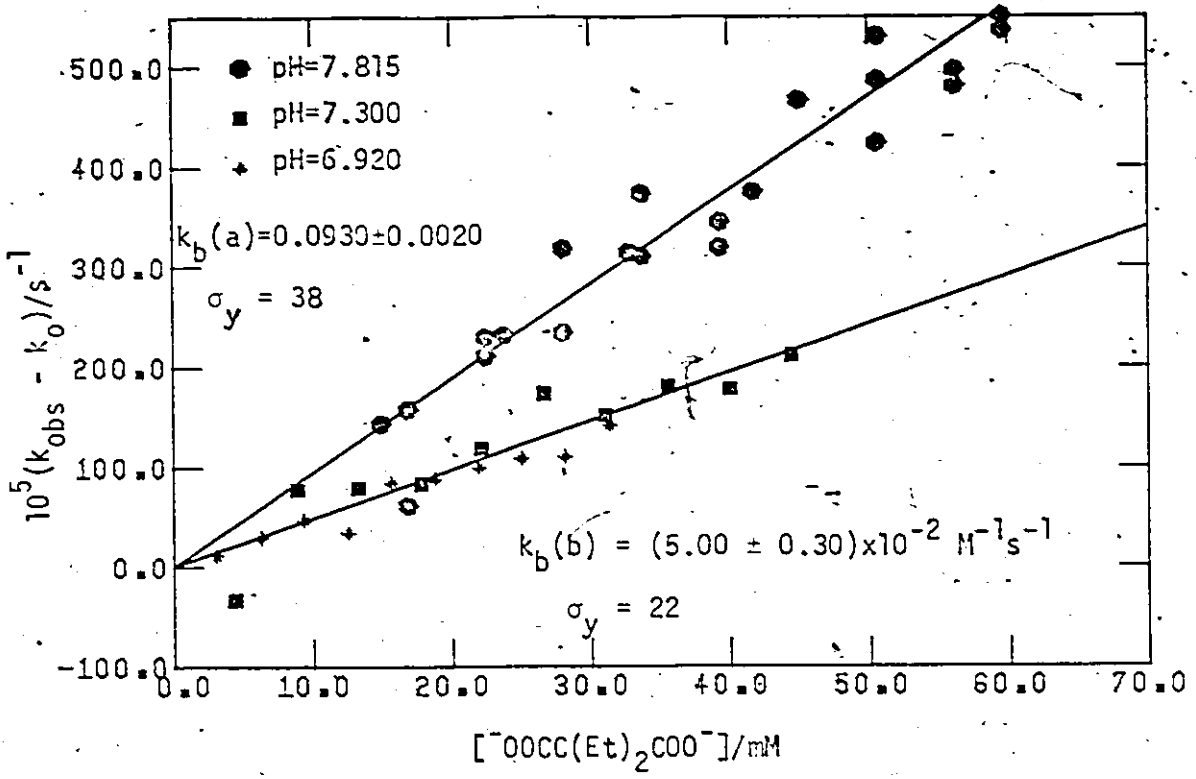

Figure A3.3 Diethylmalonate dianion buffer catalytic constant.

Figure A3.4 Hydrogen phosphate dianion buffer catalytic constant.

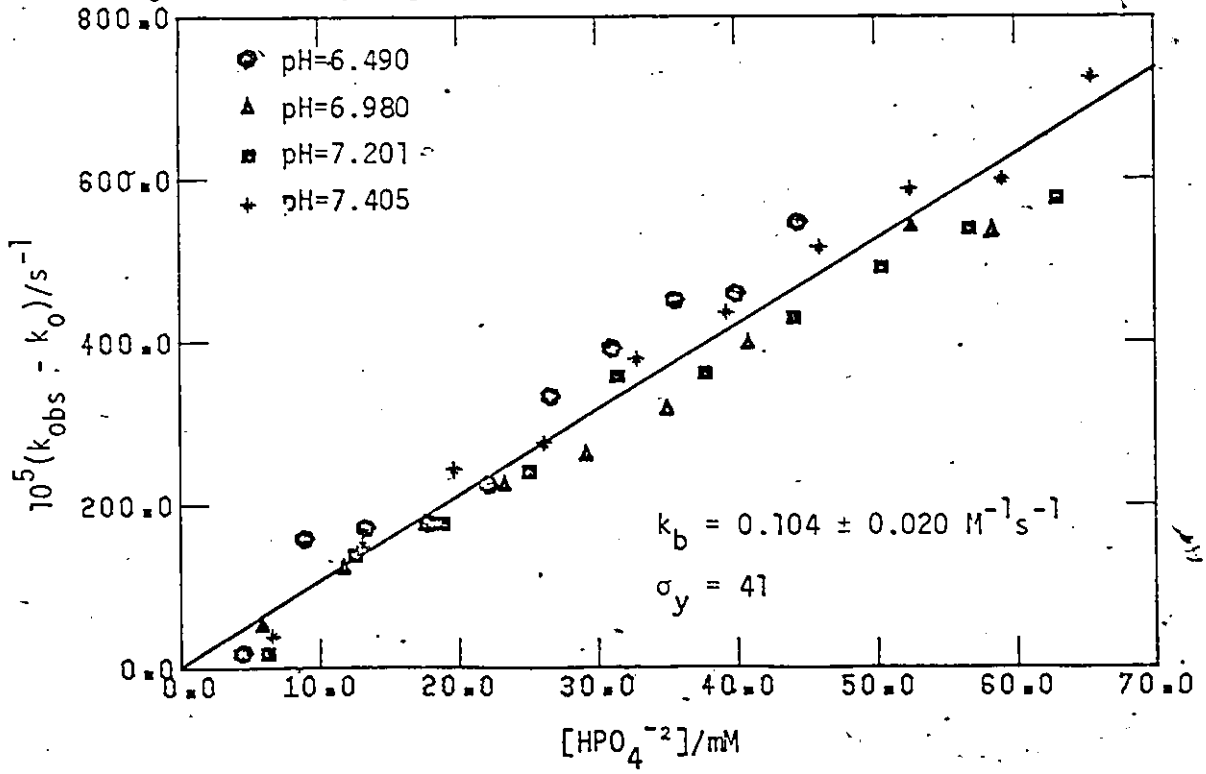

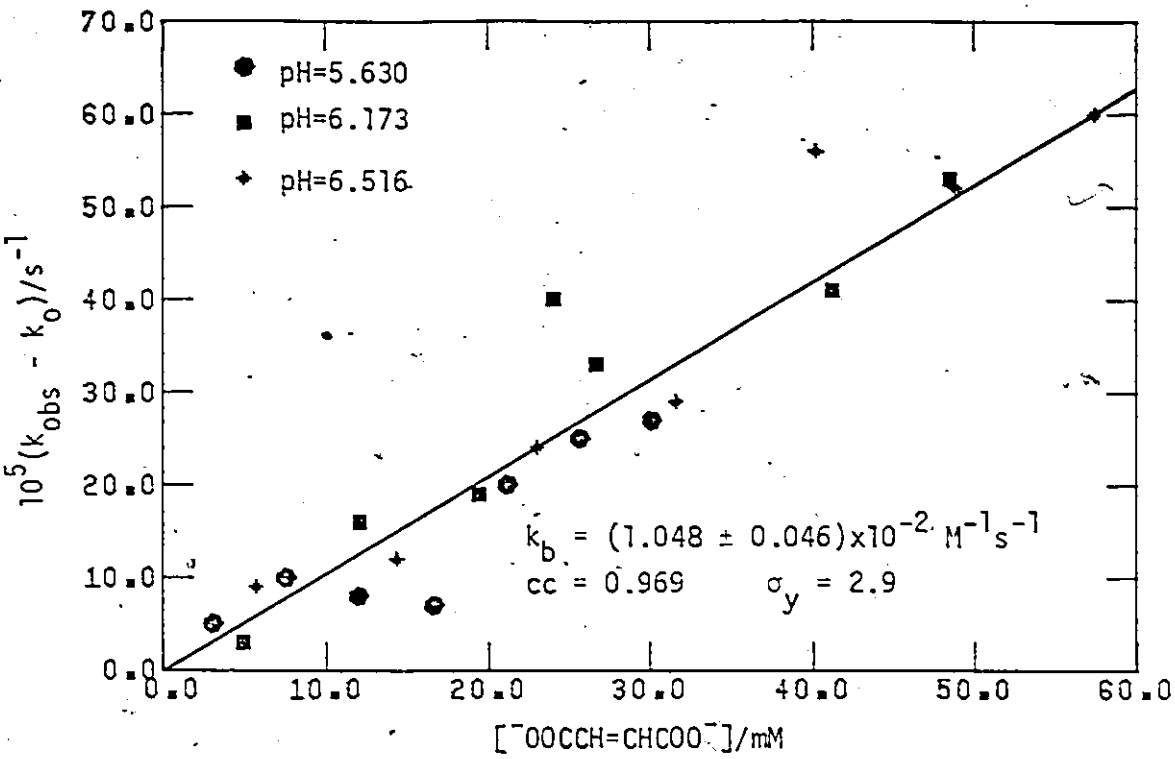

Figure A3.5 Maleate dianion buffer catalytic constant.

Figure A3.6 Acetate ion buffer catalytic constant.

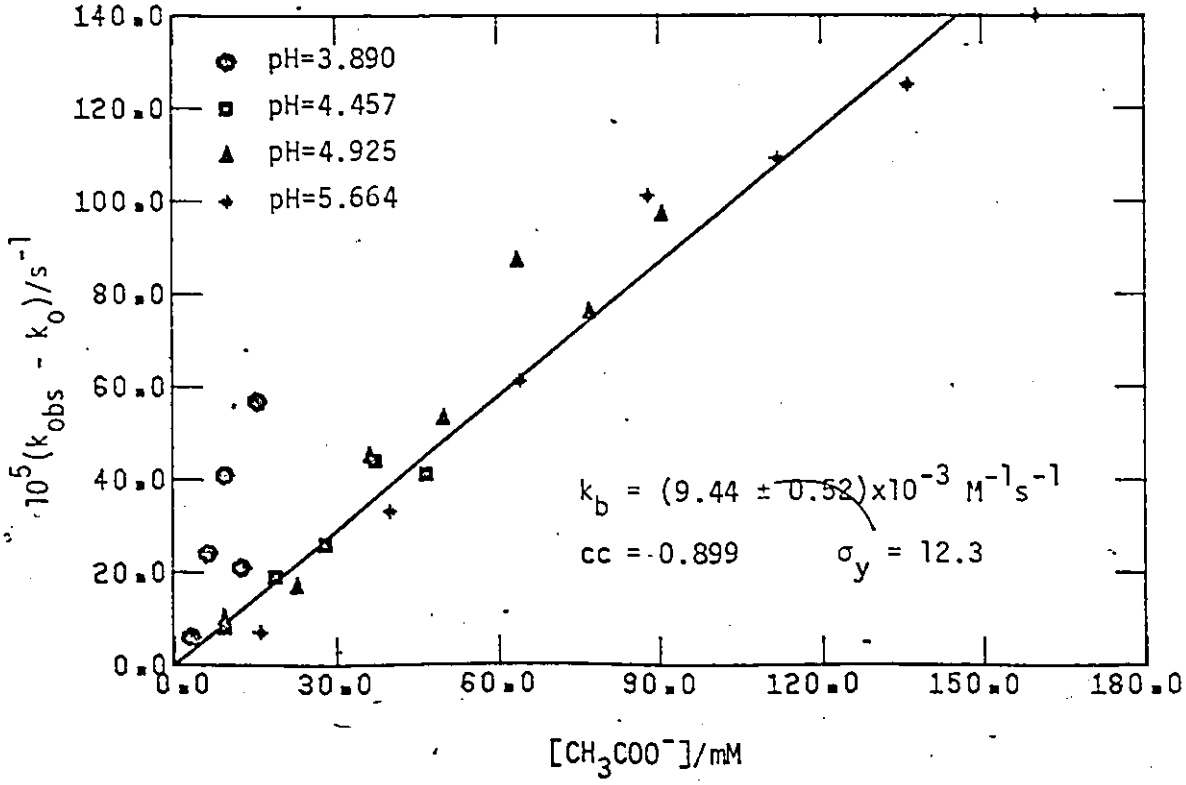

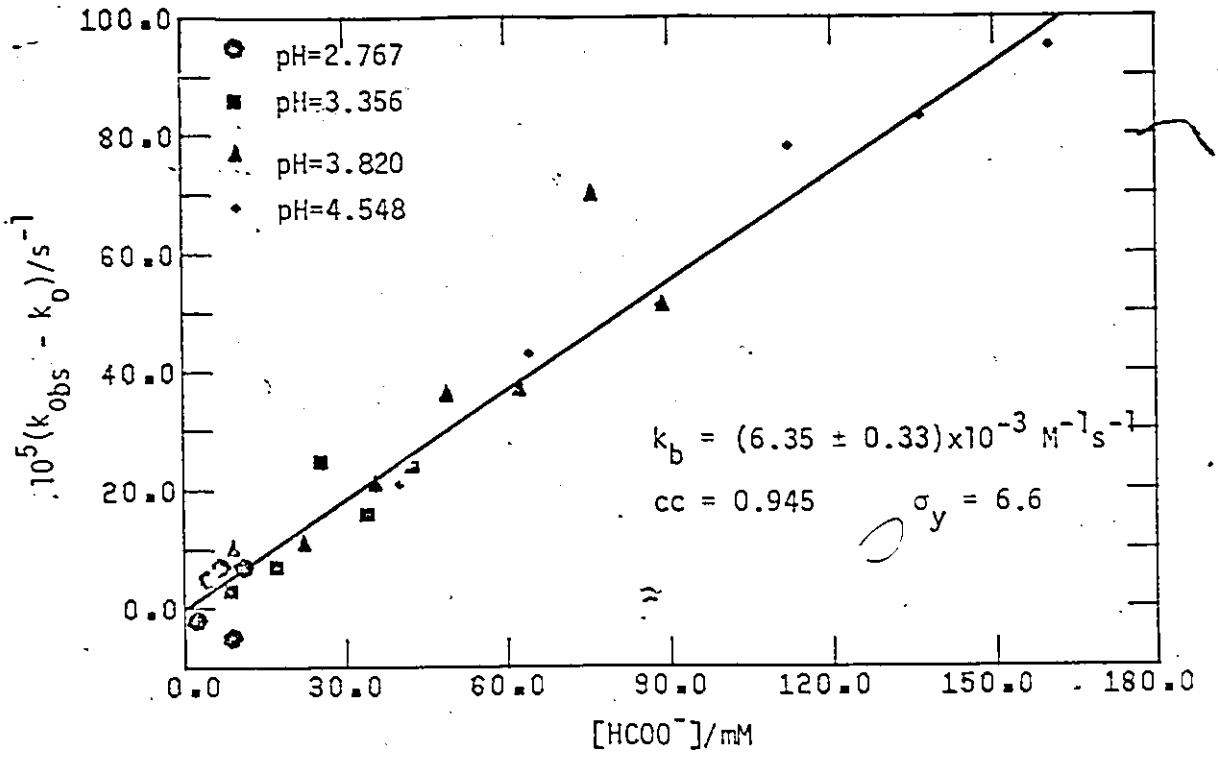

Figure A3.7 Formate anion buffer catalytic constant.

Figure A3.8 Apparent order in water for hydrolysis of 1-$(PhCH_2)_2$ in aqueous DMF (0.200 M HCl). Attempted extrapolation to pure water.

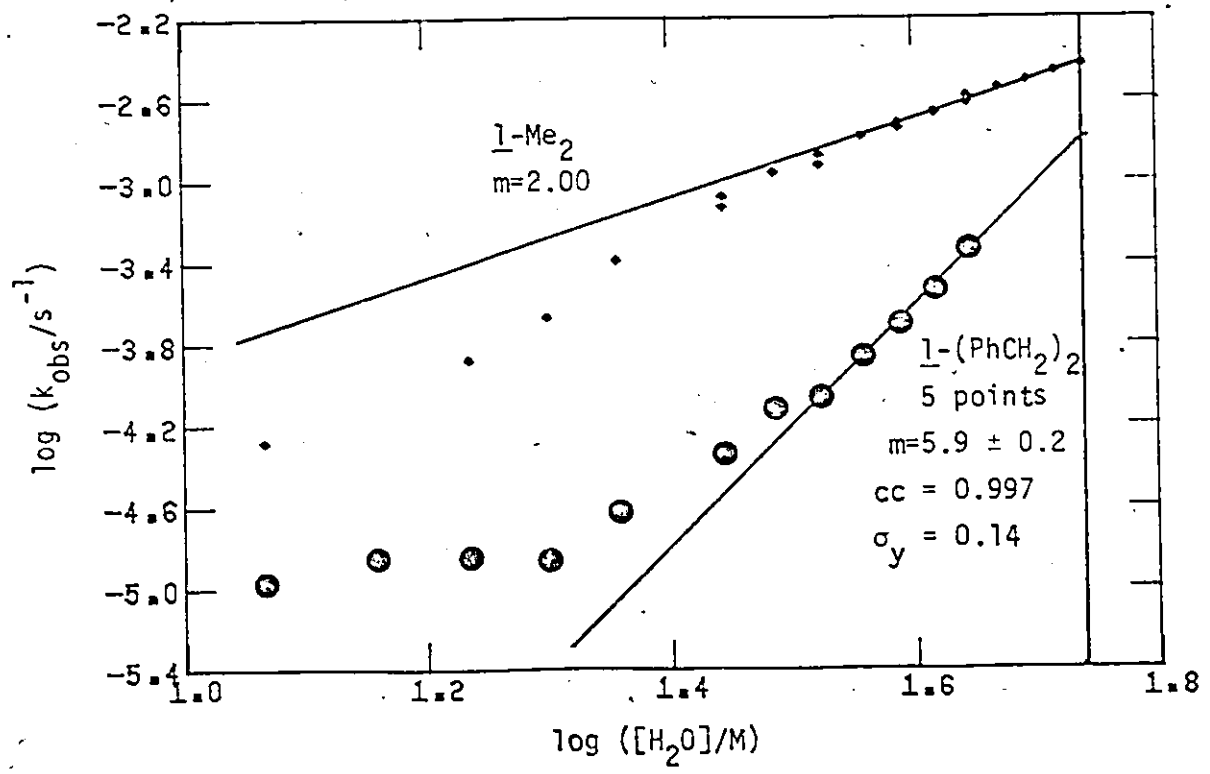

REFERENCES

1. S. Patai, Ed. The Chemistry of Diazonium and Diazo Groups. Wiley Interscience. New York, N.Y. (1978).
2. G.W. Cowell and A. Ledwith. Quart. Revs. Chem. Soc. 24, 119 (1970).
3. M. Regitz. Synthesis, 71 (1972).
4. E. Heilbronner and H.D. Martin. Chem. Ber. 106, 3376 (1973).
5. M. Regitz, I.K. Korobitsyna, and L.L. Rodina. Method. Chim. 6, 205 (1975).
6. M. Regitz. Diazoalkanes: Properties and Synthesis. Georg Thieme Pub. Suttgart, Germany (1977).
7. M. Jones, Jr., Ed. Carbenes. Wiley Interscience. New York, N.Y. (1973).
8. R. Fields, M.S. Gibson, and G. Holt. in Rodd's Chemistry of Carbon Compounds, 2nd Ed. Vol 1. Ed. M.F. Ansell. Elsevier Pub. Amersterdam, Netherlands (1975), Part A-B, Suppl., p. 125-50.
9. J.B. Moffat. J. Phys. Chem. 82, 1083 (1978).
10. R.G. Lawler. Accts. Chem. Res. 5, 25 (1972).
11. A.R. Lepley and G.L. Closs. Chemically Induced Magnetic Polarization. John Wiley and Sons. New York, N.Y. (1973).
12. D. Bethell and M.R. Brinkman. Adv. Phys. Org. Chem. 10, 53 (1973).
13. P.G. Frith and K.A. McLauchlan. Nuc. Mag. Res. 3, 378 (1974).
14. G.L. Closs. Adv. Mag. Res. 7, 157 (1974).
15. C. Richard and P. Granger. Chemically Induced Dynamic Nuclear and Electron Polarization - CIDNP and CIDEP. NMR Basic Principles

and Progress. Vol. 8. Ed. P. Diehl, E. Fluck, and R. Kosfeld. Springer Verlag. New York, N.Y. (1974).

16. R. Kaptein. Adv. Free-Rad. Chem. 5, 319 (1975).
17. H.D. Roth. Accts. Chem. Res. 10, 85 (1977).
18. Chemically Induced Magnetic Polarization. Proceedings of the NATO Advanced Study Institutes held at Sogesta, Urbino, Italy, April 1977. Ed. L.T. Muus, P.W. Atkins, K.A. McLauchlan and J.B. Pedersen. D. Reidel Publishing Co. Boston, Mass. (1977).
19. J.H. Freed and J.B. Pedersen. Adv. Mag. Res. 8, 1 (1976).
20. R. Kaptein. J. Chem. Soc. Chem. Commun., 732 (1971).
21. G.L. Closs and C.E. Doubleday. J. Am. Chem. Soc. 95, 2735 (1973).
22. G.L. Closs and C.E. Doubleday. J. Am. Chem. Soc. 94, 9248 (1972).
23. R. Kaptein, R. Freeman and H.D.W. Hill. Chem. Phys. Lett. 26, 104 (1974).
24. D.W. Turner, A.D. Baker, C. Baker, and C.R. Brundle. High Resolution Molecular Photoelectron Spectroscopy. John Wiley and Sons. New York, N.Y. (1970).
25. D.W. Turner. Ann. Rev. Phys. Chem. 21, 107 (1970)
26. C.E. Brion. Recent Advances in Electron Spectroscopy. MTP International Review of Science. Butterworths, London, U.K. (1971).
27. A.D. Baker. Accts. Chem. Res. 3, 17 (1970).
28. S.D. Worley. Chem. Revs. 71, 295 (1971).
29. T.A. Carlson. Ann. Rev. Phys. Chem. 26, 211 (1975).
30. J.W. Rabalais. Principles of Ultraviolet Photoelectron Spectros-

copy. Wiley-Interscience. New York, N.Y. (1977).

31. K. Siegbahn, D.A. Allison, and J. Allison. Handbook of Spectroscopy. Ed. J.W. Robinson. Vol 1, p. 258-749. CRC Press, Cleveland, Ohio (1974).

32. P. Carlier, R. Hernandez, P. Masclet, and G. Mouvier. J. Electron Spectrosc. Relat. Phenom. 5, 1103 (1974).

33. P. Masclet and G. Mouvier. J. Electron. Spectrosc. Relat. Phenom. 14, 77 (1978).

34. D.C. Frost, S.T. Lee, C.A. McDowell, and N.P.C. Westwood. J. Chem. Phys. 64, 4719 (1976).

35. F. Brogli, W. Eberbach, E. Haselbach, E. Heilbronner, V. Hornung, and D.M. Lemal. Helv. Chim. Acta, 56, 1933 (1973).

36. K.N. Houk, Y.-M. Chang, and P.S. Engel. J. Am. Chem. Soc. 97, 1824 (1975).

37. K.N. Houk, L.N. Domelsmith, J.W. Timberlake, and S. Szilagyi. Chem. Phys. Lett. 48, 471 (1977).

38. R.J. Boyd, J.C.G. Bünzli, and J.P. Snyder. J. Am. Chem. Soc. 98, 2398 (1976).

39. W.L. Jorgensen and L. Salem. The Organic Chemist's Book of Orbitals. Academic Press. New York, N.Y. (1973).

40. J.A. Pople and D.L. Beveridge. Approximate Molecular Orbital Theory. McGraw-Hill. New York, N.Y. (1970).

41. W.H. Miller, H.F. Schaefer III, B.J. Berne, and G.A. Segal, Eds. Modern Theoretical Chemistry. Vols 1-8. Plenum Press. New York, N.Y. (1977).

42. K. Fukui. Topics in Current Chemistry 16, 1 (1970).

43. T.L. Gilchrist and R.C. Storr. Organic Reactions and Orbital Symmetry. Cambridge University Press. London, U.K. (1972).

44. I. Fleming. Frontier Orbitals and Organic Chemical Reactions. Wiley-Interscience. London, U.K. (1976).

45. K.N. Houk in Pericyclic Reactions. Vol 2. Ed. A.P. Marchand and R.E. Lehr. Academic Press. New York, N.Y. (1977), p. 181.

46. K. Fukui and H. Fujimoto. in Chemical Reactivity and Reaction Paths. Ed. G. Klopman. Wiley-Interscience. New York, N.Y. (1974), p. 23.

47. G. Klopman, ref. 46, p. 55.

48. K. Fukui. Accts. Chem. Res. 4, 57 (1971).

49. K.N. Houk. Accts. Chem. Res. 8, 361 (1975).

50. M.J.S. Dewar and R.C. Dougherty. The PMO Theory of Organic Chemistry. Plenum Press. New York, N.Y. (1975).

51. R.B. Woodward and R. Hoffmann. The Conservation of Orbital Symmetry. Verlag Chemie. Weinheim, Ger. (1970).

52. M.J.S. Dewar. Angew. Chem. Int. Ed. 10, 761 (1971).

53. H.E. Zimmerman. Accts. Chem. Res. 4, 272 (1971).

54. S. Inagaki, H. Fujimoto, and K. Fukui. J. Am. Chem. Soc. 98, 4693 (1976).

55. G. Klopman. J. Am. Chem. Soc. 90, 223 (1968).

56. R.G. Pearson. J. Am. Chem. Soc. 85, 3533 (1963).

57. R.G. Pearson and J. Songstad. J. Am. Chem. Soc. 89, 1827 (1967).

58. R. Sustmann. Pure and Appl. Chem. 40, 569 (1974).

59. K.N. Houk. J. Sims, R.E. Duke, R.W. Strozier, and J.K. George. J. Am. Chem. Soc. 95, 7287 (1973).

60. K.N. Houk, J. Sims, C.R. Watts, and L.J. Luskus. J. Am. Chem. Soc. 95, 7301 (1973).

61. J. Bastide, N. El Ghandour, and O. Henri-Rousseau. Tett. Lett., 4225 (1972); Bull. Soc. Chim. France, 2290 (1973).

62. J. Bastide and O. Henri-Rousseau. Bull. Soc. Chim. France, 2294 (1973); and 1037 (1974).

63. P. Caramella and K.N. Houk. J. Am. Chem. Soc. 98, 6397 (1976).

64. P. Caramella, R.W. Gandour, J.A. Hall, C.G. Deville, and K.N. Houk. J. Am. Chem. Soc. 99, 385 (1977).

65. R. Huisgen. Angew. Chem. Int. Ed. 2, 565 and 633 (1963).

66. R. Huisgen. J. Org. Chem. 33, 2291 (1968).

67. R. Huisgen. J. Org. Chem. 41, 403 (1976).

68. R.A. Firestone. J. Org. Chem. 33, 2285 (1968).

69. R.A. Firestone. J. Org. Chem. 37, 2181 (1972).

70. R.A. Firestone. Tetrahedron 33, 3009 (1977).

71. R.F.W. Bader. Mol. Phys. 3, 137 (1960).

72. R.F.W. Bader. Can. J. Chem. 40, 1164 (1962).

73. L. Salem. Chem. Phys. Lett. 3, 99 (1969).

74. L. Salem and J.S. Wright. J. Am. Chem. Soc. 91, 5947 (1969).

75. R.G. Pearson. J. Am. Chem. Soc. 91, 1252 (1969) and 94, 8287 (1972).

76. R.G. Pearson. Accts. Chem. Res. 4, 152 (1971).

77. C. Reichardt. Angew. Chem. Int. Ed. 18, 98 (1979) and 4, 29 (1965).

78. P.A. Chopard, R.F. Hudson, and R.W. Taft. J. Am. Chem. Soc. 99, 6027 (1977).

79. P.S. Engel, R.A. Hayes, L. Keifer, S. Szilagyi, and J. W. Timberlake. J. Am. Chem. Soc. 100, 1876 (1978).

80. A.F. Hegarty. in The Chemistry of the Hydrazo, Azo, and Azoxy Groups. S. Patai, Ed. Wiley Interscience. New York, N.Y. (1975), Vol 2, Chapter 16, p. 643.

81. P.S. Engel, J.L. Wood, J.A. Sweet, and J.L. Margrave. J. Am. Chem. Soc. 96, 2381 (1974).

82. P.S. Engel. J. Am. Chem. Soc. 98, 1972 (1976).

83. H. Wieland, H. Hove, and K. Borner. Justus Liebigs Ann. Chem. 446, 31 (1926).

84. R. Askani. Chem. Ber. 98, 2551 (1965).

85. H.C. Ramsperger, J. Am. Chem. Soc. 51, 2134 (1929).

86. R.J. Crawford and K. Takagi. J. Am. Chem. Soc. 94, 7406 (1972).

87. M.N. Ackermann, M.R. Hallmark, S.K. Hammond and A.N. Roe. Inorg. Chem. 11, 3076 (1972).

88. E.M. Kosower. Accts. Chem. Res. 4, 193 (1971).

89. C. Willis and R.A. Back. Can. J. Chem. 51, 3605 (1973).

90. N. Wiberg, G. Fischer, and H. Bachhuber. Chem. Ber. 107, 1456 (1974).

91. W.T. Evanochko and P.B. Shevlin. J. Am. Chem. Soc. 100, 6428 (1978).

92. R. Galland, A. Heesing, and B.-U. Kaiser. Justus Liebigs Ann. Chem., 97 (1976).

93. C. Willis, R.A. Back, J.M. Parsons, and J.G. Purdon. J. Am. Chem. Soc. 99, 4451 (1977).

94. A. Streitweiser, Jr., R.H. Jagow, R.C. Fahey, and S. Suzuki. J. Am. Chem. Soc. 80, 2326 (1958).

95. E.A. Halevi. Progr. Phys. Org. Chem. 1, 109 (1963).

96. L. Melander. Isotope Effects on Reaction Rates. Ronald Press, New York, N.Y. (1964).

97. C.J. Collins and N.S. Bowman. Isotope Effects in Chemical Reactions. ACS Monograph 167. Van Nostrand Reinhold Co. New York, N.Y. (1970).

98. S.E. Schepple. Chem. Revs. 72, 511 (1972).

99. R. Shaw. Ref. 80, Vol 1, Chapter 3, p. 53 (1975).

100. S.W. Benson, F.R. Cruickshank, D.M. Golden, G.R. Haugen, H.E. O'Neal, A.S. Rodgers, R. Shaw, and R. Walsh. Chem. Revs. 69, 279 (1969).

101. S.W. Benson and H.E. O'Neal. Nat. Stand. Ref. Data Ser., Nat. Bur. Stand., No. 21, 31 (1970).

102. S.W. Benson. Thermochemical Kinetics. Wiley-Interscience. New York, N.Y. (1976).

103. S. Seltzer and S.G. Mylonakis. J. Am. Chem. Soc. 89, 6584 (1967).

104. S.E. Schepple, P.L. Grizzle, and D.W. Miller. J. Am. Chem. Soc. 97, 6165 (1975).

105. S. Seltzer. J. Am. Chem. Soc. 83, 2625 (1961) and 85, 14 (1963).

106. S.E. Schepple and S. Seltzer. J. Am. Chem. Soc. 90, 358 (1968).

107. S.E. Schepple, W.H. Rapp, D.W. Miller, D. Wright, and T. Marriott. J. Am. Chem. Soc. 94, 539 (1972).

108. S.G. Mylonakis and S. Seltzer. J. Am. Chem. Soc. 90, 5487 (1968).

109. S. Seltzer and F.T. Dunne. J. Am. Chem. Soc. 87, 2628 (1965).

110. H.E. Zimmerman, R.J. Böttcher, N.E. Bühler, G.E. Keck, and M.G.

Steinmetz. J. Am. Chem. Soc. 98, 7680 (1976).

111. S.G. Cohen and C.H. Wang. J. Am. Chem. Soc. 77, 3628 (1955).

112. C.G. Overberger and A.V. DiGuilio. J. Am. Chem. Soc. 81, 2154 (1959).

113. C. Steel and K.J. Laidler. J. Chem. Phys. 34, 1827 (1961).

114. B.K. Bandlish, A.W. Garner, M.L. Hodges, and J.W. Timberlake. J. Am. Chem. Soc. 97, 5856 (1975).

115. P.S. Engel and D.J. Bishop. J. Am. Chem. Soc. 97, 6754 (1975).

116. A. Tsolis, S.G. Mylonakis, M.T. Nieh, and S. Seltzer. J. Am. Chem. Soc. 94, 829 (1972).

117. K.R. Kopecky and T. Gillan. Can. J. Chem. 47, 2371 (1969).

118. F.D. Greene, M.A. Berwick, and J.C. Stowell. J. Am. Chem. Soc. 92 867 (1970).

119. K.R. Kopecky, T.W. Mojelsky, T. Gillan, J.A. Barry, and J.A.L. Sastre. Can. J. Chem. 55, 1001 (1977).

120. K.R. Kopecky, P.M. Pope, and J.A.L. Sastre. Can. J. Chem. 54, 2639 (1976).

121. S. Dincturk, R.A. Jackson, and M. Townson. J. Chem. Soc. Chem. Commun., 172 (1979).

122. A. Ohno and Y. Ohnishi. Tett. Lett., 4405 (1969).

123. J. W. Timberlake and M.L. Hodges. Tett. Lett., 4147 (1970).

124. J.W. Timberlake, A.W. Garner, and M.L. Hodges. Tett. Lett., 309 (1973).

125. R.C. Petersen, J.H. Markgraf, and S.D. Ross. J. Am. Chem. Soc. 83, 3819 (1961).

126. W.A. Pryor and K. Smith. J. Am. Chem. Soc. 89, 1741 (1967) and

92, 5403 (1970).

127. R.A. Johnson and S. Seltzer. J. Am. Chem. Soc. 95, 938 (1973).

128. R.C. Neuman, Jr. Accts. Chem. Res. 5, 381 (1972).

129. R.C. Neuman, Jr. and R.J. Bussey. J. Am. Chem. Soc. 92, 2440 (1970).

130. G.L. Closs and A.D. Trifunac. J. Am. Chem. Soc. 91, 4554 (1969) and 92, 2186 (1970).

131. K.G. Seifert and F. Gerhardt. Tett. Lett., 829 (1974).

132. N.A. Porter, G.R. Dubay, and J.G. Green. J. Am. Chem. Soc. 100, 920 (1978).

133. R.J. Drewer, Ref. 80 Vol 2, Chapter 20, p. 935 (1975).

134. P.S. Engel and C. Steel. Accts. Chem. Res. 6, 275 (1973).

135. N.A. Porter, L.J. Marnett, C.H. Lochmüller, G.L. Closs and M. Shobataki. J. Am. Chem. Soc. 94, 3664 (1972).

136. N.A. Porter and M.O. Funk. J. Chem. Soc. Chem. Commun., 263 (1973).

137. N.A. Porter and L.J. Marnett. J. Am. Chem. Soc. 95, 4361 (1973).

138. N.A. Porter, M.E. Landis, and L.J. Marnett. J. Am. Chem. Soc. 93, 795 (1971).

139. N.A. Porter and P.M. Iloff. J. Chem. Soc. Chem. Commun., 1575 (1971).

140. N.A. Porter, J.G. Green, and G.R. Dubay. Tett. Lett., 3363 (1975).

141. J.G. Green, G.R. Dubay, and N.A. Porter. J. Am. Chem. Soc. 99, 1264 (1977).

142. J.M. Howell and L.J. Kirschenbaum. J. Am. Chem. Soc. 98, 877 (1976).

143. P. Haberfield, P.M. Block, and M.S. Lux. J. Am. Chem. Soc. 97,

5804 (1975).

144. T. Mill and R.S. Stringham. Tett. Lett., 1853 (1969).

145. A. Schulz and C. Ruchardt. Tett. Lett., 3883 (1976).

146. M.N. Ackermann, N.C. Craig, R.R. Isberg, D.M. Lauler, R.A. MacPhail, and W.G. Young. J. Am. Chem. Soc. 99, 1661 (1977).

147. R.C. Weast, Ed. Handbook of Chemistry and Physics. 51 st. ed. CRC Press. Cleveland, Ohio. (1970), p. E-70.

148. F. Arndt, E. Milde, and G. Eckert. Chem. Ber. 56, 1976 (1923).

149. R. Stolle and W. Reichert. J. Prakt. Chem. 123, 82 (1929).

150. E.I. Fedetova, R.Y. Khvilivitskii, and I.I. Zmachinskaya. Chem. Abstr. 50, 8461d (1956).

151. V. Malatesta and K.U. Ingold. Tett. Lett., 3311 (1973).

152. P. Gray and J.C.J. Thynne. Nature (London) 191, 1357 (1961).

153. M.J. Perkins and B.P. Roberts. J. Chem. Soc. Perkin II, 297 (1974).

154. D.Y. Curtin and T.C. Miller. J. Org. Chem. 25, 885 (1960).

155. J.E. Leffler and W.B. Bond. J. Am. Chem. Soc. 78, 335 (1956).

156. D. Mackay, V.F. Marx, and W.A. Waters. J. Chem. Soc. C, 4793 (1964).

157. D.E. Zabel and W.S. Trahanovsky. J. Org. Chem. 37, 2413 (1972).

158. J.E. Herweh and R.M. Fantazier. J. Org. Chem. 39, 786 (1974).

159. P.L. Southwick, N. Latif, J. Kliganowicz, and J.G. O'Connor. Tett. Lett., 1767 (1970).

160. W. Nagata and S. Kamata. J. Chem. Soc. C, 540 (1970).

161. S. Hünig and J. Kramer. Angew. Chem. Int. Ed. 7, 943 (1968).

162. S. Hünig and G. Büttner. Angew. Chem. Int. Ed. 8, 451 (1969).

163. G. Büttner and S. Hünig. Chem. Ber. 104, 1088 and 1104 (1971).

164. G. Büttner, J. Cramer, L. Geldern, and S. Hünig. Chem. Ber. 104, 1118 (1971).

165. J.P. Freeman and C.P. Rathjen. J. Org. Chem. 37, 1686 (1972).

166. P. Knittel. Ph.D. Thesis. McMaster University, Hamilton, Ont. (1975).

167. P. Knittel and J. Warkentin. Can. J. Chem. 53, 2275 (1975).

168. P. Knittel and J. Warkentin. Can. J. Chem. 54, 1341 (1976).

169. D.W.K. Yeung. Ph.D. Thesis. McMaster University, Hamilton, Ont. (1977).

170. D.W.K. Yeung and J. Warkentin. Can. J. Chem. 54, 1345 and 1349 (1976).

171. R.C. Neuman, Jr. and E.W. Ertley, J. Am. Chem. Soc. 97, 3130 (1975).

172. R. Bonneau, J. Joussot-Dubien, L. Salem, and A.Y. Yarwood. J. Am. Chem. Soc. 98, 4329 (1976).

173. R.J. Crawford, D.M. Cameron, and H. Tokunaga. Can. J. Chem. 52, 4025 (1974).

174. D.E. McGreer, N.W.K. Chiu, M.G. Vinje, and K.C.K. Wong. Can. J. Chem. 43, 1407 (1965).

175. H. Olsen and J.P. Snyder. J. Am. Chem. Soc. 100, 285 (1978).

176. M.T.H. Liu and B.M. Jennings. J. Am. Chem. Soc. 98, 6416 (1976).

177. M.T.H. Liu and K. Ramakrishnan. J. Org. Chem. 42, 3451 (1977).

178. R.D. Harcourt and W. Roso. Can. J. Chem. 56, 1093 (1978).

179. N. Rieber, J. Alberts, J.A. Lipsky, and D.M. Lemal. J. Am. Chem. Soc. 91, 5668 (1969).

180. F.D. Greene and K.E. Gilbert. J. Org. Chem. 40, 1409 (1975).

181. D.K. White and F.D. Greene. J. Am. Chem. Soc. 100, 6760 (1978).

182. N.J. Turro, P. Lechtken, N.E. Schore, G. Schuster, H.-C. Steinmetzer, and A. Yekta. Accts. Chem. Res. 7, 97 (1974).

183. D.S. Noyce and E.H. Banitt. J. Org. Chem. 31, 4043 (1966).

184. M.U.S. Sultanbawa. Tett. Lett., 4569 (1968).

185. L.A. Paquette, M.J. Wyvratt, and G.R. Allen. J. Am. Chem. Soc. 92, 1763 (1970).

186. R.J. Crawford and A. Mishra. J. Am. Chem. Soc. 88, 3963 (1966).

187. P.S. Engel and L. Shen. Can. J. Chem. 52, 4040 (1974).

188. R.J. Crawford and H. Tokunaga. Can. J. Chem. 52, 4033 (1974).

189. O.P. Strausz, J.W. Lowa, and H.E. Gunning in Comprehensive Chemical Kinetics. Vol. 5. Ed. C.H. Bamford and C.F.H. Tipper. Elsevier. Amsterdam, Neth. (1972) Chapter 5, p. 566.

190. R.J. Crawford and D.M. Cameron. Can. J. Chem. 45, 691 (1967).

191. R.J. Crawford and M. Ohno. Can. J. Chem. 52, 3134 (1974).

192. M. Schneider and H. Strohacker. Tetrahedron 32, 619 (1976).

193. J.W. Timberlake and B.K. Bandlish. Tett. Lett., 1393 (1971).

194. T.C. Clarke, L.A. Wendling, and R.G. Bergman. J. Am. Chem. Soc. 99, 2740 (1977).

195. R.J. Crawford, H. Tokunaga, L.M.H.C. Schrijver, and J.C. Godard. Can. J. Chem. 56, 998 (1976).

196. R. Huisgen. Accts. Chem. Res. 10, 117 (1977).

197. D.E. McGreer, R.S. McDaniel, and M.G. Vinje. Can. J. Chem. 43, 1389 (1965).

198. B.H. Al-Sader and R.J. Crawford. Can. J. Chem. 46, 3301 (1968).

199. D.E. McGreer and I.M.E. Masters. Can. J. Chem. 47, 3975 (1969).

200. D.W. Setser and B.S. Rabinovitch. J. Am. Chem. Soc. 86, 564 (1964).

201. A.P. Marchand and R.E. Lehr. Pericyclic Reactions. Vols 1 and 2. Academic Press. New York, N.Y. (1977).

202. K. Tortschanoff, H. Kisch, and O.E. Polansky. Justus Liebigs Annalen , 449 (1975).

203. R. Danion-Bougot and R. Carrie. Bull. Soc. Chim. Fr., 313 (1969).

204. R.W. Alder, R. Baker, and J.M. Brown. Mechanism in Organic Chemistry. Wiley Interscience. New York, N.Y. (1971).

205. E.L. Allred and C.R. Flynn. J. Am. Chem. Soc. 94, 5891 (1972).

206. E.L. Allred, B.K. Stevenson, and T.-C. Chou. J. Am. Chem. Soc. 101, 1181 (1979).

207. M. Schneider and B. Csacsko. Angew. Chem. Int. Ed. 16, 867 (1977).

208. M.P. Schneider and R.J. Crawford. Can. J. Chem. 48, 628 (1970).

209. P.B. Condit and R.G. Bergman. J. Chem. Soc. Chem. Commun., 4 (1971).

210. V. Georgian and N. Kundu. Chem. and Ind. (London), 1755 (1962).

211. G.L. Closs and W.A. Böll. J. Am. Chem. Soc. 85, 3904 (1963).

212. R. Anet and F.A.L. Anet. J. Am. Chem. Soc. 86, 525 (1964).

213. A.C. Day and M. Whiting. J. Chem. Soc. Chem. Commun., 292 (1965).

214. P.B. Dervan, T. Uyehara, and D.S. Santilli. J. Am. Chem. Soc. 101, 2069 (1979).

215. J.A. Berson, E. Petrillo, and P. Bickart. J. Am. Chem. Soc. 96, 636 (1974).

216. J.A. Berson, S.S. Olin, E.W. Petrillo, and P. Bickart. Tetrahedron 30, 1639 (1974).

217. P.B. Dervan and T. Uyehara. J. Am. Chem. Soc. 101, 2076 (1979).

218. D.M. Lemal and S.D. McGregor. J. Am. Chem. Soc. 88, 1335 (1966).

219. J.A. Berson and S.S. Olin. J. Am. Chem. Soc. 91, 777 (1969).

220. H. Kwart and K. King. Chem. Revs. 68, 415 (1968).

221. F. Arndt and B. Eistert. Chem. Ber. 61, 1118 (1928).

222. N. Shimizu and P.D. Bartlett. J. Am. Chem. Soc. 100, 4260 (1978).

223. F. Cordt, R.M. Frank, and D. Lenoir. Tett. Lett., 505 (1979).

224. M. Godfrey. J. Chem. Res. (S), 258 (1978).

225. L. Salem and C. Rowland. Angew. Chem. Int. Ed. 11, 92 (1972).

226. R. Huisgen. Accts. Chem. Res. 10, 199 (1977).

227. M.J.S. Dewar and S. Kirschner. J. Am. Chem. Soc. 96, 5244 (1974).

228. M.J.S. Dewar. Angew. Chem. Int. Ed. 10, 761 (1971).

229. M.J.S. Dewar, S. Olivella, and H.S. Rzepa. J. Am. Chem. Soc. 100, 5650 (1978).

230. R. Hoffmann, S. Swaminathan, B. Odell, and R. Gleiter. J. Am. Chem. Soc. 92, 7091 (1970).

231. R.W. Hoffmann and H.J. Luthardt. Chem. Ber. 101, 3861 (1968).

232. J. Buter, S. Wassenaar, and R.M. Kellog. J. Org. Chem. 37, 4045 (1972).

233. C.J. Michejda. Tett. Lett., 2281 (1968).

234. D.W.K. Yeung, G.A. MacAlpine, and J. Warkentin. J. Am. Chem. Soc. 100, 1962 (1978).

235. A. Schulz, N.T. Giac, and C. Ruchardt. Tett. Lett., 845 (1977).

236. M. Bekhazi. M.Sc. Thesis. McMaster University, Hamilton, Ontario (1979).

237. T. Kealy. J. Am. Chem. Soc. 84, 966 (1962).

238. R.A. Clement. J. Org. Chem. 27, 1115 (1962) and 25, 1724 (1960).

239. R.C. Cookson, S.S.H. Gilani, and I.D.R. Stevens. Tett. Lett., 615 (1962).

240. J.C. Stickler and W.H. Pirkle, J. Org. Chem. 31, 3444 (1966).

241. J.E. Herweh and R.M. Fantazier. Tett. Lett., 2101 (1973).

242. E.J. Corey and B.B. Snider. J. Org. Chem. 38, 3632 (1973).

243. A.B. Evnin, A.Y. Lam, J.J. Maherand, and J.J. Blyskal. Tett. Lett., 4497 (1969).

244. B.T. Gillis and R.A. Izydore. J. Org. Chem. 34, 3181 (1969).

245. B.T. Gillis and R. Weinkam. J. Org. Chem. 32, 3321 (1967).

246. E.M. Kosower, B. Pazhenchevsky, and E. Hershkowitz. J. Am. Chem. Soc. 100, 6516 (1978).

247. C.W. Rees and M. Yelland. J. Chem. Soc. Perkin I, 221 (1973).

248. R.H. Kent and J.-P. Anselme. Can. J. Chem. 46, 2322 (1968).

249. E.F. Ullman and E.A. Bartkus. Chem. Ind. (London), 93 (1962).

250. M. Rosenblum. J. Am. Chem. Soc. 82, 3797 (1960).

251. K.M. Ibne-Rasa and E. Koubek. J. Org. Chem. 28, 3240 (1963).

252. B.T. Gillis and J.G. Dain. J. Org. Chem. 36, 518 (1971).

253. M. Rosenblum, A. Longroy, M. Neveu, and C. Steel. J. Am. Chem. Soc. 87, 5716 (1965).

254. B. Fuchs, W.D. Kwalwasser, and M. Rosenblum. Israel. J. Chem. 13, 107 (1975).

255. D.H.R. Barton and B.J. Willis. J. Chem. Soc. Chem. Commun., 1225 (1970).

256. D. Daniil, G. Gauglitz, and H. Meier. Photochem. and Photobiol. 26, 225 (1977).

257. D. Daniil and H. Meier. J. Heterocyclic Chem. 13, 649 (1976).

258. D. Daniil and H. Meier. Tett. Lett., 3155 (1977).

259. S.L. Lee, A.M. Cameron, and J. Warkentin. Can. J. Chem. 50, 2326 (1972).

260. P.R. West. Ph.D. Thesis. McMaster University, Hamilton, Ontario (1967).

261. P.R. West and J. Warkentin. J. Org. Chem. 34, 3233 (1969).

262. A.M. Cameron. Ph.D. Thesis. McMaster University, Hamilton, Ontario (1972).

263 N.J. Turro, D.C. Neckers, P.A. Leermakers, D. Seldner, and P. D'Angelo. J. Am. Chem. Soc. 87, 4097 (1965).

264. J.B. Fulton. Ph.D. Thesis. McMaster University, Hamilton, Ontario (1978).

265. K. Ramakrishnan. Ph.D. Thesis. McMaster University, Hamilton, Ontario (1975).

266. K. Ramakrishnan, J.B. Fulton, and J. Warkentin. Tetrahedron 32, 2685 (1976).

267. L.M. Cabelkova-Taguchi. Ph.D. Thesis. McMaster University, Hamilton, Ontario (1977).

268. E.M. Kosower and T. Tsuji. J. Am. Chem. Soc. 93, 1992 (1971).

269. W.P. Jencks and J. Regenstein. in Handbook of Biochemistry. 2nd. Ed. H.A. Sober, Ed. Chemical Rubber Co., Cleveland, Ohio (1970), pp J187-J230.

270. E. Fahr and H. Lind. Angew. Chem. Int. Ed. 4, 372 (1966).

271. E. Pechhold. Ph.D. Thesis. Ohio State University (1968).

272. G. Koga, N. Koga, and J.-P. Anselme. Ref. 80, Vol 2, Chap. 19 (1975), especially pp 903-910.

273. R.W. Hoffmann. Chem. Ber. 97, 2772 (1964).

274. R.W. Hoffmann and G. Guhn. Chem. Ber. 100, 1474 (1967).

275. R.W. Hoffmann and K.R. Eicken. Chem. Ber. 100, 1465 (1967).

276. G. Fraenkel and E. Pechhold. Tett. Lett., 4821 (1969).

277. W.H. Urry, F.W. Stacey, E.S. Huyser, and O.O. Juveland. J. Am. Chem. Soc. 76, 450 (1954).

278. J.H. Hall and M. Wojciechowska. J. Org. Chem. 43, 4869 (1978).

279. H.B. Milne and W. Kilday. J. Org. Chem. 30, 64 (1965).

280. S.G. Cohen and J. Nicholson. J. Org. Chem. 30, 1162 (1965), and J. Am. Chem. Soc. 86, 3862 (19[illegible]

281. L.A. Carpino and E.G.S. Rundberg. J. Org. Chem. 34, 1717 (1969).

282. P.J. Kocienski. J.M. Ansell, and R.W. Ostrow. J. Org. Chem. 41, 3625 (1976).

283. P.J. Kocienski. J.M. Ansell, and B.E. Norcross. J. Org. Chem. 41, 3650 (1976).

284. O. Diels. Justus Liebigs' Ann. Chem. 429, 1 (1922).

285. R. Huisgen and F. Jakob. Justus Liebigs' Ann. Chem. 596, 37 (1954).

286. H. Bock, E. Baltin, and J. Kroner. Chem. Ber. 99, 3337 (1966).

287. E.M. Kosower and P.C. Huang. J. Am. Chem. Soc. 90, 2354 (1968).

288. C.V. King. J. Am. Chem. Soc. 62, 379 (1940).

289. C.V. King and J.J. Josephs. J. Am. Chem. Soc. 66, 767 (1944).

290. T. Koopmans. Physica 1, 104 (1934).

291. A. Prakash, C. Calvo, A.M. Cameron, and J. Warkentin. J. Cryst. Mol. Struct. 3, 71 (1973).

292. Tables of Interatomic Distances. Chemical Society. London, U.K. (1958).

293. G. Berthier and J. Serre, in the Chemistry of the Carbonyl Group. Ed. S. Patai. Interscience, New York, N.Y. (1970), Chapter 1.

294. E.M. Kosower. An Introduction to Physical Organic Chemistry. John Wiley and Sons. New York, N.Y. (1968), p 49.

295. N.L. Alpert, W.E. Keiser, and H.A. Szymanski. IR-Theory and Practice of Infrared Spectroscopy. Plenum Press. New York, N.Y. (1970).

296. J. Bernstein and I. Izak, J. Chem. Soc. Perkin II, 429 (1976) and refs cited therein.

297. R.K. Kakar, E.A. Rinehart, C.R. Quade, and T. Kojima. J. Chem. Phys. 52, 3803 (1970).

298. J.A. Pople, D.P. Santry, and G.A. Segal. J. Chem. Phys. 43, 5129 and 5135 (1965).

299. J.A. Pople and G.A. Segal. J. Chem. Phys. 44, 3289 (1966).

300. L. Salem. J. Am. Chem. Soc. 90, 543 and 553 (1968).

301. S.P. McGlynn and J.L. Meeks. J. Electron Spectrosc. Relat. Phenom. 8, 85 (1976).

302. A.D. Bain. M.Sc. Thesis. Department of Chemistry, University of British Columbia, Vancouver, B.C. (1972).

303. Sadtler Standard Grating Spectra. Sadtler Research Labs. Philadelphia, PA. (1972) (a) No. 25048; (b) No. 20236.

304. C.C. Price and J.M. Judge. Org. Syn. 45, 22 (1965).

305. V.A. Palm, U.L. Haldna, and A.J. Talvik. in The Chemistry of the Carbonyl Group. S. Patai, Ed. Wiley-Interscience. New York, N.Y. (1966), Chapter 9, p 421.

306. D.W. Davies. Chem. Phys. Lett. 2, 173 (1968).

307. D.C. Frost, F.G. Herring, C.A. McDowell, and I.A. Stenhouse. Chem. Phys. Lett. 4, 533 (1970).

308. E. Haselbach and A. Schmelzer. Helv. Chim. Acta. 54, 1575 (1971) and refs cited therein.

309. M.B. Robin. Higher Excited States of Polyatomic Molecules. Vol. 2. Academic Press. New York, N.Y. (1975) pp 68-75.

310. D.H. Williams and I. Fleming. Spectroscopic Methods in Organic Chemistry. McGraw-Hill. New York, N.Y. (1973).

311. I.L. Karle and J. Karle. J. Chem. Phys. 17, 1052 (1949).

312. G. Herzberg. Molecular Spectra and Molecular Structure. D. Van Nostrand Co. New York, N.Y. (1966).

313. G.A. MacAlpine and J. Warkentin. Can. J. Chem. 56, 308 (1978).

314. S.L. Lee, G.B. Gubelt, A.M. Cameron, and J. Warkentin. J. Chem. Soc. Chem. Commun., 1074 (1970).

315. T.H. Lowry and K.S. Richardson. Mechanism and Theory in Organic Chemistry. Harper and Row. New York, N.Y. (1976).

316. M.K. Karapet'yants and M.L. Karapet'yants. Thermodynamic Constants of Inorganic and Organic Compounds. Ann Arbor-Humphrey Science Pub. Ann Arbor, Mich. (1970).

317. Y. Yukawa and Y. Tsuno. Bull. Chem. Soc. Japan 32, 971 (1959).

318. F.W. McLafferty. Interpretation of Mass Spectra. 2nd Ed. W.A. Benjamin. Inc. Reading, Mass. (1973), p. 189.

319. M.J. Perona, P.C. Beadle, and D.M. Golden. Int. J. Chem. Kinet. 5, 495 (1973).

320. S.G. Cohen, S.J. Groszos, and D.B. Sparrow. J. Am. Chem. Soc. 72, 3947 (1950).

321. J.C. Martin and J.W. Timberlake. J. Am. Chem. Soc. 92, 978 (1970).

322. S.F. Nelson and P.D. Bartlett. J. Am. Chem. Soc. 88, 137 (1966).

323. R. Wheland and P.D. Bartlett. J. Am. Chem. Soc. 92, 6057 (1970).

324. G.S. Hammond. J. Am. Chem. Soc. 77, 334 (1955).

325. A.J. Duke and B.P. Stark. Extrusion Reactions. Pergammon Press. Oxford, U.K. (1967).

326. F.A. Cotton and G. Wilkinson. Advanced Inorganic Chemistry. 3rd Ed. Wiley-Interscience. New York, N.Y. (1972).

327. C. Wentrup. Tetrahedron 30, 1301 (1974).

328. R.J. Gillespie and T.E. Peel. J. Am. Chem. Soc. 95, 5173 (1973).

329. C.H. Rochester. Acidity Functions. Academic Press. N.Y. (1970).

330. K. Yates and R.A. McClelland. Prog. Phys. Org. Chem. 11, 323 (1974).

331. R.A. Cox and K. Yates. J. Am. Chem. Soc. 100, 3861 (1978), and supplemental information available from the Journal.

332. J.F. McGarrity and T. Smyth. J. Chem. Soc. Chem. Commun., 347 (1977).

333. J.N. Bronsted. Chem. Revs. 5, 322 (1928).

334. D.M. Bishop and K.J. Laidler. J. Chem. Phys. 42, 1688 (1965).

335. S.W. Benson. J. Am. Chem. Soc. 80, 5151 (1958).

336. D.R. Coulson. J. Am. Chem. Soc. 100, 2992 (1978).

337. E. Pollak and P. Pechukas. J. Am. Chem. Soc. 100, 2984 (1978).

338. Reference 147, p. D-122.

339. S.L. Johnson. Adv. Phys. Org. Chem. 5, 237 (1967).

340. M. Eigen. Angew. Chem. Int. Ed. 3, 1 (1964).

341. M. Eigen. Disc. Far. Soc. 39, 7 (1965).

342. K.C. Chao and R.A. Greenhorn. Thermodynamics of Fluids - an Introduction to Equilibrium Theory. Marcel Dekker Inc. New York, N.Y. (1975).

343. R. Haase. Physical Chemistry 1, 293 (1971).

344. A.G. Williamson. An Introduction to Non-Electrolyte Solutions. John Wiley and Sons Inc. New York, N.Y. (1967).

345. H. Chen and D.E. Irish. J. Phys. Chem. 75, 2672 (1971).

346. H.S. Gutowsky and A. Saika. J. Chem. Phys. 21, 1688 (1953).

347. Reference 147, p. F-7.

348. L.P. Hammett. Physical Organic Chemistry. McGraw-Hill, New York, N.Y. (1970), p. 271.

349. P. Tickle, A.G. Briggs, and J.M. Wilson. J. Chem. Soc. B., 65 (1970).

350. C.H. Bamford and C.F.H. Tipper. Comprehensive Chemical Kinetics. Vol.10. Ester Formation and Hydrolysis and Related Reactions. Elsevier Co., Amsterdam, Neth. (1972).

351. A. Skrabal and A. Zahorka. Monatsh. Chem. 53-54, 562 (1929).

352. M. Charton. J. Org. Chem. 44, 903 (1979).

353. L.S. Levitt and H.F. Widing. Progr. Phys. Org. Chem. 12, 119 (1976).

354. C.G. Screttas. J. Org. Chem. 44, 1471 (1979).

355. R.T. Morrison and R.N. Boyd. Organic Chemistry. 2nd Ed. Allyn and

Bacon Inc., Boston, Mass. (1966), p. 288-298.

356. M.L. Bender. Chem. Revs. 60, 53 (1960).

357. D. Samuel and B.L. Silver. Adv. Phys. Org. Chem. 3, 123 (1965).

358. W.G. Klemperer. Angew. Chem. Int. Ed. 17, 246 (1978).

359. H. Danh, H.-P. Schunke, and J. Temler. Helv. Chim. Acta. 55, 907 (1972).

360. D. Canet, C. Gouïon-Ginet, and J.P. Marchal. J. Mag. Res. 22, 537 (1976).

361. C. Delseth and J.-P. Kintzinger. Helv. Chim. Acta. 59, 466 (1976).

362. K. Pihlaja and E. Taskinen in Physical Methods in Heterocyclic Chemistry. Vol. 6. A.R. Katritzky, Ed. Academic Press. New York, N.Y. (1974) p. 210.

363. P. Deslongchamps. Tetrahedron 31, 2463 (1975).

364. J. Hine. Adv. Phys. Org. Chem. 15, 1 (1977).

365. J.-M. Lehn and G. Wipff. Helv. Chim. Acta. 61, 1274 (1978).

366. M.H. Lien, A.C. Hopkinson, M.R. Peterson, K. Yates and I.G. Csizmadia in Progress in Theoretical Chemistry. Vol. 2. Applications of MO Theory in Organic Chemistry. I.G. Csizmadia. Ed. Elsevier. Amsterdam, Neth. (1977), p. 162.

367. F.A. Long and L. Friedman. J. Am. Chem. Soc. 72, 3692 (1952).

368. D.R. Storm and D.E. Koshland, Jr. J. Am. Chem. Soc. 94, 5815 (1972).

369. M. Balakrishnan, G.V. Rao, and N. Venkatasubramanian. J. Chem. Soc. Perkin II, 6 and 1093 (1974).

370. G.M. Blackburn and H.L.H. Dodds. J. Chem. Soc. Perkin II, 377 (1974).

371. M.L. Bender, H. Matsui, R.J. Thomas, and S.W. Tobey. J. Am. Chem. Soc. 83 4193 (1961).

372. C.G. Overberger, M.T. O'Shaugnesy, and H. Shalit. J. Am. Chem. Soc. 71, 2661 (1949).

373. S.J. Yeh and H.H. Jaffe. J. Am. Chem. Soc. 81, 3274 (1959).

374. D.G. Lee and M.H. Sadar. J. Am. Chem. Soc. 96, 2862 (1974).

375. A.R. Butler. J. Chem. Soc. Perkin II, 959 (1976).

376. B. Dickie and R.F. Childs. Personal Communication.

377. H.H. Jaffe and R.W. Gardner. J. Am. Chem. Soc. 80, 319 (1958).

378. S.J. Yeh and H.H. Jaffe. J. Am. Chem. Soc. 81, 3279 and 3283 (1959).

379. J.H. Collins and H.H. Jaffe. J. Am. Chem. Soc. 84, 4708 (1962).

380. M. Izaks and H.H. Jaffe. J. Am. Chem. Soc. 86, 2209 (1964).

381. F. Gerson and E. Heilbronner. Helv. Chim. Acta. 45, 51 (1962).

382. E. Haselbach. Helv. Chim. Acta. 53, 1526 (1970).

383. E. Haselbach, A. Henriksson, A. Schmelzer, and H. Berthou. Helv. Chim. Acta. 56, 705 (1973).

384. W.A. Spitzer, T.W. Toone, and R. Stewart. Can. J. Chem. 54, 440 (1976).

385. H.W. Thompson and D.G. Melillo. J. Am. Chem. Soc. 92, 3218 (1970).

386. J. Gasteiger and R. Huisgen. J. Am. Chem. Soc. 94, 6541 (1972).

387. R.E. Partch. J. Am. Chem. Soc. 89, 3662 (1967).

388. Sadtler Standard NMR Spectra. Sadtler Research Labs, Philadelphia, PA. (1972) (a) No. 6023; (b) No. 425.

389. J.B. Stothers. Carbon-13 NMR Spectroscopy. Academic Press. New York, N.Y. (1972).

390. D.C. Frost, N.P.C. Westwood, N.H. Werstiuk, L. Cabelkova-Taguchi, and J. Warkentin. Can. J. Chem. 55, 3677 (1977).

391. F.D. Rossini. Experimental Methods in Thermochemistry. Wiley Interscience. New York, N.Y. (1956).

392. J. Lee and H.H. Seliger. Photochem. Photobiol. 4, 1015 (1965).

393. K. Mukai, N. Nishiguchi, K. Ishizu, Y. Deguchi, and H. Takaki. Bull. Chem. Soc. Japan. 40, 2731 (1967).

394. T.W. Bentley and P.v.R. Schleyer. J. Am. Chem. Soc. 98, 7667 (1976).

395. D.K. Edwards. J. Opt. Soc. Am. 50, 617 (1960).

396. M.A. Zoglio, J.J. Windheuser, R. Vatti, H.V. Maulding. S.S. Kornblum, A. Jacobs, and H. Hamot. J. Pharm. Sci. 57, 2080 (1968).

397. H.V. Maulding and M.A. Zoglio. J. Pharm. Sci. 59, 333 (1970).

398. P. Ahlberg. Acta. Chem. Scand. 24, 1883 (1970).

399. S. Wold. Acta. Chem. Scand. 24, 2321 (1970), and 25, 336 (1971).

400. S. Wold and P. Ahlberg. Acta. Chem. Scand. 24, 618 (1970).

401. J. Zsako and Z. Finta. Rev. Roum. Chim. 16, 483 (1971).

402. D.T.Y. Chen. J. Thermal Anal. 7, 61 (1975).

403. M.J. Blandamer. J. Burgess, and M. Dupree. J. Chem. Soc. Dalton, 63 (1977).

404. E.D. Becker. High Resolution NMR. Academic Press. New York, N.Y. (1969), p. 219.

405. H.D. Young. Statistical Treatment of Experimental Data. McGraw-Hill Co. Inc. New York, N.Y. (1962).

406. C. Mack. Essentials of Statistics for Scientists and Technologists. Plenum Press. London, U.K. (1975).

407. P.R. Bevington. Data Reduction and Error Analysis for the Physical Sciences. McGraw-Hill Co. Inc. New York, N.Y. (1969).

408. D.W. Marquardt. J. Soc. Ind. Appl. Math. 11, 431 (1963).

409. K.J. Laidler. Reaction Kinetics. Vol. 1. Homogeneous Gas Reactions. Pergammon Press. New York, N.Y. (1970).

410. K.B. Wiberg. Physical Organic Chemistry. John Wiley and Sons Inc. New York, N.Y. (1966).

411. E.A. Guggenheim. Phil. Mag. 2, 538 (1926).

412. C. Capellos and B.H.J. Bielski. Kinetic Systems - Mathematical Description of Chemical Kinetics in Solution. Wiley-Interscience. New York, N.Y. (1972).

413. H. Eyring. Chem. Revs. 17, 65 (1935).